ISSN 1007-9327 (print)
ISSN 2219-2840 (online)

World Journal of *Gastroenterology*

World J Gastroenterol 2021 January 7; 27(1): 1-142

Published by Baishideng Publishing Group Inc

World Journal of Gastroenterology

Contents

Weekly Volume 27 Number 1 January 7, 2021

World Journal of Gastroenterology

Weekly Volume 27 Number 1 January 7, 2021

Contents

ABOUT COVER

Editorial Board Member of *World Journal of Gastroenterology*, King-Wah Chiu is a Distinguished Professor at the Cheng Shui University in Kaohsiung, Taiwan, Republic of China. Having received his Bachelor's degree from China Medical University College of Medicine in 1985, he rose to Chief in the Gastroenterology Division of the Kaohsiung Chang Gung Memorial Hospital Affiliated to Chang Gung University of College of Medicine in 2002. Dr. Chiu is a recognized expert in hepato-gastroenterology, having practiced for 30 years, and the pioneer of transplant hepatology in the field of liver transplantation, practicing in Kaohsiung Chang Gung Memorial Hospital since 1998. His ongoing research interests involve the application of molecular biology in transplant hepatology, particularly to study the effects of integrative basic medicine on and management of living-donor liver transplantation establishment. (L-Editor: Filipodia)

AIMS AND SCOPE

The primary aim of *World Journal of Gastroenterology* (*WJG*, *World J Gastroenterol*) is to provide scholars and readers from various fields of gastroenterology and hepatology with a platform to publish high-quality basic and clinical research articles and communicate their research findings online. *WJG* mainly publishes articles reporting research results and findings obtained in the field of gastroenterology and hepatology and covering a wide range of topics including gastroenterology, hepatology, gastrointestinal endoscopy, gastrointestinal surgery, gastrointestinal oncology, and pediatric gastroenterology.

INDEXING/ABSTRACTING

The *WJG* is now indexed in Current Contents®/Clinical Medicine, Science Citation Index Expanded (also known as SciSearch®), Journal Citation Reports®, Index Medicus, MEDLINE, PubMed, PubMed Central, and Scopus. The 2020 edition of Journal Citation Report® cites the 2019 impact factor (IF) for *WJG* as 3.665; IF without journal self cites: 3.534; 5-year IF: 4.048; Ranking: 35 among 88 journals in gastroenterology and hepatology; and Quartile category: Q2.

RESPONSIBLE EDITORS FOR THIS ISSUE

NAME OF JOURNAL
World Journal of Gastroenterology

ISSN
ISSN 1007-9327 (print) ISSN 2219-2840 (online)

LAUNCH DATE
October 1, 1995

FREQUENCY
Weekly

EDITORS-IN-CHIEF
Andrzej S Tarnawski, Subrata Ghosh

EDITORIAL BOARD MEMBERS
http://www.wjgnet.com/1007-9327/editorialboard.htm

PUBLICATION DATE
January 7, 2021

INSTRUCTIONS TO AUTHORS
https://www.wjgnet.com/bpg/gerinfo/204

GUIDELINES FOR ETHICS DOCUMENTS
https://www.wjgnet.com/bpg/GerInfo/287

GUIDELINES FOR NON-NATIVE SPEAKERS OF ENGLISH
https://www.wjgnet.com/bpg/gerinfo/240

PUBLICATION ETHICS
https://www.wjgnet.com/bpg/GerInfo/288

PUBLICATION MISCONDUCT
https://www.wjgnet.com/bpg/gerinfo/208

ARTICLE PROCESSING CHARGE
https://www.wjgnet.com/bpg/gerinfo/242

STEPS FOR SUBMITTING MANUSCRIPTS
https://www.wjgnet.com/bpg/GerInfo/239

ONLINE SUBMISSION
https://www.f6publishing.com

E-mail: bpgoffice@wjgnet.com https://www.wjgnet.com

World Journal of Gastroenterology

Submit a Manuscript: https://www.f6publishing.com

World J Gastroenterol 2021 January 7; 27(1): 1-18

DOI: 10.3748/wjg.v27.i1.1

ISSN 1007-9327 (print) ISSN 2219-2840 (online)

REVIEW

Experimental models of metabolic and alcoholic fatty liver disease

Delfin Gerard Buyco, Jasmin Martin, Sookyoung Jeon, Royce Hooks, Chelsea Lin, Rotonya Carr

ORCID number: Delfin Gerard Buyco 0000-0001-5477-0316; Jasmin Martin 0000-0002-6581-2005; Sookyoung Jeon 0000-0002-3620-0851; Royce Hooks 0000-0003-0899-9907; Chelsea Lin 0000-0003-3696-121X; Rotonya Carr 0000-0003-0235-6994.

Author contributions: Buyco DG wrote the first draft of the paper; Buyco DG, Martin J, Jeon S, Hooks R, Lin C and Carr RM performed the research for the manuscript and edited all drafts of the paper.

Conflict-of-interest statement: The authors report no conflicts of interest.

Manuscript source: Unsolicited Manuscript

Specialty type: Gastroenterology and hepatology

Delfin Gerard Buyco, Jasmin Martin, Sookyoung Jeon, Royce Hooks, Chelsea Lin, Rotonya Carr, Division of Gastroenterology, University of Pennsylvania, Philadelphia, PA 19104, United States

Corresponding author: Rotonya Carr, MD, Assistant Professor, Division of Gastroenterology, University of Pennsylvania, 421 Curie Boulevard 907 Biomedical Research Center, Philadelphia, PA 19104, United States. rotonya.carr@pennmedicine.upenn.edu

Abstract

Non-alcoholic fatty liver disease (NAFLD) is a multi-systemic disease that is considered the hepatic manifestation of metabolic syndrome (MetS). Because alcohol consumption in NAFLD patients is common, there is a significant overlap in the pathogenesis of NAFLD and alcoholic liver disease (ALD). Indeed, MetS also significantly contributes to liver injury in ALD patients. This "syndrome of metabolic and alcoholic steatohepatitis" (SMASH) is thus expected to be a more prevalent presentation in liver patients, as the obesity epidemic continues. Several pre-clinical experimental models that couple alcohol consumption with NAFLD-inducing diet or genetic obesity have been developed to better understand the pathogenic mechanisms of SMASH. These models indicate that concomitant MetS and alcohol contribute to lipid dysregulation, oxidative stress, and the induction of innate immune response. There are significant limitations in the applicability of these models to human disease, such as the ability to induce advanced liver injury or replicate patterns in human food/alcohol consumption. Thus, there remains a need to develop models that accurately replicate patterns of obesogenic diet and alcohol consumption in SMASH patients.

Key Words: Non-alcoholic fatty liver disease; Alcoholic liver disease; Non-alcoholic steatohepatitis; Animal models; Insulin resistance; Oxidative stress

Core Tip: Experimental animal and cell culture models have been developed to study the "syndrome of metabolic and alcoholic steatohepatitis" (SMASH), in which concomitant non-alcoholic fatty liver disease and alcoholic liver disease risk factors play a role in liver injury. These models demonstrate that obesity, metabolic syndrome, and alcohol consumption synergistically contribute to lipid dysregulation, oxidative stress, inflammation, and fibrogenesis. The pathogenesis of SMASH in these

Country/Territory of origin: United States

Peer-review report's scientific quality classification
Grade A (Excellent): 0
Grade B (Very good): 0
Grade C (Good): C
Grade D (Fair): 0
Grade E (Poor): 0

Received: September 3, 2020
Peer-review started: September 3, 2020
First decision: October 17, 2020
Revised: November 1, 2020
Accepted: December 6, 2020
Article in press: December 6, 2020
Published online: January 7, 2021

P-Reviewer: Jin H
S-Editor: Zhang H
L-Editor: A
P-Editor: Liu JH

experimental models is dependent on obesogenic diet composition, alcohol consumption patterns, alcohol dosage, and genetic background.

Citation: Buyco DG, Martin J, Jeon S, Hooks R, Lin C, Carr R. Experimental models of metabolic and alcoholic fatty liver disease. *World J Gastroenterol* 2021; 27(1): 1-18
URL: https://www.wjgnet.com/1007-9327/full/v27/i1/1.htm
DOI: https://dx.doi.org/10.3748/wjg.v27.i1.1

INTRODUCTION

The two most common causes of liver disease worldwide are non-alcoholic fatty liver disease (NAFLD) and alcoholic liver disease (ALD)[1]. NAFLD is a multi-system disease whose major risk factors are genetic susceptibility, obesity, insulin resistance, and metabolic syndrome (MetS). MetS is the constellation of obesity, insulin resistance, hypercholesterolemia, hypertriglyceridemia, and hypertension; and NAFLD is considered the hepatic manifestation of MetS[2-4]. ALD also has a multi-factorial etiology, including alcohol consumption quantity and pattern, environmental factors, and genetics. Alcohol consumption patterns can be described in terms of long-term (chronic) or acute (binge) drinking episodes.

Clinicians recognize the existence of an overlap condition between NAFLD and ALD, despite the absence of significant alcohol intake in NAFLD diagnostic criteria[5]. For example, among ALD patients, obesity increases the likelihood for the development of alcoholic cirrhosis[6], while both long-term alcohol consumption and obesity have been found to independently promote advanced fibrosis[7]. Obesity and MetS also increase mortality in ALD[8]. Obesity, insulin resistance, and MetS are the most significant contributors to ALD severity, with as many as 50% of ALD patients estimated to have liver disease as a consequence of both alcohol overconsumption and obesity[9,10]. Obese individuals who overconsume alcohol are more likely to develop hepatic steatosis and cirrhosis compared to normal weight individuals[7]. As the obesity epidemic persists, this "syndrome of metabolic and alcoholic steatohepatitis" or SMASH is expected to become a more common presentation in liver patients[11].

Several experimental models have been developed to understand the metabolic factors that exacerbate liver disease in patients with coexistent NAFLD and ALD risk factors. Studies that incorporated both obesogenic diet (*e.g.*, high-fat, high-fructose) or genetic obesity and some form of alcohol consumption in a rodent model were included in this critical review, while human retrospective studies, human clinical trials, and *in vitro* models were excluded. While these models couple NAFLD risk factors with alcohol exposure, they differ in the animal genetic background, obesogenic diet composition, type and duration of alcohol consumption, and ability to induce significant liver injury. Here, we review the pre-clinical experimental models developed to study the interactive effects of NAFLD and ALD risk factors on hepatic injury, as well as limitations of the various models with regards to human disease.

PATHOLOGICAL OVERLAP BETWEEN NAFLD AND ALD

Lipid dysregulation

Lipid metabolism dysregulation is a key factor in the pathogenesis of NAFLD and ALD. *De novo* lipogenesis and fatty acid oxidation (FAO) are implicated in NAFLD pathogenesis, although lipid uptake, storage, and export also play a role[12]. Meanwhile, experimental models indicate that alcohol (EtOH) consumption further exacerbates lipid dysregulation in MetS. AMP-activated protein kinase (AMPK) is a key regulator of lipid metabolism, and its inhibition has been implicated in both NAFLD and ALD[13-15]. AMPK has reciprocal effects on *de novo* lipogenesis and fatty acid (FA) uptake through the regulation of the transcription factor sterol response element binding protein 1 (SREBP-1)[16]. SREBP-1 is upregulated in NAFLD patients and in high-fat diet (HFD)-induced NAFLD rodent models[17]. Pharmacological inhibition of SREBP-1 increases insulin sensitivity and suppresses FA synthesis[18]. AMPK also modulates FAO by regulating peroxisome proliferator-activated receptor

(PPAR) α and sirtuin 1 (SIRT-1), the latter of which is inhibited by EtOH consumption[19-22]. FAO is induced in NAFLD as a compensatory effect of increased lipid uptake and *de novo* lipogenesis[23]. In obese patients, EtOH is also known to increase adiponectin levels, which induces AMPK activation[24].

Oxidative stress

NAFLD risk factors and EtOH consumption also contribute to oxidative stress in fatty liver disease by dysregulating oxidative biochemical processes and producing reactive oxygen species (ROS). Obesogenic diet contributes to the formation of ROS such as hydrogen peroxide (H_2O_2), superoxide (O_2-), 4-hydroxynonenal (4-HNE), malondialdehyde (MDA), and oxysterols as byproducts of FAO[25]. EtOH metabolism by alcohol and acetaldehyde dehydrogenases, and cytochrome P450 2E1 (CYP2E1) also produces ROS[26]. CYP2E1, in particular, is implicated in the pathogenesis of both NAFLD and ALD in humans[5,27]. CYP2E1 metabolizes EtOH and other xenobiotics in a nicotinamide adenine dinucleotide phosphate ($NADP^+$/NADPH)-mediated process and produces H_2O_2 and O_2^-[28]. Mouse models also indicate that CYP2E1 plays a role in lipid dysregulation[29] and diabetes[30]. Inhibition of CYP2E1 has been found to be protective against lipid metabolism dysregulation and oxidative stress induced by combined FA and EtOH treatment *in vitro*[31].

Concomitant NAFLD risk factors and EtOH consumption also dysregulate the unfolded protein response (UPR), resulting in the production of ROS in the endoplasmic reticulum (ER)[32]. In the UPR, misfolded proteins sequester binding immunoglobulin protein (BIP), inducing the protein kinase R-like ER kinase (PERK), activating transcription factor 6 (ATF-6), and inositol-requiring kinase (IRE-1) transduction pathways. The UPR involves the formation of disulfide bonds, an oxidative process that produces H_2O_2 and other ROS[32]. Protein folding dysregulation is associated with oxidative stress in fatty liver disease[33]; saturated FA, oleic acid, and cholesterol interact with the UPR and induce ER stress[34]. Lipids and EtOH have a reciprocal relationship with the ER: PERK induces protein and lipid metabolism, and apoptosis, while ATF-6 and IRE-1 mediate protein trafficking and inflammation[35,36].

Three enzymes are key to the elimination of ROS: Superoxide dismutase (SOD) metabolizes O_2- to O_2 and H_2O_2; while catalase and glutathione peroxidase (GPx) metabolize H_2O_2 to O_2 and H_2O[37,38]. H_2O_2 oxidation by GPx is coupled to the metabolism of reduced glutathione (GSH) to oxidized glutathione disulfide (GSSG). GSSG is reduced back to GSH by glutathione reductase (GR), which requires NADPH[39,40]. Clinical observations indicate that patients with NAFLD have increased SOD, GPx, and GR activities, as well as elevated levels of GSH[41,42]. Similarly, patients with ALD have upregulated SOD activity[43], although GSH/GSSG ratio is decreased[44].

Immune response

Macrophage and neutrophil activation play important roles in liver injury in the context of MetS and EtOH consumption[45,46]. Macrophages adopt a number of functional states that are traditionally categorized into two groups. Pro-inflammatory M1 polarization is distinguished by the presence of cell surface marker CD68, and secretion of interleukin (IL) 6, tumor necrosis factor α (TNFα), and other cytokines. Conversely, anti-inflammatory M2 polarization is distinguished by CD163, transforming growth factor β (TGFβ), IL-10, and arginase 1 (ARG-1)[47]. Saturated FAs and cholesterol are known to induce a predominantly M1-like phenotype in Kupffer cells, liver-resident macrophages[48]. M1 polarization is associated with severity of disease, CD68+ Kupffer cells, and TNFα expression were both found to be significantly higher in non-alcoholic steatohepatitis (NASH) patients compared to patients with simple steatosis[49]. However, CD45+ leukocytes and CD163+ Kupffer cells are also increased in pediatric NAFLD patients[50]. Meanwhile, hepatocyte damage in ALD increases lipopolysaccharide (LPS) leakage into the liver by enhancing intestinal permeability, resulting in TNFα and IL-10 secretion by Kupffer cells[51,52]. The two-state model of macrophage polarization may thus be insufficient to describe immune response under concomitant NAFLD and ALD risk factors. Kupffer cells also release IL-1β in response to hepatic tissue damage and necrosis, which results in neutrophil recruitment from bone marrow to the liver[53]. Neutrophil infiltration, distinguished by upregulation in TNFα, IL-1, and osteopontin (OPN), contributes to hepatocyte death and correlates with ALD severity[54].

Apoptosis and fibrosis

NAFLD pathogenesis involves hepatocellular apoptosis, which occurs *via* the extrinsic

and intrinsic pathways. In the intrinsic pathway, apoptosis occurs as a result of cellular, ER, or mitochondrial stress[55]. In the extrinsic pathway, apoptosis arises as a response to extracellular signaling[56]. One particularly important extrinsic mechanism in NAFLD is the tumor necrosis factor α (TNFα) pathway. TNFα activates anti-apoptotic NF-κB and apoptotic caspase-3[57,58].

Oxidative stress, inflammation, and hepatocyte apoptosis contribute to hepatic fibrosis in NAFLD and ALD, and these pathways are mediated by hepatic stellate cells (HSC)[59]. One important fibrogenic mechanism in NAFLD and ALD is the TGFβ pathway, which induces the expression of collagens, a component of extracellular matrix (ECM), *via* the signal transducer SMAD-3. Another important signaling pathway is that of toll-like receptor 4 (TLR-4), which responds to LPS, and produces pro-inflammatory cytokines[60,61]. TLR-4 is upregulated in obese patients with NAFLD[62]; and in patients with ALD, alcohol increases gut permeability and promotes LPS-producing Gram-negative bacteria[63]. However, in one study, mRNA expression of TLR-4 tended to decrease in biopsy-diagnosed NAFLD patients who drank at most 20 g/kg/d EtOH compared to those who did not drink[64]. Activated HSCs also produce tissue inhibitor of metalloproteinases (TIMP), which inhibits ECM-degrading matrix metalloproteinases (MMPs)[65].

EXPERIMENTAL MODELS OF NAFLD AND ALD

Despite the pathological overlap between NAFLD and ALD, most studies model NAFLD risk factors and EtOH consumption independent of each other. Although individually these models are limited in their capacity to recapitulate SMASH pathogenesis, they form the foundation for many SMASH models.

NAFLD models

A variety of animal models have been proposed for studying NAFLD, which can be largely divided into three categories: dietary, genetic, and combined models. Dietary manipulations can induce NAFLD development by using obesogenic or nutrient-deficient diets[66]. Obesogenic diets are typically rich in fat with additional sugar and/or cholesterol, representing metabolic and histological features of human NAFLD. There are a number of obesogenic diets, varying in the macronutrient composition, sources of fat, types of sugar, and cholesterol content. Nutrient-deficient diets, such as methionine- and choline-deficient, and choline-deficient L-amino acid-defined (CDAA) diets, are also capable of inducing NAFLD[66-68]. Choline-deficient and CDAA diets are used because methionine and choline are required for phosphatidylcholine synthesis, and are thus intimately involved in lipoprotein synthesis, lipid storage, and lipid regulation[69]. Nutrient-deficient diets can rapidly induce NAFLD within a few weeks of feeding, but some metabolic features including body weight, hyperglycemia, and insulin sensitivity do not manifest as they do in human NAFLD.

Various genetic animal models have also been created to study NAFLD, and are especially valuable for studying the mechanisms of NAFLD pathogenesis[67,70]. Genetic mouse models of NAFLD include leptin-deficient (ob/ob), leptin receptor-deficient (db/db), insulin resistant (KK-A^{y}), SREBP-1c transgenic, PPARα null, phosphatase and tensin homolog (PTEN) null, and acyl-coenzyme A oxidase (ACOX) null mice. For rats, genetic models include leptin receptor-deficient (fa/fa) and cholecystokinin knockout (OLETF). Dietary and genetic models are also combined to replicate the multifactorial nature of human NAFLD. A detailed discussion of NAFLD animal models is beyond the scope of this review and described in other reviews[66-68,70].

ALD models

Pre-clinical models have also been developed to understand the pathogenesis of ALD. EtOH can be administered to animals either orally or intravenously. Four models have been developed for studying ALD: (1) Binge feeding, in which animals are acutely administered EtOH by gavage; (2) Chronic feeding, in which animals are given access to EtOH through diet or drinking water for a prolonged period of time (*e.g.*, Lieber-DeCarli diet model[71]); (3) Intragastric (iG) infusion feeding (*e.g.*, Tsukamoto-French model[72-74]); and (4) Chronic-binge feeding, in which animals are given chronic EtOH for a certain period of time, then administered EtOH acutely (*e.g.*, Gao model[75,76]). Variations in these models exist, such as multiple binge feeding and combined models. In addition, experimental models vary in EtOH concentration and feeding period. Animal models should thus be selected depending on the purpose of the study, as

there have been no animal models that fully recapitulate the full spectrum of ALD.

EXPERIMENTAL MODELS OF SMASH

Experimental rodent models (Table 1) of SMASH couple one of the dietary or genetic models of NAFLD described above with EtOH consumption models of ALD. While obesity and EtOH consumption models vary considerably, studies that combine the two generally indicate a synergistic increase in steatosis, inflammation, and fibrosis by obesity and EtOH.

Dietary models of SMASH

The most common type of dietary SMASH model couples HFD with either chronic or binge (acute) EtOH consumption. For example, Gäbele *et al*[77] gave Balb/c mice *ad libitum* access to either chow diet or HFD, along with water or 5% EtOH in drinking water. HFD-EtOH diet upregulated TNFα, TGFβ, collagen I, α smooth muscle actin (αSMA) expression, synergistically contributing to inflammation and fibrosis. HFD upregulated TLR-4 expression, but EtOH did not have an effect on TLR-4. However, combined HFD-EtOH increased serum LPS levels and had increased fibrosis compared to the other groups, suggesting that obesity increases LPS sensitivity by upregulating TLR-4, while EtOH promotes fibrosis by increasing intestinal permeability and LPS leakage.

Wang *et al*[78] used high-fat (HF) Lieber-DeCarli (LD) diet and observed increased inflammation and apoptosis in HF-EtOH treated rats. Sprague-Dawley rats were given *ad libitum* access to control LD or HF LD diet for 6 wk. The HF LD-fed rats were then given either HF LD and HF-EtOH LD for another 4 wk. HF-EtOH LD increased hepatic steatosis and number of inflammatory foci compared to controls. HF-EtOH LD also increased TUNEL+ apoptotic hepatocytes compared to control diet, but EtOH did not significantly affect TUNEL+ hepatocyte count, suggesting that obesogenic diet contributes more to apoptosis than EtOH in this model. There was no difference in B-cell lymphoma (BCL) 2 or BCL-2-associated X protein (Bax) between the groups, while Fas death receptor and Fas ligand were upregulated in the HF-EtOH LD group, suggesting that hepatocyte apoptosis occurs *via* the extrinsic pathway in SMASH.

Similarly, Gopal *et al*[79] developed a model using both solid diet and LD to determine the effect of exogenous SOD-1 on inflammation and fibrosis in SMASH. C57BL/6 mice were fed either chow or HFD for 10 wk, then either control LD or 5% EtOH LD for an additional 4 wk. The HFD-fed mice were also administered SOD-1 for 2 wk. HFD-EtOH upregulated CYP2E1, ADH, catalase, FA oxidizing ACOX-1, pro-inflammatory CCL-2, and pro-fibrotic MMP-12 compared to controls. These results corroborate the findings in the other aforementioned HFD-EtOH models that dietary obesity and EtOH both contribute to lipid dysregulation, inflammation, and fibrosis. SOD-1 treatment attenuated the increases in CYP2E1, ADH, CCL-2, and MMP-12, but further upregulated catalase, PPARα, and ACOX-1. The effects of SOD indicate that dysregulation of antioxidant mechanisms plays a role in SMASH pathogenesis, but targeting these mechanisms pharmacologically may have adverse effects on lipid metabolism (Figure 1).

The aforementioned models used chronic EtOH feeding to induce liver injury, but Duly *et al*[80] took a different approach to modeling SMASH by coupling HFD to repeated binge EtOH consumption. C57BL/6 mice were fed chow or HFD for 12 wk, and administered saline or 2 g EtOH/kg BW twice per week. ALT/AST activity did not differ between experimental groups, but HFD-EtOH increased hepatic TG levels compared to controls. HFD-EtOH also upregulated SREBP-1 and stearoyl-CoA desaturase 1, a transcriptional target of SREBP-1 involved in FA synthesis[16], compared to controls. HFD-EtOH also increased vimentin+ cells in the hepatic parenchyma and collagen deposition compared to controls, but did not affect expression of pro-fibrotic collagen I, TGFβ, and plasminogen activator inhibitor (PAI-1). These results suggest that obesity and EtOH synergistically contribute to lipid dysregulation and fibrosis, although through a yet unknown mechanism. The application of this study to human disease is also limited because HFD alone did not promote TG accumulation, a diagnostic criterion for NAFLD.

HFD intragastric infusion is also used in overfeeding models of SMASH. For example, Lazaro *et al*[81] fed C57BL/6 mice high saturated fat, high cholesterol (HFHC) diet for 2 wk, then liquid HFD or HFD-EtOH by intragastric infusion for 8 wk, with some HFD-EtOH-fed mice also receiving additional EtOH by gavage. HFHC and chronic-binge EtOH upregulated myeloperoxidase, CXCL-1, and OPN, and increased

Table 1 Experimental studies modeling the effect of metabolic syndrome risk factors and alcohol consumption on liver injury outcomes in rodent and cell culture models

Ref.	Experimental model details	Biochemistry	Anatomy and histology	mRNA and protein expression
Alwahsh *et al*[84]	(1) Animal: 10 wk male Sprague- Dawley rat; (2) Initial weight: 270-310 g; (3) Diet: LD control, LD with 30% kcal from fructose, 30% kcal from EtOH, or LD with both fructose and EtOH; and (4) Duration: 28 d	(1) ↑ ALT; (2) ↑ liver and plasma TG; (3) ↑ plasma leptin; (4) ↓ plasma HDL; (5) ↓ plasma albumin; and (6) No dif. in leptin or hepatic TG between LD-EtOH and LD- fructose-EtOH	(1) Portal inflammatory infiltration and stage 1 fibrosis (LD-EtOH); (2) Periportal macrosteatosis (LD-fructose); and (3) Portal inflammation, periportal macrosteatosis, fibrosis (LD-fructose-EtOH)	(1) ↑ leptin; (2) ↑ ACC-2; (3) ↑ lipase in LD-EtOH, but ↓ in LD-fructose and LD-fructose-EtOH; (4) ↓ IRS-1, IRS-2 (fructose groups); and (5) ↑ CD36, CPT-1α, PPARα in LD- EtOH and LD-fructose, but no change in LD-fructose-EtOH
Bucher *et al*[112]	(1) Animal: 7 wk male C57BL/6J Mouse; (2) Initial weight: 20-23 g; (3) Diet: Control (3 kcal/g food; 16% kcal protein) or HFD (5.5 kcal/g; 60% kcal SFA); 10 g/kg/d EtOH in drinking water; and (4) Duration: 4 mo	(1) ↑ ALT, but ↓ ALT compared to EtOH-naïve HFD; (2) ↑ cholesterol, but ↓ cholesterol compared to EtOH-naïve HFD; (3) ↑ TG↑ serum glucose; (4) ↑ serum insulin; and (5) ↑ MUFA and ↓ SFA (compared to HFD)	(1) Mediovesicular and macrovacular steatosis and (2) No dif. in necroinflammation or perisinusoidal fibrosis between HFD and HFD-EtOH	(1) ↑ genes for apoptosis inhibition, acetyl-CoA synthesis, lipogenesis, mitochondrial functions (NADH dehydrogenase, COX, ATP synthase), and proteolysis; (2) ↓ genes for apoptosis (BCL-2 homologs), fibrosis (collagen), chemotaxis, oxidative stress (GPx, HMOX-1, SOD); and (3) ↓ CYP2E1 protein levels
Carmiel-Haggai *et al*[94]	(1) Animal: 15 wk male fa/fa Zucker Rat; (2) Initial weight: 595 ± 35 g (obese), 316 ± 32 g (lean controls); and (3) Diet: 35% v/v EtOH in saline every 12 h for 3 d; final dose was 4 g/kg EtOH	(1) ↑ ALT; (2) ↑ NEFA; (3) ↑ LPO by-products (4-HNE, MDA); and (4) ↓ CYP2E1 activity	(1) Macrovesicular steatosis (EtOH-naïve fa/fa) and (2) Lobular microvesicular, central macrosteatosis, inflammation (EtOH-fed fa/fa)	(1) ↓ GSH, GPx, GR; (2) ↓ GSSG (EtOH-fed and EtOH-naïve fa/fa); (3) ↓ catalase, SOD; (4) ↑ iNOS; (5) ↑ caspase 3, caspase 8; (6) ↑ BCL-XL, FAS ligand; and (7) ↑ BCL-2, BAX (EtOH-fed and EtOH-naïve fa/fa)
Duly *et al*[80]	(1) Animal: 6-8 wk male C57BL/6 Mouse; (2) Initial weight: 20 g; (3) Diet: chow (12% kcal fat) or HFD (45% kcal fat, 0.25% cholesterol); 2 g/kg EtOH in saline twice per wk; and (4) Duration: 12 wk	(1) ↑ TG (chow-EtOH, but not HFD or HFD-EtOH); (2) ↑ cholesterol, HDL, LDL (but no difference between HFD and HFD- EtOH); and (3) ↑ serum insulin	(1) Steatosis and lipid accumulation; (2) Collagen deposition; (3) ↑ cellular infiltration; (4) ↑ CD45+ leukocytes; (5) ↑ F4/80+ Kupffer cells; and (6) ↑ vimentin+ HSCs	(1) ↑ SREBP-1; (2) ↑ SCD-1; (3) ↑ PPARα; (4) ↓ ACOX-1; (5) No dif. in TGFβ or HSP90; and (6) ↑ collagen I, PAI-1 (EtOH-naïve HFD)
Everitt *et al*[87]	(1) Animal: 12 wk male ob/ob C57BL/6-J/Rj-ob mouse; (2) Diet: PUFA-enriched LD with 27.5% EtOH or isocaloric maltodextrin; and (3) Duration: 4 wk	(1) ↑ ALT/AST; (2) ↑ hepatic TG; (3) ↑ hepatic cholesterol; (4) ↑ hepatic lactate; (5) ↓ hepatic pyruvate; (6) No dif. in BAL between EtOH-fed; and (7) ob/ob and EtOH-fed lean mice	Steatosis in EtOH-fed ob/ob	(1) ↑ mTOR, PPARγ, FGF-21, FSP-27; (2) ↑ SIRT-1, pAMPKα, AMPKα, pACC (ob compared to lean; EtOH did not have an effect); (3) ↑ adipose TNFα, ↓ hepatic TNFα; (4) ↑ cytosolic lipin-1 protein levels; (5) ↓ nuclear lipin-1 protein levels; (6) ↓ PGC-1α; and (7) ↓ ACOX-1
Gäbele *et al*[77]	(1) Animal: 12 wk female Balb/c mouse; (2) Diet: Chow or HFD [17% fat (50% lard, 50% cacao-butter), 1.25% cholesterol, 0.5% cholate]; 5% EtOH in *ad libitum*; and (3) Duration: 6 wk	(1) ↑ hepatic TG; (2) ↑ portal blood LPS; and (3) ↓ BAL (not statistically significant)	(1) Steatosis in HFD-fed mice; (2) ↑ 4-HNE; (3) ↑ αSMA+ cells; (4) ↑ collagen I; and (5) ↑ ECM deposition	(1) ↑ p47phox, TNF, TGFβ, collagen I; (2) ↑ TLR-4 in HFD mice, with no effect by EtOH; (3) ↑ αSMA protein levels; and (4) ↓ CYP2E1 protein levels in HFD
Gopal *et al*[79]	(1) Animal: 6-8 wk male C57BL/6 mouse; (2) Diet: Chow or HFD (45% kcal fat) for 10 wk, then LD control or 5% v/v EtOH LD for 4 wk additionally; and (3) Drug: HFD mice also given 1000 U/kg Cu/Zn SOD-1 with polylysine- PEG copolymer in 10 mM HEPES every 2 d for 2 wk	(1) ↑ ALT; (2) ↑ FFA; (3) ↓ leptin; (4) nanoSOD treatment counteracted the above effects; and (5) No dif. in MDA between groups	(1) ↑ adipose mass by HFD, but ↓ fat/body weight ratio by HFD- EtOH; (2) ↑ microvesicular steatosis (in all mice); (3) ↑ macrovesicular steatosis; (4) ↑ inflammatory nodules; (5) ↑ hepatocyte ballooning; and (6) ↑ MCP-1 protein levels, ↓ MCP-1 in HFD-EtOH mice treated with nanoSOD	(1) ↑ adipose CYP2E1 protein levels, ↓ CYP2E1 by nanoSOD; (2) ↑ hepatic CYP2E1, ADH, catalase, ↓ CYP2E1 and ADH, but ↑ catalase by nanoSOD; (3) ↑ PPARα, ACOX-1 in HFD, further ↑ ACOX-1 by EtOH, further ↑ for both by nanoSOD; and (4) ↑ CCL-2, MMP-12; ↓ by nanoSOD
Jung *et al*[108]	(1) Animal: Female C57BL/6J mouse; (2) Diet: Control (69% carbohydrates, 12% fat, 19% protein) or FFC (60% carbohydrates, 25% fat, 15% protein, 50% wt/wt	(1) ↑ TG; ↓ in beer-treated FFC compared to EtOH-treated or naïve and (2) ↓ glucose tolerance in all FFC-fed groups	(1) ↑ neutrophil granulocytes; ↓ by beer in FFC-fed mice; (2) ↑ NAS; ↓ by beer in FFC-fed mice; (3) ↑ iNOS protein levels; ↓ by beer and EtOH in FFC-fed mice; and (4) ↑ 4-HNE; ↓ by beer and EtOH in FFC-fed mice	(1) ↑ IR, IRS-2 in FFC-EtOH and FFC- beer compared to naïve; no dif. in IRS-1; (2) ↓ adiponectin in FFC and FFC- EtOH, but ↑ in FFC-beer; (3) ↑ hepatic AdipoR1 and SIRT-1 in FFC-beer; and (4)

	fructose, 0.16% wt/wt cholesterol); Diets enriched with 2.5 g/kg EtOH, isocaloric beer (4.9% v/v EtOH), or isocaloric diet; and (3) Duration: 7 wk			No dif. in PPARγ, AdipoR2, FASN, SREBP-1c, ACOX-1 between groups
Kanuri *et al*[106]	(1) Animal: 6 wk male ob/ob C57BL/6 mouse; (2) Diet: 2.5 g/kg/d EtOH in drinking water; and (3) Duration: 6 wk	(1) ↑ ALT/AST in ob/ob, but ↓ slightly by EtOH in ob/ob; (2) ↑ TG, cholesterol, HDL, LDL in ob/ob, but no effect by EtOH; and (3) No dif. in FFA	(1) Steatosis, hepatomegaly in ob/ob; (2) Macrovesicular steatosis in EtOH-naïve ob/ob; (3) Microvesicular steatosis in EtOH- fed ob/ob; and (4) ↓ hepatic neutrophils	(1) ↑ PLIN-2, PLIN-3, TNFα, PAI-1 in ob/ob, ↓ PAI-1, PLIN-2, PLIN-3 by EtOH; (2) ↓ IRS-1, IRS-2, adiponectin, SIRT- 1 in ob/ob; ↑ adiponectin, SIRT-1 by EtOH; (3) No effect by EtOH on PPARγ, ACOX-1, SREBP-1c, IRS-1, IRS02, GLUT-4, glucokinase, PEPCK; and (4) No dif. in hepatic ACOX-1, PPARγ
Kitagawa *et al*[95]	(1) Animal: 8 wk female KK-A^{y} mouse; (2) Diet: LD with 5% EtOH or isocaloric maltodextrin; Single gavage of 4 g/kg EtOH or gavage on after 11 d; (3) Drug: 0.1 g/L rifaximin (RFX); and (4) Duration: 10 d	(1) ↑ ALT; (2) ↑ serum and hepatic TG; (3) ↑ portal blood LPS; (4) ↑ CYP2E1 activity; and (5) ↓ ALT, TG, LPS (but not to basal levels) in EtOH-fed treated with RFX	(1) Lipid droplet accumulation in hepatic lobule; (2) Hepatomegaly; (3) ↑ 4-HNE; and (4) RFX counteractedthe aboveeffects	(1) ↑ ACCα, FASN; TNFα, IL-6, ILNγ; CCL-2; CD14, TLR-4, TLR-2; HMOX- 1, NOX-1; (2) ↓ CPT-1α; (3) ↑ CYP2E1 protein levels; no effect by RFX; and (4) RFX counteracted effects of EtOH on ACCα, FASN, TNFα, IFNγ, TLR-4, HMOX-1, and NOX-2, CPT-1α
Lazaro *et al*[81]	(1) Animal: Male WT and OPN- knockout C57BL/6 mice and (2) Diet: High-fat, high-cholesterol diet for 2 wk, then iG liquid HFD-EtOH (36% kcal from corn oil; 27 g/kg/d EtOH) or isocaloric HFD for 8 wk; Some HFD-EtOH given 4-5 g/kg/wk EtOH by gavage	(1) ↑ ALT, but ↓ with binge EtOH; ↓ ALT in binge-treated OPN KO compared to binge-treated WT; (2) ↑ bilirubin, ↓ albumin; (3) ↑ TG; and (4) No dif. in BAL	(1) Steatosis, hepatomegaly, mononuclear cell inflammation, neutrophil infiltration, perisinusoidal and percellular fibrosis in HFD-EtOH and (2) Splenomegaly, ↑ TLR-4 in binge-treated mice; effect of binge greater in OPN KO	(1) ↑ collagen I, αSMA, TIMP-1 by EtOH; further ↑ by EtOH binge; (2) ↑ myeloperoxidase, CXCL-1, OPN in binge-treated; and (3) ↑ myeloperoxidase, IL-17α in binge-treated OPN KO
Minato *et al*[96]	(1) Animal: 30 wk male OLET and OLETF rat; (2) Initial weight: 620 ± 15 g (OLETF), 460 ± 10 g (OLET); (3) Diet: 10 mL 10% EtOH by gavage for 1-5 d/wk; and (4) Duration: 3 wk	(1) ↑ ALT/AST; (2) ↑ serum and hepatic TG; (3) ↑ serum glucose; (4) ↑ serum insulin in OLETF, with no effect from EtOH; and (5) ↑ serum adiponectin in OLETF, ↓ by EtOH in OLETF	(1) Mild pericentral microvesicular steatosis in EtOH-naïve OLETF; (2) Steatohepatitis, focal hepatic necrosis, and hepatocyte ballooning in EtOH-treated OLETF; (3) ↑ hepatic CYP2E1; and (4) ↑ 4-HNE	(1) ↑ PPARγ in OLETF, with no effect from EtOH and (2) ↑ TNFα
Nieto *et al*[85]	(1) Animal: 12 wk male Lewis rat; (2) Initial weight: 100 g; (3) Diet: Choline deficient (CD) diet; (4) 15 mL/kg whiskey by gavage 3 times per wk; and (5) Duration: 3 mo	(1) ↑ ALT/AST; (2) ↑ TG; (3) ↑ NEFA; (4) ↑ MDA, protein carbonyls; (5) ↑ serum TNFα, but ↓ in CD- whiskey; (6) ↑ CYP2E1 activity; (7) ↑ caspase-3, caspase-8 activity	(1) Minimal steatosis in whiskey-naïve CD rats and (2) Periportal and percentral microvesicular steatosis in CD-whiskey rats	(1) ↑ collagen 1, αSMA, cytochrome *c*, HSP47, CYP2E1; (2) ↑ leptin, TIMP-1, and BAX protein levels by CD, with no effect by whiskey; and (3) ↓ MMP-2, MMP-9, MMP-13, BCL-2, BCL-XL by CD, with no effect by whiskey
Osaki *et al*[101]	(1) Animal: Male Sprague-Dawley rat; (2) Initial weight: 106 g; (3) Diet: HFD (30% beef tallow, 20% casein, 20% sucrose); 1%-2% v/v EtOH *ad libitum*; and (4) Duration: 12 wk	(1) ↓ ALT; no dif. in AST; (2) ↓ ammonia, urate; (3) No dif. in serum glucose, FFA, cholesterol, HDL, bilirubin, alkaline phosphatase levels, urea, creatinine, lactate, acetate; (4) No dif. in hepatic TG, MDA; (5) No dif. in hepatic, renal, or pulmonary thiobarbituric acid-reactive substances	No dif. in hepatic TG, MDA No dif. in weight of liver, epididymal adipose tissue, perirenal adipose tissue, or gastrocnemius muscle	No dif. in TNFα, adiponectin, insulin-like growth factor binding protein 1, hemoglobin
Robin *et al*[86]	(1) Animal: Male ob/ob C57BL/6J mouse; (2) Initial weight: 49-56 g (obese), 26-30 g (lean); (3) Diet: 2.5 g/kg/d EtOH by gastric intubation; (4) Drug: 100 mg/kg/d pentoxifylline (PTX) by iP; and (5) Duration: 4 d	(1) ↑ ALT in ob/ob; no effect by EtOH; (2) ↑ caspase-3,CYP2E1, SOD activities; ↓ caspase 3 by PTX; (3) ↓ GPx, cytosolic GT activity in ob/ob, but no effect by EtOH; (4) ↓ mitochondrial GT activity by EtOH; and (5) No dif. in GR activity	(1) Steatosis, caspase-3 activation in ob/ob; (2) TUNEL+ hepatocytes; and (3) Necrosis, inflammation in EtOH-naïve ob/ob	(1) ↑ TNFα protein levels; ↓ by PTX; (2) ↑ IκBα protein levels, ↓ NF-κB p65; ↓ NF-κB activity; (3) ↓ iNOS, BCL-XL; (4) ↓ cytosolic GSH, mitochondrial GSSG; and (5) ↑ HSP70
Song *et al*[124]	(1) Animal: 6 wk male C57BL/6J mouse; (2) Diet: high-fructose diet (20.2% kcal protein, 66.96% kcal carbohydrates, 12.9% kcal fat); 10% v/v EtOH for 2 d,	(1) ↑ ALT/AST; (2) ↑ plasma TG, NEFA, cholesterol by EtOH, but not fructose; (3) ↑ plasma glucose by fructose diet, ↓ glucose by EtOH; (4) ↑ insulin by fructose and EtOH, but not combined	(1) ↑ microvesicular steatosis and (2) ↑ macrovesicular steatosis in EtOH-naïve fructose; ↓ by fructose-EtOH diet	(1) ↑ hepatic CYP2E1 protein levels; (2) ↑ KHK in EtOH-naïve fructose; (3) ↑ F4/80, CD68, and TNFα, MyD88, IRF-3, and TRAF-6; (4) ↑ CCL-2, TLR-4, and IRF-7 only in fructose-EtOH; (5) ↑

	15% for 5 d, 20% for 17 wk; and (3) Duration: 18 wk	fructose-EtOH; (5) ↓ copper by fructose and EtOH, but not combined fructose-EtOH		CD163, IL-1β, or ARG-1 by EtOH, but no effect by fructose; and (6) No dif. in IL-6, IL-10
Sun *et al*[107]	(1) Animal: Male Sprague-Dawley rats; (2) Initial weight: 80-100 g; (3) Diet: HFD (38% fat, 2% cholesterol, 1% cholate) or control (38% kcal from fat); 4 g/kg/d EtOH by gavage beginning after 3 wk; and (4) Duration: 12 wk	No dif. in plasma LPS levels	(1) ↑ steatosis, fibrosis in HFD mice compared to HFD-EtOH and (2) ↑ Kupffer cell and HSC activation in HFD mice compared to HFD- EtOH	↑ inflammatory cytokines (TNFα, CXCL-1, CXCL-2, IL-1β, IL-6), pro- fibrotic markers (αSMA, collagen, TGF-β, TIMP-1, MMP-2, MMP-9) in HFD compared to HFD-EtOH
Suzuki *et al*[92]	(1) Animal: 8 wk male KK-A^{y} mouse; (2) Diet: LD containing 5% EtOH or isocaloric maltodextrin; 4 g/kg EtOH or isocaloric maltodextrin by gavage on day 11; (3) Drug: 120 mg/kg/d phenylbutyric acid (PBA); and (4) Duration: 10 d	(1) ↑ ALT/AST in chronic-binge mice; no dif. in ALT/AST between chronic-only and controls; (2) ↑ serum and hepatic TG; (3) No dif. in blood glucose; and (4) PBA ↓ ALT/AST, TG in EtOH-fed mice compared to PBA-naïve	(1) ↑ steatosis, PMN infiltration, ccCK18+ hepatocytes, 4-HNE+ cells in chronic-binge mice and (2) PBA alleviated liver injury, but did not decrease 4-HNE+ cell count	(1) ↑ inflammatory cytokines (TNFα, IL-6), ER stress markers (BiP, uXBP-1, sXBP-1, IP3R1, CHOP), and HMOX-1 by chronic-binge; PBA ↓ aforementioned genes; (2) ↑ BiP, uXBP-1 in chronic, but not sXBP-1, IP3R1, CHOP, HMOX-1; and (3) ↑ CYP2E1; PBA had no effect
Wang *et al*[78]	(1) Animal: 8 wk male Sprague-Dawley rat; (2) Diet: LD control (35% kcal from fat) or LD HFD (71% kcal from fat) for 6 wk; then LD HFD were given either solid HFD (55% kcal fat) or HF-EtOH diet (55% kcal fat, 16% kcal EtOH) for 4 wk; (3) Duration: 10 wk	(1) ↑ TUNEL+ hepatocytes; (2) ↑ cleaved caspase-3 levels; and (3) No dif. in 4-HNE or MDA levels between HFD and HFD-EtOH, but ↑ compared to controls	(1) Lipid droplet accumulation; (2) ↑ steatosis; and (3) ↑ number of inflammatory foci	(1) ↑ Fas death receptor and ligand; (2) No dif. in caspase-3 expression; (3) No dif. in CYP2E1, TNFα, TNFR-1, IL-1β, IL-12 between HFD and HFD-EtOH, but ↑ compared to controls
Xu *et al*[83]	(1) Animal: 8 wk male C57BL/6J mouse; (2) Diet: 580 kcal/kg/d (control) or 986 kcal/kg/d (overfed) of liquid HFD (37% kcal corn oil) by iG infusion for 45 d; 23 g/kg/d (low dose) or 32 g/kg/d (high dose) *via* iG infusion added to diet after 45; controls received isocaloric amount of diet; and (3) Duration: 10 wk	(1) ↑ hepatic TG, hepatic MDA, BAL in EtOH-treated overfed mice and (2) ↑ ALT in overfed mice; dose- dependent ↑ ALT by EtOH	(1) Steatosis, mononuclear cell infiltration in EtOH-treated (high dose) control mice; (2) Steatohepatitis and pericellular fibrosis in EtOH-treated (high dose) overfed mice; (3) ↑ macrophage infiltration in WAT in EtOH-treated overfed mice; and (4) No dif. in liver histology between EtOH-naïve overfed mice and controls	(1) ↑ M1 polarization markers (iNOS, TNFα) in liver and WAT for overfed-EtOH mice; (2) ↑ M2 markers (IL-10, ARG-1) in WAT, but ↓in liver for overfed- EtOH mice; (3) ↓ AdipoR, mitochondrial function genes (PGC-1α, PPARα, COX, cytochrome *c*, ACOX-1), in overfed-EtOH; (4) ↑ SREBP-1, ↓ pACC in EtOH; and (5) No effect on AMPK, PPARδ by overfeeding or EtOH

Results listed refer to experimental groups with concomitant metabolic syndrome risk factor and alcohol consumption compared to healthy or EtOH-naïve controls, unless stated otherwise. ACC: Acetyl-CoA carboxylase; ACOX: Acyl-CoA oxidase; AdipoR: Adiponectin receptor; ALT: Alanine aminotransferase; αSMA: Alpha smooth muscle actin; AUC: Area under the curve; ARG: Arginase; AST: Aspartate aminotransferase; BCL: B-cell lymphoma; BAX: BCL-2-associated X protein; BiP: Binding immunoglobulin protein; BAL: Blood alcohol level; CPT: Carnitine palmitoyltransferase; CHOP: C/EBP homologous protein; DGAT-2: Diacylglycerol O-acyltransferase 1; ER: Endoplasmic reticulum; EtOH: Ethanol; FA: Fatty acid; FASN: Fatty acid synthase; FAO: Fatty acid oxidation; FGF: Fibroblast growth factor; GTT: Glucose tolerance test; GSSG: Glutathione, oxidized; GSH: Glutathione, reduced; GPx: Glutathione peroxidases; GR: Glutathione reductase; GT: Glutathione transferase; H&E: Hematoxylin and eosin stain; HMOX: Heme oxygenase; HSP: Heat shock protein; HSC: Hepatic stellate cells; HCC: Hepatocellular carcinoma; HDL: High density lipoprotein; HFD: High-fat diet; HFHC: High-fat, high cholesterol diet; FFC: High-fat, high-fructose, high-cholesterol diet; 4-HNE: 4-hydroxynonenal; iNOS: Inducible nitric oxide synthase; IP3R1: Inositol trisphosphate receptor type 1; IR: Insulin receptor; IRS: Insulin receptor substrate; IFN: Interferon; IRF: Interferon regulatory factor; IL: Interleukin; iG: Intragastric; iP: Intraperitoneal; JNK: c-Jun N-terminal kinase; KHK: Ketohexokinase; LD: Lieber- DeCarli; LDL: Low density lipoprotein; MDA: Malondialdehyde; MMP: Matrix metallopeptidase; MCP: Monocyte chemoattractant protein; MUFA: Monounsaturated fatty acids; MyD88: Myeloid differentiation primary response 88; NOX: NADPH oxidase; NOX: NAFLD activity score; OLET: Otsuka Long-Evans Tokushima; OLETF: Otsuka Long-Evans Tokushima fatty; PLIN: Perilipin; PPAR: Peroxisome proliferator-activated receptor; PEPCK: Phosphoenolpyruvate carboxykinase; PAI-1: Plasminogen activator inhibitor 1; PUFA: Polyunsaturated fatty acids; PGC-1α: PPARγ coactivator 1 α; PHH: Primary human hepatocytes; Akt: Protein kinase B; SFA: Saturated fatty acids; SIRT-1: Sirtuin 1; SCD-1: Stearoyl-CoA desaturase 1; SREBP-1: Steroid response-element binding protein 1; SOD: Superoxide dismutase; TGFβ: Transforming growth factor β; TG: Triglycerides; TNFα: Tumor necrosis factor α; TRAF: TNF receptor associated factor; WAT: White adipose tissue; XBP-1: X-box binding protein 1.

the presence of necrotic hepatocytes, suggesting increased hepatic neutrophil infiltration. HFHC-EtOH with additional EtOH binge also upregulated collagen I, αSMA, and TIMP-1 compared to controls. Unlike the Gäbele study, EtOH also upregulated TLR-4 expression in HFHC-fed mice. Since OPN is associated with increased ALD severity[82], HFHC-EtOH diet was also given to OPN-knockout (KO) mice to determine the role of OPN in liver disease. HFHC-EtOH diet increased neutrophil infiltration, plasma ALT activity, and αSMA in OPN KO mice, suggesting

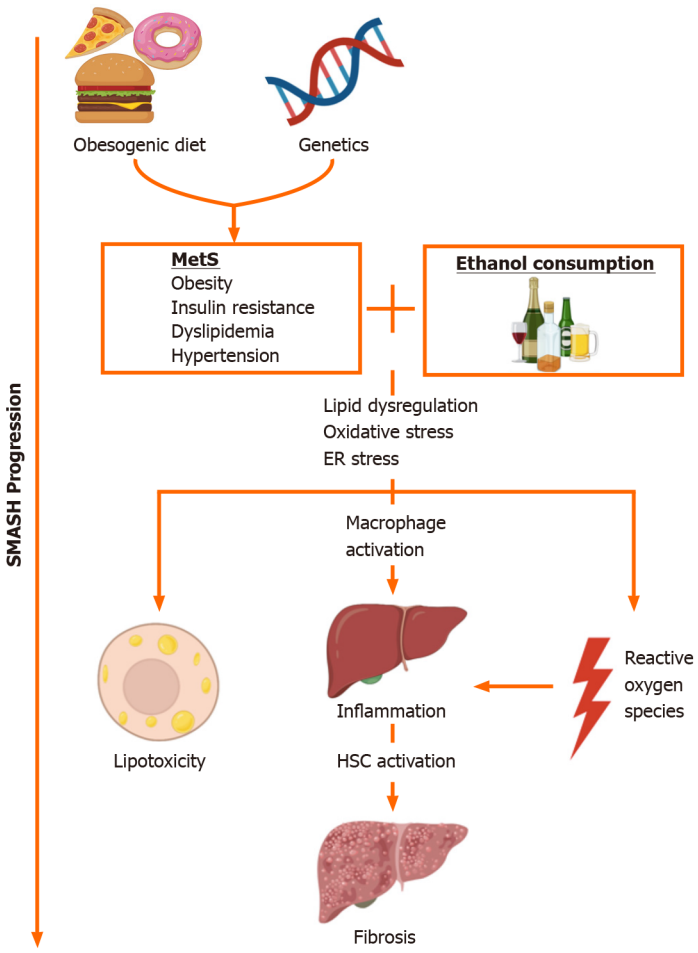

Figure 1 Pathogenesis and progression of the syndromes of metabolic and alcoholic steatohepatitis. Metabolic syndrome (MetS) is a cluster of factors–obesity, insulin resistance, hypertension, high triglyceride levels, and low high-density lipoproteins cholesterol levels–that arise from obesogenic diet and genetic factors. Coupled with heavy alcohol consumption, MetS promotes lipid dysregulation, oxidative stress, and endoplasmic reticulum stress. These biochemical processes reciprocally mediate each other and contribute to lipotoxic cellular dysfunction, immune response, inflammation, and fibrosis in syndromes of metabolic and alcoholic steatohepatitis.

that OPN plays a protective role in fatty liver disease. Similarly, Xu *et al*[83] overfed C57BL/6 mice HFD by iG infusion for 45 d, after which different dosages of EtOH was introduced for another 4 wk. Compared to controls, overfeeding and EtOH elevated hepatic TG levels, increased fibrosis, upregulated induced nitric oxide synthase (iNOS) activity, and induced the PERK and IRE-1 pathways. HFD and high-dose EtOH increased liver weight, hepatic TG levels, plasma adiponectin levels, ALT activity, and fibrosis compared to low-dose EtOH treatment. These results suggest that concomitant overfeeding and EtOH consumption induce fibrosis, oxidative stress, and ER stress. Furthermore, these results indicate that the effects of EtOH on NAFLD progression are dose-dependent, as evidenced by the differential effects on liver injury by low and high dose EtOH.

To recapitulate SMASH pathogenesis, EtOH is also coupled with other dietary models of NAFLD other than HFD. These other dietary models of SMASH are similar to the HFD-based models in that they induce lipid dysregulation, oxidative stress, apoptosis, and fibrosis. Alwahsh *et al*[84] fed Sprague-Dawley rats either control LD, fructose LD, EtOH LD, or combined fructose-EtOH LD diet for 28 d. EtOH and fructose independently elevated hepatic TG and cholesterol, and upregulated PPARα and carnitine palmitoyltransferase I (CPT-1) compared to controls. However, combined fructose-EtOH decreased cholesterol, and downregulated PPARα and CPT-1 compared to controls. Combined treatment also upregulated leptin receptor and acetyl-CoA carboxylase (ACC). This study suggests that in either NAFLD or ALD, PPARα compensates for the increase in lipid accumulation, but FAO capacity is diminished under concomitant in SMASH. Nieto *et al*[85] developed a model in which Lewis rats were administered a choline-deficient (CD) diet and multiple whiskey gavages. Compared to controls, CD-whiskey treatment elevated MDA and protein carbonyl levels, upregulated TNFα, collagen I, αSMA, and β-tubulin, increased

collagen deposition, and increased caspase-3 and caspase-8 activity. These results suggest that CD-whiskey induces oxidative stress, inflammation, and fibrosis. CD diet also downregulated BCL-XL, suggesting greater susceptibility to apoptosis, although whiskey did not affect its expression.

Genetic models of SMASH

Experimental rodent models of SMASH also employ genetic models of NAFLD coupled with EtOH consumption. One commonly used genetic mouse model is ob/ob leptin deficiency. For example, Robin *et al*[86] developed a model in which ob/ob mice were administered EtOH daily by gavage for 4 d. EtOH upregulated TNFα and heat shock protein 70 (HSP70) expression, increased caspase-3 activity, and downregulated NF-κB expression and activity in obese mice compared to controls. Treatment with TNFα inhibitor pentoxifylline attenuated these effects in EtOH-treated obese mice. These results suggest that combined multiple binge EtOH dysregulates TNFα signaling and induces hepatocellular apoptosis in genetic obesity. However, EtOH did not increase serum ALT in either lean or obese mice, suggesting that it does not contribute to acute liver injury in this model.

Everitt *et al*[87] also used ob/ob mice to determine the effect of polyunsaturated fatty acids (PUFA) and chronic EtOH on obesity. EtOH increased ALT/AST, TG and cholesterol levels, and AMPK expression in obese mice compared to controls. EtOH also downregulated SIRT-1 and SFRS-10, a SIRT-1 target. SFRS-10 modulates splicing for the transcription factor lipin 1, which has two isoforms: FA oxidizing lipin 1α and TG synthetic lipin 1β[88]. The decrease in SFRS-10 resulted in an upregulation of the β isoform, which is also seen in human obesity and *in vitro* models[89]. In PUFA-fed ob/ob mice, EtOH also upregulated PPARγ which regulates adipocyte differentiation, glucose homeostasis, lipogenesis, and lipid droplet formation[90]. Although PPARγ is not upregulated in NASH patients[91], increased PPARγ and lipin-1β in the Everitt model underscores the potential synergistic effects of obesogenic factors and EtOH on AMPK-mediated *de novo* lipogenesis in human disease.

Another genetic mouse model is KK-A^{y}, which induces obesity and hyperinsulinemia by dysregulating appetite suppression. Suzuki *et al*[92] fed KK-A^{y} mice control or 5% EtOH LD diet for 10 d, then administered a single 4 g/kg EtOH dose by gavage in a chronic-binge EtOH model. In obese mice, EtOH upregulated spliced and unspliced XBP-1, BIP, inositol trisphosphate receptor, and C/EBP homologous protein, and oxidative stress markers CYP2E1 and heme oxygenase 1 (HMOX-1). Treatment with the chemical chaperone 4-phenylbutyric acid decreased the aforementioned UPR genes, ALT/AST activity, and hepatic TG levels. These results suggest that EtOH induces the UPR, exacerbates ER stress, and promotes oxidative stress in genetic obesity. In another study from the same lab, Kitagawa *et al*[93] used a similar feeding regiment and found elevated serum LPS, and upregulated inflammatory cytokines TNFα, IL-1β, and interferon γ, and upregulated TLR-4. Furthermore, with regards to the small intestinal microbiota, EtOH decreased *Lactobacillales* and increased *Erysipelotrichales* in the KK-A^{y} mice. Treatment with rifaximin, an antibiotic, restored the *Erysipelotrichales* population and increased *Bacteroidales*, while restoring cytokine expression to basal levels.

In rat studies, one commonly used genetic model is the fa/fa Zucker rat. For example, Carmiel-Haggai *et al*[94] administered fa/fa Zucker rats multiple binges of 35% EtOH or saline over 3 days to determine the effect of concomitant genetic obesity and EtOH consumption on oxidative stress. In obese fa/fa rats, EtOH decreased basal GSH levels, increased GSSG levels, and upregulated CYP2E1 and iNOS compared to controls. EtOH also decreased SOD, catalase, and GR activity in obese rats, suggesting that EtOH exacerbates oxidative stress in obesity by straining antioxidant mechanisms. Another genetic rat model is the Otsuka Long Evans Tokushima Fatty (OLETF) rat, which is a cholecystokinin KO model that dysregulates appetite suppression[95]. Minato *et al*[96] administered lean OLET and obese OLETF rats 10% EtOH gavage every few days for 3 wk in a multiple binge EtOH model of SMASH. In obese rats, EtOH increased inflammation, CYP2E1 protein levels, TNFα expression, 4-HNE levels compared to controls. However, EtOH did not affect PPARγ expression or steatosis in OLETF rats compared to EtOH-naïve OLETF rats. These results suggest that while this model recapitulates inflammation and oxidative stress in SMASH, it does not feature lipid metabolism dysregulation.

Apparent alleviation of NAFLD/NASH by ethanol

Some experimental models that couple obesity and EtOH consumption do not induce severe liver injury, and instead show evidence for a possible protective effect by moderate EtOH consumption in NAFLD. The amount of alcohol that constitutes "mild

or moderate" (referred to as "moderate" hereafter) consumption is difficult to define, and there are varied definitions of moderate alcohol consumption in both humans and rodent models. In retrospective studies of NAFLD, moderate alcohol consumption is less than 20-40 g EtOH daily[97-99], although other studies define it as less than 2 alcoholic drinks per day[100]. Moderate alcohol consumption is associated with improved insulin sensitivity, decreased fibrosis, and improved cardiovascular outcomes in NAFLD/NASH patients[101-103], which is a significant finding because fibrosis is a major factor in NAFLD mortality[104]. However, the effects of BMI, insulin resistance, socioeconomic status, drinking pattern, or type of alcoholic beverage on human fatty liver disease have not been fully elucidated[103]. Nevertheless, there are rodent models that describe an apparent alleviation of NAFLD symptoms associated with moderate alcohol consumption. Moderate alcohol consumption is less rigorously defined for rodent models, although of the studies reviewed in this paper, those that model "moderate alcohol consumption" generally have less than a daily 5 g EtOH/kg body weight dosage for rodents[105-108].

Osaki *et al*[105] developed a model in which chronic consumption of 1%-2% v/v EtOH reduced blood markers for liver injury in HFD-fed Sprague-Dawley rats for 12 wk. EtOH did not affect body weight, liver mass, or adipose tissue mass, nor did it affect serum cholesterol, FFA, or TG levels. EtOH decreased serum ALT activity, lactate dehydrogenase, urate, and ammonia levels. In a similar study by Sun *et al*[107], a 4 g/kg EtOH binge by gavage downregulated expression of pro-inflammatory TNFα, CXCL-1, CXCL-2, and IL-1β, and pro- fibrotic αSMA, collagen, TGFβ, TIMP1, MMP2, and MMP9 in Sprague-Dawley rats fed HFHC for 12 wk. Using a genetic obesity model, Kanuri *et al*[106] determined the effect of chronic EtOH consumption on lipid storage and thrombosis. *Ad libitum* access to 2.5 g/kg EtOH was not found to affect TNFα, insulin receptor substrate (IRS)-1, or IRS-2 expression in ob/ob C57BL/6 mice. EtOH downregulated the expression of lipid droplet-associated proteins perilipin (PLIN) 2 and PLIN-3, suggesting decreased lipid accumulation due to EtOH. PLIN2 expression and lipid accumulation are known to be upregulated in ALD[109,110], but PLIN3 may instead play a protective role by facilitating lipid export from the ER[111]. Expression of pro-thrombotic PAI-1 was comparable between EtOH- treated ob/ob mice and control WT mice, despite upregulation of PAI-1 in EtOH-naïve ob/ob mice compared to WT.

Experimental animal studies have suggested the possible role of adiponectin signaling and sensitivity in apparent EtOH-mediated amelioration of NAFLD. For example, Bucher *et al*[112] found a decrease in serum adiponectin levels in C57BL/6 mice administered HFD and 10 g/kg/d EtOH in drinking water compared to mice fed HFD only. Decreased adiponectin in EtOH-treated mice accompanied lower serum TG and cholesterol levels, and downregulated collagen I, collagen III, and CYP2E1 expression. Similarly, Jung *et al*[108] found upregulated SIRT-1 and insulin receptor expression in high-fat, high-fructose, high-cholesterol-fed C57BL/6 mice administered pure EtOH or beer, compared to alcohol-naïve mice. Beer, but not pure EtOH, also upregulated adiponectin and adiponectin receptor 1 expression. In both of the aforementioned studies, AMPK activation by adiponectin suggests a possible compensatory effect in response to concomitant EtOH and lipid intake. However, the differential effects of beer and pure EtOH suggest that the alcohol-associated alleviation of fatty liver may instead be due to other components in alcoholic beverages. In an intervention study, serum adiponectin was elevated, although not significantly, in overweight (BMI ≥ 27 kg/m^2) adults who consumed 100 mL whiskey daily for 4 wk, compared to overweight adults who were asked to drink mineral water[24].

CONCLUSION

Various pre-clinical experimental models have been developed to study the interactive effects of NAFLD and ALD risk factors on hepatic injury resulting in SMASH. While each model differs in obesity etiology, as well as pattern and duration of alcohol consumption, they all demonstrate that obesity and heavy alcohol consumption synergistically contribute to hepatic injury. The models suggest that both sets of risk factors contribute to increased steatosis and fibrosis, as well as an M1-like phenotype in activated macrophages. There is also evidence that obesity and alcohol consumption synergistically interfere with antioxidant defense, but the effect of alcohol seems to be dose-dependent. Despite the advantages of these animal models, there are still limitations with regards to replicating what we understand from human disease.

New models should consider the effect of alcohol consumption patterns on fatty liver disease pathogenesis. For example, the highest risk group for ALD are

individuals who already drink heavily, then dramatically increase alcohol intake in a short period[113]. There are already models, such as the NIAAA model[75], that replicate chronic-binge alcohol consumption patterns in ALD. In the NIAAA model, mice are fed Lieber-DeCarli EtOH diet for 10 d and given EtOH gavage on the eleventh day, with a set of chronic-binge feedings that can repeated multiple times. However, repeated sets of chronic-binge feedings only slightly elevate ALT/AST levels compared to a single set, and does not result in liver fibrosis. Thus, future models should also induce advanced liver injury in the context of repeated chronic-binge alcohol consumption to fully recapitulate fatty liver disease in humans.

Furthermore, while most current experimental models use high-fat diets to induce obesity, future models should more closely replicate the diets that are composed of high-fat and high glycemic index foods that are commonly found in Western countries and have been identified as risk factors for NAFLD/NASH[114]. Fructose, in particular, is known to increase hepatic *de novo* lipogenesis and impair fatty acid oxidation in humans, and promote gut permeability in mice. Fructose also promotes insulin resistance in both the liver and skeletal muscle[115]. There are studies that model NAFLD progression that combine saturated fats, cholesterol, and fructose into a single diet[116,117], but the specific composition of fats and fructose source (*e.g.*, sucrose or high fructose corn syrup) varies between studies. Future experimental models should thus also determine the effect of fructose on multi-system lipid dysregulation, insulin resistance, and inflammation.

Animal studies are also limited in replicating the genetic factors for NAFLD and ALD. For example, genetic models for obesity and insulin resistance in mice include ob/ob (leptin), db/db (leptin receptor), and foz/foz (ALMS-1)[118]. These do not parallel genetic polymorphisms known to predispose humans to NAFLD/NASH. Human genetic predispositions to fatty liver disease include polymorphisms in PNPLA3, TM6SF2, GCKR, MBOAT7, HSD17B3, PPARγ, IRS-1, PLIN2, and adiponectin, among others[119-121]. Furthermore, different rodent strains may also have an inherent bias towards certain disease states. For example, TNFα and iNOS are upregulated in C57BL/6 mice compared to Balb/c mice, despite being administered the same diet. Likewise, ARG-1 is increased in Balb/c compared to C57BL/6[122]. C57BL/6 mice may thus have a bias towards M1 polarization; and Balb/c, to M2 polarization. Future studies should further compare the roles that different human polymorphisms play in fatty liver disease pathogenesis, while also controlling for possible bias in the animal model used.

Finally, further research is needed to determine the interaction between multiple factors in fatty liver disease pathogenesis. In the established "two-hit" model of NAFLD pathogenesis, lipid accumulation results in a cascade of other dysfunctions, such as inflammation and fibrogenesis. Meanwhile, in the competing "multi-hit" model, multiple factors, such as insulin resistance and gut microbiome dysregulation, along with lipid metabolism dysregulation, synergistically result in liver injury[123]. For example, approximately 70% of all patients with insulin resistance will develop NAFLD. To determine possible interactions or causal relationships between these factors and alcohol, future experimental models should monitor fatty liver disease progression over time.

The development of novel pre-clinical experimental models may help elucidate new mechanisms and the interactions between alcohol and metabolic abnormalities in fatty liver disease. Specifically, feeding regimens that better model food and alcohol consumption in patients with SMASH should be developed. These models should incorporate both chronic-binge alcohol consumption and Western diet and also consider how those dietary factors interact with human genetics.

REFERENCES

1 **Asrani SK**, Devarbhavi H, Eaton J, Kamath PS. Burden of liver diseases in the world. *J Hepatol* 2019; **70**: 151-171 [PMID: 30266282 DOI: 10.1016/j.jhep.2018.09.014]

2 **Rinella ME**. Nonalcoholic fatty liver disease: a systematic review. *JAMA* 2015; **313**: 2263-2273 [PMID: 26057287 DOI: 10.1001/jama.2015.5370]

3 **Younossi ZM**, Marchesini G, Pinto-Cortez H, Petta S. Epidemiology of Nonalcoholic Fatty Liver Disease and Nonalcoholic Steatohepatitis: Implications for Liver Transplantation. *Transplantation* 2019; **103**: 22-27 [PMID: 30335697 DOI: 10.1097/TP.0000000000002484]

4 **Marchesini G**, Brizi M, Bianchi G, Tomassetti S, Bugianesi E, Lenzi M, McCullough AJ, Natale S, Forlani G, Melchionda N. Nonalcoholic fatty liver disease: a feature of the metabolic syndrome. *Diabetes* 2001; **50**: 1844-1850 [PMID: 11473047 DOI: 10.2337/diabetes.50.8.1844]

5 **Chalasani N**, Gorski JC, Asghar MS, Asghar A, Foresman B, Hall SD, Crabb DW. Hepatic

cytochrome P450 2E1 activity in nondiabetic patients with nonalcoholic steatohepatitis. *Hepatology* 2003; **37**: 544-550 [PMID: 12601351 DOI: 10.1053/jhep.2003.50095]

6 **Naveau S**, Giraud V, Borotto E, Aubert A, Capron F, Chaput JC. Excess weight risk factor for alcoholic liver disease. *Hepatology* 1997; **25**: 108-111 [PMID: 8985274 DOI: 10.1002/hep.510250120]

7 **Hart CL**, Morrison DS, Batty GD, Mitchell RJ, Davey Smith G. Effect of body mass index and alcohol consumption on liver disease: analysis of data from two prospective cohort studies. *BMJ* 2010; **340**: c1240 [PMID: 20223873 DOI: 10.1136/bmj.c1240]

8 **Stepanova M**, Rafiq N, Younossi ZM. Components of metabolic syndrome are independent predictors of mortality in patients with chronic liver disease: a population-based study. *Gut* 2010; **59**: 1410-1415 [PMID: 20660697 DOI: 10.1136/gut.2010.213553]

9 **Raynard B**, Balian A, Fallik D, Capron F, Bedossa P, Chaput JC, Naveau S. Risk factors of fibrosis in alcohol-induced liver disease. *Hepatology* 2002; **35**: 635-638 [PMID: 11870378 DOI: 10.1053/jhep.2002.31782]

10 **Åberg F**, Puukka P, Salomaa V, Männistö S, Lundqvist A, Valsta L, Perola M, Jula A, Färkkilä M. Combined Effects of Alcohol and Metabolic Disorders in Patients With Chronic Liver Disease. *Clin Gastroenterol Hepatol* 2020; **18**: 995-997. e2 [PMID: 31255807 DOI: 10.1016/j.cgh.2019.06.036]

11 **Carr RM**, Correnti J. Insulin resistance in clinical and experimental alcoholic liver disease. *Ann N Y Acad Sci* 2015; **1353**: 1-20 [PMID: 25998863 DOI: 10.1111/nyas.12787]

12 **Lambert JE**, Ramos-Roman MA, Browning JD, Parks EJ. Increased de novo lipogenesis is a distinct characteristic of individuals with nonalcoholic fatty liver disease. *Gastroenterology* 2014; **146**: 726-735 [PMID: 24316260 DOI: 10.1053/j.gastro.2013.11.049]

13 **Mihaylova MM**, Shaw RJ. The AMPK signalling pathway coordinates cell growth, autophagy and metabolism. *Nat Cell Biol* 2011; **13**: 1016-1023 [PMID: 21892142 DOI: 10.1038/ncb2329]

14 **You M**, Matsumoto M, Pacold CM, Cho WK, Crabb DW. The role of AMP-activated protein kinase in the action of ethanol in the liver. *Gastroenterology* 2004; **127**: 1798-1808 [PMID: 15578517 DOI: 10.1053/j.gastro.2004.09.049]

15 **Smith BK**, Marcinko K, Desjardins EM, Lally JS, Ford RJ, Steinberg GR. Treatment of nonalcoholic fatty liver disease: role of AMPK. *Am J Physiol Endocrinol Metab* 2016; **311**: E730-E740 [PMID: 27577854 DOI: 10.1152/ajpendo.00225.2016]

16 **Jung EJ**, Kwon SW, Jung BH, Oh SH, Lee BH. Role of the AMPK/SREBP-1 pathway in the development of orotic acid-induced fatty liver. *J Lipid Res* 2011; **52**: 1617-1625 [PMID: 21757781 DOI: 10.1194/jlr.M015263]

17 **Kohjima M**, Higuchi N, Kato M, Kotoh K, Yoshimoto T, Fujino T, Yada M, Yada R, Harada N, Enjoji M, Takayanagi R, Nakamuta M. SREBP-1c, regulated by the insulin and AMPK signaling pathways, plays a role in nonalcoholic fatty liver disease. *Int J Mol Med* 2008; **21**: 507-511 [PMID: 18360697]

18 **Tang JJ**, Li JG, Qi W, Qiu WW, Li PS, Li BL, Song BL. Inhibition of SREBP by a small molecule, betulin, improves hyperlipidemia and insulin resistance and reduces atherosclerotic plaques. *Cell Metab* 2011; **13**: 44-56 [PMID: 21195348 DOI: 10.1016/j.cmet.2010.12.004]

19 **Pawlak M**, Lefebvre P, Staels B. Molecular mechanism of PPARα action and its impact on lipid metabolism, inflammation and fibrosis in non-alcoholic fatty liver disease. *J Hepatol* 2015; **62**: 720-733 [PMID: 25450203 DOI: 10.1016/j.jhep.2014.10.039]

20 **Schug TT**, Li X. Sirtuin 1 in lipid metabolism and obesity. *Ann Med* 2011; **43**: 198-211 [PMID: 21345154 DOI: 10.3109/07853890.2010.547211]

21 **Lin J**, Yang R, Tarr PT, Wu PH, Handschin C, Li S, Yang W, Pei L, Uldry M, Tontonoz P, Newgard CB, Spiegelman BM. Hyperlipidemic effects of dietary saturated fats mediated through PGC-1beta coactivation of SREBP. *Cell* 2005; **120**: 261-273 [PMID: 15680331 DOI: 10.1016/j.cell.2004.11.043]

22 **You M**, Liang X, Ajmo JM, Ness GC. Involvement of mammalian sirtuin 1 in the action of ethanol in the liver. *Am J Physiol Gastrointest Liver Physiol* 2008; **294**: G892-G898 [PMID: 18239056 DOI: 10.1152/ajpgi.00575.2007]

23 **Ipsen DH**, Lykkesfeldt J, Tveden-Nyborg P. Molecular mechanisms of hepatic lipid accumulation in non-alcoholic fatty liver disease. *Cell Mol Life Sci* 2018; **75**: 3313-3327 [PMID: 29936596 DOI: 10.1007/s00018-018-2860-6]

24 **Beulens JW**, van Loon LJ, Kok FJ, Pelsers M, Bobbert T, Spranger J, Helander A, Hendriks HF. The effect of moderate alcohol consumption on adiponectin oligomers and muscle oxidative capacity: a human intervention study. *Diabetologia* 2007; **50**: 1388-1392 [PMID: 17492425 DOI: 10.1007/s00125-007-0699-8]

25 **Bellanti F**, Villani R, Facciorusso A, Vendemiale G, Serviddio G. Lipid oxidation products in the pathogenesis of non-alcoholic steatohepatitis. *Free Radic Biol Med* 2017; **111**: 173-185 [PMID: 28109892 DOI: 10.1016/j.freeradbiomed.2017.01.023]

26 **Peter Guengerich F**, Avadhani NG. Roles of Cytochrome P450 in Metabolism of Ethanol and Carcinogens. *Adv Exp Med Biol* 2018; **1032**: 15-35 [PMID: 30362088 DOI: 10.1007/978-3-319-98788-0_2]

27 **Niemelä O**, Parkkila S, Juvonen RO, Viitala K, Gelboin HV, Pasanen M. Cytochromes P450 2A6, 2E1, and 3A and production of protein-aldehyde adducts in the liver of patients with alcoholic and non-alcoholic liver diseases. *J Hepatol* 2000; **33**: 893-901 [PMID: 11131450 DOI: 10.1016/s0168-8278(00)80120-8]

28 **Chen Y**, Han M, Matsumoto A, Wang Y, Thompson DC, Vasiliou V. Glutathione and Transsulfuration in Alcohol-Associated Tissue Injury and Carcinogenesis. *Adv Exp Med Biol* 2018; **1032**: 37-53 [PMID: 30362089 DOI: 10.1007/978-3-319-98788-0_3]

29 **Kamada Y**, Matsumoto H, Tamura S, Fukushima J, Kiso S, Fukui K, Igura T, Maeda N, Kihara S, Funahashi T, Matsuzawa Y, Shimomura I, Hayashi N. Hypoadiponectinemia accelerates hepatic tumor formation in a nonalcoholic steatohepatitis mouse model. *J Hepatol* 2007; **47**: 556-564 [PMID: 17459514 DOI: 10.1016/j.jhep.2007.03.020]

30 **Leclercq IA**, Field J, Enriquez A, Farrell GC, Robertson GR. Constitutive and inducible expression of hepatic CYP2E1 in leptin-deficient ob/ob mice. *Biochem Biophys Res Commun* 2000; **268**: 337-344 [PMID: 10679205 DOI: 10.1006/bbrc.2000.2125]

31 **Mahli A**, Thasler WE, Patsenker E, Müller S, Stickel F, Müller M, Seitz HK, Cederbaum AI, Hellerbrand C. Identification of cytochrome CYP2E1 as critical mediator of synergistic effects of alcohol and cellular lipid accumulation in hepatocytes in vitro. *Oncotarget* 2015; **6**: 41464-41478 [PMID: 26497211 DOI: 10.18632/oncotarget.6203]

32 **Ozgur R**, Uzilday B, Iwata Y, Koizumi N, Turkan I. Interplay between the unfolded protein response and reactive oxygen species: a dynamic duo. *J Exp Bot* 2018; **69**: 3333-3345 [PMID: 29415271 DOI: 10.1093/jxb/ery040]

33 **Liu X**, Green RM. Endoplasmic reticulum stress and liver diseases. *Liver Res* 2019; **3**: 55-64 [PMID: 32670671 DOI: 10.1016/j.livres.2019.01.002]

34 **Henkel A**, Green RM. The unfolded protein response in fatty liver disease. *Semin Liver Dis* 2013; **33**: 321-329 [PMID: 24222090 DOI: 10.1055/s-0033-1358522]

35 **Liu Z**, Lv Y, Zhao N, Guan G, Wang J. Protein kinase R-like ER kinase and its role in endoplasmic reticulum stress-decided cell fate. *Cell Death Dis* 2015; **6**: e1822 [PMID: 26225772 DOI: 10.1038/cddis.2015.183]

36 **Han J**, Kaufman RJ. The role of ER stress in lipid metabolism and lipotoxicity. *J Lipid Res* 2016; **57**: 1329-1338 [PMID: 27146479 DOI: 10.1194/jlr.R067595]

37 **Marí M**, Morales A, Colell A, García-Ruiz C, Fernández-Checa JC. Mitochondrial glutathione, a key survival antioxidant. *Antioxid Redox Signal* 2009; **11**: 2685-2700 [PMID: 19558212 DOI: 10.1089/ARS.2009.2695]

38 **He L**, He T, Farrar S, Ji L, Liu T, Ma X. Antioxidants Maintain Cellular Redox Homeostasis by Elimination of Reactive Oxygen Species. *Cell Physiol Biochem* 2017; **44**: 532-553 [PMID: 29145191 DOI: 10.1159/000485089]

39 **Weydert CJ**, Cullen JJ. Measurement of superoxide dismutase, catalase and glutathione peroxidase in cultured cells and tissue. *Nat Protoc* 2010; **5**: 51-66 [PMID: 20057381 DOI: 10.1038/nprot.2009.197]

40 **Moreno-Sánchez R**, Marín-Hernández Á, Gallardo-Pérez JC, Vázquez C, Rodríguez-Enríquez S, Saavedra E. Control of the NADPH supply and GSH recycling for oxidative stress management in hepatoma and liver mitochondria. *Biochim Biophys Acta Bioenerg* 2018; **1859**: 1138-1150 [PMID: 30053395 DOI: 10.1016/j.bbabio.2018.07.008]

41 **Świderska M**, Maciejczyk M, Zalewska A, Pogorzelska J, Flisiak R, Chabowski A. Oxidative stress biomarkers in the serum and plasma of patients with non-alcoholic fatty liver disease (NAFLD). Can plasma AGE be a marker of NAFLD? *Free Radic Res* 2019; **53**: 841-850 [PMID: 31234658 DOI: 10.1080/10715762.2019.1635691]

42 **Asghari S**, Hamedi-Shahraki S, Amirkhizi F. Systemic redox imbalance in patients with nonalcoholic fatty liver disease. *Eur J Clin Invest* 2020; **50**: e13211 [PMID: 32017057 DOI: 10.1111/eci.13211]

43 **Chien YW**, Chen YL, Peng HC, Hu JT, Yang SS, Yang SC. Impaired homocysteine metabolism in patients with alcoholic liver disease in Taiwan. *Alcohol* 2016; **54**: 33-37 [PMID: 27565754 DOI: 10.1016/j.alcohol.2016.06.002]

44 **Szuster-Ciesielska A**, Daniluk J, Kandefer-Szerszeń M. Oxidative stress in the blood of patients with alcohol-related liver cirrhosis. *Med Sci Monit* 2002; **8**: CR419-CR424 [PMID: 12070432]

45 **Bieghs V**, Trautwein C. Innate immune signaling and gut-liver interactions in non-alcoholic fatty liver disease. *Hepatobiliary Surg Nutr* 2014; **3**: 377-385 [PMID: 25568861 DOI: 10.3978/j.issn.2304-3881.2014.12.04]

46 **Byun JS**, Yi HS. Hepatic Immune Microenvironment in Alcoholic and Nonalcoholic Liver Disease. *Biomed Res Int* 2017; **2017**: 6862439 [PMID: 28852648 DOI: 10.1155/2017/6862439]

47 **Zhou D**, Huang C, Lin Z, Zhan S, Kong L, Fang C, Li J. Macrophage polarization and function with emphasis on the evolving roles of coordinated regulation of cellular signaling pathways. *Cell Signal* 2014; **26**: 192-197 [PMID: 24219909 DOI: 10.1016/j.cellsig.2013.11.004]

48 **Kitade H**, Chen G, Ni Y, Ota T. Nonalcoholic Fatty Liver Disease and Insulin Resistance: New Insights and Potential New Treatments. *Nutrients* 2017; **9** [PMID: 28420094 DOI: 10.3390/nu9040387]

49 **Park JW**, Jeong G, Kim SJ, Kim MK, Park SM. Predictors reflecting the pathological severity of non-alcoholic fatty liver disease: comprehensive study of clinical and immunohistochemical findings in younger Asian patients. *J Gastroenterol Hepatol* 2007; **22**: 491-497 [PMID: 17376039 DOI: 10.1111/j.1440-1746.2006.04758.x]

50 **De Vito R**, Alisi A, Masotti A, Ceccarelli S, Panera N, Citti A, Salata M, Valenti L, Feldstein AE, Nobili V. Markers of activated inflammatory cells correlate with severity of liver damage in children with nonalcoholic fatty liver disease. *Int J Mol Med* 2012; **30**: 49-56 [PMID: 22505182 DOI:

10.3892/ijmm.2012.965]
51 **Kazankov K**, Jørgensen SMD, Thomsen KL, Møller HJ, Vilstrup H, George J, Schuppan D, Grønbæk H. The role of macrophages in nonalcoholic fatty liver disease and nonalcoholic steatohepatitis. *Nat Rev Gastroenterol Hepatol* 2019; **16**: 145-159 [PMID: 30482910 DOI: 10.1038/s41575-018-0082-x]
52 **Hosseini N**, Shor J, Szabo G. Alcoholic Hepatitis: A Review. *Alcohol Alcohol* 2019; **54**: 408-416 [PMID: 31219169 DOI: 10.1093/alcalc/agz036]
53 **Xu R**, Huang H, Zhang Z, Wang FS. The role of neutrophils in the development of liver diseases. *Cell Mol Immunol* 2014; **11**: 224-231 [PMID: 24633014 DOI: 10.1038/cmi.2014.2]
54 **Gao B**, Bataller R. Alcoholic liver disease: pathogenesis and new therapeutic targets. *Gastroenterology* 2011; **141**: 1572-1585 [PMID: 21920463 DOI: 10.1053/j.gastro.2011.09.002]
55 **Alkhouri N**, Carter-Kent C, Feldstein AE. Apoptosis in nonalcoholic fatty liver disease: diagnostic and therapeutic implications. *Expert Rev Gastroenterol Hepatol* 2011; **5**: 201-212 [PMID: 21476915 DOI: 10.1586/egh.11.6]
56 **Youle RJ**, Strasser A. The BCL-2 protein family: opposing activities that mediate cell death. *Nat Rev Mol Cell Biol* 2008; **9**: 47-59 [PMID: 18097445 DOI: 10.1038/nrm2308]
57 **Yang YM**, Seki E. TNFα in liver fibrosis. *Curr Pathobiol Rep* 2015; **3**: 253-261 [PMID: 26726307 DOI: 10.1007/s40139-015-0093-z]
58 **Luedde T**, Schwabe RF. NF-κB in the liver--linking injury, fibrosis and hepatocellular carcinoma. *Nat Rev Gastroenterol Hepatol* 2011; **8**: 108-118 [PMID: 21293511 DOI: 10.1038/nrgastro.2010.213]
59 **Wallace MC**, Friedman SL, Mann DA. Emerging and disease-specific mechanisms of hepatic stellate cell activation. *Semin Liver Dis* 2015; **35**: 107-118 [PMID: 25974897 DOI: 10.1055/s-0035-1550060]
60 **Seki E**, Brenner DA. Recent advancement of molecular mechanisms of liver fibrosis. *J Hepatobiliary Pancreat Sci* 2015; **22**: 512-518 [PMID: 25869468 DOI: 10.1002/jhbp.245]
61 **Tsuchida T**, Friedman SL. Mechanisms of hepatic stellate cell activation. *Nat Rev Gastroenterol Hepatol* 2017; **14**: 397-411 [PMID: 28487545 DOI: 10.1038/nrgastro.2017.38]
62 **Sharifnia T**, Antoun J, Verriere TG, Suarez G, Wattacheril J, Wilson KT, Peek RM Jr, Abumrad NN, Flynn CR. Hepatic TLR4 signaling in obese NAFLD. *Am J Physiol Gastrointest Liver Physiol* 2015; **309**: G270-G278 [PMID: 26113297 DOI: 10.1152/ajpgi.00304.2014]
63 **Petrasek J**, Mandrekar P, Szabo G. Toll-like receptors in the pathogenesis of alcoholic liver disease. *Gastroenterol Res Pract* 2010; **2010** [PMID: 20827314 DOI: 10.1155/2010/710381]
64 **Yamada K**, Mizukoshi E, Seike T, Horii R, Kitahara M, Sunagozaka H, Arai K, Yamashita T, Honda M, Kaneko S. Light alcohol consumption has the potential to suppress hepatocellular injury and liver fibrosis in non-alcoholic fatty liver disease. *PLoS One* 2018; **13**: e0191026 [PMID: 29342182 DOI: 10.1371/journal.pone.0191026]
65 **Gandhi CR**. Hepatic stellate cell activation and pro-fibrogenic signals. *J Hepatol* 2017; **67**: 1104-1105 [PMID: 28939135 DOI: 10.1016/j.jhep.2017.06.001]
66 **Denk H**, Abuja PM, Zatloukal K. Animal models of NAFLD from the pathologist's point of view. *Biochim Biophys Acta Mol Basis Dis* 2019; **1865**: 929-942 [PMID: 29746920 DOI: 10.1016/j.bbadis.2018.04.024]
67 **Santhekadur PK**, Kumar DP, Sanyal AJ. Preclinical models of non-alcoholic fatty liver disease. *J Hepatol* 2018; **68**: 230-237 [PMID: 29128391 DOI: 10.1016/j.jhep.2017.10.031]
68 **Hebbard L**, George J. Animal models of nonalcoholic fatty liver disease. *Nat Rev Gastroenterol Hepatol* 2011; **8**: 35-44 [PMID: 21119613 DOI: 10.1038/nrgastro.2010.191]
69 **Sherriff JL**, O'Sullivan TA, Properzi C, Oddo JL, Adams LA. Choline, Its Potential Role in Nonalcoholic Fatty Liver Disease, and the Case for Human and Bacterial Genes. *Adv Nutr* 2016; **7**: 5-13 [PMID: 26773011 DOI: 10.3945/an.114.007955]
70 **Lau JK**, Zhang X, Yu J. Animal models of non-alcoholic fatty liver disease: current perspectives and recent advances. *J Pathol* 2017; **241**: 36-44 [PMID: 27757953 DOI: 10.1002/path.4829]
71 **Lieber CS**, DeCarli LM. Liquid diet technique of ethanol administration: 1989 update. *Alcohol Alcohol* 1989; **24**: 197-211 [PMID: 2667528]
72 **Tsukamoto H**, French SW, Benson N, Delgado G, Rao GA, Larkin EC, Largman C. Severe and progressive steatosis and focal necrosis in rat liver induced by continuous intragastric infusion of ethanol and low fat diet. *Hepatology* 1985; **5**: 224-232 [PMID: 3979954 DOI: 10.1002/hep.1840050212]
73 **French SW**, Miyamoto K, Tsukamoto H. Ethanol-induced hepatic fibrosis in the rat: role of the amount of dietary fat. *Alcohol Clin Exp Res* 1986; **10**: 13S-19S [PMID: 3544925 DOI: 10.1111/j.1530-0277.1986.tb05175.x]
74 **Ueno A**, Lazaro R, Wang PY, Higashiyama R, Machida K, Tsukamoto H. Mouse intragastric infusion (iG) model. *Nat Protoc* 2012; **7**: 771-781 [PMID: 22461066 DOI: 10.1038/nprot.2012.014]
75 **Bertola A**, Mathews S, Ki SH, Wang H, Gao B. Mouse model of chronic and binge ethanol feeding (the NIAAA model). *Nat Protoc* 2013; **8**: 627-637 [PMID: 23449255 DOI: 10.1038/nprot.2013.032]
76 **Mathews S**, Xu M, Wang H, Bertola A, Gao B. Animals models of gastrointestinal and liver diseases. Animal models of alcohol-induced liver disease: pathophysiology, translational relevance, and challenges. *Am J Physiol Gastrointest Liver Physiol* 2014; **306**: G819-G823 [PMID: 24699333 DOI: 10.1152/ajpgi.00041.2014]
77 **Gäbele E**, Dostert K, Dorn C, Patsenker E, Stickel F, Hellerbrand C. A new model of interactive

effects of alcohol and high-fat diet on hepatic fibrosis. *Alcohol Clin Exp Res* 2011; **35**: 1361-1367 [PMID: 21463337 DOI: 10.1111/j.1530-0277.2011.01472.x]

78 **Wang Y**, Seitz HK, Wang XD. Moderate alcohol consumption aggravates high-fat diet induced steatohepatitis in rats. *Alcohol Clin Exp Res* 2010; **34**: 567-573 [PMID: 20028348 DOI: 10.1111/j.1530-0277.2009.01122.x]

79 **Gopal T**, Kumar N, Perriotte-Olson C, Casey CA, Donohue TM Jr, Harris EN, Talmon G, Kabanov AV, Saraswathi V. Nanoformulated SOD1 ameliorates the combined NASH and alcohol-associated liver disease partly *via* regulating CYP2E1 expression in adipose tissue and liver. *Am J Physiol Gastrointest Liver Physiol* 2020; **318**: G428-G438 [PMID: 31928222 DOI: 10.1152/ajpgi.00217.2019]

80 **Duly AM**, Alani B, Huang EY, Yee C, Haber PS, McLennan SV, Seth D. Effect of multiple binge alcohol on diet-induced liver injury in a mouse model of obesity. *Nutr Diabetes* 2015; **5**: e154 [PMID: 25915743 DOI: 10.1038/nutd.2015.4]

81 **Lazaro R**, Wu R, Lee S, Zhu NL, Chen CL, French SW, Xu J, Machida K, Tsukamoto H. Osteopontin deficiency does not prevent but promotes alcoholic neutrophilic hepatitis in mice. *Hepatology* 2015; **61**: 129-140 [PMID: 25132354 DOI: 10.1002/hep.27383]

82 **Seth D**, Duly A, Kuo PC, McCaughan GW, Haber PS. Osteopontin is an important mediator of alcoholic liver disease *via* hepatic stellate cell activation. *World J Gastroenterol* 2014; **20**: 13088-13104 [PMID: 25278703 DOI: 10.3748/wjg.v20.i36.13088]

83 **Xu J**, Lai KKY, Verlinsky A, Lugea A, French SW, Cooper MP, Ji C, Tsukamoto H. Synergistic steatohepatitis by moderate obesity and alcohol in mice despite increased adiponectin and p-AMPK. *J Hepatol* 2011; **55**: 673-682 [PMID: 21256905 DOI: 10.1016/j.jhep.2010.12.034]

84 **Alwahsh SM**, Xu M, Schultze FC, Wilting J, Mihm S, Raddatz D, Ramadori G. Combination of alcohol and fructose exacerbates metabolic imbalance in terms of hepatic damage, dyslipidemia, and insulin resistance in rats. *PLoS One* 2014; **9**: e104220 [PMID: 25101998 DOI: 10.1371/journal.pone.0104220]

85 **Nieto N**, Rojkind M. Repeated whiskey binges promote liver injury in rats fed a choline-deficient diet. *J Hepatol* 2007; **46**: 330-339 [PMID: 17156887 DOI: 10.1016/j.jhep.2006.09.010]

86 **Robin MA**, Demeilliers C, Sutton A, Paradis V, Maisonneuve C, Dubois S, Poirel O, Lettéron P, Pessayre D, Fromenty B. Alcohol increases tumor necrosis factor alpha and decreases nuclear factor-kappab to activate hepatic apoptosis in genetically obese mice. *Hepatology* 2005; **42**: 1280-1290 [PMID: 16317704 DOI: 10.1002/hep.20949]

87 **Everitt H**, Hu M, Ajmo JM, Rogers CQ, Liang X, Zhang R, Yin H, Choi A, Bennett ES, You M. Ethanol administration exacerbates the abnormalities in hepatic lipid oxidation in genetically obese mice. *Am J Physiol Gastrointest Liver Physiol* 2013; **304**: G38-G47 [PMID: 23139221 DOI: 10.1152/ajpgi.00309.2012]

88 **Bi L**, Jiang Z, Zhou J. The role of lipin-1 in the pathogenesis of alcoholic fatty liver. *Alcohol Alcohol* 2015; **50**: 146-151 [PMID: 25595739 DOI: 10.1093/alcalc/agu102]

89 **Pihlajamäki J**, Lerin C, Itkonen P, Boes T, Floss T, Schroeder J, Dearie F, Crunkhorn S, Burak F, Jimenez-Chillaron JC, Kuulasmaa T, Miettinen P, Park PJ, Nasser I, Zhao Z, Zhang Z, Xu Y, Wurst W, Ren H, Morris AJ, Stamm S, Goldfine AB, Laakso M, Patti ME. Expression of the splicing factor gene SFRS10 is reduced in human obesity and contributes to enhanced lipogenesis. *Cell Metab* 2011; **14**: 208-218 [PMID: 21803291 DOI: 10.1016/j.cmet.2011.06.007]

90 **Lefterova MI**, Haakonsson AK, Lazar MA, Mandrup S. PPARγ and the global map of adipogenesis and beyond. *Trends Endocrinol Metab* 2014; **25**: 293-302 [PMID: 24793638 DOI: 10.1016/j.tem.2014.04.001]

91 **Gross B**, Pawlak M, Lefebvre P, Staels B. PPARs in obesity-induced T2DM, dyslipidaemia and NAFLD. *Nat Rev Endocrinol* 2017; **13**: 36-49 [PMID: 27636730 DOI: 10.1038/nrendo.2016.135]

92 **Suzuki M**, Kon K, Ikejima K, Arai K, Uchiyama A, Aoyama T, Yamashina S, Ueno T, Watanabe S. The Chemical Chaperone 4-Phenylbutyric Acid Prevents Alcohol-Induced Liver Injury in Obese KK-A^{y} Mice. *Alcohol Clin Exp Res* 2019; **43**: 617-627 [PMID: 30748014 DOI: 10.1111/acer.13982]

93 **Kitagawa R**, Kon K, Uchiyama A, Arai K, Yamashina S, Kuwahara-Arai K, Kirikae T, Ueno T, Ikejima K. Rifaximin prevents ethanol-induced liver injury in obese KK-A^{y} mice through modulation of small intestinal microbiota signature. *Am J Physiol Gastrointest Liver Physiol* 2019; **317**: G707-G715 [PMID: 31509430 DOI: 10.1152/ajpgi.00372.2018]

94 **Carmiel-Haggai M**, Cederbaum AI, Nieto N. Binge ethanol exposure increases liver injury in obese rats. *Gastroenterology* 2003; **125**: 1818-1833 [PMID: 14724834 DOI: 10.1053/j.gastro.2003.09.019]

95 **Moran TH**. Unraveling the obesity of OLETF rats. *Physiol Behav* 2008; **94**: 71-78 [PMID: 18190934 DOI: 10.1016/j.physbeh.2007.11.035]

96 **Minato T**, Tsutsumi M, Tsuchishima M, Hayashi N, Saito T, Matsue Y, Toshikuni N, Arisawa T, George J. Binge alcohol consumption aggravates oxidative stress and promotes pathogenesis of NASH from obesity-induced simple steatosis. *Mol Med* 2014; **20**: 490-502 [PMID: 25180626 DOI: 10.2119/molmed.2014.00048]

97 **Dunn W**, Sanyal AJ, Brunt EM, Unalp-Arida A, Donohue M, McCullough AJ, Schwimmer JB. Modest alcohol consumption is associated with decreased prevalence of steatohepatitis in patients with non-alcoholic fatty liver disease (NAFLD). *J Hepatol* 2012; **57**: 384-391 [PMID: 22521357 DOI: 10.1016/j.jhep.2012.03.024]

98 **Cotrim HP**, Freitas LA, Alves E, Almeida A, May DS, Caldwell S. Effects of light-to-moderate alcohol consumption on steatosis and steatohepatitis in severely obese patients. *Eur J Gastroenterol*

Hepatol 2009; **21**: 969-972 [PMID: 19194305 DOI: 10.1097/MEG.0b013e328328f3ec]
99 **Kwon HK**, Greenson JK, Conjeevaram HS. Effect of lifetime alcohol consumption on the histological severity of non-alcoholic fatty liver disease. *Liver Int* 2014; **34**: 129-135 [PMID: 23809459 DOI: 10.1111/liv.12230]
100 **Ascha MS**, Hanouneh IA, Lopez R, Tamimi TA, Feldstein AF, Zein NN. The incidence and risk factors of hepatocellular carcinoma in patients with nonalcoholic steatohepatitis. *Hepatology* 2010; **51**: 1972-1978 [PMID: 20209604 DOI: 10.1002/hep.23527]
101 **Hsu CC**, Kowdley KV. The Effects of Alcohol on Other Chronic Liver Diseases. *Clin Liver Dis* 2016; **20**: 581-594 [PMID: 27373618 DOI: 10.1016/j.cld.2016.02.013]
102 **Ajmera VH**, Terrault NA, Harrison SA. Is moderate alcohol use in nonalcoholic fatty liver disease good or bad? *Hepatology* 2017; **65**: 2090-2099 [PMID: 28100008 DOI: 10.1002/hep.29055]
103 **Weng G**, Dunn W. Effect of alcohol consumption on nonalcoholic fatty liver disease. *Transl Gastroenterol Hepatol* 2019; **4**: 70 [PMID: 31620652 DOI: 10.21037/tgh.2019.09.02]
104 **Hagström H**. Alcohol Consumption in Concomitant Liver Disease: How Much is Too Much? *Curr Hepatol Rep* 2017; **16**: 152-157 [PMID: 28706775 DOI: 10.1007/s11901-017-0343-0]
105 **Osaki A**, Okazaki Y, Kimoto A, Izu H, Kato N. Beneficial effect of a low dose of ethanol on liver function and serum urate in rats fed a high-fat diet. *J Nutr Sci Vitaminol (Tokyo)* 2014; **60**: 408-412 [PMID: 25866304 DOI: 10.3177/jnsv.60.408]
106 **Kanuri G**, Landmann M, Priebs J, Spruss A, Löscher M, Ziegenhardt D, Röhl C, Degen C, Bergheim I. Moderate alcohol consumption diminishes the development of non-alcoholic fatty liver disease (NAFLD) in ob/ob mice. *Eur J Nutr* 2016; **55**: 1153-1164 [PMID: 26003186 DOI: 10.1007/s00394-015-0929-7]
107 **Sun F**, Zhuang Z, Zhang D, Chen Y, Liu S, Gao N, Shi J, Wang B. Chronic moderate alcohol consumption relieves high-fat high-cholesterol diet-induced liver fibrosis in a rat model. *Clin Exp Pharmacol Physiol* 2018; **45**: 1046-1055 [PMID: 29851129 DOI: 10.1111/1440-1681.12976]
108 **Jung F**, Lippmann T, Brandt A, Jin CJ, Engstler AJ, Baumann A. Moderate consumption of fermented alcoholic beverages diminishes diet-induced non-alcoholic fatty liver disease through mechanisms involving hepatic adiponectin signaling in mice. *Eur J Nutr* 2020; **59**: 787-799 [PMID: 30879098 DOI: 10.1007/s00394-019-01945-2]
109 **Carr RM**, Dhir R, Yin X, Agarwal B, Ahima RS. Temporal effects of ethanol consumption on energy homeostasis, hepatic steatosis, and insulin sensitivity in mice. *Alcohol Clin Exp Res* 2013; **37**: 1091-1099 [PMID: 23398239 DOI: 10.1111/acer.12075]
110 **Carr RM**, Peralta G, Yin X, Ahima RS. Absence of perilipin 2 prevents hepatic steatosis, glucose intolerance and ceramide accumulation in alcohol-fed mice. *PLoS One* 2014; **9**: e97118 [PMID: 24831094 DOI: 10.1371/journal.pone.0097118]
111 **Jeon S**, Carr R. Alcohol effects on hepatic lipid metabolism. *J Lipid Res* 2020; **61**: 470-479 [PMID: 32029510 DOI: 10.1194/jlr.R119000547]
112 **Bucher S**, Begriche K, Catheline D, Trak-Smayra V, Tiaho F, Coulouarn C, Pinon G, Lagadic-Gossmann D, Rioux V, Fromenty B. Moderate chronic ethanol consumption exerts beneficial effects on nonalcoholic fatty liver in mice fed a high-fat diet: possible role of higher formation of triglycerides enriched in monounsaturated fatty acids. *Eur J Nutr* 2020; **59**: 1619-1632 [PMID: 31161349 DOI: 10.1007/s00394-019-02017-1]
113 **Choi G**, Runyon BA. Alcoholic hepatitis: a clinician's guide. *Clin Liver Dis* 2012; **16**: 371-385 [PMID: 22541704 DOI: 10.1016/j.cld.2012.03.015]
114 **Hosseini Z**, Whiting SJ, Vatanparast H. Current evidence on the association of the metabolic syndrome and dietary patterns in a global perspective. *Nutr Res Rev* 2016; **29**: 152-162 [PMID: 27955720 DOI: 10.1017/s095442241600007x]
115 **Weber KS**, Simon MC, Strassburger K, Markgraf DF, Buyken AE, Szendroedi J, Müssig K, Roden M; GDS Group. Habitual Fructose Intake Relates to Insulin Sensitivity and Fatty Liver Index in Recent-Onset Type 2 Diabetes Patients and Individuals without Diabetes. *Nutrients* 2018; **10** [PMID: 29914103 DOI: 10.3390/nu10060774]
116 **Dorn C**, Engelmann JC, Saugspier M, Koch A, Hartmann A, Müller M, Spang R, Bosserhoff A, Hellerbrand C. Increased expression of c-Jun in nonalcoholic fatty liver disease. *Lab Invest* 2014; **94**: 394-408 [PMID: 24492282 DOI: 10.1038/labinvest.2014.3]
117 **Ganz M**, Bukong TN, Csak T, Saha B, Park JK, Ambade A, Kodys K, Szabo G. Progression of non-alcoholic steatosis to steatohepatitis and fibrosis parallels cumulative accumulation of danger signals that promote inflammation and liver tumors in a high fat-cholesterol-sugar diet model in mice. *J Transl Med* 2015; **13**: 193 [PMID: 26077675 DOI: 10.1186/s12967-015-0552-7]
118 **Stephenson K**, Kennedy L, Hargrove L, Demieville J, Thomson J, Alpini G, Francis H. Updates on Dietary Models of Nonalcoholic Fatty Liver Disease: Current Studies and Insights. *Gene Expr* 2018; **18**: 5-17 [PMID: 29096730 DOI: 10.3727/105221617X15093707969658]
119 **Miyaaki H**, Nakao K. Significance of genetic polymorphisms in patients with nonalcoholic fatty liver disease. *Clin J Gastroenterol* 2017; **10**: 201-207 [PMID: 28290069 DOI: 10.1007/s12328-017-0732-5]
120 **Anstee QM**, Reeves HL, Kotsiliti E, Govaere O, Heikenwalder M. From NASH to HCC: current concepts and future challenges. *Nat Rev Gastroenterol Hepatol* 2019; **16**: 411-428 [PMID: 31028350 DOI: 10.1038/s41575-019-0145-7]
121 **Eslam M**, George J. Genetic contributions to NAFLD: leveraging shared genetics to uncover

systems biology. *Nat Rev Gastroenterol Hepatol* 2020; **17**: 40-52 [PMID: 31641249 DOI: 10.1038/s41575-019-0212-0]

122 **Maina V**, Sutti S, Locatelli I, Vidali M, Mombello C, Bozzola C, Albano E. Bias in macrophage activation pattern influences non-alcoholic steatohepatitis (NASH) in mice. *Clin Sci (Lond)* 2012; **122**: 545-553 [PMID: 22142284 DOI: 10.1042/CS20110366]

123 **Buzzetti E**, Pinzani M, Tsochatzis EA. The multiple-hit pathogenesis of non-alcoholic fatty liver disease (NAFLD). *Metabolism* 2016; **65**: 1038-1048 [PMID: 26823198 DOI: 10.1016/j.metabol.2015.12.012]

124 **Song M**, Chen T, Prough RA, Cave MC, McClain CJ. Chronic alcohol consumption causes liver injury in high-fructose-fed male mice through enhanced hepatic inflammatory response. *Alcohol Clin Exp Res* 2016; **40**: 518-528 [PMID: 26858005 DOI: 10.1111/acer.12994]

World Journal of Gastroenterology

Submit a Manuscript: https://www.f6publishing.com

World J Gastroenterol 2021 January 7; 27(1): 19-36

DOI: 10.3748/wjg.v27.i1.19

ISSN 1007-9327 (print) ISSN 2219-2840 (online)

REVIEW

Human hepatitis viruses-associated cutaneous and systemic vasculitis

Chrong-Reen Wang, Hung-Wen Tsai

ORCID number: Chrong-Reen Wang 0000-0001-9881-7024; Hung-Wen Tsai 0000-0001-9223-2535.

Author contributions: Wang CR designed the report and wrote the paper; Wang CR and Tsai HW collected and analyzed the clinical data.

Conflict-of-interest statement: The authors declare no conflicts of interest.

Manuscript source: Invited manuscript

Specialty type: Gastroenterology and hepatology

Country/Territory of origin: Taiwan

Peer-review report's scientific

Chrong-Reen Wang, Department of Internal Medicine, National Cheng Kung University Hospital, Tainan 70403, Taiwan

Hung-Wen Tsai, Department of Pathology, National Cheng Kung University Hospital, Tainan 70403, Taiwan

Corresponding author: Chrong-Reen Wang, MD, PhD, Department of Internal Medicine, National Cheng Kung University Hospital, No. 138 Sheng-Li Road, Tainan 70403, Taiwan. wangcr@mail.ncku.edu.tw

Abstract

Human hepatitis viruses (HHVs) include hepatitis A virus, hepatitis B virus (HBV), hepatitis C virus (HCV), hepatitis delta virus, and hepatitis E virus and can cause liver inflammation in their common human host. Usually, HHV is rapidly cleared by the immune system, following acute HHV invasion. The morbidities associated with hepatitis A virus and hepatitis E virus infection occur shortly after their intrusion, in the acute stage. Nevertheless, the viral infectious process can persist for a long period of time, especially in HBV and HCV infection, leading to chronic hepatitis and further progressing to hepatic cirrhosis and liver cancer. HHV infection brings about complications in other organs, and both acute and chronic hepatitis have been associated with clinical presentations outside the liver. Vascular involvement with cutaneous and systemic vasculitis is a well-known extrahepatic presentation; moreover, there is growing evidence for a possible causal relationship between viral pathogens and vasculitis. Except for hepatitis delta virus, other HHVs have participated in the etiopathogenesis of cutaneous and systemic vasculitis *via* different mechanisms, including direct viral invasion of vascular endothelial cells, immune complex-mediated vessel wall damage, and autoimmune responses with stimulation of autoreactive B-cells and impaired regulatory T-cells. Cryoglobulinemic vasculitis and polyarteritis nodosa are recognized for their association with chronic HHV infection. Although therapeutic guidelines for HHV-associated vasculitis have not yet been established, antiviral therapy should be initiated in HBV and HCV-related systemic vasculitis in addition to the use of corticosteroids. Plasma exchange and/or combined cyclophosphamide and corticosteroid therapy can be considered in patients with severe life-threatening vasculitis manifestations.

Key Words: Human hepatitis viruses; Hepatitis B virus; Hepatitis C virus; Cryoglobulinemic vasculitis; Polyarteritis nodosa; Antiviral therapy

quality classification
Grade A (Excellent): 0
Grade B (Very good): B, B
Grade C (Good): 0
Grade D (Fair): 0
Grade E (Poor): 0

Received: November 21, 2020
Peer-review started: November 21, 2020
First decision: December 17, 2020
Revised: December 19, 2020
Accepted: December 27, 2020
Article in press: December 27, 2020
Published online: January 7, 2021

P-Reviewer: Liang XS, Wang K
S-Editor: Zhang L
L-Editor: A
P-Editor: Ma YJ

Core Tip: The human hepatitis viruses (HHVs) hepatitis A virus, hepatitis B virus, hepatitis C virus, hepatitis delta virus, and hepatitis E virus can cause liver inflammation in their common human host. With the exception of hepatitis delta virus, all other HHVs can participate in the pathogenesis of cutaneous and systemic vasculitis *via* different mechanisms like direct viral invasion of vascular endothelial cells and immune complex-mediated vessel wall damage. Cryoglobulinemic vasculitis and polyarteritis nodosa are recognized for their association with chronic HHV infection. Antiviral therapy should be initiated in hepatitis B virus and hepatitis C virus-related systemic vasculitis.

Citation: Wang CR, Tsai HW. Human hepatitis viruses-associated cutaneous and systemic vasculitis. *World J Gastroenterol* 2021; 27(1): 19-36
URL: https://www.wjgnet.com/1007-9327/full/v27/i1/19.htm
DOI: https://dx.doi.org/10.3748/wjg.v27.i1.19

INTRODUCTION

Hepatocellular injury caused by acute or chronic inflammation of the liver is derived from adverse factors, including alcohol consumption, autoimmune response, drug use, steatosis, and viruses[1]. Hepatotropic viruses are known for their role in the etiology of viral hepatitis, and, from the public health perspective, the disease is associated with heavy health burden and higher annual mortality[2]. In addition to uncommon herpes viruses-related hepatitis due to Epstein-Barr virus, cytomegalovirus, and herpes simplex virus infection[3], human hepatitis viruses (HHVs) are the most common causes of acute and chronic hepatitis in their human host[4]. The discovery of HHV starts with clinical description of disease, antigen/antibody reaction establishment, virus-like particles visualization, and finally viral genomes sequencing[5]. Early experiments illustrated two types, infectious hepatitis and serum hepatitis[6]. Australia antigens in serum hepatitis yielded the detection of 42-nm Dane particles[7,8]. Subsequently, deoxyribonucleic acid (DNA) sequencing was performed and hepatitis B virus (HBV) was found[9]. Later, virus-like particles were observed in infectious hepatitis, and complementary DNA (cDNA) from hepatitis A virus (HAV) was sequenced[10,11]. Hepatitis C virus (HCV) was identified in non-A, non-B hepatitis patients receiving multiple transfusions[12], transmission to chimpanzees[13], and cDNA library screens[14]. Hepatitis delta virus (HDV), a HBV-associated virus[15], is a separate defective virus requiring the help of HBV for its infection[16]. After elucidating the hepatitis E virus (HEV) cDNA[17], an endemic non-A, non-B hepatitis[18], there are five members of HHVs[5].

Typically following HHV invasion into humans, there is rapid clearance of viruses by the host defense system, with a self-limiting disease course[4]. The morbidities associated with HAV and HEV infection, commonly transmitted *via* the fecal-oral route, occur shortly after their intrusion in the acute stage[19-21]. The infectious processes can persist for a long period of time in HBV, HCV, and HDV infection, progressing to chronic hepatitis and leading to liver fibrosis, irreversible cirrhosis, and hepatocellular carcinoma[22-24]. Table 1 summarizes and compares the common characteristics of the five HHV members[4,5,19-29].

EXTRAHEPATIC MANIFESTATIONS OF HUMAN HEPATITIS VIRUSES INFECTION

Although HHVs primarily affect hepatocytes, they can cause extrahepatic manifestations, with damage to other organs[30-34]. Both acute and chronic forms of viral hepatitis are associated with various clinical presentations outside of the liver, which may precede or follow hepatic dysfunction. The crucial pathogenic mechanism is caused by the immune responses against viral pathogens, with the deposition of immune complexes (IC) in targeted tissues.

Table 1 Common characteristics and comparative features in five members of human hepatitis viruses

	HAV	HBV	HCV	HDV[1]	HEV
Family; Genus	*Picornaviridae Hepatovirus*	*Hepadnavirida Orthohepadnavirus*	*Flaviviridae Hepacivirus*	*Deltaviridae Deltavirus*	*Hepeviridae Orthohepevirus*
Discovery[2]; Frequency	1983 Highest in AH	1979 Highest in CH	1989 Second in CH	1986 Less in CH	1990 Less in AH
Genome[3]; Length; Diameter[4]; Envelope[5]; Receptor	Linear ssRNA; 7500 nt; 27-32 nm; Quasi-envelope; Unknown	Circular dsDNA; 3200 nt; 42 nm; Envelope; NTCP, HSP	Linear ssRNA; 9600 nt; 55-65 nm; Envelope; CD81, SR-BI	Circular ssRNA; 1700 nt; 36-43 nm; Envelope; NTCP, HSP	Linear ssRNA; 7200 nt; 30-34 nm; Quasi-envelope; Unknown
Incubation; Age[6]; Course	14-30 d; Children; Acute	30-180 d; Any; Acute/chronic	14-180 d; Any; Acute/chronic	14-160 d; Any; Acute/chronic[7]	14-70 d; Adults; Acute
Route of spread	Enteric, sexual	Parental, sexual, vertical	Parental, sexual	Parental, sexual, vertical	Enteric, vertical, parenteral
Hepatitis diagnosis	Anti-HAV IgM	Anti-HBc IgM, HBs antigen, DNA by PCR	Anti-HCV IgG, RNA by PCR	Anti-HDV IgM, RNA by PCR	Anti-HEV IgM, RNA by PCR
Vaccine; Post-exp; Av agent	Available; Ig/vaccine; Not available	Available; Ig/vaccine; NA, IFN-α	Not available; Not effective; DAA agent	HBV vaccine; Not available; IFN-α	Available in China; Not available; Not available
FH[8]; LC/HCC; Prognosis[9]	Very rare; Nil; Full recovery	Very rare; Yes; Chronic carrier	Extremely rare; Yes; High carrier rate	Yes; Yes; Chronic carrier	Yes; Nil; Full recovery

[1]Co-infection/superinfection with hepatitis B virus.
[2]By cloning and sequencing.
[3]Partial dsRNA in hepatitis B virus.
[4]Diameter of virion.
[5]Quasi-envelop with internal protein rather than viral glycoprotein.
[6]Commonly affected age.
[7]Progress to chronicity in 80% superinfection/5% co-infection hepatitis B virus.
[8]Up to 20% in superinfection with hepatitis B virus and pregnant women.
[9]Poorer in hepatitis B virus superinfection with hepatitis delta virus and pregnant woman with hepatitis E virus. AH: Acute hepatitis; Av: Antiviral; CH: Chronic hepatitis; DAA: Direct-acting antiviral; DNA: Deoxyribonucleic acid; ds: Double-stranded; Post-exp: Post-exposure; FH: Fulminant hepatitis; HBc: Hepatitis B virus core antigen; HBs: Hepatitis B virus surface antigen; HCC: Hepatocellular carcinoma; HSP: Heparan sulfate proteoglycans; IFN: Interferon; Ig: Immunoglobulins; LC: Liver cirrhosis; NA: Nucleoside/nucleotide analogues; nt: Nucleotide; NTCP: Sodium taurocholate co-transporting polypeptide, PCR: Polymerase chain reaction; RNA: Ribonucleic acid; SR-BI: Scavenger receptor class B type I; ss: Single-stranded.

Extrahepatic manifestations with evanescent rash and transient arthralgia that develop in acute HAV infection are rare[35]. In the protracted clinical course with cholestasis or relapsing disease, cutaneous vasculitis and arthritis occur with a predilection for lower extremities[36-38], and usually there is spontaneous recovery after the clearance of HAV. Other infrequently observed presentations include glomerulonephritis, myocarditis, thrombocytopenia, and neurological complications like Guillain-Barre syndrome[20,32,39-41].

Acute HEV infection can be asymptomatic or manifest as fulminant hepatitis[21]. Neurological involvement is the most frequently encountered extrahepatic disorder, followed by hematological and gastrointestinal manifestations, possibly caused by autoimmune responses related to molecular mimicry[42,43]. Neuralgic amyotrophy and Guillain-Barre syndrome are two common neuromuscular disorders[44,45], and other uncommon presentations include mononeuritis multiplex, meningoradiculitis, and encephalitis[46-48]. Thrombocytopenia is a frequently identified hematological disorder[49,50], and pancreatitis is the most common gastrointestinal abnormality[51,52]. Myocarditis and glomerulonephritis are rarely observed complications[53,54]. Although there is evidence to support the treatment of HEV-related neurological manifestations with corticosteroids[42,55], the currently recommended therapy is plasma exchange and immune modulation with intravenous immunoglobulin[42,56].

Although extrahepatic manifestations exist with acute infection of all HHVs, such presentations are more commonly identified in HBV, with up to 20% occurrence[57]. Acute HBV infection is often subclinical and asymptomatic in around two-thirds of cases[58]. In the pre-icteric prodromal phase, there is serum sickness-like illness with arthritis and dermatitis due to the deposition of circulating IC composed of HBV surface (HBs) antigen and further activation of complements[59]. These manifestations are usually transient and are resolved after the onset of jaundice. Guillain-Barre syndrome has been reported to be associated with acute HBV infection, and both

plasma exchange and intravenous immunoglobulin are effective treatments[60], implying that there is autoimmune-mediated damage to the myelin sheath of peripheral nerves.

Owing to the availability of viral markers and our understanding of pathogenic pathways, extrahepatic manifestations of chronic HBV infection have been well-elucidated for a while[33,57]. The etiopathogenesis outside the liver in the chronic phase involves the deposition of IC comprised of HBs and/or HBe antigens, followed by the local activation of complement cascades and the recruitment of inflammatory cells[61]. Notably, higher viral load or persistent infection can promote the production of IC, leading to deposition at small or medium-sized arteries[62]. In addition, viral replication has been demonstrated in the endothelium of targeted vessels[63]. Taken together, both mechanisms suggest that inhibition of viral replication, either spontaneously or under antiviral therapy, can reduce extrahepatic manifestations. Up to one-fifth of victims with chronic HBV infection have morbidities outside the liver[61], and these are comprised of arthritis, glomerulonephritis, uveitis, peripheral neuropathy, Raynaud phenomenon, Sjögren syndrome, cutaneous vasculitis, and systemic vasculitis, including polyarteritis nodosa and cryogobulinemic vasculitis[57,62,64,65]. Since the administration of immunosuppressive agents increases the risk of additional hepatic HBV replication with worsening liver disease[61], the treatment of HBV-associated glomerulonephritis and vasculitis is mainly based on antiviral agents, interferon (IFN)-α or nucleoside/nucleotide analogues (NAs)[66-70].

In most cases, symptomatic manifestations are uncommon during acute HCV infection[71]. Extrahepatic presentations include arthralgia, myalgia, and rash[72]. Patients with HCV infection usually progress to chronic stage without recovery[71,72]. Nevertheless, antiviral therapy is highly effective for the acute infection, resulting in the clearance of HCV with sustained virological response (SVR)[72,73].

Persistent HCV infection is a leading cause of chronic liver disease[74]. Although essentially curable with direct-acting antiviral (DAA) therapy, only a portion of patients are diagnosed. Notably, extrahepatic manifestations occur in up to three-quarter of victims with chronic HCV infection[75], and cryoglobulinemia is the most frequently encountered presentation (in 40% to 60% of infected patients)[76]. Direct viral invasion and deposits of soluble IC are two pathogenic processes involved in the development of disease outside the liver[75,76]. The clinical presentations include arthralgia, myalgia, glomerulonephritis, Raynaud phenomenon, Sjögren's syndrome, Hashimoto's thyroiditis, Graves' disease, ulcerative keratitis, peripheral neuropathy, and cryoglobulinemia vasculitis[74-78]. Occasionally, extrahepatic-related autoimmune comorbidities such as cryoglobulinemia vasculitis can lead to the diagnosis of HCV infection[76]. Sustained eradication of HCV by IFN-α or DAA agents has shown to be beneficial for outcomes following these manifestations[78,79]. Notably, a prospective study with 9895 HCV-infected cases receiving DAA medications revealed that viral clearance is responsible for a significant decrease in HCV extrahepatic mortality[80].

VASCULITIS MANIFESTATION IN HUMAN HEPATITIS VIRUSES INFECTION

There is growing evidence demonstrating a causal relationship between viral pathogens and vasculitis. Except for HDV[24,25], other HHVs have been shown to participate in the etiopathogenesis of cutaneous and systemic vasculitis *via* different mechanisms, including direct viral invasion of vascular endothelium, IC-mediated vessel wall damage, and autoimmune responses with stimulation of autoreactive B-cells and impaired regulatory T cells[81-83].

Cutaneous leukocytoclastic vasculitis (CLV) rarely occurs during acute HAV infection, and it may resolve after the regression of hepatitis[36-38,84]. In chronic HBV infection, CLV is rarely observed, with an 1% incidence[62]. HBs antigen has been identified in affected skin lesions[85]. Notably, IFN-α therapy is effective against HBV-associated CLV[86]. The histopathological picture of HHV-triggered CLV shows relatively less eosinophils and lymphocytes compared with those in drug-induced CLV[81].

Acute HAV or HEV infection can induce Henoch-Schönlein purpura (referred to as HSP)[87-89], a systemic vasculitis caused by the widespread deposition of circulating immunoglobulin (Ig)A IC in small-sized blood vessels of skin, joint, lung, kidney, testis, gastrointestinal tract, and nervous system[90]. HAV- and HEV-related HSP usually have a spontaneous recovery. Owing to the defective liver catabolism of IgA IC with further tissue deposits, HSP occurs in HBV or HCV chronic liver diseases,

usually requiring antiviral and corticosteroid therapy[91-94].

Vascular involvement with systemic vasculitis in HHV infection is a recognized extrahepatic morbidity with potential life-threatening organ dysfunction[31,95]. Among them, cryoglobulinemic vasculitis and polyarteritis nodosa are well-known vascular comorbidities in HHV infection[96,97].

HUMAN HEPATITIS VIRUSES-ASSOCIATED CRYOGLOBULINEMIC VASCULITIS

Cryoglobulinemic vasculitis is caused by IC-mediated inflammation of small-sized blood vessels and is accompanied by the activation of complements[96]. Cryoglobulins are circulating antibodies that precipitate *in vitro* at temperatures less than 37 °C and dissolve after rewarming, and these are either Ig or a mixture of Ig and complement components[98]. Individuals with cryoglobulinemia may remain asymptomatic without clinical abnormalities[96,98]. A typical triad of purpura, arthralgia, and weakness associated with organic dysfunction and elevated levels of rheumatoid factor (RF) was defined as cryoglobulinemic disease in 1966 by Meltzer *et al*[99]. Based on the composition of Ig, cryoglobulinemia can be classified into type I with monoclonal Ig (usually IgM), type II with polyclonal IgG and monoclonal IgM RF, and type III with polyclonal IgG and polyclonal IgM RF[100]. Type I is an infrequently encountered subgroup and is only found in hematological malignancies[101], whereas mixed types II and III can be associated with viral hepatitis caused by HBV, most commonly observed with HCV, and rarely identified with HAV infection[96,102-104]. Despite the presence of cryoglobulins in up to 60% of chronic HCV patients, cryoglobulinemic vasculitis only appears in around 10% of cases[76]. In chronic HHV infection, envelope glycoproteins can help the virus enter intrahepatic and circulating B lymphocytes to produce Ig with RF activity, resulting in the generation of cryoglobulins and formation of IC with vascular wall deposition[105,106].

Recurrent palpable purpura with the characteristic histopathological finding of leukocytoclastic vasculitis is the most common clinical manifestation[107]. Other cutaneous presentations are ischemic ulcers, digital gangrene, and Raynaud's phenomenon. In Figure 1, the presence of leukocytoclastic vasculitis in biopsied skin lesions from a HCV-infected patient with cryoglobulinemia-associated purpura is shown. In addition, the presence of Meltzer triad was identified in most patients at the onset of disease[108], and skin, joint, kidney, and peripheral nerve are frequently affected organs in cryoglobulinemic vasculitis[96,108]. Renal involvement with membranoproliferative glomerulonephritis as the most common finding is associated with significant morbidity and even mortality[109]. HCV core protein and Ig are major components of IC and are distributed along the capillary walls of glomeruli[110]. Peripheral neuropathy with mononeuritis multiplex is commonly observed, which can be the first clinical manifestation[111]. Other rarely involved organs include the central nervous system, gastrointestinal tract, myocardium, and lung, and their involvement leads to the clinical presentations of impaired cognitive function, intestinal ischemia, hypertrophic cardiomyopathy, and diffuse alveolar hemorrhage[96,108,112-115].

Sporadic cases with cryoglobulinemic vasculitis, either in adults or children, have been observed during acute HAV infection[36,84,104,116,117]. These patients had biopsy-proven CLV plus arthritis or glomerulonephritis, and the use of corticosteroids were required to control these complications.

Based on clinical observations, the Meltzer triad had been regarded as an IC-mediated disease secondary to the HBV infection[118]. Since then, HBs antigen in biopsied vessel wall and HBs antigen/anti-HBs in circulating cryoprecipitates have been identified in cryoglobulinemic vasculitis[119]. A retrospective study from 913 cases with cryoglobulinemia demonstrated a HBs antigen positivity of 5.8%[120], whereas analyzed data from 231 patients with mixed cryoglobulinemia only revealed an HBV infection rate of 1.8%[107]. Nevertheless, HBV is among three common infectious etiologies in patients with cryoglobulinemia[108]. This virus is predominantly associated with type II cryoglobulinemia, and its common extrahepatic manifestations are purpura, arthralgia, and neuropathy[121]. Furthermore, compared to adults, children with symptomatic cryogobulinemia have a lower occurrence of HBV infection but higher frequencies of articular and cutaneous involvement[122]. Notably, the presence of HBs antigen represents one of the main independent predictors of mortality in cryogobulinemic vasculitis[70].

Accumulated evidence indicates that the use of NAs for viral suppression in HBV-related cryogobulinemic vasculitis can cause the disappearance of cryoglobulins,

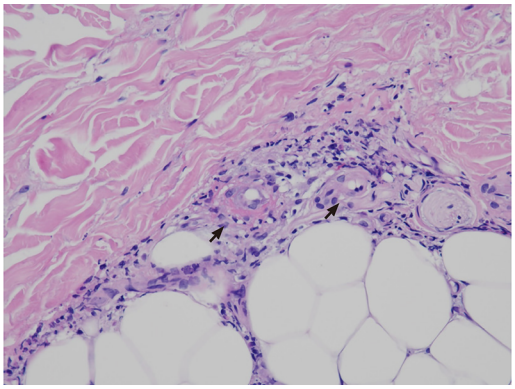

Figure 1 Cryoglobulinemic vasculitis. The small vessels show neutrophilic inflammation, with fibrinoid necrosis and fragmented neutrophil nuclei (black arrows). Hematoxylin and eosin staining, 400 ×.

normalize liver function, and significantly clinically improve most patients with mild disease, indicating a role for HBV replication in the pathogenesis[70,123]. Antiviral therapy with NAs should be a life-long prescription, and discontinuation is considered only after persistent HBs antigen loss with the seroconversion and undetectable HBV DNA[70,124]. Despite an observation with ineffective responses[70], IFN-α can be an alternative therapeutic modality[123]. The use of corticosteroids without NA therapy is ineffective for suppression of HBV viremia, resulting in refractory or relapsing disease[121]. Nevertheless, only a portion of patients with severe disease, including peripheral neuropathy and renal involvement, can achieve clinical regression under NA therapy[70,123,125]. CD20-positive B-cells are expanded and activated in mixed cryogobulinemia, and they participate in the production of cryoglobulins[126]. Clinical remission has been reported in patients with glomerulonephritis treated with NA in combination with rituximab, a monoclonal antibody against CD20 on the surface of B-cells[127,128]. Considering the risk of viral reactivation in patients with positive HBs or an occult infection with negative HBs and positive anti-HBc, prophylaxis with NAs should be initiated before the rituximab treatment[70,124,129]. Because of a potentially fatal complication, its use should be avoided during an active flare of HBV infection[70,130]. Prescription of this biologic as a second-line agent can be considered in patients with severe disease refractory to NA therapy[70,123].

Among the underlying diseases in cryoglobulinemia, HCV infection is the most common cause, with a 73% positive frequency of anti-HCV and a 86% occurrence of HCV ribonucleic acid[102,108,131]. Nevertheless, only a small portion of cryoglobulinemia with HCV infection develops significant vasculitis manifestations[96]. Similar to HBV infection, HCV is mainly associated with type II cryoglobulinemia[108]. The interaction of HCV envelope proteins with CD81 surface receptor can stimulate B-cells to expand clonally and produce monoclonal IgM RF that binds polyclonal anti-HCV core antigen, which suggests that cryoglobulinemia is due to host immune responses against HCV infection[132-134]. Although the HCV-related mixed cryoglobulinemia is a benign B-cell lymphoproliferative condition, chronic viral stimulation on the immune system leads to the selection of abnormal clones[135]. An epidemiological survey elucidated a link between HCV infection and B-cell non-Hodgkin's lymphoma (NHL)[135]. A large-scale cohort with 146394 HCV-infected patients demonstrated a more than 20% increased risk of this malignancy[136]. Furthermore, the overall risk of B-cell NHL in mixed cryoglobulinemia patients was estimated to be 35 times higher than that in the general population[137]. Collectively, these observations have indicated a pathogenic role of HCV in B-cell NHL.

Since HCV-related cryoglobulinemic vasculitis is an antigen-driven process and its activity usually correlates with viremia, the most effective treatment is the eradication of underlying viral infection[96]. Anti-HCV therapy can follow the existing guideline as cryoglobulinemia does not specifically influence the choice of antiviral drug[138]. DAA agents alone induce SVR with less adverse events and are more effective than the combined IFN-α and ribavirin regimen in cryoglobulinemic vasculitis[79]. In a prospective multicenter study carried out in these patients, all achieved SVR with a 90% complete clinical response after DAA therapy for 12 wk or more[139]. Altogether, patients with HCV-associated cryoglobulinemic vasculitis had higher SVR (74%-100%) and clinical remission (61%-100%) rates after receiving DAA medications[79]. Higher complete response rates (75%-100%) were observed in cutaneous and musculoskeletal

presentations, while lower responses (30%-70%) were identified in peripheral nerve and renal involvement[139]. In addition, DAA therapy is beneficial for HCV-associated B-cell malignancy, resulting in higher SVR and lymphoproliferative disease response rates in indolent NHL patients[140].

In addition to optimized DAA agents, corticosteroids in combination with cyclophosphamide are also considered as first-line therapy in severe fulminant manifestations, such as intestinal necrotizing vasculitis, rapid progressive glomerulonephritis, and diffuse alveolar hemorrhage[108,141]. Plasma exchange with warm apheresis solution to avoid cryoglobulin precipitation is an adjunct treatment that is useful in life-threatening disease by removing circulating cryoglobulins to interrupt the IC-mediated pathogenesis[141]. An earlier investigation showed that the addition of rituximab to the combined IFN-α and ribavirin regimen can enhance the clearance of cryoglobulins and shorten the time to clinical remission[142]. A subsequent randomized controlled trial in patients with severe disease revealed that rituximab monotherapy is as effective as conventional immunosuppressive treatment[143]. Despite the promise of rituximab as a therapeutic agent[144], there is a substantial risk for IC formation between this biologic and RF-positive IgM to exacerbate the vasculitis activity in HCV-associated type II cryoglobulinemic vasculitis[145].

HUMAN HEPATITIS VIRUSES-ASSOCIATED POLYARTERITIS NODOSA

Polyarteritis nodosa is a rare disease, with an annual incidence ranging from 0 to 2 cases per million population[97]. It is a necrotizing vasculitis affecting small- and medium-sized arteries, with systemic involvement but usually sparing the lungs. A skin-restricted form involving the area below the knees can progress to the systemic form, suggesting the same entity for both forms[146,147]. Most patients with polyarteritis nodosa belong to the idiopathic type with autoimmune-mediated mechanisms[97,148]. The secondary type is often observed in viral diseases, like cytomegalovirus, human immunodeficiency virus, and HHV infections. The association between HBV and polyarteritis nodosa was first recognized in 1970[149,150], and since then a substantial portion of cases have been identified after HBV infection. Later on, owing to the introduction of the vaccination protocol, the occurrence of HBV-related polyarteritis nodosa has gradually disappeared from clinical practice[151]. Although HCV positivity has been observed in this disorder, it is not a dominant etiological factor[152]. The occlusion and rupture of inflamed arteries can produce ischemia and hemorrhage in various organs and tissues, including skin, joint, kidney, testis, gastrointestinal tract, and peripheral nerve[97,148]. The most frequently involved organ system is the skin, presenting manifestations of palpable purpura, livedoid lesions, subcutaneous nodules, and necrotic ulcers[153]. Figure 2 demonstrates the histopathological findings of transmural necrotizing arteritis with neutrophilic infiltration and fibrinoid necrosis in a cutaneous biopsy specimen from a patient with polyarteritis nodosa-associated nodules (Case No. 2 in Table 2). Mononeuritis multiplex and symmetrical polyneuropathy are common neurological complications[154]. Gastrointestinal manifestations are usually associated with significant morbidity and can manifest as an acute surgical abdomen[155]. Renal involvement without glomerulonephritis is related to infarction or hemorrhage caused by the rupture of renal micro-aneurysms[97]. Although rare as an initial presentation, orchitis due to testicular ischemia is a characteristic finding of polyarteritis nodosa[156].

As supported by clinical evidence, the idiopathic type benefits from combined corticosteroids and cyclophosphamide therapy, which induce remission in severe disease with organ dysfunction; whereas, mild manifestations can be treated with corticosteroids alone[97,148]. After the completion of cyclophosphamide therapy, azathioprine or methotrexate can be prescribed as a remission-maintenance agent[97]. Currently, small-molecule targeted drugs and biologics have been used in refractory patients naïve to HBV infection with successful outcomes, including Janus kinase inhibitor, B-cell targeted agent, tumor necrosis factor blocker, and interleukin-6 blockade[157-161]. The clinical data and medication profiles with biologics in polyarteritis nodosa patients recently diagnosed by authors are shown in Table 2. Although poor prognosis in earlier years is due to a delayed diagnosis[97], the overall outcome has improved to a 5-year survival rate of 80%. Outcomes are significantly worsened in association with HBV infection, age above 65 years, new-onset hypertension, renal impairment with high creatinine levels, gastrointestinal involvement requiring surgery, and peripheral nerve involvement[153].

There are no available reports related to the association of polyarteritis nodosa with

Table 2 Clinical and medication profiles in five polyarteritis nodosa patients naïve to human hepatitis virus infection[1]

No	Age/sex	Initial symptom	Diagnosisperiod[2]	BVAS/FFS[3]	HHV status[4]	Follow-up manifestation	Therapy	Outcome
1	23/F	Arthralgia, rash[5]	2 mo	6/0	Negative	Joint, PN, skin	Az, Cs	Survival, remission
2	29/F	Arthralgia, fever, rash[5]	1 yr	11/0	Negative	FN, GI, joint, PN, skin	Az, Cs	Survival, remission
3	38/F	Fever, rash[5]	1 yr 5 mo	14/0	Negative	Joint, PN, skin	Az, Cs, Cy	Survival, remission
4	39/M	Rash	3 yr 10 mo	18/1	Negative	Kidney, skin	Az, Cs, RTX	Survival, chronic renal insufficiency
5	42/M	Arthralgia, rash	6 mo	7/0	Negative	Joint, PN, skin, kidney, testis	ADA, Az, Cs, Cy	Survival, remission

[1]Enrollment from 2012 to 2019.
[2]Time period from initial symptoms to the established diagnosis.
[3]Calculation at the disease diagnosis.
[4]Human hepatitis virus status, including examinations for hepatitis A virus, hepatitis B virus, hepatitis C virus, and hepatitis delta virus.
[5]Erythematous nodosum-like skin lesions. ADA: Adalimumab; Az: Azathioprine; BVAS: Birmingham vasculitis activity score; Cs: Corticosteroids, Cy: Cyclophosphamide; F: Female; FFS: Four-factor score, including age above 65 years, cardiac symptoms, gastrointestinal involvement, and renal insufficiency; FN: Foot necrosis; GI: Gastrointestinal; HHV: Human hepatitis virus; M: Male; PAN: Polyarteritis nodosa; PN: Peripheral neuropathy; RTX: Rituximab.

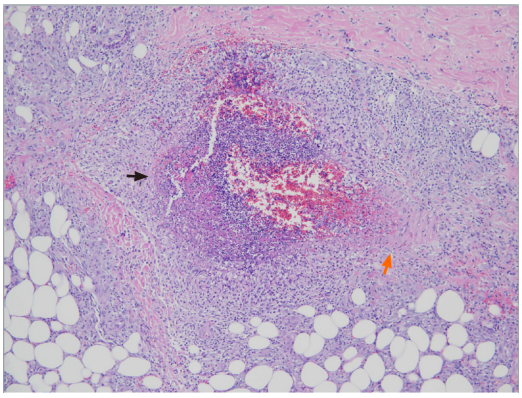

Figure 2 Polyarteritis nodosa. The vascular wall shows transmural necrotizing inflammation, with intense neutrophilic infiltration and fibrinoid necrosis (black arrow). There is residual muscular wall of the vessel (orange arrow). Hematoxylin and eosin staining, 100 ×.

HAV. Nevertheless, published cases with cutaneous or renal manifestations have shown histopathological evidence of medium-sized blood vessels' involvement compatible with the diagnosis of polyarteritis nodosa[162,163].

Simultaneous development of mixed cryoglobulinemia and polyarteritis nodosa has been documented in patients with coinfection of HCV and HBV[164,165]. In a clinical survey on polyarteritis nodosa, the positive frequency of anti-HCV was 20% (5% with detectable HCV ribonucleic acid and they were more likely to have cutaneous manifestation)[166]. In a large cohort with 161 cases of HCV-related vasculitis (19% polyarteritis nodosa and 81% cryoglobulinemic vasculitis), there were more acute and severe clinical presentations in the former group, including constitutional symptoms, new-onset hypertension, gastrointestinal tract involvement, and mononeuritis multiplex[167]. Despite no differences in the 5-year survival rates, there was a higher complete remission rate for polyarteritis nodosa than for cryoglobulinemic vasculitis. The therapeutic guidelines for HCV-related polyarteritis nodosa have not been established yet. Reported cases have received various combinations of corticosteroids, cyclophosphamide, and antiviral agents. B-cell targeted therapy has been applied to patients with HCV-related polyarteritis nodosa[167,168]. A higher clinical relapse rate was observed for rituximab treatment than for a combined regimen with IFN-α and ribavirin in this disease[167].

During the 1970s to 1980s, HBV was a major cause of polyarteritis nodosa, with

nearly half of cases having this infection, but the frequency has decreased due to improved blood safety and a viral vaccine campaign since early the 1990s, indicating HBV as a causal etiology[169]. Although histopathological studies have rarely confirmed the presence of HBV antigens in the vessel wall[151], the pathogenesis of HBV-related type is related to the deposits of IC, different from the idiopathic disease[169]. When comparing HBV- with HCV-associated polyarteritis nodosa[167,169], the former group has more general symptoms and orchitis, less cutaneous manifestation and new-onset hypertension, a lower survival rate, and a much shorter average period from viral infection to vasculitis development, 7 mo *vs* 20 years. In the HBV-related type, most cases have higher viral replication and HBV DNA levels, leading to the persistent presence of circulating IC[169].

The prevalence of HBs antigen in the general Taiwan population used to be near 20%, but the HBV seropositive rate in children has decreased dramatically from 11% to less than 1% after the initiation of the national vaccination program in 1984[170]. Despite a high inpatient prevalence with more than 10 cases per 100000 discharges in the United States[171], polyarteritis nodosa has been very rarely encountered by practicing physicians in Taiwan. In particular, even with more than 2 million infected patients, there is no reported association between HBV and polyarteritis nodosa[159,172-177]. Perinatal mother-to-infant HBV transmission is the most important factor responsible for a high carriage rate of HBs antigen in Taiwan[178]. Vertical transmission in infants is asymptomatic until adulthood and associated with a greater risk of chronic infection, suggesting that HBV infection causes an immunotolerant status in children who are less prone to develop full immune responses[179]. Parenteral HBV infection during adult life can induce polyarteritis nodosa within 1 year after viral infection, indicating an early post-infectious disease *via* this transmission route[169]. In Table 3, polyarteritis nodosa from various larger-number case series with different HBV-associated frequencies is compared[153,172-177,180-184]. Patients reported from Taiwan have no HBV infection, younger female predominance, and more cutaneous or testicular manifestation than those from other series with a HBV association.

After initial therapy with corticosteroids to reduce acute vascular inflammation, the therapeutic approach in HBV-associated polyarteritis nodosa is to clear circulating IC and suppress HBV replication by plasma exchange and antiviral agents with NAs or IFN-α[169]. Since the addition of cyclophosphamide to corticosteroids has shown to benefit patients presenting with poor prognostic factors[185], this regimen can be considered in patients with severe disease. Notably, plasma exchange has not been shown to be beneficial in polyarteritis nodosa patients without HBV infection[186]. Furthermore, antiviral agents can be used concurrently with corticosteroids or combined cyclophosphamide and corticosteroids therapy[97,148]. Contradictory to the idiopathic disease, relapses have rarely been observed in HBV-related type, especially when viral replication has ceased and seroconversion from HBe antigen to antibody has been achieved after antiviral therapy[148,169].

CONCLUSION

Although HHVs primarily affect hepatocytes, they can also cause complications in other organs, and both acute and chronic viral hepatitis are associated with clinical presentations outside the liver. Vascular involvement with cutaneous and systemic vasculitis is a well-known extrahepatic morbidity. There is growing evidence suggesting a causal relationship between viral pathogens and vasculitis. Except for HDV, other HHVs have participated in the etiopathogenesis of cutaneous and systemic vasculitis *via* different mechanisms, including direct viral invasion of vascular endothelial cells, IC-mediated vessel wall damage, and autoimmune responses with stimulation of autoreactive B-cells and impaired regulatory T cells. Cryoglobulinemic vasculitis and polyarteritis nodosa are recognized for their association with chronic HHV infection. Therapeutic guidelines for HHV-associated vasculitis have not been established yet. Antiviral therapy should be initiated in HBV and HCV-related systemic vasculitis in addition to the use of corticosteroids. Plasma exchange and/or combined cyclophosphamide and corticosteroid therapy can be considered in patients with severe life-threatening vasculitis manifestations.

Table 3 Comparisons of clinical and outcome profiles in polyarteritis nodosa from various case series with different hepatitis B virus-infected frequencies

Source of cases	No/age[1] F%	HBV status	Fever	AM	Skin	PN	GI	Renal	TestisM%	Therapy	Death
Taiwan	12/31, 67%	0%	67%	58%	75%	42%	50%	75%	50%	Az, Cs, Cy, Bio	33%
United Kingdom	17/49, 24%	31%	76%	77%	65%	59%	65%	77%	NA	Cs, Is	38%
United States	53/54, 34%	11%	31%	55%	58%	60%	25%	66%	NA	Cs, Cy	42%
Canada	45/54, 47%	19%	63%	51%	44%	51%	53%	44%	4%	Cs, Cy	53%
South Korea	27/47, 37%	56%	52%	30%	44%	63%	48%	48%	24%	Az, Cs, Cy, Is	15%
France	348/51,37%	35%	64%	59%	50%	74%	38%	51%	17%	Av, Cs, Cy, Is	25%
India	27/38, 26%	26%	52%	37%	37%	82%	30%	59%	30%	Av, Az, Cs, Cy	11%

[1]Mean age at disease diagnosis. AM: Articulomuscular; Az: Azathioprine; Av: Antiviral agent; Bio: Biologics; Cs: Corticosteroids; Cy: Cyclophosphamide; F: Female; GI: Gastrointestinal; Is: Immunosuppressive agent, M: Male; NA: Not available; PN: Peripheral neuropathy.

ACKNOWLEDGEMENTS

The authors are indebted to Dr. Wu IC, Division of Gastroenterology and Hepatology, for his valuable comments on HHV-related clinical manifestations, and to other physicians at the National Cheng Kung University Hospital involved in the diagnosis and management of reported patients. The Institutional Review Board of National Cheng Kung University Hospital approved this study (No. B-ER-105-108).

REFERENCES

1 **Arroyo V**, Moreau R, Jalan R. Acute-on-Chronic Liver Failure. *N Engl J Med* 2020; **382**: 2137-2145 [PMID: 32459924 DOI: 10.1056/NEJMra1914900]
2 **Razavi H**. Global Epidemiology of Viral Hepatitis. *Gastroenterol Clin North Am* 2020; **49**: 179-189 [PMID: 32389357 DOI: 10.1016/j.gtc.2020.01.001]
3 **Noor A**, Panwala A, Forouhar F, Wu GY. Hepatitis caused by herpes viruses: A review. *J Dig Dis* 2018; **19**: 446-455 [PMID: 29923691 DOI: 10.1111/1751-2980.12640]
4 **Rasche A**, Sander AL, Corman VM, Drexler JF. Evolutionary biology of human hepatitis viruses. *J Hepatol* 2019; **70**: 501-520 [PMID: 30472320 DOI: 10.1016/j.jhep.2018.11.010]
5 **Khuroo MS**, Sofi AA. The Discovery of Hepatitis Viruses: Agents and Disease. *J Clin Exp Hepatol* 2020; **10**: 391-401 [PMID: 32655240 DOI: 10.1016/j.jceh.2020.04.006]
6 **Krugman S**, Giles JP, Hammond J. Infectious hepatitis. Evidence for two distinctive clinical, epidemiological, and immunological types of infection. *JAMA* 1967; **200**: 365-373 [PMID: 4164595 DOI: 10.1001/jama.200.5.365]
7 **BLUMBERG BS**, ALTER HJ, VISNICH S. A "NEW" ANTIGEN IN LEUKEMIA SERA. *JAMA* 1965; **191**: 541-546 [PMID: 14239025 DOI: 10.1001/jama.1965.03080070025007]
8 **Dane DS**, Cameron CH, Briggs M. Virus-like particles in serum of patients with Australia-antigen-associated hepatitis. *Lancet* 1970; **1**: 695-698 [PMID: 4190997 DOI: 10.1016/s0140-6736(70)90926-8]
9 **Burrell CJ**, Mackay P, Greenaway PJ, Hofschneider PH, Murray K. Expression in Escherichia coli of hepatitis B virus DNA sequences cloned in plasmid pBR322. *Nature* 1979; **279**: 43-47 [PMID: 377093 DOI: 10.1038/279043a0]
10 **Koff RS**. Feinstone SM, Kapikian AZ, Purcell RH. Hepatitis A: detection by immune electron microscopy of a virus like antigen associated with acute illness [Science 1973;182:1026-1028]. *J Hepatol* 2002; **37**: 2-6 [PMID: 12076855 DOI: 10.1016/s0168-8278(02)00169-1]
11 **Ticehurst JR**, Racaniello VR, Baroudy BM, Baltimore D, Purcell RH, Feinstone SM. Molecular cloning and characterization of hepatitis A virus cDNA. *Proc Natl Acad Sci USA* 1983; **80**: 5885-5889 [PMID: 6310601 DOI: 10.1073/pnas.80.19.5885]
12 **Alter HJ**, Holland PV, Morrow AG, Purcell RH, Feinstone SM, Moritsugu Y. Clinical and serological analysis of transfusion-associated hepatitis. *Lancet* 1975; **2**: 838-841 [PMID: 53329 DOI: 10.1016/s0140-6736(75)90234-2]
13 **Alter HJ**, Purcell RH, Holland PV, Popper H. Transmissible agent in non-A, non-B hepatitis. *Lancet* 1978; **1**: 459-463 [PMID: 76017 DOI: 10.1016/s0140-6736(78)90131-9]

14 **Choo QL**, Kuo G, Weiner AJ, Overby LR, Bradley DW, Houghton M. Isolation of a cDNA clone derived from a blood-borne non-A, non-B viral hepatitis genome. *Science* 1989; **244**: 359-362 [PMID: 2523562 DOI: 10.1126/science.2523562]

15 **Rizzetto M**, Canese MG, Aricò S, Crivelli O, Trepo C, Bonino F, Verme G. Immunofluorescence detection of new antigen-antibody system (delta/anti-delta) associated to hepatitis B virus in liver and in serum of HBsAg carriers. *Gut* 1977; **18**: 997-1003 [PMID: 75123 DOI: 10.1136/gut.18.12.997]

16 **Rizzetto M**, Hoyer B, Canese MG, Shih JW, Purcell RH, Gerin JL. delta Agent: association of delta antigen with hepatitis B surface antigen and RNA in serum of delta-infected chimpanzees. *Proc Natl Acad Sci USA* 1980; **77**: 6124-6128 [PMID: 6934539 DOI: 10.1073/pnas.77.10.6124]

17 **Khuroo MS**. Study of an epidemic of non-A, non-B hepatitis. Possibility of another human hepatitis virus distinct from post-transfusion non-A, non-B type. *Am J Med* 1980; **68**: 818-824 [PMID: 6770682 DOI: 10.1016/0002-9343(80)90200-4]

18 **Reyes GR**, Purdy MA, Kim JP, Luk KC, Young LM, Fry KE, Bradley DW. Isolation of a cDNA from the virus responsible for enterically transmitted non-A, non-B hepatitis. *Science* 1990; **247**: 1335-1339 [PMID: 2107574 DOI: 10.1126/science.2107574]

19 **Hofmeister MG**, Foster MA, Teshale EH. Epidemiology and Transmission of Hepatitis A Virus and Hepatitis E Virus Infections in the United States. *Cold Spring Harb Perspect Med* 2019; **9** [PMID: 29712684 DOI: 10.1101/cshperspect.a033431]

20 **Abutaleb A**, Kottilil S. Hepatitis A: Epidemiology, Natural History, Unusual Clinical Manifestations, and Prevention. *Gastroenterol Clin North Am* 2020; **49**: 191-199 [PMID: 32389358 DOI: 10.1016/j.gtc.2020.01.002]

21 **Aslan AT**, Balaban HY. Hepatitis E virus: Epidemiology, diagnosis, clinical manifestations, and treatment. *World J Gastroenterol* 2020; **26**: 5543-5560 [PMID: 33071523 DOI: 10.3748/wjg.v26.i37.5543]

22 **Yuen MF**, Chen DS, Dusheiko GM, Janssen HLA, Lau DTY, Locarnini SA, Peters MG, Lai CL. Hepatitis B virus infection. *Nat Rev Dis Primers* 2018; **4**: 18035 [PMID: 29877316 DOI: 10.1038/nrdp.2018.35]

23 **Kaplan DE**. Hepatitis C Virus. *Ann Intern Med* 2020; **173**: ITC33-ITC48 [PMID: 32866406 DOI: 10.7326/AITC202009010]

24 **Gilman C**, Heller T, Koh C. Chronic hepatitis delta: A state-of-the-art review and new therapies. *World J Gastroenterol* 2019; **25**: 4580-4597 [PMID: 31528088 DOI: 10.3748/wjg.v25.i32.4580]

25 **Taylor JM**. Infection by Hepatitis Delta Virus. *Viruses* 2020; **12** [PMID: 32560053 DOI: 10.3390/v12060648]

26 **Feng Z**, Hirai-Yuki A, McKnight KL, Lemon SM. Naked Viruses That Aren't Always Naked: Quasi-Enveloped Agents of Acute Hepatitis. *Annu Rev Virol* 2014; **1**: 539-560 [PMID: 26958733 DOI: 10.1146/annurev-virology-031413-085359]

27 **Cheung A**, Kwo P. Viral Hepatitis Other than A, B, and C: Evaluation and Management. *Clin Liver Dis* 2020; **24**: 405-419 [PMID: 32620280 DOI: 10.1016/j.cld.2020.04.008]

28 **Cao Y**, Bing Z, Guan S, Zhang Z, Wang X. Development of new hepatitis E vaccines. *Hum Vaccin Immunother* 2018; **14**: 2254-2262 [PMID: 29708836 DOI: 10.1080/21645515.2018.1469591]

29 **World Health Organization**. Hepatitis 2020. https://www.who.int/health-topics/hepatitis#tab=tab_1

30 **Schiff ER**. Atypical clinical manifestations of hepatitis A. *Vaccine* 1992; **10** Suppl 1: S18-S20 [PMID: 1475999 DOI: 10.1016/0264-410x(92)90534-q]

31 **Pyrsopoulos NT**, Reddy KR. Extrahepatic manifestations of chronic viral hepatitis. *Curr Gastroenterol Rep* 2001; **3**: 71-78 [PMID: 11177698 DOI: 10.1007/s11894-001-0044-1]

32 **Amarapurkar DN**, Amarapurkar AD. Extrahepatic manifestations of viral hepatitis. *Ann Hepatol* 2002; **1**: 192-195 [PMID: 15280806]

33 **Han SH**. Extrahepatic manifestations of chronic hepatitis B. *Clin Liver Dis* 2004; **8**: 403-418 [PMID: 15481347 DOI: 10.1016/j.cld.2004.02.003]

34 **Romano C**, Cuomo G, Ferrara R, Del Mastro A, Esposito S, Sellitto A, Adinolfi LE. Uncommon immune-mediated extrahepatic manifestations of HCV infection. *Expert Rev Clin Immunol* 2018; **14**: 1089-1099 [PMID: 30338718 DOI: 10.1080/1744666X.2018.1538790]

35 **Shin EC**, Jeong SH. Natural History, Clinical Manifestations, and Pathogenesis of Hepatitis A. *Cold Spring Harb Perspect Med* 2018; **8** [PMID: 29440324 DOI: 10.1101/cshperspect.a031708]

36 **Inman RD**, Hodge M, Johnston ME, Wright J, Heathcote J. Arthritis, vasculitis, and cryoglobulinemia associated with relapsing hepatitis A virus infection. *Ann Intern Med* 1986; **105**: 700-703 [PMID: 3021038 DOI: 10.7326/0003-4819-105-5-700]

37 **Ilan Y**, Hillman M, Oren R, Zlotogorski A, Shouval D. Vasculitis and cryoglobulinemia associated with persisting cholestatic hepatitis A virus infection. *Am J Gastroenterol* 1990; **85**: 586-587 [PMID: 2337062]

38 **Dan M**, Yaniv R. Cholestatic hepatitis, cutaneous vasculitis, and vascular deposits of immunoglobulin M and complement associated with hepatitis A virus infection. *Am J Med* 1990; **89**: 103-104 [PMID: 2368780 DOI: 10.1016/0002-9343(90)90107-o]

39 **Shenoy R**, Nair S, Kamath N. Thrombocytopenia in hepatitis A--an atypical presentation. *J Trop Pediatr* 2004; **50**: 241-242 [PMID: 15357567 DOI: 10.1093/tropej/50.4.241]

40 **Allen O**, Edhi A, Hafeez A, Halalau A. A Very Rare Complication of Hepatitis A Infection: Acute Myocarditis-A Case Report with Literature Review. *Case Rep Med* 2018; **2018**: 3625139 [PMID:

30302093 DOI: 10.1155/2018/3625139]
41 **Stübgen JP**. Neuromuscular complications of hepatitis A virus infection and vaccines. *J Neurol Sci* 2011; **300**: 2-8 [PMID: 20920814 DOI: 10.1016/j.jns.2010.09.015]
42 **Dalton HR**, Kamar N, van Eijk JJ, Mclean BN, Cintas P, Bendall RP, Jacobs BC. Hepatitis E virus and neurological injury. *Nat Rev Neurol* 2016; **12**: 77-85 [PMID: 26711839 DOI: 10.1038/nrneurol.2015.234]
43 **Rawla P**, Raj JP, Kannemkuzhiyil AJ, Aluru JS, Thandra KC, Gajendran M. A Systematic Review of the Extra-Hepatic Manifestations of Hepatitis E Virus Infection. *Med Sci (Basel)* 2020; **8** [PMID: 32033102 DOI: 10.3390/medsci8010009]
44 **Avila JD**, Lacomis D, Lam EM. Neuralgic Amyotrophy Associated With Hepatitis E Virus Infection: First Case in the United States. *J Clin Neuromuscul Dis* 2016; **18**: 96-100 [PMID: 27861224 DOI: 10.1097/CND.0000000000000137]
45 **Loly JP**, Rikir E, Seivert M, Legros E, Defrance P, Belaiche J, Moonen G, Delwaide J. Guillain-Barré syndrome following hepatitis E. *World J Gastroenterol* 2009; **15**: 1645-1647 [PMID: 19340910 DOI: 10.3748/wjg.15.1645]
46 **Perrin HB**, Cintas P, Abravanel F, Gérolami R, d'Alteroche L, Raynal JN, Alric L, Dupuis E, Prudhomme L, Vaucher E, Couzigou P, Liversain JM, Bureau C, Vinel JP, Kamar N, Izopet J, Peron JM. Neurologic Disorders in Immunocompetent Patients with Autochthonous Acute Hepatitis E. *Emerg Infect Dis* 2015; **21**: 1928-1934 [PMID: 26490255 DOI: 10.3201/eid2111.141789]
47 **Dalton HR**, van Eijk JJJ, Cintas P, Madden RG, Jones C, Webb GW, Norton B, Pique J, Lutgens S, Devooght-Johnson N, Woolson K, Baker J, Saunders M, Househam L, Griffiths J, Abravanel F, Izopet J, Kamar N, van Alfen N, van Engelen BGM, Hunter JG, van der Eijk AA, Bendall RP, Mclean BN, Jacobs BC. Hepatitis E virus infection and acute non-traumatic neurological injury: A prospective multicentre study. *J Hepatol* 2017; **67**: 925-932 [PMID: 28734938 DOI: 10.1016/j.jhep.2017.07.010]
48 **Despierres LA**, Kaphan E, Attarian S, Cohen-Bacrie S, Pelletier J, Pouget J, Motte A, Charrel R, Gerolami R, Colson P. Neurologic disorders and hepatitis E, France, 2010. *Emerg Infect Dis* 2011; **17**: 1510-1512 [PMID: 21801637 DOI: 10.3201/eid1708.102028]
49 **Marion O**, Abravanel F, Del Bello A, Esposito L, Lhomme S, Puissant-Lubrano B, Alric L, Faguer S, Izopet J, Kamar N. Hepatitis E virus-associated cryoglobulinemia in solid-organ-transplant recipients. *Liver Int* 2018; **38**: 2178-2189 [PMID: 29845733 DOI: 10.1111/liv.13894]
50 **Woolson KL**, Forbes A, Vine L, Beynon L, McElhinney L, Panayi V, Hunter JG, Madden RG, Glasgow T, Kotecha A, Dalton HC, Mihailescu L, Warshow U, Hussaini HS, Palmer J, Mclean BN, Haywood B, Bendall RP, Dalton HR. Extra-hepatic manifestations of autochthonous hepatitis E infection. *Aliment Pharmacol Ther* 2014; **40**: 1282-1291 [PMID: 25303615 DOI: 10.1111/apt.12986]
51 **Nayak HK**, Kamble NL, Raizada N, Garg S, Daga MK. Acute pancreatitis complicating acute hepatitis e virus infection: a case report and review. *Case Reports Hepatol* 2013; **2013**: 531235 [PMID: 25374721 DOI: 10.1155/2013/531235]
52 **Raj M**, Kumar K, Ghoshal UC, Saraswat VA, Aggarwal R, Mohindra S. Acute Hepatitis E-Associated Acute Pancreatitis: A Single Center Experience and Literature Review. *Pancreas* 2015; **44**: 1320-1322 [PMID: 26390412 DOI: 10.1097/MPA.0000000000000402]
53 **Sengupta P**, Biswas S, Roy T. Hepatitis E-Induced Acute Myocarditis in an Elderly Woman. *Case Rep Gastroenterol* 2019; **13**: 342-349 [PMID: 31572104 DOI: 10.1159/000501998]
54 **Del Bello A**, Guilbeau-Frugier C, Josse AG, Rostaing L, Izopet J, Kamar N. Successful treatment of hepatitis E virus-associated cryoglobulinemic membranoproliferative glomerulonephritis with ribavirin. *Transpl Infect Dis* 2015; **17**: 279-283 [PMID: 25708383 DOI: 10.1111/tid.12353]
55 **van Eijk JJ**, van Alfen N, Berrevoets M, van der Wilt GJ, Pillen S, van Engelen BG. Evaluation of prednisolone treatment in the acute phase of neuralgic amyotrophy: an observational study. *J Neurol Neurosurg Psychiatry* 2009; **80**: 1120-1124 [PMID: 19321467 DOI: 10.1136/jnnp.2008.163386]
56 **Osman C**, Jennings R, El-Ghariani K, Pinto A. Plasma exchange in neurological disease. *Pract Neurol* 2020; **20**: 92-99 [PMID: 31300488 DOI: 10.1136/practneurol-2019-002336]
57 **Trepo C**, Guillevin L. Polyarteritis nodosa and extrahepatic manifestations of HBV infection: the case against autoimmune intervention in pathogenesis. *J Autoimmun* 2001; **16**: 269-274 [PMID: 11334492 DOI: 10.1006/jaut.2000.0502]
58 **McMahon BJ**, Alward WL, Hall DB, Heyward WL, Bender TR, Francis DP, Maynard JE. Acute hepatitis B virus infection: relation of age to the clinical expression of disease and subsequent development of the carrier state. *J Infect Dis* 1985; **151**: 599-603 [PMID: 3973412 DOI: 10.1093/infdis/151.4.599]
59 **Kappus MR**, Sterling RK. Extrahepatic manifestations of acute hepatitis B virus infection. *Gastroenterol Hepatol (N Y)* 2013; **9**: 123-126 [PMID: 23983659]
60 **Yimam KK**, Merriman RB, Todd Frederick R. A rare case of acute hepatitis B virus infection causing guillain-barré syndrome. *Gastroenterol Hepatol (N Y)* 2013; **9**: 121-123 [PMID: 23983658]
61 **Cacoub P**, Terrier B. Hepatitis B-related autoimmune manifestations. *Rheum Dis Clin North Am* 2009; **35**: 125-137 [PMID: 19481001 DOI: 10.1016/j.rdc.2009.03.006]
62 **Cacoub P**, Saadoun D, Bourlière M, Khiri H, Martineau A, Benhamou Y, Varastet M, Pol S, Thibault V, Rotily M, Halfon P. Hepatitis B virus genotypes and extrahepatic manifestations. *J Hepatol* 2005; **43**: 764-770 [PMID: 16087273 DOI: 10.1016/j.jhep.2005.05.029]
63 **Mason A**, Theal J, Bain V, Adams E, Perrillo R. Hepatitis B virus replication in damaged

endothelial tissues of patients with extrahepatic disease. *Am J Gastroenterol* 2005; **100**: 972-976 [PMID: 15784044 DOI: 10.1111/j.1572-0241.2005.41308.x]

64 **Levo Y**, Gorevic PD, Kassab HJ, Zucker-Franklin D, Franklin EC. Association between hepatitis B virus and essential mixed cryoglobulinemia. *N Engl J Med* 1977; **296**: 1501-1504 [PMID: 865530 DOI: 10.1056/NEJM197706302962605]

65 **Stübgen JP**. Neuromuscular disorders associated with hepatitis B virus infection. *J Clin Neuromuscul Dis* 2011; **13**: 26-37 [PMID: 22361623 DOI: 10.1097/CND.0b013e3181df2b2b]

66 **Guillevin L**, Lhote F, Sauvaget F, Deblois P, Rossi F, Levallois D, Pourrat J, Christoforov B, Trépo C. Treatment of polyarteritis nodosa related to hepatitis B virus with interferon-alpha and plasma exchanges. *Ann Rheum Dis* 1994; **53**: 334-337 [PMID: 7912504 DOI: 10.1136/ard.53.5.334]

67 **Guillevin L**, Mahr A, Cohen P, Larroche C, Queyrel V, Loustaud-Ratti V, Imbert B, Hausfater P, Roudier J, Bielefeld P, Petitjean P, Smadja D; French Vasculitis Study Group. Short-term corticosteroids then lamivudine and plasma exchanges to treat hepatitis B virus-related polyarteritis nodosa. *Arthritis Rheum* 2004; **51**: 482-487 [PMID: 15188337 DOI: 10.1002/art.20401]

68 **Tang S**, Lai FM, Lui YH, Tang CS, Kung NN, Ho YW, Chan KW, Leung JC, Lai KN. Lamivudine in hepatitis B-associated membranous nephropathy. *Kidney Int* 2005; **68**: 1750-1758 [PMID: 16164651 DOI: 10.1111/j.1523-1755.2005.00591.x]

69 **Chung DR**, Yang WS, Kim SB, Yu E, Chung YH, Lee Y, Park JS. Treatment of hepatitis B virus associated glomerulonephritis with recombinant human alpha interferon. *Am J Nephrol* 1997; **17**: 112-117 [PMID: 9096440 DOI: 10.1159/000169083]

70 **Mazzaro C**, Dal Maso L, Visentini M, Gitto S, Andreone P, Toffolutti F, Gattei V. Hepatitis B virus-related cryogobulinemic vasculitis. The role of antiviral nucleot(s)ide analogues: a review. *J Intern Med* 2019; **286**: 290-298 [PMID: 31124596 DOI: 10.1111/joim.12913]

71 **Martinello M**, Hajarizadeh B, Grebely J, Dore GJ, Matthews GV. Management of acute HCV infection in the era of direct-acting antiviral therapy. *Nat Rev Gastroenterol Hepatol* 2018; **15**: 412-424 [PMID: 29773899 DOI: 10.1038/s41575-018-0026-5]

72 **Loomba R**, Rivera MM, McBurney R, Park Y, Haynes-Williams V, Rehermann B, Alter HJ, Herrine SK, Liang TJ, Hoofnagle JH, Heller T. The natural history of acute hepatitis C: clinical presentation, laboratory findings and treatment outcomes. *Aliment Pharmacol Ther* 2011; **33**: 559-565 [PMID: 21198704 DOI: 10.1111/j.1365-2036.2010.04549.x]

73 **Morin T**, Pariente A, Lahmek P, Rabaud C, Silvain C, Cadranel JF; Association Nationale des Hépato-gastroentérologues des Hôpitaux généraux (ANGH) Société de Pathologie Infectieuse de Langue Française (SPILF) Fédération des Pôles de Référence et Réseaux Hépatites (FPRRH). Acute hepatitis C: analysis of a 126-case prospective, multicenter cohort. *Eur J Gastroenterol Hepatol* 2010; **22**: 157-166 [PMID: 19734798 DOI: 10.1097/MEG.0b013e328330a8e8]

74 **Spearman CW**, Dusheiko GM, Hellard M, Sonderup M. Hepatitis C. *Lancet* 2019; **394**: 1451-1466 [PMID: 31631857 DOI: 10.1016/S0140-6736(19)32320-7]

75 **Cacoub P**, Poynard T, Ghillani P, Charlotte F, Olivi M, Piette JC, Opolon P. Extrahepatic manifestations of chronic hepatitis C. MULTIVIRC Group. Multidepartment Virus C. *Arthritis Rheum* 1999; **42**: 2204-2212 [PMID: 10524695 DOI: 10.1002/1529-0131(199910)42:10<2204::AID-ANR24>3.0.CO;2-D]

76 **Kuna L**, Jakab J, Smolic R, Wu GY, Smolic M. HCV Extrahepatic Manifestations. *J Clin Transl Hepatol* 2019; **7**: 172-182 [PMID: 31293918 DOI: 10.14218/JCTH.2018.00049]

77 **Zegans ME**, Anninger W, Chapman C, Gordon SR. Ocular manifestations of hepatitis C virus infection. *Curr Opin Ophthalmol* 2002; **13**: 423-427 [PMID: 12441848 DOI: 10.1097/00055735-200212000-00014]

78 **Petta S**, Craxì A. Extrahepatic Manifestations of Chronic Viral C Hepatitis. *Gastroenterol Clin North Am* 2020; **49**: 347-360 [PMID: 32389367 DOI: 10.1016/j.gtc.2020.01.012]

79 **Comarmond C**, Cacoub P, Saadoun D. Treatment of chronic hepatitis C-associated cryoglobulinemia vasculitis at the era of direct-acting antivirals. *Therap Adv Gastroenterol* 2020; **13**: 1756284820942617 [PMID: 32782479 DOI: 10.1177/1756284820942617]

80 **Carrat F**, Fontaine H, Dorival C, Simony M, Diallo A, Hezode C, De Ledinghen V, Larrey D, Haour G, Bronowicki JP, Zoulim F, Asselah T, Marcellin P, Thabut D, Leroy V, Tran A, Habersetzer F, Samuel D, Guyader D, Chazouilleres O, Mathurin P, Metivier S, Alric L, Riachi G, Gournay J, Abergel A, Cales P, Ganne N, Loustaud-Ratti V, D'Alteroche L, Causse X, Geist C, Minello A, Rosa I, Gelu-Simeon M, Portal I, Raffi F, Bourliere M, Pol S; French ANRS CO22 Hepather cohort. Clinical outcomes in patients with chronic hepatitis C after direct-acting antiviral treatment: a prospective cohort study. *Lancet* 2019; **393**: 1453-1464 [PMID: 30765123 DOI: 10.1016/S0140-6736(18)32111-1]

81 **Thomas K**, Vassilopoulos D. Infections and vasculitis. *Curr Opin Rheumatol* 2017; **29**: 17-23 [PMID: 27662570 DOI: 10.1097/BOR.0000000000000348]

82 **Lidar M**, Lipschitz N, Langevitz P, Shoenfeld Y. The infectious etiology of vasculitis. *Autoimmunity* 2009; **42**: 432-438 [PMID: 19811260 DOI: 10.1080/08916930802613210]

83 **Vergani D**, Mieli-Vergani G. Autoimmune manifestations in viral hepatitis. *Semin Immunopathol* 2013; **35**: 73-85 [PMID: 23010889 DOI: 10.1007/s00281-012-0328-6]

84 **Cozzani E**, Herzum A, Burlando M, Parodi A. Cutaneous manifestations of HAV, HBV, HCV. *G Ital Dermatol Venereol* 2019 [PMID: 31804053 DOI: 10.23736/S0392-0488.19.06488-5]

85 **Grigorescu I**, Dumitrascu DL. Spontaneous and antiviral-induced cutaneous lesions in chronic hepatitis B virus infection. *World J Gastroenterol* 2014; **20**: 15860-15866 [PMID: 25400473 DOI:

10.3748/wjg.v20.i42.15860]
86 **Glück T**, Weber P, Wiedmann KH. [Hepatitis-B-associated vasculitis. Clinical course with glucocorticoid and alpha-interferon therapy]. *Dtsch Med Wochenschr* 1994; **119**: 1388-1392 [PMID: 7924948 DOI: 10.1055/s-2008-1058850]
87 **Chemli J**, Zouari N, Belkadhi A, Abroug S, Harbi A. [Hepatitis A infection and Henoch-Schonlein purpura: a rare association]. *Arch Pediatr* 2004; **11**: 1202-1204 [PMID: 15475276 DOI: 10.1016/j.arcped.2004.06.014]
88 **Altinkaynak S**, Ertekin V, Selimoglu MA. Association of Henoch-Schonlein purpura and hepatitis A. *J Emerg Med* 2006; **30**: 219-220 [PMID: 16567262 DOI: 10.1016/j.jemermed.2005.12.011]
89 **Thapa R**, Biswas B, Mallick D. Henoch-Schönlein purpura triggered by acute hepatitis E virus infection. *J Emerg Med* 2010; **39**: 218-219 [PMID: 19201130 DOI: 10.1016/j.jemermed.2008.10.004]
90 **Heineke MH**, Ballering AV, Jamin A, Ben Mkaddem S, Monteiro RC, Van Egmond M. New insights in the pathogenesis of immunoglobulin A vasculitis (Henoch-Schönlein purpura). *Autoimmun Rev* 2017; **16**: 1246-1253 [PMID: 29037908 DOI: 10.1016/j.autrev.2017.10.009]
91 **Maggiore G**, Martini A, Grifeo S, De Giacomo C, Scotta MS. Hepatitis B virus infection and Schönlein-Henoch purpura. *Am J Dis Child* 1984; **138**: 681-682 [PMID: 6731386 DOI: 10.1001/archpedi.1984.02140450063019]
92 **Ergin S**, Sanli Erdoğan B, Turgut H, Evliyaoğlu D, Yalçin AN. Relapsing Henoch-Schönlein purpura in an adult patient associated with hepatitis B virus infection. *J Dermatol* 2005; **32**: 839-842 [PMID: 16361739 DOI: 10.1111/j.1346-8138.2005.tb00856.x]
93 **Ogawa M**, Makino Y, Ueda S, Ohto M, Akikusa B. Rapidly progressive glomerulonephritis in association with Henoch-Schönlein purpura in a patient with advanced liver cirrhosis. *Nephron* 1995; **71**: 365-366 [PMID: 8569993 DOI: 10.1159/000188750]
94 **Madison DL**, Allen E, Deodhar A, Morrison L. Henoch-Schönlein purpura: a possible complication of hepatitis C related liver cirrhosis. *Ann Rheum Dis* 2002; **61**: 281-282 [PMID: 11830445 DOI: 10.1136/ard.61.3.281-a]
95 **Nishida N**, Kudo M. Clinical features of vascular disorders associated with chronic hepatitis virus infection. *Dig Dis* 2014; **32**: 786-790 [PMID: 25376297 DOI: 10.1159/000368023]
96 **Silva F**, Pinto C, Barbosa A, Borges T, Dias C, Almeida J. New insights in cryoglobulinemic vasculitis. *J Autoimmun* 2019; **105**: 102313 [PMID: 31383568 DOI: 10.1016/j.jaut.2019.102313]
97 **De Virgilio A**, Greco A, Magliulo G, Gallo A, Ruoppolo G, Conte M, Martellucci S, de Vincentiis M. Polyarteritis nodosa: A contemporary overview. *Autoimmun Rev* 2016; **15**: 564-570 [PMID: 26884100 DOI: 10.1016/j.autrev.2016.02.015]
98 **Desbois AC**, Cacoub P, Saadoun D. Cryoglobulinemia: An update in 2019. *Joint Bone Spine* 2019; **86**: 707-713 [PMID: 30731128 DOI: 10.1016/j.jbspin.2019.01.016]
99 **Meltzer M**, Franklin EC. Cryoglobulinemia--a study of twenty-nine patients. I. IgG and IgM cryoglobulins and factors affecting cryoprecipitability. *Am J Med* 1966; **40**: 828-836 [PMID: 4956870 DOI: 10.1016/0002-9343(66)90199-9]
100 **Brouet JC**, Clauvel JP, Danon F, Klein M, Seligmann M. Biologic and clinical significance of cryoglobulins. A report of 86 cases. *Am J Med* 1974; **57**: 775-788 [PMID: 4216269 DOI: 10.1016/0002-9343(74)90852-3]
101 **Harel S**, Mohr M, Jahn I, Aucouturier F, Galicier L, Asli B, Malphettes M, Szalat R, Brouet JC, Lipsker D, Fermand JP. Clinico-biological characteristics and treatment of type I monoclonal cryoglobulinaemia: a study of 64 cases. *Br J Haematol* 2015; **168**: 671-678 [PMID: 25363150 DOI: 10.1111/bjh.13196]
102 **Trejo O**, Ramos-Casals M, García-Carrasco M, Yagüe J, Jiménez S, de la Red G, Cervera R, Font J, Ingelmo M. Cryoglobulinemia: study of etiologic factors and clinical and immunologic features in 443 patients from a single center. *Medicine (Baltimore)* 2001; **80**: 252-262 [PMID: 11470986 DOI: 10.1097/00005792-200107000-00004]
103 **Charles ED**, Dustin LB. Hepatitis C virus-induced cryoglobulinemia. *Kidney Int* 2009; **76**: 818-824 [PMID: 19606079 DOI: 10.1038/ki.2009.247]
104 **Cheema SR**, Arif F, Charney D, Meisels IS. IgA-dominant glomerulonephritis associated with hepatitis A. *Clin Nephrol* 2004; **62**: 138-143 [PMID: 15356971 DOI: 10.5414/cnp62138]
105 **Chen PP**, Fong S, Goni F, Silverman GJ, Fox RI, Liu MF, Frangione B, Carson DA. Cross-reacting idiotypes on cryoprecipitating rheumatoid factor. *Springer Semin Immunopathol* 1988; **10**: 35-55 [PMID: 3137675 DOI: 10.1007/]
106 **Quartuccio L**, Fabris M, Salvin S, Isola M, Soldano F, Falleti E, Beltrami CA, De Re V, De Vita S. Bone marrow B-cell clonal expansion in type II mixed cryoglobulinaemia: association with nephritis. *Rheumatology (Oxford)* 2007; **46**: 1657-1661 [PMID: 17893101 DOI: 10.1093/rheumatology/kem209]
107 **Ferri C**, Sebastiani M, Giuggioli D, Cazzato M, Longombardo G, Antonelli A, Puccini R, Michelassi C, Zignego AL. Mixed cryoglobulinemia: demographic, clinical, and serologic features and survival in 231 patients. *Semin Arthritis Rheum* 2004; **33**: 355-374 [PMID: 15190522 DOI: 10.1016/j.semarthrit.2003.10.001]
108 **Ramos-Casals M**, Stone JH, Cid MC, Bosch X. The cryoglobulinaemias. *Lancet* 2012; **379**: 348-360 [PMID: 21868085 DOI: 10.1016/S0140-6736(11)60242-0]
109 **Roccatello D**, Fornasieri A, Giachino O, Rossi D, Beltrame A, Banfi G, Confalonieri R, Tarantino A, Pasquali S, Amoroso A, Savoldi S, Colombo V, Manno C, Ponzetto A, Moriconi L, Pani A,

Rustichelli R, Di Belgiojoso GB, Comotti C, Quarenghi MI. Multicenter study on hepatitis C virus-related cryoglobulinemic glomerulonephritis. *Am J Kidney Dis* 2007; **49**: 69-82 [PMID: 17185147 DOI: 10.1053/j.ajkd.2006.09.015]

110 **Johnson RJ**, Gretch DR, Yamabe H, Hart J, Bacchi CE, Hartwell P, Couser WG, Corey L, Wener MH, Alpers CE. Membranoproliferative glomerulonephritis associated with hepatitis C virus infection. *N Engl J Med* 1993; **328**: 465-470 [PMID: 7678440 DOI: 10.1056/NEJM199302183280703]

111 **Ammendola A**, Sampaolo S, Ambrosone L, Ammendola E, Ciccone G, Migliaresi S, Di Iorio G. Peripheral neuropathy in hepatitis-related mixed cryoglobulinemia: electrophysiologic follow-up study. *Muscle Nerve* 2005; **31**: 382-385 [PMID: 15515001 DOI: 10.1002/mus.20184]

112 **Casato M**, Saadoun D, Marchetti A, Limal N, Picq C, Pantano P, Galanaud D, Cianci R, Duhaut P, Piette JC, Fiorilli M, Cacoub P. Central nervous system involvement in hepatitis C virus cryoglobulinemia vasculitis: a multicenter case-control study using magnetic resonance imaging and neuropsychological tests. *J Rheumatol* 2005; **32**: 484-488 [PMID: 15742440]

113 **Retamozo S**, Díaz-Lagares C, Bosch X, Bové A, Brito-Zerón P, Gómez ME, Yagüe J, Forns X, Cid MC, Ramos-Casals M. Life-Threatening Cryoglobulinemic Patients With Hepatitis C: Clinical Description and Outcome of 279 Patients. *Medicine (Baltimore)* 2013; **92**: 273-284 [PMID: 23974248 DOI: 10.1097/MD.0b013e3182a5cf71]

114 **Cavalli G**, Berti A, Fragasso G, De Cobelli F. Hypertrophic cardiomyopathy secondary to hepatitis C virus-related vasculitis. *J Cardiovasc Med (Hagerstown)* 2016; **17** Suppl 2: e156-e157 [PMID: 24979124 DOI: 10.2459/JCM.0000000000000109]

115 **Terrier B**, Saadoun D, Sène D, Scerra S, Musset L, Cacoub P. Presentation and outcome of gastrointestinal involvement in hepatitis C virus-related systemic vasculitis: a case-control study from a single-centre cohort of 163 patients. *Gut* 2010; **59**: 1709-1715 [PMID: 20841367 DOI: 10.1136/gut.2010.218123]

116 **Muñoz-Martínez SG**, Díaz-Hernández HA, Suárez-Flores D, Sánchez-Ávila JF, Gamboa-Domínguez A, García-Juárez I, Torre A. Atypical manifestations of hepatitis A virus infection. *Rev Gastroenterol Mex* 2018; **83**: 134-143 [PMID: 29685743 DOI: 10.1016/j.rgmx.2017.10.004]

117 **Nassih H**, Bourrahouat A, Sab IA. Hepatitis A Virus Infection Associated with Cryoglobulinemic Vasculitis. *Indian Pediatr* 2020; **57**: 71-72 [PMID: 31937705]

118 **Levo Y**, Gorevic PD, Kassab HJ, Tobias H, Franklin EC. Liver involvement in the syndrome of mixed cryoglobulinemia. *Ann Intern Med* 1977; **87**: 287-292 [PMID: 900672 DOI: 10.7326/0003-4819-87-3-287]

119 **Gower RG**, Sausker WF, Kohler PF, Thorne GE, McIntosh RM. Small vessel vasculitis caused by hepatitis B virus immune complexes. Small vessel vasculitis and HBsAG. *J Allergy Clin Immunol* 1978; **62**: 222-228 [PMID: 701656 DOI: 10.1016/0091-6749(78)90211-7]

120 **Monti G**, Galli M, Invernizzi F, Pioltelli P, Saccardo F, Monteverde A, Pietrogrande M, Renoldi P, Bombardieri S, Bordin G. Cryoglobulinaemias: a multi-centre study of the early clinical and laboratory manifestations of primary and secondary disease. GISC. Italian Group for the Study of Cryoglobulinaemias. *QJM* 1995; **88**: 115-126 [PMID: 7704562]

121 **Mazzaro C**, Dal Maso L, Urraro T, Mauro E, Castelnovo L, Casarin P, Monti G, Gattei V, Zignego AL, Pozzato G. Hepatitis B virus related cryoglobulinemic vasculitis: A multicentre open label study from the Gruppo Italiano di Studio delle Crioglobulinemie - GISC. *Dig Liver Dis* 2016; **48**: 780-784 [PMID: 27106525 DOI: 10.1016/j.dld.2016.03.018]

122 **Liou YT**, Huang JL, Ou LS, Lin YH, Yu KH, Luo SF, Ho HH, Liou LB, Yeh KW. Comparison of cryoglobulinemia in children and adults. *J Microbiol Immunol Infect* 2013; **46**: 59-64 [PMID: 22237397 DOI: 10.1016/j.jmii.2011.12.027]

123 **Mazzaro C**, Dal Maso L, Visentini M, Ermacora A, Tonizzo M, Gattei V, Andreone P. Recent news in the treatment of hepatitis B virus-related cryogobulinemic vasculitis. *Minerva Med* 2020; **111**: 566-572 [PMID: 32573522 DOI: 10.23736/S0026-4806.20.06771-3]

124 **European Association for the Study of the Liver**. ; European Association for the Study of the Liver. EASL 2017 Clinical Practice Guidelines on the management of hepatitis B virus infection. *J Hepatol* 2017; **67**: 370-398 [PMID: 28427875 DOI: 10.1016/j.jhep.2017.03.021]

125 **Kamimura H**, Setsu T, Kimura N, Yokoo T, Sakamaki A, Kamimura K, Tsuchiya A, Takamura M, Yamagiwa S, Terai S. Renal Impairment in Chronic Hepatitis B: A Review. *Diseases* 2018; **6** [PMID: 29921773 DOI: 10.3390/diseases6020052]

126 **Ferri C**, Antonelli A, Mascia MT, Sebastiani M, Fallahi P, Ferrari D, Giunti M, Pileri SA, Zignego AL. B-cells and mixed cryoglobulinemia. *Autoimmun Rev* 2007; **7**: 114-120 [PMID: 18035320 DOI: 10.1016/j.autrev.2007.02.019]

127 **Pasquet F**, Combarnous F, Macgregor B, Coppere B, Mausservey C, Ninet J, Hot A. Safety and efficacy of rituximab treatment for vasculitis in hepatitis B virus-associated type II cryoglobulinemia: a case report. *J Med Case Rep* 2012; **6**: 39 [PMID: 22284897 DOI: 10.1186/1752-1947-6-39]

128 **Terrier B**, Marie I, Lacraz A, Belenotti P, Bonnet F, Chiche L, Graffin B, Hot A, Kahn JE, Michel C, Quemeneur T, de Saint-Martin L, Hermine O, Léger JM, Mariette X, Senet P, Plaisier E, Cacoub P. Non HCV-related infectious cryoglobulinemia vasculitis: Results from the French nationwide CryoVas survey and systematic review of the literature. *J Autoimmun* 2015; **65**: 74-81 [PMID: 26320984 DOI: 10.1016/j.jaut.2015.08.008]

129 **Tsutsumi Y**, Yamamoto Y, Ito S, Ohigashi H, Shiratori S, Naruse H, Teshima T. Hepatitis B virus

reactivation with a rituximab-containing regimen. *World J Hepatol* 2015; **7**: 2344-2351 [PMID: 26413224 DOI: 10.4254/wjh.v7.i21.2344]

130 **Khan ZH**, Ilyas K, Ghazanfar H, Khan HH, Hussain Q, Hammad S, Munir A, Asim R. Fatal Fulminant Hepatitis from Rituximab-induced Hepatitis B Reactivation in a Patient with Follicular Lymphoma: A Case Report and a Brief Review of Literature. *Cureus* 2018; **10**: e2257 [PMID: 29725560 DOI: 10.7759/cureus.2257]

131 **Ferri C**, Greco F, Longombardo G, Palla P, Moretti A, Marzo E, Mazzoni A, Pasero G, Bombardieri S, Highfield P. Association between hepatitis C virus and mixed cryoglobulinemia [see comment]. *Clin Exp Rheumatol* 1991; **9**: 621-624 [PMID: 1662567]

132 **Rosa D**, Saletti G, De Gregorio E, Zorat F, Comar C, D'Oro U, Nuti S, Houghton M, Barnaba V, Pozzato G, Abrignani S. Activation of naïve B lymphocytes *via* CD81, a pathogenetic mechanism for hepatitis C virus-associated B lymphocyte disorders. *Proc Natl Acad Sci* 2005; **102**: 18544-18549 [PMID: 16339892 DOI: 10.1073/pnas.0509402102]

133 **Charles ED**, Green RM, Marukian S, Talal AH, Lake-Bakaar GV, Jacobson IM, Rice CM, Dustin LB. Clonal expansion of immunoglobulin M+CD27+ B cells in HCV-associated mixed cryoglobulinemia. *Blood* 2008; **111**: 1344-1356 [PMID: 17942751 DOI: 10.1182/blood-2007-07-101717]

134 **Ferri C**, La Civita L, Zignego AL, Pasero G. Viruses and cancers: possible role of hepatitis C virus. *Eur J Clin Invest* 1997; **27**: 711-718 [PMID: 9352239 DOI: 10.1046/j.1365-2362.1997.1790728.x]

135 **Mele A**, Pulsoni A, Bianco E, Musto P, Szklo A, Sanpaolo MG, Iannitto E, De Renzo A, Martino B, Liso V, Andrizzi C, Pusterla S, Dore F, Maresca M, Rapicetta M, Marcucci F, Mandelli F, Franceschi S. Hepatitis C virus and B-cell non-Hodgkin lymphomas: an Italian multicenter case-control study. *Blood* 2003; **102**: 996-999 [PMID: 12714514 DOI: 10.1182/blood-2002-10-3230]

136 **Giordano TP**, Henderson L, Landgren O, Chiao EY, Kramer JR, El-Serag H, Engels EA. Risk of non-Hodgkin lymphoma and lymphoproliferative precursor diseases in US veterans with hepatitis C virus. *JAMA* 2007; **297**: 2010-2017 [PMID: 17488966 DOI: 10.1001/jama.297.18.2010]

137 **Monti G**, Pioltelli P, Saccardo F, Campanini M, Candela M, Cavallero G, De Vita S, Ferri C, Mazzaro C, Migliaresi S, Ossi E, Pietrogrande M, Gabrielli A, Galli M, Invernizzi F. Incidence and characteristics of non-Hodgkin lymphomas in a multicenter case file of patients with hepatitis C virus-related symptomatic mixed cryoglobulinemias. *Arch Intern Med* 2005; **165**: 101-105 [PMID: 15642884 DOI: 10.1001/archinte.165.1.101]

138 **Bunchorntavakul C**, Mitrani R, Reddy KR. Advances in HCV and Cryoglobulinemic Vasculitis in the Era of DAAs: Are We at the End of the Road? *J Clin Exp Hepatol* 2018; **8**: 81-94 [PMID: 29743799 DOI: 10.1016/j.jceh.2017.11.012]

139 **Saadoun D**, Pol S, Ferfar Y, Alric L, Hezode C, Si Ahmed SN, de Saint Martin L, Comarmond C, Bouyer AS, Musset L, Poynard T, Resche Rigon M, Cacoub P. Efficacy and Safety of Sofosbuvir Plus Daclatasvir for Treatment of HCV-Associated Cryoglobulinemia Vasculitis. *Gastroenterology* 2017; **153**: 49-52. e5 [PMID: 28288791 DOI: 10.1053/j.gastro.2017.03.006]

140 **Arcaini L**, Besson C, Frigeni M, Fontaine H, Goldaniga M, Casato M, Visentini M, Torres HA, Loustaud-Ratti V, Peveling-Oberhag J, Fabris P, Rossotti R, Zaja F, Rigacci L, Rattotti S, Bruno R, Merli M, Dorival C, Alric L, Jaccard A, Pol S, Carrat F, Ferretti VV, Visco C, Hermine O. Interferon-free antiviral treatment in B-cell lymphoproliferative disorders associated with hepatitis C virus infection. *Blood* 2016; **128**: 2527-2532 [PMID: 27605512 DOI: 10.1182/blood-2016-05-714667]

141 **Ramos-Casals M**, Zignego AL, Ferri C, Brito-Zerón P, Retamozo S, Casato M, Lamprecht P, Mangia A, Saadoun D, Tzioufas AG, Younossi ZM, Cacoub P; International Study Group of Extrahepatic Manifestations related to HCV (ISG-EHCV). Evidence-based recommendations on the management of extrahepatic manifestations of chronic hepatitis C virus infection. *J Hepatol* 2017; **66**: 1282-1299 [PMID: 28219772 DOI: 10.1016/j.jhep.2017.02.010]

142 **Saadoun D**, Resche Rigon M, Sene D, Terrier B, Karras A, Perard L, Schoindre Y, Coppéré B, Blanc F, Musset L, Piette JC, Rosenzwajg M, Cacoub P. Rituximab plus Peg-interferon-alpha/ribavirin compared with Peg-interferon-alpha/ribavirin in hepatitis C-related mixed cryoglobulinemia. *Blood* 2010; **116**: 326-34; quiz 504 [PMID: 20439619 DOI: 10.1182/blood-2009-10-248518]

143 **De Vita S**, Quartuccio L, Isola M, Mazzaro C, Scaini P, Lenzi M, Campanini M, Naclerio C, Tavoni A, Pietrogrande M, Ferri C, Mascia MT, Masolini P, Zabotti A, Maset M, Roccatello D, Zignego AL, Pioltelli P, Gabrielli A, Filippini D, Perrella O, Migliaresi S, Galli M, Bombardieri S, Monti G. A randomized controlled trial of rituximab for the treatment of severe cryoglobulinemic vasculitis. *Arthritis Rheum* 2012; **64**: 843-853 [PMID: 22147661 DOI: 10.1002/art.34331]

144 **Desbois AC**, Comarmond C, Saadoun D, Cacoub P. Cryoglobulinemia vasculitis: how to handle. *Curr Opin Rheumatol* 2017; **29**: 343-347 [PMID: 28368978 DOI: 10.1097/BOR.0000000000000390]

145 **Sène D**, Ghillani-Dalbin P, Amoura Z, Musset L, Cacoub P. Rituximab may form a complex with IgMkappa mixed cryoglobulin and induce severe systemic reactions in patients with hepatitis C virus-induced vasculitis. *Arthritis Rheum* 2009; **60**: 3848-3855 [PMID: 19950292 DOI: 10.1002/art.25000]

146 **Ishiguro N**, Kawashima M. Cutaneous polyarteritis nodosa: a report of 16 cases with clinical and histopathological analysis and a review of the published work. *J Dermatol* 2010; **37**: 85-93 [PMID: 20175828 DOI: 10.1111/j.1346-8138.2009.00752.x]

147 **Morgan AJ**, Schwartz RA. Cutaneous polyarteritis nodosa: a comprehensive review. *Int J Dermatol* 2010; **49**: 750-756 [PMID: 20618492 DOI: 10.1111/j.1365-4632.2010.04522.x]

148 **Hernández-Rodríguez J**, Alba MA, Prieto-González S, Cid MC. Diagnosis and classification of polyarteritis nodosa. *J Autoimmun* 2014; **48-49**: 84-89 [PMID: 24485157 DOI: 10.1016/j.jaut.2014.01.029]

149 **Gocke DJ**, Hsu K, Morgan C, Bombardieri S, Lockshin M, Christian CL. Association between polyarteritis and Australia antigen. *Lancet* 1970; **2**: 1149-1153 [PMID: 4098431 DOI: 10.1016/s0140-6736(70)90339-9]

150 **Trepo C**, Thivolet J. Hepatitis associated antigen and periarteritis nodosa (PAN). *Vox Sang* 1970; **19**: 410-411 [PMID: 4396040]

151 **Ozen S**. The changing face of polyarteritis nodosa and necrotizing vasculitis. *Nat Rev Rheumatol* 2017; **13**: 381-386 [PMID: 28490787 DOI: 10.1038/nrrheum.2017.68]

152 **Sharma A**, Sharma K. Hepatotropic viral infection associated systemic vasculitides-hepatitis B virus associated polyarteritis nodosa and hepatitis C virus associated cryoglobulinemic vasculitis. *J Clin Exp Hepatol* 2013; **3**: 204-212 [PMID: 25755502 DOI: 10.1016/j.jceh.2013.06.001]

153 **Pagnoux C**, Seror R, Henegar C, Mahr A, Cohen P, Le Guern V, Bienvenu B, Mouthon L, Guillevin L; French Vasculitis Study Group. Clinical features and outcomes in 348 patients with polyarteritis nodosa: a systematic retrospective study of patients diagnosed between 1963 and 2005 and entered into the French Vasculitis Study Group Database. *Arthritis Rheum* 2010; **62**: 616-626 [PMID: 20112401 DOI: 10.1002/art.27240]

154 **Imboden JB**. Involvement of the Peripheral Nervous System in Polyarteritis Nodosa and Antineutrophil Cytoplasmic Antibodies-Associated Vasculitis. *Rheum Dis Clin North Am* 2017; **43**: 633-639 [PMID: 29061248 DOI: 10.1016/j.rdc.2017.06.011]

155 **Pagnoux C**, Mahr A, Cohen P, Guillevin L. Presentation and outcome of gastrointestinal involvement in systemic necrotizing vasculitides: analysis of 62 patients with polyarteritis nodosa, microscopic polyangiitis, Wegener granulomatosis, Churg-Strauss syndrome, or rheumatoid arthritis-associated vasculitis. *Medicine (Baltimore)* 2005; **84**: 115-128 [PMID: 15758841 DOI: 10.1097/01.md.0000158825.87055.0b]

156 **Brimo F**, Lachapelle J, Epstein JI. Testicular vasculitis: a series of 19 cases. *Urology* 2011; **77**: 1043-1048 [PMID: 21419476 DOI: 10.1016/j.urology.2011.01.021]

157 **Rimar D**, Alpert A, Starosvetsky E, Rosner I, Slobodin G, Rozenbaum M, Kaly L, Boulman N, Awisat A, Ginsberg S, Zilber K, Shen-Orr SS. Tofacitinib for polyarteritis nodosa: a tailored therapy. *Ann Rheum Dis* 2016; **75**: 2214-2216 [PMID: 27558986 DOI: 10.1136/annrheumdis-2016-209330]

158 **Seri Y**, Shoda H, Hanata N, Nagafuchi Y, Sumitomo S, Fujio K, Yamamoto K. A case of refractory polyarteritis nodosa successfully treated with rituximab. *Mod Rheumatol* 2017; **27**: 696-698 [PMID: 25671401 DOI: 10.3109/14397595.2015.1014153]

159 **Wang CR**, Yang CC. Adalimumab therapy in hepatitis B virus-negative polyarteritis nodosa: A case report. *Medicine (Baltimore)* 2018; **97**: e11053 [PMID: 29923995 DOI: 10.1097/MD.0000000000011053]

160 **Ginsberg S**, Rosner I, Slobodin G, Rozenbaum M, Kaly L, Jiries N, Boulman N, Awisat A, Hussein H, Novofastovski I, Silawy A, Rimar D. Infliximab for the treatment of refractory polyarteritis nodosa. *Clin Rheumatol* 2019; **38**: 2825-2833 [PMID: 30972576 DOI: 10.1007/s10067-019-04474-9]

161 **Krusche M**, Ruffer N, Kötter I. Tocilizumab treatment in refractory polyarteritis nodosa: a case report and review of the literature. *Rheumatol Int* 2019; **39**: 337-344 [PMID: 30465270 DOI: 10.1007/s00296-018-4210-2]

162 **Press J**, Maslovitz S, Avinoach I. Cutaneous necrotizing vasculitis associated with hepatitis A virus infection. *J Rheumatol* 1997; **24**: 965-967 [PMID: 9150090]

163 **Candan F**, Ayan S, Tas F, Gökce G, Elagoz S. Spontaneous renal laceration as the presenting feature of polyarteritis nodosa in a patient with familial Mediterranean fever after hepatitis A infection. *Rheumatol Int* 2005; **25**: 475-477 [PMID: 15765217 DOI: 10.1007/s00296-005-0597-7]

164 **Della Rossa A**, Tavoni A, Lorefice P, Casula F, Bombardieri S. HBV and HCV infection, polyarteritis nodosa and mixed cryoglobulinaemia: a case report. *Clin Rheumatol* 2000; **19**: 502-504 [PMID: 11147768 DOI: 10.1007/s100670070018]

165 **Garcia de La Peña Lefebvre P**, Mouthon L, Cohen P, Lhote F, Guillevin L. Polyarteritis nodosa and mixed cryoglobulinaemia related to hepatitis B and C virus coinfection. *Ann Rheum Dis* 2001; **60**: 1068-1069 [PMID: 11602482 DOI: 10.1136/ard.60.11.1068]

166 **Carson CW**, Conn DL, Czaja AJ, Wright TL, Brecher ME. Frequency and significance of antibodies to hepatitis C virus in polyarteritis nodosa. *J Rheumatol* 1993; **20**: 304-309 [PMID: 8097250]

167 **Saadoun D**, Terrier B, Semoun O, Sene D, Maisonobe T, Musset L, Amoura Z, Rigon MR, Cacoub P. Hepatitis C virus-associated polyarteritis nodosa. *Arthritis Care Res (Hoboken)* 2011; **63**: 427-435 [PMID: 20981809 DOI: 10.1002/acr.20381]

168 **Néel A**, Masseau A, Hervier B, Bossard C, Cacoub P, Pagnoux C, Hamidou MA. Life-threatening hepatitis C virus-associated polyarteritis nodosa successfully treated by rituximab. *J Clin Rheumatol* 2011; **17**: 439-441 [PMID: 22089995 DOI: 10.1097/RHU.0b013e31823a58d7]

169 **Guillevin L**, Mahr A, Callard P, Godmer P, Pagnoux C, Leray E, Cohen P; French Vasculitis Study Group. Hepatitis B virus-associated polyarteritis nodosa: clinical characteristics, outcome, and

impact of treatment in 115 patients. *Medicine (Baltimore)* 2005; **84**: 313-322 [PMID: 16148731 DOI: 10.1097/01.md.0000180792.80212.5e]

170 **Lin CL**, Kao JH. Perspectives and control of hepatitis B virus infection in Taiwan. *J Formos Med Assoc* 2015; **114**: 901-909 [PMID: 26184565 DOI: 10.1016/j.jfma.2015.06.003]

171 **Ungprasert P**, Koster MJ, Cheungpasitporn W, Wijarnpreecha K, Thongprayoon C, Kroner PT. Inpatient burden and association with comorbidities of polyarteritis nodosa: National Inpatient Sample 2014. *Semin Arthritis Rheum* 2020; **50**: 66-70 [PMID: 31362895 DOI: 10.1016/j.semarthrit.2019.07.009]

172 **Chen WY**, Lin KT, Chuang CY, Chen CY. Clinical studies of polyarteritis nodosa. *Taiwan Yi Xue Hui Za Zhi* 1977; **76**: 982-989 [PMID: 25312]

173 **Wang CR**, Liu MF, Tsai RT, Chuang CY, Chen CY. Circulating intercellular adhesion molecules-1 and autoantibodies including anti-endothelial cell, anti-cardiolipin, and anti-neutrophil cytoplasma antibodies in patients with vasculitis. *Clin Rheumatol* 1993; **12**: 375-380 [PMID: 8258240 DOI: 10.1007/BF02231583]

174 **Tsai WL**, Tsai IC, Lee T, Hsieh CW. Polyarteritis nodosa: MDCT as a "one-stop shop" modality for whole-body arterial evaluation. *Cardiovasc Intervent Radiol* 2008; **31** Suppl 2: S26-S29 [PMID: 17508232 DOI: 10.1007/s00270-007-9059-9]

175 **Huang MN**, Wu CH. Polyarteritis nodosa and antiphospholipid syndrome causing bilateral renal infarction. *J Rheumatol* 2009; **36**: 197 [PMID: 19208533 DOI: 10.3899/jrheum.080601]

176 **Li KJ**, Hsieh SC, Toh YC, Yu CL. Clinical images: non-hepatitis B virus-related polyarteritis nodosa presenting with fever and diffuse intra-abdominal microaneurysms. *Arthritis Rheum* 2011; **63**: 3597 [PMID: 21834065 DOI: 10.1002/art.30579]

177 **Tsai HC**, Liao HT, Tsai CY. Polyarteritis nodosa with intra-hepatic arterial haemorrhage. *Liver Int* 2020; **40**: 2858-2859 [PMID: 32810375 DOI: 10.1111/liv.14641]

178 **Lu FT**, Ni YH. Elimination of Mother-to-Infant Transmission of Hepatitis B Virus: 35 Years of Experience. *Pediatr Gastroenterol Hepatol Nutr* 2020; **23**: 311-318 [PMID: 32704492 DOI: 10.5223/pghn.2020.23.4.311]

179 **Hong M**, Bertoletti A. Tolerance and immunity to pathogens in early life: insights from HBV infection. *Semin Immunopathol* 2017; **39**: 643-652 [PMID: 28685270 DOI: 10.1007/s00281-017-0641-1]

180 **Travers RL**, Allison DJ, Brettle RP, Hughes GR. Polyarteritis nodosa: a clinical and angiographic analysis of 17 cases. *Semin Arthritis Rheum* 1979; **8**: 184-199 [PMID: 34221 DOI: 10.1016/s0049-0172(79)80007-4]

181 **Cohen RD**, Conn DL, Ilstrup DM. Clinical features, prognosis, and response to treatment in polyarteritis. *Mayo Clin Proc* 1980; **55**: 146-155 [PMID: 6101626]

182 **Fortin PR**, Larson MG, Watters AK, Yeadon CA, Choquette D, Esdaile JM. Prognostic factors in systemic necrotizing vasculitis of the polyarteritis nodosa group--a review of 45 cases. *J Rheumatol* 1995; **22**: 78-84 [PMID: 7699687]

183 **Bae YD**, Choi HJ, Lee JC, Park JJ, Lee YJ, Lee EB, Song YW. Clinical features of polyarteritis nodosa in Korea. *J Korean Med Sci* 2006; **21**: 591-595 [PMID: 16891798 DOI: 10.3346/jkms.2006.21.4.591]

184 **Sharma A**, Pinto B, Dhooria A, Rathi M, Singhal M, Dhir V, Sharma K, Parkash M, Modi M, Vijayvergiya R, Sinha SK, Nada R, Minz RW, Singh S. Polyarteritis nodosa in north India: clinical manifestations and outcomes. *Int J Rheum Dis* 2017; **20**: 390-397 [PMID: 27990777 DOI: 10.1111/1756-185X.12954]

185 **Guillevin L**, Lhote F, Gayraud M, Cohen P, Jarrousse B, Lortholary O, Thibult N, Casassus P. Prognostic factors in polyarteritis nodosa and Churg-Strauss syndrome. A prospective study in 342 patients. *Medicine (Baltimore)* 1996; **75**: 17-28 [PMID: 8569467 DOI: 10.1097/00005792-199601000-00003]

186 **Guillevin L**, Lhote F, Cohen P, Jarrousse B, Lortholary O, Généreau T, Léon A, Bussel A. Corticosteroids plus pulse cyclophosphamide and plasma exchanges versus corticosteroids plus pulse cyclophosphamide alone in the treatment of polyarteritis nodosa and Churg-Strauss syndrome patients with factors predicting poor prognosis. A prospective, randomized trial in sixty-two patients. *Arthritis Rheum* 1995; **38**: 1638-1645 [PMID: 7488285 DOI: 10.1002/art.1780381116]

World Journal of Gastroenterology

Submit a Manuscript: https://www.f6publishing.com

World J Gastroenterol 2021 January 7; 27(1): 37-54

DOI: 10.3748/wjg.v27.i1.37

ISSN 1007-9327 (print) ISSN 2219-2840 (online)

MINIREVIEWS

Lipidome is lipids regulator in gastrointestinal tract and it is a life collar in COVID-19: A review

Khaled Mohamed Mohamed Koriem

ORCID number: Khaled Mohamed Mohamed Koriem 0000-0002-1323-1700.

Author contributions: Koriem KMM designed the review study, conceived of the manuscript, conducted the literature search and wrote the first and final versions of the manuscript.

Conflict-of-interest statement: The author declares no conflict of interest.

Manuscript source: Invited manuscript

Specialty type: Gastroenterology and hepatology

Country/Territory of origin: Egypt

Khaled Mohamed Mohamed Koriem, Medical Physiology Department, Medical Research Division, National Research Centre, Dokki 12622, Cairo, Egypt

Corresponding author: Khaled Mohamed Mohamed Koriem, PhD, Professor, Medical Physiology Department, Medical Research Division, National Research Centre, 33 El-Buhouth Street, Dokki 12622, Cairo, Egypt. kkoriem@yahoo.com

Abstract

The term lipidome is mentioned to the total amount of the lipids inside the biological cells. The lipid enters the human gastrointestinal tract through external source and internal source. The absorption pathway of lipids in the gastrointestinal tract has many ways; the 1st way, the lipid molecules are digested in the lumen before go through the enterocytes, digested products are re-esterified into complex lipid molecules. The 2nd way, the intracellular lipids are accumulated into lipoproteins (chylomicrons) which transport lipids throughout the whole body. The lipids are re-synthesis again inside the human body where the gastrointestinal lipids are: (1) Transferred into the endoplasmic reticulum; (2) Collected as lipoproteins such as chylomicrons; or (3) Stored as lipid droplets in the cytosol. The lipids play an important role in many stages of the viral replication cycle. The specific lipid change occurs during viral infection in advanced viral replication cycle. There are 47 lipids within 11 lipid classes were significantly disturbed after viral infection. The virus connects with blood-borne lipoproteins and apolipoprotein E to change viral infectivity. The viral interest is cholesterol- and lipid raft-dependent molecules. In conclusion, lipidome is important in gastrointestinal fat absorption and coronavirus disease 2019 (COVID-19) infection so lipidome is basic in gut metabolism and in COVID-19 infection success.

Key Words: Lipidome; Gastrointestinal tract; Fat metabolism; COVID-19; Viral infection; Future therapy

Core Tip: The lipidome is mentioned to the total amount of the lipids inside the biological cells. The lipid enters the human gastrointestinal tract through external

Peer-review report's scientific quality classification
Grade A (Excellent): A, A
Grade B (Very good): 0
Grade C (Good): 0
Grade D (Fair): 0
Grade E (Poor): 0

Received: November 16, 2020
Peer-review started: November 16, 2020
First decision: November 25, 2020
Revised: December 2, 2020
Accepted: December 17, 2020
Article in press: December 17, 2020
Published online: January 7, 2021

P-Reviewer: Alberca RW
S-Editor: Fan JR
L-Editor: A
P-Editor: Ma YJ

source and internal source. The tissue distribution of lipid is completely different among different species. The lipids play an important role in many stages of the viral replication cycle. The specific lipid change occurs during viral infection. The virus connects with blood-borne lipoproteins and apolipoprotein E. The viral interest is cholesterol- and lipid raft-dependent molecules. This review focuses on the important of lipidome in both gastrointestinal fat absorption and coronavirus disease 2019 infection.

Citation: Koriem KMM. Lipidome is lipids regulator in gastrointestinal tract and it is a life collar in COVID-19: A review. *World J Gastroenterol* 2021; 27(1): 37-54
URL: https://www.wjgnet.com/1007-9327/full/v27/i1/37.htm
DOI: https://dx.doi.org/10.3748/wjg.v27.i1.37

INTRODUCTION

The term lipidome or lipidomic is mentioned to the total amount of the lipids inside the biological cells. There are 4 principal constituents occurs inside the biological cells or organs and these 4 constituents are lipids, proteins, sugars and nucleic acids. Lipids are the most important compounds in the living organisms, where they build blocks for cellular membranes, energy storage, and signaling molecules. The technique used in lipidome is generally mass spectrometry (MS)[1]. Lipid metabolism plays an important role in the regulation of cellular homeostasis. Lipid compositions are often used to evaluate lipid metabolism though the application of lipodome[2]. The lipidome or lipidomic is one of the omics science applies in modern biology[3]. There are a tight correlation between lipidomic, metabolomics, genomic and proteomic especially in protective and therapeutic studies[4-6]. Figure 1 explores different types of omics. The lipidome technique applies either by MS or by bioinformatics or ordinary lab-based methods[7,8]. The repeated doses of the drug to micro-tissues lead to collect lipid molecules for 5 time points (2, 4, 7, 9, and 11 d) and hepatotoxic effect occurs[9]. The absorption pathway of lipids in the gastrointestinal tract has many ways; the 1st way, the lipid molecules are digested in the lumen before go through the enterocytes (inside the enterocytes), digested products are re-esterified into complex lipid molecules. The 2nd way, the intracellular lipids are accumulated into lipoproteins (chylomicrons) which transport lipids throughout the whole body[10]. The chylomicrons carrying most of lipids which secreted into the intercellular space, then into the lamina propria, then the lipids enter into the lacteals, and then into the lymphatic system. Thus, the gastrointestinal lymphatic system has a principal role in the absorption of lipids[11-13]. The gastrointestinal lipid metabolism is important to supply of energy (in the form of lipids) to the different organs in the body where the defects in the process of lipid absorption can lead to severe pathological diseases.

Coronavirus disease 2019 (COVID-19) is the last coronavirus outbreak. Coronavirus is derived its name from Latin corona word. Corona virus is first discovered in 1930, while first diagnostic in 1940 in animal models. The first human case of coronavirus is reported in China in 2003 but the COVID-19 was discovered in 2019. This is 3rd serious coronavirus outbreak during the last 20 years, after severe acute respiratory syndrome-related coronavirus (SARS-CoV) in 2002-2003 and Middle East respiratory syndrome-related coronavirus (MERS-CoV) in 2012[14]. There are 7 coronaviruses induce human infections (4 of which, cause cold symptoms in humans while the other 3 coronaviruses called SARS-CoV, MERS-CoV, and COVID-19) cause severe respiratory illness[15]. The coronavirus RNA genome size = 27-34 kilo-bases and this size is the largest RNA genome size. The life cycle of coronavirus is summarized into 3 successive steps: (1) Viral entry; (2) Viral replication; and (3) Viral release. The transmission of COVID-19 in human is occurred though a specific connection process between viral protein and host cell receptor. There are 4 types of coronavirus: (1) *Alphacoronavirus*; (2) *Betacoronavirus*; (3) *Gammacoronavirus*; and (4) *Deltacoronavirus*. Table 1 reveals different genus of coronaviruses. *Betacoronavirus* is the dangerous one because it contains Human coronavirus *e.g.*,., COVID-19, MERS, and severe acute respiratory syndrome-related coronavirus-2 (SARS-CoV-2, SARS-CoV-2). In COVID-19 cases, the attention of blood safety is recommended where coronaviruses have globally arisen especially in endemic areas[16].

Table 1 Different genus of coronaviruses

Coronaviruses	Genus	Type species	Species
Coronaviruses	Alphacoronavirus	Alphacoronavirus 1	Alphacoronavirus 1
			Human coronavirus 229E
			Human coronavirus NL63
			Miniopterus bat coronavirus 1
			Miniopterus bat coronavirus HKU8
			Porcine epidemic diarrhea virus
			Rhinolophus bat coronavirus HKU2
			Scotophilus bat coronavirus 512
	Betacoronavirus	Murine coronavirus	Betacoronavirus 1 (Bovine , Human coronavirus OC43)
			Hedgehog coronavirus 1
			Human coronavirus HKU1
			MERS-CoV
			Murine coronavirus
			Pipistrellus bat coronavirus HKU5
			Rousettus bat coronavirus HKU9
			SARS-CoV, SARS-CoV-2
			Tylonycteris bat coronavirus HKU4
	Gammacoronavirus	Avian coronavirus	Avian coronavirus
			Beluga whale coronavirus SW1
	Deltacoronavirus	Bulbul coronavirus	Bulbul coronavirus HKU11
			Porcine coronavirus HKU15

MERS-CoV: Middle East respiratory syndrome-related coronavirus; SARS-CoV: Severe acute respiratory syndrome-related coronavirus.

The aim of this review is to provide a link between the lipid important in both gastrointestinal fat absorption and COVID-19 infection success. So, this review deals with lipidome in gastrointestinal metabolism and in COVID-19 infection success.

GASTROINTESTINAL UPTAKE OF LIPIDS

The lipid enters the human gastrointestinal tract through 2 sources; external source such as dietary food and internal source such as enterocytes emerge from the gastrointestinal mucosa and from liver bile[17]. The dietary lipids include non-polar lipids, triacylglycerols, cholesterol esters, and polar phospholipids. The liver bile lipids are dissolved in bile acid (include cholesterols and phospholipids). In the gut, the external lipids in diet are hydrolysis by gut lipase to diacylglycerols and fatty acids. The gastrointestinal lipids such as high density lipoproteins, very low density lipoprotein excretion, cytosolic lipid drops and fatty acid oxidation are also included in gastrointestinal lipids[18]. The lipids, as well as, proteins and mucins adhere to plastic particles such as polyvinyl chloride, polyethylene, polyethylene terephthalate polypropylene, and polystyrene. The human gastrointestinal tract do not decays these particles[19]. The high lipid containing-diet for 1 d declined the number of small intestinal intraepithelial lymphocytes and lamina propria lymphocytes. The effect of high lipid containing-diet on the intestinal immune system was independent of the gut microbes. The oral intake of free fatty acids declined the number of small intestinal intraepithelial lymphocytes and lamina propria lymphocytes. So, free fatty acids damaged the intestines and intestinal lipotoxicity occurred as in the case of colorectal cancer or food allergy[20]. The deficiency of fatty acid lead to tissue-resident memory T (Trm) cells death. The gastric adenocarcinoma cells pushed Trm cells for lipid uptake

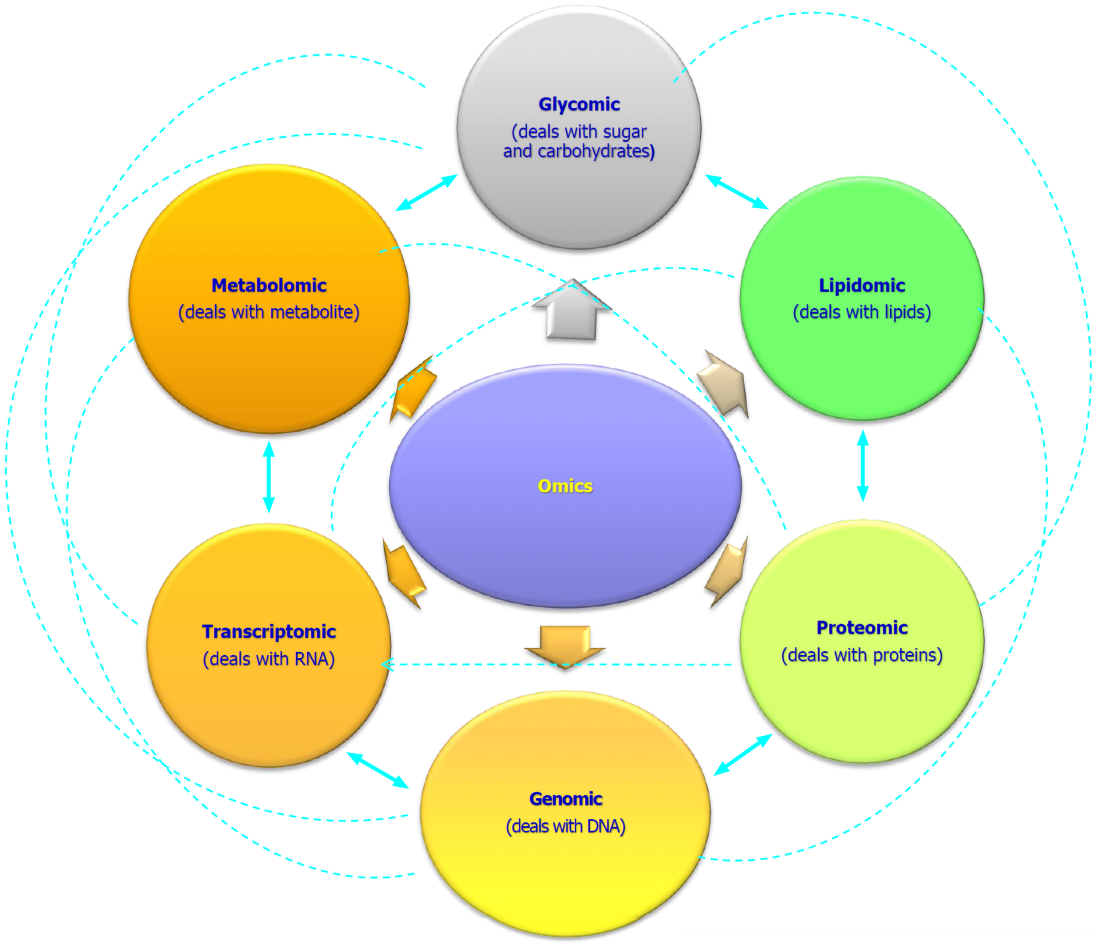

Figure 1 Different types of omics.

and caused Trm cell death[21]. The cancer-associated fibroblasts, through lipidomic technique, accumulate more fatty acids and phospholipids in colorectal cancer cells that plays a principal role in colorectal cancer progress. The fatty acids synthase enzyme, which increased fatty acids synthesis, is considerably increased in cancer-associated fibroblasts[22]. The lipidomics technique in dextran sulfate sodium-induced intestinal barrier dysfunction inhibited the transport and uptake of most of bee pollen lipids such as glycerophospholipids, sphingomyelins, and glycosylsphingolipids. The administration with bee pollen lipids controlled glycerophospholipid and sphingolipid metabolisms that correlated with gastrointestinal permeability barriers and improving gastrointestinal oxidative stress[23]. The gastrointestinal-fatty acid binding protein connected with high-fat diet, leads to changes in gut motility and morphology which caused thinner phenotype occurring at the human whole body. So, gastrointestinal-fatty acid binding protein is incorporated in dietary lipid sensing and signaling which effecting gastrointestinal motility, intestinal configuration, and nutrient absorption and consequently effecting total energy metabolism[24].

GASTROINTESTINAL UPTAKE OF FATTY ACIDS

Fatty acids are uptake by the gastrointestinal tract through 2 ways; the 1st way, fatty acids transfer from the intestinal membrane from higher concentration to lower concentration inside the cell while the 2nd way occurs from the cell to the lumen when the fatty acids concentration inside the cell is higher than lumen fatty acids concentration. The gastrointestinal bile acids are essential for the conservation of their enterohepatic flow. Most of the bile acids are absorbed by gastrointestinal tract *via* certain carrier proteins. These proteins are up-regulate in the distal ileum. The bile acids uptake by gastrointestinal cells reduces the stimulation of cytosolic and membrane receptors (farnesoid X receptor and guanine nucleotide-binding proteins-coupled bile acid receptor 1). These receptors effect on hepatic synthesis of bile acids,

glucose, and lipid metabolism. The increase in bile acid absorption leads to the pathophysiology of liver and metabolic disorders such as fatty liver diseases and type 2 diabetes mellitus[25]. Short-chain fatty acids *e.g.*,. butyrates are bacterial metabolites formed in the gastrointestinal tract and these fatty acids are benefit for host cells. These short-chain fatty acids are stimulators of gastrointestinal cellular gene expression. The propionate and butyrate exert higher efficacy for controlling cell differentiation and gene expression[26]. The tumor necrosis factor-α (TNF-α) is an inflammatory agent associated with gastrointestinal inflammation while omega-3 polyunsaturated fatty acids exert anti-inflammatory activities and stop TNF-α inhibition of sugar uptake by gastrointestinal tract in the human colon cancer cell line (Caco-2). In Caco-2 cancer cells, TNF-α reduces glutamine uptake which counteracts by pro-resolving lipid mediators. So, pro-resolving lipid mediators are favorable biomolecules to restore intestinal nutrients transport during intestinal inflammation[27]. The long-chain fatty acids uptake is an essential physiological process that controls cellular energy homeostasis. The 5' adenosine monophosphate-activated protein kinase accelerates the gastrointestinal long-chain fatty acids uptake by up-regulating human protein is encoded by the CD36 gene (CD36 protein) and stimulating its membrane translocation in the same time[28]. The metabolite of intestinal microbes (TMAVA) level increased in plasma from subjects with liver steatosis compared with controls. The TMAVA declined synthesis of carnitine. The TMAVA changed fecal microbiomes and declined cold tolerance. The TMAVA decreased plasma and liver levels of carnitine and acyl-carnitine. The hepatocytes possessed lower liver fatty acid oxidation. The high fat diet stimulated liver steatosis which declined by carnitine administration. The decrease levels of carnitine and fatty acid oxidation leads to the increase of uptake and liver accumulation of free fatty acids[29]. The colorectal cancer is correlated with the change of fatty acids level in serum and tumor tissues. The colorectal cancer tissues had higher levels of polyunsaturated fatty acids than normal large intestinal mucosa. The change in tumor and serum polyunsaturated fatty acids level is due to the uptake of these fatty acids by cancer cells. The polyunsaturated fatty acids are essential for formation of cell membrane phospholipids during rapid multiplying of cancer cells[30]. The fatty acid system possessed a memory. The memory of the fatty acid system consists of small intestine enterocytes [CD36, scavenger receptor class B type 1, long-chain fatty acid transport protein 4 (FATP4), fatty acid-binding protein 1 (FABP1), FABP2] and hepatocytes. In these cells, the short-term memory fatty acids are found. These short-term fatty acids consist of cytoplasmic lipid droplet cycles. The short-term memory of enterocytes and hepatocytes are united together to form long-term fatty acids memory. These long-term fatty acids memory are found in the adipocyte and in cellular membranes. The formation of fatty acids memory depend on sensing environmental material, encoding, consolidation, long-term storage, retrieval, re-encoding, re-consolidation, and renewed long-term storage[31]. The gastrointestinal microbiome controls many homeostatic processes in the healthy host such as immune function and gut barrier protection. Loss of normal gastrointestinal microbial configuration and function correlated with diseases such as clostridioides difficile infection, asthma, and epilepsy. The change of gastrointestinal microbiome stimulate sepsis by many processes such as: (1) Stimulates pathogenic intestinal bacteria; (2) Instructs the immune system for inflammatory response; and (3) Decreases section of beneficial microbial products such as short-chain fatty acids[32]. 2 meal/d against 12 meal/d declined peri-renal fat weight and serum triglyceride and liposaccharide levels in high fat diet-fed pigs. The decline of meal frequncy down-regulated mRNA expression of lipoprotein lipase, CD36 molecule, interleukin 1 beta, tumor necrosis factor alpha, toll-like receptor 4, myeloid differentiation factor 88, and nuclear factor kappa beta 1 as well as protein expression of myeloid differentiation primary response 88 (MYD88) in perirenal fat of high fat diet-fed pigs. So, the 2 meal/d against the 12 meal/d enhanced high fat diet-induced fat deposition and inflammatory response by decreasing fatty acid uptake[33].

GASTROINTESTINAL UPTAKE OF CHOLESTEROL

The aryl hydrocarbon receptor (AHR) modifies hepatic expression of cholesterol synthesis. Niemann-Pick C1-like intracellular cholesterol transporter (NPC1L1) facilitates the intestinal absorption of dietary cholesterol. The transcription of NPC1L1 involved in the cholesterol synthesis pathway is controlled by sterol-regulatory element-binding protein-2. So, the AHR possessed a role in the homeostatic regulation of cholesterol synthesis and absorption which referred to the application of this

receptor in the treatment of hyperlipidosis-associated metabolic diseases[34]. The decrease of gastrointestinal microbiota diminished albuminuria and tubulointerstitial damage. The serum acetate level was declined in antibiotics-treated diabetic rats and associated with the cholesterol level in the kidney. The acetate increased cholesterol increase in human kidney-2 (HK-2) cells which was induced by higher expression of proteins that reducing cholesterol synthesis and uptake. So, the acetate formed from gastrointestinal microbiota facilitated the imbalance of cholesterol homeostasis and consequently gastrointestinal microbiota reprogramming helping in diabetic nephropathy prevention and therapy[35]. Higher secretion of bile salts into the canalicular lumen increases bile formation and promotes biliary cholesterol and phospholipid output. Disturbing hepatic bile salt uptake was found to limit bile salt flux *via* the liver and consequently decrease biliary lipid excretion. Higher lysosomal discharge into bile increased biliary lipid secretion. The higher bile salts exposed to canalicular membrane leads to more cholesterol and phospholipid molecules to be excreted per bile salt. The increase of biliary lipid secretion is independent on variations in bile salt output, biliary bile salt hydrophobicity, or cholesterol and phospholipid transporters activities. Consequently, increase exposure of the canalicular membrane to bile salts associated with increased biliary cholesterol secretion and this process controls biliary cholesterol and phospholipid secretion[36]. The low-density lipoprotein, high-density lipoprotein and cholesterol levels in the blood become low in Plasmodium falciparum parasites infections in humans. These parasites import cholesterol from the surrounding environment. So, cholesterol import by Plasmodium falciparum includes hepatocytes and cholesterol uptake by the parasites[37]. Lipid structure of liposome alters the cell response for permeability, transport, and uptake in small intestine. The surface statuses of cholesterol-containing liposomes were smooth but they did not affect their transport and uptake through Caco-2 cell and microfold cells monolayers[38]. The sterols occur in the blood circulation either from cholesterol synthesis or gastrointestinal uptake. They are esterified or oxygenated. The cholesterol, cholesterol precursors, plant sterols and oxysterols accumulated in carotid artery plates. The circulating sterols were not reflected sterols levels. The normal cholesterol level occurs when plant sterol (but not oxysterol level) connected between plasma and plates. The oxysterols were lower in plates. Both cholesterol and plant sterols were lower esterified in plates than in plasma. The cholesterol, cholesterol precursors, plant sterols, and oxysterols were increased in symptomatic compared to asymptomatic patients[39]. The brown fat stimulation increases the uptake of cholesterol by the liver and so lowers plasma cholesterol and protects against atherosclerosis occurs. The hepatic cholesterol is converted into bile acids which secreted into the intestine. The bile acids seizure prevents the higher level of plasma bile acids which induced by brown fat activation. This process improves cholesterol metabolism and declines atherosclerosis occurs. Consequently, the collection of both brown fat activation and bile acids seizure is a favorable new therapeutic strategy to decline hyperlipidaemia and cardiovascular diseases[40]. The human Caco-2 cell line is well known *in vitro* model of the gastrointestinal epithelial barrier. The intestine is a major border in cholesterol uptaking and represents a non-biliary way for cholesterol excretion. The Caco-2 cells are a valuable model for investigating cholesterol homeostasis such as cholesterol uptake and efflux[41]. The Caco-2 cells signify the structure and functional properties of small intestinal cells. It is able of expressing brush borders, tight junctions, intestinal efflux and uptake and this control infusion of drugs and food extracts from intestinal lumen to blood circulation. The functional foods and their constituents had anti-proliferative and anti-cancer effects through apoptosis, cell cycle halt and decrease of all signal paths include in Caco-2 cell lines. The transportation, bioavailability, metabolism, mechanisms of actions, cellular paths created by food stuffs in Caco-2 cell lines are affected by their molecular weight, structures and physicochemical properties[42]. The cholesterol homeostasis is controlled by external factors such as diet and internal factors such as certain receptors, enzymes and transcription factors. The receptor 36 (CD36) is a membrane receptor takes place in fatty acid uptake, lipid metabolism, atherothrombosis and inflammation. The CD36 is vital molecule for cholesterol homeostasis in many processes such as absorption/reabsorption, synthesis, and transport of cholesterol and bile acids. The amount of fatty acids and fatty acid structure in the diet affects the CD36 Level and CD36 facilitated cholesterol metabolism in the liver, intestine and macrophages. The CD36 facilitated cholesterol and lipoprotein homeostasis counteracted by dietary saturated fatty acids and *trans*-fatty acids in the diet[43].

UPTAKE OF LYSOPHOSPHOLIPIDS

The bee venom caused skin inflammation which includes erythema, blisters, edemas, pain, and itching. The bee venom has an inhibitory effect on toll-like receptors. The toll-like receptors caused by secretory phospholipase A2. This secretory phospholipase A2 facilitates the hydrolysis of membrane phospholipids into lysophospholipids and free fatty acids[44]. The metabolic analysis in human cancers increased uptake of lysophospholipids and lipid storage, associated with increased fatty acid oxidation that maintains both adenosine triphosphate (ATP) levels and reactive oxygen species (ROS)-detoxifying reduced form of nicotinamide adenine dinucleotide phosphate (NADPH)[45]. The glycerol phosphate process creates higher than 90% of the hepatic triacylglycerol. The lysophosphatidic acid (an intermediate in this process) is created by glycerol-3-phosphate acyltransferase domain containing 3. The glycerophosphodiester phosphodiesterase creates lysophosphatidic acid from lysophospholipids. In human, liver glycerophosphodiester phosphodiesterase overexpression caused increased both lysophosphatidic acid and fatty acids uptake. The liver steatosis patients have increased glycerol-3-phosphate acyltransferase domain containing 3 mRNA levels compared with normal one. Consequently, the glycerol-3-phosphate acyltransferase domain containing 3 overexpression have a vital role in liver triacylglycerol increase and controls liver steatosis[46]. The microalga (Chlorella vulgaris) when exposed to the flame retardant triphenyl phosphate increase the synthesis of membrane lipids but decrease of lysoglycerolipids, fatty acids, and glyceryl-glucoside. On the other side, the microalga Scenedesmus obliquus when exposed to the flame retardant triphenyl phosphate increase lipolysis process such as accumulation of fatty acids, lysophospholipids, and glycerol phosphate[47]. The breathing of sphingosine increased the levels of sphingosine in the luminal membrane of bronchi and the trachea. The breathing of sphingosine without any side effects even with high doses[48]. The lysophosphatidic acid (LPA) is a bioactive lipid mediator which is incorporated in development, physiology, and pathological processes of the cardiovascular system. The LPA created both inside the cells and in the biological fluids. Most of the LPA is created by the secreted lysophospholipase D, autotaxin, *via* its binding to various β integrins or heparin sulfate on cell surface and hydrolyzing many lysophospholipids. The LPA possessed many effects on many blood cells and vascular cells that associated in the development of cardiovascular diseases such as atherosclerosis and aortic valve sclerosis. The LPA caused diversity of monocytes into macrophages and arouses oxidized low-density lipoproteins uptake by macrophages to form foam cells during atherosclerosis[49]. The docosahexaenoic acid-associated lysophosphatidyl choline declined triacylglycerol level due to the increase of carnitine palmitoyltransferase 2 and acyl-CoA oxidase levels and the decrease of acetyl-CoA carboxylase and glucose-6-phosphate dehydrogenase levels in the liver. So, the docosahexaenoic acid-associated lysophosphatidylcholine rich oil has hypolipidemic effect[50].

GASTROINTESTINAL METABOLISM OF ABSORBED LIPIDS

The tissue distribution of lipid is completely different among different species. Tiger puffer possesses lipid storage in the liver. There are 29 lipid metabolism-associated genes. These genes are included in lipogenesis, fatty acid oxidation, biosynthesis and hydrolysis of glycerides, lipid transport, and lipid transcription control. The intestine possesses the high transcription of lipogenic genes while the liver and muscle possesses low lipid gene expression. The intestine also has the highest transcription genes of most apolipoproteins and lipid metabolism-associated transcription factors. The fatty acid oxidation occurs in the mitochondrial β-oxidation in the liver and intestine. The re-acylation of absorbed lipids occurs in the intestine. In conclusion, the intestine is the center of lipid metabolism while the liver is the pure storage organ for lipid[51]. The highly lipophilic food stuffs are occurred in higher concentrations in the medium-chain triglycerides than the long-chain triglycerides. The 30% of the lipophilic food stuffs in medium-chain triglycerides are crossed the Caco-2 cells and 50% of the lipophilic food stuffs in medium-chain triglycerides were metabolized. The 60% of the lipophilic food stuffs in long-chain triglycerides were crossed the Caco-2 cells and 10% of the lipophilic food stuffs in long-chain triglycerides were metabolized. The higher lipid droplets and chylomicrons were formed for the long-chain triglycerides referring to of the lipophilic food stuffs transported through lymph. Although the medium-chain triglycerides possesses the higher of the lipophilic food stuffs, the final amount

of the lipophilic food stuffs absorbed and transported to the lymph was lower to that of the long-chain triglycerides formulation[52]. Vitamin B_6 is found in the diet in many forms but only pyridoxal 5'-phosphate (PLP) can serve as an enzymes cofactor. The intestine absorbs nonphosphorylated B_6 vitamers, which are changed to the active PLP form. Many human processes dependent on PLP such as amino acid and neurotransmitter metabolism, folate metabolism, protein and polyamine synthesis, carbohydrate and lipid metabolism, mitochondrial function and erythropoiesis. There are many roles of PLP beside the role of PLP as a cofactor B_6 vitamers and these roles are antioxidants, altering expression and action of steroid hormone receptors, affecting immune function, and antagonist of adenosine-5'-triphosphate (ATP)[53]. The oxysterols are oxidized forms of cholesterol which created by enzymes or by reactive oxygen species or both. The cholesterol or oxysterols are absorbed and stored in lipoproteins by hepatic cells. Inside the liver, additional cholesterol is metabolized to form bile acids. The endoplasmic reticulum is the main place for bile acid synthesis process. The metabolized sterols from this process are stored in the other places and in the cell membrane. The changes in membrane oxysterol: Sterol ratio affects the cell membrane stucture. The oxysterols changes membrane flexibility and receptor location. The hydroxylase enzymes in the mitochondria expedite oxysterol formation by an acidic process. In lysosomes, the oxysterols are also detected. The biochemical and physiological properties of oxysterols are many and important. Oxysterol levels are associated in many diseases such as chronic inflammatory diseases (Alzheimer's disease, atherosclerosis, and bowel disease), cancer and many neurodegenerative diseases[54]. The lipins possess vital roles in adipogenesis, insulin sensitivity, and gene regulation/mutation in these genes induces lipodystrophy, myoglobinuria, and inflammatory disorders. The lipids (lipid 1, 2, and 3) serve as phosphatidic acid phosphatase enzymes (need for triacylglycerol synthesis). The alteration of fatty acids in diet into triglycerides has been done by lipid 2 and 3. These 2 Lipids phosphatidic acid phosphatase enzymes activities have an important role in phospholipid homeostasis and chylomicron accumulation in enterocytes[55].

THE FINAL FORMS OF GASTROINTESTINAL LIPIDS

The lipids are re-synthesis again inside the human body where the gastrointestinal lipids are: (1) Transferred into the endoplasmic reticulum; (2) Collected as lipoproteins such as chylomicrons; or (3) Stored as lipid droplets in the cytosol. Both chylomicrons and cytosolic lipid droplets possess similar structure. The decrease of the microbiota which produces acetyl-CoA from acetate leads to suppress the change of fructose into hepatic acetyl-CoA and fatty acids. So, the higher fructose consumption facilitates fructose absorption in the small intestine and citrate breakdown in hepatocytes through lipogenesis process. But, the lipogenic transcriptional program stimulates by fructose that is independent of acetyl-CoA metabolism. Consequently, 2 mechanisms regulate hepatic lipogenesis by fructose inside the hepatocytes and these 2 mechanisms are: (1) The expression of lipogenic genes; and (2) The generation of microbial acetate feeds lipogenic pools of acetyl-CoA[56]. There are lower small intestine muscle mass, increase Bacteroidetes, decrease Firmicutes in the large intestine, and decrease of circulating short-chain fatty acids (SCFA) values in non-obese diabetic animals. These changes are correlated with increase body weight, hyperlipidemia, and severe insulin and glucose intolerance. Also, insulin resistance disturbances which related to energy metabolism such as decrease overall respiratory exchange rates but increase liver oxidative activity. There are changes related to gut and microbiota structure which accompanied with decrease of circulating SCFA that leads to metabolic disorders occurs[57]. Vitamin E includes 8 compounds; α-, β-, γ-, and delta-tocopherol and α-, β-, γ-, and delta-tocotrienol. α-tocopherol is found in the human diet. All the above forms of the vitamin E are absorbed in the small intestine, and then the liver metabolizes only α-tocopherol. The liver then removes and excretes the remaining vitamin E forms. Vitamin E deficiency is caused by a diet with low vitamin E or is caused by irregularities in dietary fat absorption or metabolism. Vitamin E is a lipid-soluble vitamin. Vitamin E reduces atherosclerosis and decrease rates of cardiac disease[58]. The different lipids during passage in gastrointestinal tract depend on lipid type and the microenvironment surrounding. The protein is the problem for pancreas lipase to catalyze lipid hydrolysis following gastric digestion. The higher free fatty acids secretion level and rate persistent in small intestine digestion in triacylglycerols (glycerol tripalmitate, glycerol tristearate, glycerol trioleate) in the order of glycerol tripalmitate > glycerol tristearate > glycerol trioleate, respectively[59]. The free fatty

acids secretion during 240 min in-vitro gastrointestinal digestion were measured, and the results proved that the release rate of short-chain saturated fatty acids were higher than the long-chain poly-unsaturated fatty acids. Also, the location of fatty acids inside triacylglycerols possesses an effect on the lipid hydrolysis process through pancreas lipase in gastrointestinal tract using in-vitro digestion model[60]. In the biological system, the gasotransmitters [nitric oxide (NO), hydrogen sulfide (H_2S), and carbon monoxide (CO)] are molecules do neural purposes in the whole body. Also, the gasotransmitters are small and lipid molecules control the changes in lipids rates of production or consumption. Moreover, tissue levels of the gasotransmitters are controlled by the level of O_2 and reactive oxygen species[61]. The changes in intestinal barrier permeability cause severe gastrointestinal disturbances. The leaky gut syndrome is caused by intestinal hyperpermeability due to changes in the expression levels and functioning of tight junctions. The diseases linked to intestinal hyperpermeability are found in Western countries, where a diet possesses higher fats. The fructose is a key that incorporated in the control of the intestinal permeability and induced harmful effects (such as tight junction protein dysfunction). The short chain fatty acids (such as butyrate) cause decrease of intestinal permeability but long chain fatty acids (such as *n*-3 and *n*-6 polyunsaturated fatty acids) have unknown effects[62]. The transepithelial transport rates in the Caco-2 cell were as follows: Scoparone > hydroxycinnamic acid > rutin > quercetin. The main metabolism of hydroxycinnamic acid (quercetin, and scoparone) in transepithelial transport was found to be methylation. Also, triglyceride, low-density lipoprotein cholesterol, total cholesterol, aspartate aminotransferase, and alanine aminotransferase levels in human liver cancer cell line (HepG2 cells) were suppressed by 53.64%, 23.44%, 36.49%, 27.98%, and 77.42% compared to the oleic acid-induced group[63].

COVID-19 AND LIPIDOME

The COVID-19 pandemic presents a global threat to global public health. The plasma lipidome is analyzed in mild, moderate, and severe COVID-19 patients and healthy subjects. Plasma lipidome of COVID-19 contains monosialodihexosyl ganglioside (GM3)-enriched exosomes, with sphingomyelins (SMs) and GM3s, and decrease diacylglycerols (DAGs). The COVID-19 patients with increase disease severity have an increase in GM3s. So, GM3-enriched exosomes participate in pathological cases of COVID-19 and presents the higher source on the plasma lipidome to COVID-19[64]. There is a change in lipid metabolism especially short and medium chain saturated fatty acids, acyl-carnitines, and sphingolipids in COVID-19 patients. But, there are no changes in hematological parameters (red blood cells, hematocrit, and mean corpuscular hemoglobin concentration, with slight increase in mean corpuscular volume) is observed[65,66]. MS-related methods such as lipidomics has been applied in COVID-19 disease outbreaks. Ultra-high-pressure liquid chromatographies with high-resolution mass spectrometry (UHPLC-HRMS)-based lipidomics are used to identify infectious pathogens and biomarkers related in COVID-19. Polymerase chain reaction-mass spectrometry (PCR-MS) is a new technology to determine known pathogens from the clinical specimens. Also, miniaturized MS provides an application with fast, high sensitive and easy way to analyze for COVID-19. Consequently, MS-related methods are an easy and sensitive way in studying corona outbreaks such as COVID-19[67]. MS-related, lipidomics method provides a suitable way of virus-induced changes to the host after infection and can lead to the determination of new therapeutic agents for preventing disease spreading. The omics study with MERS-CoV is used lipid extraction to develop a single sample in lipids determination in COVID-19 infection[68]. The lipidomic changes such as structural-lipids, the eicosanoids, and docosanoids lipid mediators (LMs) are important for the diagnosis of COVID-19 disease severity. The progression from moderate to severe disease is accompanied with loss of specific immune regulatory LMs and increased pro-inflammatory cytokines[69,70]. COVID-19 exerts higher effect on the metabolism. The lipidomic analysis showed pathogenic redistribution of the lipoprotein particle size and composition to increase the atherosclerotic danger. The metabolomic analysis showed abnormal high levels of ketone bodies such as acetoacetic acid, 3-hydroxybutyric acid, and acetone. Also, higher increase of 2-hydroxybutyric acid (an indication of hepatic glutathione synthesis and oxidative stress marker). So, SARS-CoV-2 infection caused liver damage correlated with dyslipidemia and oxidative stress[71]. The viral infection is depended on the lipid metabolism of the infected cells. From a lipidomics view, there are many mechanisms connecting to viral infection such as viral entry, the disorder of host cell

lipid metabolism, and the role related to different lipids in the infection efficiency. So, lipids play an important role in COVID-10 infection success especially the role of cholesterol in the success of viral infection[72]. Figure 2 exhibits lipidome and COVID-19 in gastrointestinal tract.

LIPIDOME VIEW IN VIRAL REPLICATION CYCLES

COVID-19 is a virus and this virus is dependent on its lipid cover which possesses high capability to detergent. The lipids play an important role in many stages of the virus replication cycle. The definite lipid change occurs during viral infection in higher viral replication cycle. There are 47 lipids within 11 lipid classes were significantly disturbed after viral infection. There are 4 polyunsaturated fatty acids (PUFAs): (1) Arachidonic acid (AA); (2) Docosahexaenoic acid (DHA); (3) Docosapentaenoic acid (DPA); and (4) Eicosapentaenoic acid (EPA) were upregulated during viral infection. The 3 of these 4 fatty acids (PUFAs; AA, DHA, and EPA) declined viral replication. Consequently, enteroviruses modify the host lipid pathways for higher virus replication. Higher exogenous lipids prevent effective viral replication. The control of the host lipid profile is a host-targeting antiviral strategy for enterovirus infection[73]. In hepatitis C virus (HCV) infection, the HCV reproduction depends on many lipid metabolic processes during viral life cycle. The HCV induces cells' lipidomic profile changes by controlling many key pathways of lipid synthesis, remodeling and utilization. So, the lipids play a significant role in HCV RNA replication, meeting and entrance. In viral process, there are many changes in the cell fatty acid content and variations of the membrane lipid composition during replication of the virus. In viral process, the lipids represent lipid provider during replication and as an essential hub for HCV meeting. The lipoproteins play an important role in HCV maturation and entrance[74]. There is an increase in the levels of many phosphatidylethanolamine (PE) lipids in the serum of Zika virus patients, most of them plasmenyl-phosphatidylethanolamine (pPE) (or plasmalogens) correlated with polyunsaturated fatty acids. The plasmalogens correlated with polyunsaturated fatty acids are abundant in neural membranes of the brain and these represent 20% of total phospholipids in humans. The biosynthesis of plasmalogens is necessary for efficient peroxisomes, which are important sites for Zika virus replication[75]. A stable benzoic derivative of retinoic acid (AM580) and retonic acid receptor-αagonist has greater effective in disturbing the life cycle of many viruses such as MERS-coronavirus and influenza A virus. The sterol regulatory element binding protein (SREBP) connect with AM580 and exerts antiviral effect. Consequently, lipidome technique plays a major role in human viral infections where SREBP is an effective agent in the antiviral strategies development[76]. The glycerophospholipids and fatty acids increased in human coronavirus 229E-infected cells and the linoleic acid (LA) to AA metabolism was disturbed in HCoV-229E infection by using high performance liquid chromatography-associated with lipidome technique. Supplementation with LA or AA in HCoV-229E-infected cells depressed HCoV-229E virus replication. The inhibition of LA and AA on virus replication can be seen in MERS-CoV. So, the host lipid metabolic processes correlated with human-coronavirus proliferation. Consequently, the control of lipid metabolism is the main goal for coronavirus infections[77]. The cell lipidome technique shows an increase in phospholipase A2 (PLA2) activity to produce lyso-phosphatidylcholine (lyso-PChol). The PLA2 enzyme family is activated in West Nile virus strain Kunjin virus-infected cells and produces lyso-PChol lipid molecules that need for viral reproduction. The production of lyso-PChol is increased by inhibition of PLA2 in West Nile virus strain Kunjin virus reproduction and production of infectious virus is occurred. The lyso-PChol related to the formation of the West Nile virus strain Kunjin virus replication complex (RC). Consequently, lipid homeostasis enables the researchers to understand flaviviruses replication[78]. The HCV-infected cells contain higher amounts of phosphatidylcholines and triglycerides with longer fatty acyl chains and increased use of C18 fatty acids especially oleic acid. So, decrease of fatty acid elongases and desaturases reduces HCV reproduction. There is an increase in the levels of polyunsaturated fatty acids (PUFAs) in HCV infection. The decrease of the PUFA synthesis path damaged viral reproduction, indicating that higher PUFAs are needed for viral replication. Consequently, the control of the host cell lipid metabolism is needed and caused by HCV to increase viral replication[79].

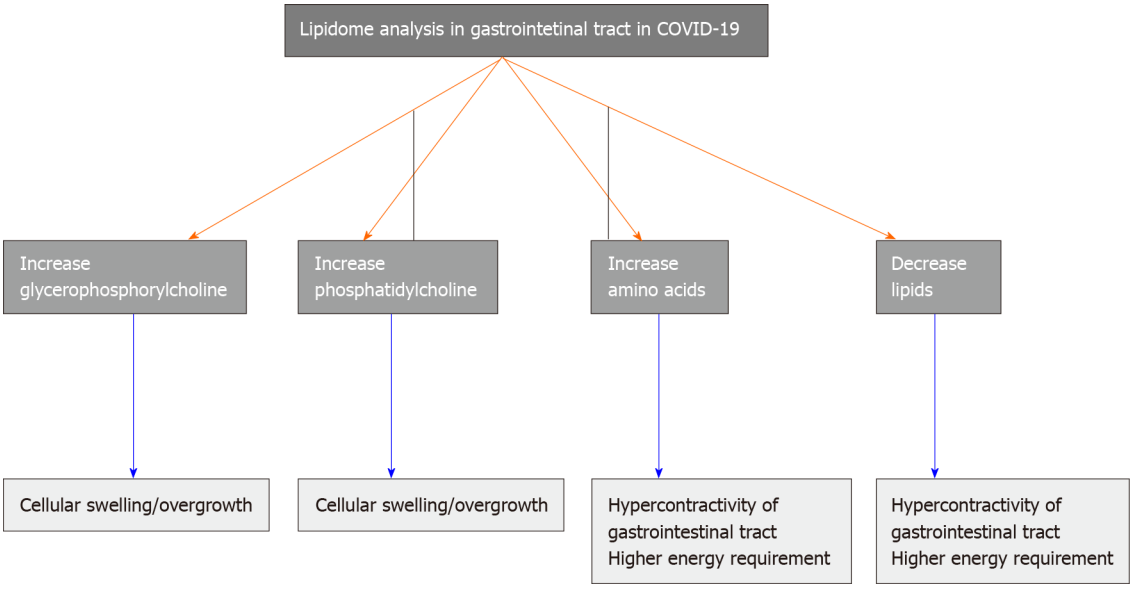

Figure 2 Lipidome and COVID-19 in gastrointestinal tract.

THE ROLE OF LIPIDOME DURING THE HOST-VIRAL INTERACTIONS

In the recent century, researches using genetic, cell biological, and biochemical techniques has led to huge increase in molecular and biological insight into interaction of virus with their hosts. Cell biological studies depend on microscope as a principal technique, of basic microbiology methods so these researches added more data to host-viral interactions. On the other hand, the biomedical researches, the main focus was on the determination of genes and proteins necessary for activity. Based on these findings there is now increased consciousness that lipids (both of host and of virus) play vital roles in regulating infection stability, entry into host cells, as well as, replication and persistence of the virus. There is a connection between the host protein disulfide isomerase (PDI) with dengue virus protein and role of lipid raft in viral infection. The PDI correlates with dengue virus nonstructural protein 1 (NS1) inside the biological cell as well as on the surface in the lipid raft molecule. Disturbance of this relation between PDI and NS1 is important in treatment strategy to stop dengue virus infection[80]. The virus connects with blood-borne lipoproteins and apolipoprotein E (apoE) to change viral infectivity. Viral interest is cholesterol- and lipid raft-dependent (24-dehydrocholesterol reductase, 3-hydroxy-3-methylglutaryl-CoA reductase, fibrin degradation products, raft-linking protein, Sterol regulatory element-binding transcription factor 1). The virus is gone to the nucleus through the dynein and kinesin motors. Amyloid precursor protein has a role nucleus invention by the virus. The viral protein removes mitochondrial DNA as in Alzheimer's disease case. The virus connects with the host transcription factors transcription factor CP2 and POU domain, class 2, transcription factor 1 that control many other genes. Viral inactivity is controlled by interleukin 6 (IL6) and IL1β. Viral avoidance occurs by inhibition of the antigen processor human gene that encodes the protein antigen peptide transporter 2, the production of an Fc immunoglobulin receptor mimic and inhibition of the viral-activated kinase eukaryotic interferon-inducible factor 2 alpha kinase[81]. The role of lipidome during the host-viral interactions includes 2 main categories: (1) cell and chemical biology in the viral-host interaction; and (2) lipid profiling in the viral-host interaction.

Cell and chemical biology in the viral-host interaction

There is an important host factor (CPSF6) connects with nuclear protein (NP1). The CPSF6 increases the nuclear production of NP1 in the same time CPSF6 possesses an important role in progress of capsid mRNAs inside the nucleus. The connection between viral NP1 and host CPSF6 gives the scientist the mechanism enables viral protein increases the viral gene expression and replication as well as antiviral drug discovery[82]. The virus infection causes spreading of the distraction of transcription termination (DoTT) of RNA polymerase II (RNAPII) in host genes. The herpes simplex virus-1 (HSV-1) immediate early protein (ICP27) causes widespread DoTT through connection with essential mRNA 3' processing factor (CPSF). The ICP27 stimulates

mRNA 3' processing for viral and host transcription. So, ICP27 possesses an important role in HSV-1-causes viral infection while CPSF stimulates regulation of transcription end[83]. The RNA binding-deficient stores in nucleoprotein (NP) bodies and the nuclear RNA export factor 1 (NXF1) is necessary for viral protein expression but not for viral RNA synthesis. The NXF1 connects with viral mRNAs but not with viral RNAs. Consequently, the NXF1 promotes the export of viral mRNA:NXF1 complexes from inclusion bodies. This provides a basis for new therapeutic approaches for viruses[84]. The ribosomal proteins (RPs) contain 60S subunit control translation of specific mRNAs. The translation process of the RPs in this process controls in the catalyzing peptide bond formation. The ribosomal protein L13 (RPL13) is a regulator of viral translation and infection. Consequently, understanding this process gives rise to the effects for the translation of viral mRNA and thus for the development of viral prevention[85]. The influenza A viruses contain RNA genome include 8 segments. Each RNA segment correlated with the NP and viral RNA polymerase to and from a viral ribonucleoprotein (vRNP) molecule. The formation of viral mRNA is dependent on the host RNA transcription and for these processes to be occurred; the vRNPs must pass through the cell nuclear pore complex (NPC) to the nucleus. The influenza A virus NS2 protein, also called the nuclear export protein and this protein connects with the host cellular nucleoporins during the nuclear export of vRNPs. The human nucleoporin 214 (Nup214) is called NS2-binding protein and NS2 protein coonects with the amino terminal FG domain of the Nup214 protein. The influenza viral replication was decreased by the Nup214 protein. Consequently, the FG domains of nucleoporins have an important role in the connection of the influenza NS2 protein with host NPC for viral RNA (vRNA) spread[86]. The importin-α3 (one of the main nuclear factor kappa-light-chain-enhancer of activated B cells (NF-κB) transporters) is the expressed nuclear factor in the mammalian respiratory tract. Importin-α3 promoter effect is controlledby TNF-α-induced NF-κB. The increasing of TNF-α increasing pathogenic avian influenza A viruses (HPAIVs) in serious human cases protecting human polymerase signatures (PB2 627K, 701N) which downregulate importin-α3 mRNA expression in the lung cells. The decrease of Importin-α3 is returned by the mutating of the HPAIV polymerase into an avian-type signature (PB2 627E, 701D) which suppresses the high TNF-α levels. The decrease of importin-α3 decreased the NF-κB antiviral gene expression and increased influenza dangerous. Consequently, importin-α3 possesses a role in antiviral immunity in influenza and so importin-α3 in the lung help in the strategy to fight respiratory virus infections[87]. During rotavirus infection, the small interfering RNA (siRNA) facilitates genetic exhaustion of ATP5B or other ATP synthase molecules (ATP5A1 and ATP5O) decreases the production of viral new generations without modification of viral RNA amounts and translation. The ATP5B controls the late-stage rotavirus growth in intestinal cells. Consequently, the role of host proteins in rotavirus RNA identifies ATP5B as a novel pro-rotavirus RNA-binding protein that help scientists to understand virus growth and pathogenesis[88]. The host protein (hnRNP C1/C2) decreases viral RNA translation. The hnRNP C1/C2 connects with stem-loop V in the Internal Ribosome Entry Site' (IRES) and transfers binding protein where this protein controls of viral translation. The hnRNP C1/C2 causes changing of viral translation to replication. Consequently, the hnRNP C1/C2 controls of viral RNA translation to replication by a specific mechanism[89]. The connection of glycyl-tRNA synthetase (GARS) increases the environmental of the initiation area of the internal IRES in the mRNA binding site of the ribosome that increasing IRES effect at the step of initiation formation[90].

Lipid profiling in the viral-host interaction

The studies of viral lipids are not new trends. The main developments in analytical biochemistry have added new information to these studies. The liquid chromatography and MS are the most important techniques applied in the field of lipidome. These techniques allow detection, characterization, and quantification of huge molecules of lipids (although it is currently not possible to determine the full "lipidome" of a cell or tissue in one study). The major biochemical information of lipid lists (*e.g.*,. of mycobacteria) is now applied to investigate the details of lipid biosynthesis and lipid transporters. Potato is a natural host of Potato spindle tuber viroid (PSTVd) which causes arresting phenotype and alteration of leaves and tubers. The PSTVd virus replicates in the nucleus and moves in the plant. The host possesses defense, stress and sugar metabolism correlated genes which alters expression levels in infection and the hormone-related genes showed up- or down-regulation. Consequently, gibberellin and brassinosteroid paths possess an important role in tuber development upon PSTVd infection[91]. In dengue virus infection, there is an increase in mRNA, myeloid differentiation 2-related lipid recognition protein (ML) and Niemann

Pick-type C1 (NPC1) genes. These 3 genes translate lipid-binding proteins which play an important role in host-viral connection. The RNA interference (RNAi)-mediated gene stops the ML and NPC1 genes. In viral infection, ML and NPC1 increase viral infection by reducing the host immune ability. Consequently, the dengue virus effects the expression of these genes to stimulate viral infection of the mosquito host[92].

FUTURE THERAPY OF CORONAVIRUS

No vaccines or antiviral drug to prevent or treat human coronavirus infections is available. The coronavirus treatment is only caring. There are many antiviral agents used *e.g.*, viral proteases, polymerases and entry proteins. Coronavirus is capable to replicate in invitro study such as human lung cancer cell line (Calu-3 cells) and causes lower transcriptomic variations before 12 h after viral infection. As infection progress, coronavirus causes a significant dysregulation of the host transcriptome greater than SARS virus. Both viruses induced a similar stimulation of host receptors and the interleukin 17 paths but coronavirus inhibits the expression of many genes such as type I and II major histocompatibility complex genes. This viral effect identifies the ability of the host response to viral infection. There are 207 genes was inhibited following coronavirus infection, and was used to detect the antiviral secretions such as kinase inhibitors and glucocorticoids. Consequently, coronavirus and SARS virus possesses host gene expression reactions that effect on *in vivo* pathogenesis and therapeutic strategies[93]. In coronavirus infection, the whole blood cytokine investigations increased the cytokine expression in the viral cell infected case. The inflammatory gene expression increased after dysfunction of respiratory function, except the expression in the IL1 path. The investigations of CD4 and CD8 expression showed that the pro-inflammatory factors increased with T cell initiation that leads to prolong the disease or prolong the infection. Consequently, the pro-inflammatory factors such as IL1 and related pro-inflammatory paths analyzes and uses as therapeutic agents for COVID-19[94].

CONCLUSION

The term lipidome is mentioned to the total amount of the lipids inside the biological cells. The lipid enters the human gastrointestinal tract through external source and internal source. The lipids are re-synthesis again inside the human body where the gastrointestinal lipids are: (1) Transferred into the endoplasmic reticulum; (2) Collected as lipoproteins such as chylomicrons; or (3) Stored as lipid droplets in the cytosol. The tissue distribution of lipid is completely different among different species. Fatty acids are uptake by the gastrointestinal tract through 2 ways; the 1st way, fatty acids transfer from the intestinal membrane from higher concentration to lower concentration inside the cell while the 2nd way occurs from the cell to the lumen when the fatty acids concentration inside the cell is higher than lumen fatty acids concentration. The lipids play an important role in many stages of the viral replication cycle. There are 47 Lipids within 11 Lipid classes were significantly disturbed after viral infection. The virus connects with blood-borne lipoproteins and apolipoprotein E to change viral infectivity. The viral interest is cholesterol- and lipid raft-dependent molecules. The future therapy of coronavirus includes the investigations of CD4 and CD8 expression where these pro-inflammatory factors increased with T cell initiation that leads to prolong the infection.

REFERENCES

1 **Züllig T**, Trötzmüller M, Köfeler HC. Lipidomics from sample preparation to data analysis: a primer. *Anal Bioanal Chem* 2020; **412**: 2191-2209 [PMID: 31820027 DOI: 10.1007/s00216-019-02241-y]

2 **Schlame M**, Xu Y, Erdjument-Bromage H, Neubert TA, Ren M. Lipidome-wide ^{13}C flux analysis: a novel tool to estimate the turnover of lipids in organisms and cultures. *J Lipid Res* 2020; **61**: 95-104 [PMID: 31712250 DOI: 10.1194/jlr.D119000318]

3 **Quehenberger O**, Armando AM, Brown AH, Milne SB, Myers DS, Merrill AH, Bandyopadhyay S, Jones KN, Kelly S, Shaner RL, Sullards CM, Wang E, Murphy RC, Barkley RM, Leiker TJ, Raetz CR, Guan Z, Laird GM, Six DA, Russell DW, McDonald JG, Subramaniam S, Fahy E, Dennis EA. Lipidomics reveals a remarkable diversity of lipids in human plasma. *J Lipid Res* 2010; **51**: 3299-3305 [PMID: 20671299 DOI: 10.1194/jlr.M009449]

4 **Koriem KMM**. A lipidomic concept in infectious diseases. *Asian Pac J Trop Biomed* 2017; **7**: 265-274 [DOI: 10.1016/j.apjtb.2016.12.010]
5 **Koriem KMM**. Protective effect of natural products and hormones in colon cancer using metabolome: A physiological overview. *Asian Pac J Trop Biomed* 2017; **7**: 957-966 [DOI: 10.1016/j.apjtb.2017.09.002]
6 **Koriem KMM**. Proteomic approach in human health and disease: Preventive and cure studies. *Asian Pac J Trop Biomed* 2018; **8**: 226-236 [DOI: 10.4103/2221-1691.231285]
7 **Subramaniam S**, Fahy E, Gupta S, Sud M, Byrnes RW, Cotter D, Dinasarapu AR, Maurya MR. Bioinformatics and systems biology of the lipidome. *Chem Rev* 2011; **111**: 6452-6490 [PMID: 21939287 DOI: 10.1021/cr200295k]
8 **Seppänen-Laakso T**, Oresic M. How to study lipidomes. *J Mol Endocrinol* 2009; **42**: 185-190 [PMID: 19060177 DOI: 10.1677/JME-08-0150]
9 **Goracci L**, Valeri A, Sciabola S, Aleo MD, Moritz W, Lichtenberg J, Cruciani G. A Novel Lipidomics-Based Approach to Evaluating the Risk of Clinical Hepatotoxicity Potential of Drugs in 3D Human Microtissues. *Chem Res Toxicol* 2020; **33**: 258-270 [PMID: 31820940 DOI: 10.1021/acs.chemrestox.9b00364]
10 **Tso P**, Balint JA. Formation and transport of chylomicrons by enterocytes to the lymphatics. *Am J Physiol* 1986; **250**: G715-G726 [PMID: 3521320 DOI: 10.1152/ajpgi.1986.250.6.G715]
11 **D'Aquila T**, Hung YH, Carreiro A, Buhman KK. Recent discoveries on absorption of dietary fat: Presence, synthesis, and metabolism of cytoplasmic lipid droplets within enterocytes. *Biochim Biophys Acta* 2016; **1861**: 730-747 [PMID: 27108063 DOI: 10.1016/j.bbalip.2016.04.012]
12 **Hung YH**, Carreiro AL, Buhman KK. Dgat1 and Dgat2 regulate enterocyte triacylglycerol distribution and alter proteins associated with cytoplasmic lipid droplets in response to dietary fat. *Biochim Biophys Acta Mol Cell Biol Lipids* 2017; **1862**: 600-614 [PMID: 28249764 DOI: 10.1016/j.bbalip.2017.02.014]
13 **Hussain MM**. Intestinal lipid absorption and lipoprotein formation. *Curr Opin Lipidol* 2014; **25**: 200-206 [PMID: 24751933 DOI: 10.1097/MOL.0000000000000084]
14 **Yang Y**, Peng F, Wang R, Yange M, Guan K, Jiang T, Xu G, Sun J, Chang C. The deadly coronaviruses: The 2003 SARS pandemic and the 2020 novel coronavirus epidemic in China. *J Autoimmun* 2020; **109**: 102434 [PMID: 32143990 DOI: 10.1016/j.jaut.2020.102434]
15 **Hasöksüz M**, Kiliç S, Saraç F. Coronaviruses and SARS-COV-2. *Turk J Med Sci* 2020; 549-556 [PMID: 32293832 DOI: 10.3906/sag-2004-127]
16 **Chang L**, Yan Y, Wang L. Coronavirus Disease 2019: Coronaviruses and Blood Safety. *Transfus Med Rev* 2020; **34**: 75-80 [PMID: 32107119 DOI: 10.1016/j.tmrv.2020.02.003]
17 **Shiau YF**, Popper DA, Reed M, Umstetter C, Capuzzi D, Levine GM. Intestinal triglycerides are derived from both endogenous and exogenous sources. *Am J Physiol* 1985; **248**: G164-G169 [PMID: 3970197 DOI: 10.1152/ajpgi.1985.248.2.G164]
18 **Ko CW**, Qu J, Black DD, Tso P. Regulation of intestinal lipid metabolism: current concepts and relevance to disease. *Nat Rev Gastroenterol Hepatol* 2020; **17**: 169-183 [PMID: 32015520 DOI: 10.1038/s41575-019-0250-7]
19 **Stock V**, Fahrenson C, Thuenemann A, Dönmez MH, Voss L, Böhmert L, Braeuning A, Lampen A, Sieg H. Impact of artificial digestion on the sizes and shapes of microplastic particles. *Food Chem Toxicol* 2020; **135**: 111010 [PMID: 31794801 DOI: 10.1016/j.fct.2019.111010]
20 **Tanaka S**, Nemoto Y, Takei Y, Morikawa R, Oshima S, Nagaishi T, Okamoto R, Tsuchiya K, Nakamura T, Stutte S, Watanabe M. High-fat diet-derived free fatty acids impair the intestinal immune system and increase sensitivity to intestinal epithelial damage. *Biochem Biophys Res Commun* 2020; **522**: 971-977 [PMID: 31810607 DOI: 10.1016/j.bbrc.2019.11.158]
21 **Lin R**, Zhang H, Yuan Y, He Q, Zhou J, Li S, Sun Y, Li DY, Qiu HB, Wang W, Zhuang Z, Chen B, Huang Y, Liu C, Wang Y, Cai S, Ke Z, He W. Fatty Acid Oxidation Controls $CD8^+$ Tissue-Resident Memory T-cell Survival in Gastric Adenocarcinoma. *Cancer Immunol Res* 2020; **8**: 479-492 [PMID: 32075801 DOI: 10.1158/2326-6066.CIR-19-0702]
22 **Gong J**, Lin Y, Zhang H, Liu C, Cheng Z, Yang X, Zhang J, Xiao Y, Sang N, Qian X, Wang L, Cen X, Du X, Zhao Y. Reprogramming of lipid metabolism in cancer-associated fibroblasts potentiates migration of colorectal cancer cells. *Cell Death Dis* 2020; **11**: 267 [PMID: 32327627 DOI: 10.1038/s41419-020-2434-z]
23 **Li Q**, Liang X, Xue X, Wang K, Wu L. Lipidomics Provides Novel Insights into Understanding the Bee Pollen Lipids Transepithelial Transport and Metabolism in Human Intestinal Cells. *J Agric Food Chem* 2020; **68**: 907-917 [PMID: 31842537 DOI: 10.1021/acs.jafc.9b06531]
24 **Lackey AI**, Chen T, Zhou YX, Bottasso Arias NM, Doran JM, Zacharisen SM, Gajda AM, Jonsson WO, Córsico B, Anthony TG, Joseph LB, Storch J. Mechanisms underlying reduced weight gain in intestinal fatty acid-binding protein (IFABP) null mice. *Am J Physiol Gastrointest Liver Physiol* 2020; **318**: G518-G530 [PMID: 31905021 DOI: 10.1152/ajpgi.00120.2019]
25 **Ticho AL**, Malhotra P, Dudeja PK, Gill RK, Alrefai WA. Intestinal Absorption of Bile Acids in Health and Disease. *Compr Physiol* 2019; **10**: 21-56 [PMID: 31853951 DOI: 10.1002/cphy.c190007]
26 **Pearce SC**, Weber GJ, van Sambeek DM, Soares JW, Racicot K, Breault DT. Intestinal enteroids recapitulate the effects of short-chain fatty acids on the intestinal epithelium. *PLoS One* 2020; **15**: e0230231 [PMID: 32240190 DOI: 10.1371/journal.pone.0230231]
27 **Castilla-Madrigal R**, Gil-Iturbe E, López de Calle M, Moreno-Aliaga MJ, Lostao MP. DHA and its derived lipid mediators MaR1, RvD1 and RvD2 block TNF-α inhibition of intestinal sugar and

glutamine uptake in Caco-2 cells. *J Nutr Biochem* 2020; **76**: 108264 [PMID: 31760230 DOI: 10.1016/j.jnutbio.2019.108264]

28 **Wu W**, Wang S, Liu Q, Shan T, Wang X, Feng J, Wang Y. AMPK facilitates intestinal long-chain fatty acid uptake by manipulating CD36 expression and translocation. *FASEB J* 2020; **34**: 4852-4869 [PMID: 32048347 DOI: 10.1096/fj.201901994R]

29 **Zhao M**, Zhao L, Xiong X, He Y, Huang W, Liu Z, Ji L, Pan B, Guo X, Wang L, Cheng S, Xu M, Yang H, Yin Y, Garcia-Barrio MT, Chen YE, Meng X, Zheng L. TMAVA, a Metabolite of Intestinal Microbes, Is Increased in Plasma From Patients With Liver Steatosis, Inhibits γ-Butyrobetaine Hydroxylase, and Exacerbates Fatty Liver in Mice. *Gastroenterology* 2020; **158**: 2266-2281. e27 [PMID: 32105727 DOI: 10.1053/j.gastro.2020.02.033]

30 **Mika A**, Kobiela J, Pakiet A, Czumaj A, Sokołowska E, Makarewicz W, Chmielewski M, Stepnowski P, Marino-Gammazza A, Sledzinski T. Preferential uptake of polyunsaturated fatty acids by colorectal cancer cells. *Sci Rep* 2020; **10**: 1954 [PMID: 32029824 DOI: 10.1038/s41598-020-58895-7]

31 **Straub RH**. The memory of the fatty acid system. *Prog Lipid Res* 2020; **79**: 101049 [PMID: 32589906 DOI: 10.1016/j.plipres.2020.101049]

32 **Adelman MW**, Woodworth MH, Langelier C, Busch LM, Kempker JA, Kraft CS, Martin GS. The gut microbiome's role in the development, maintenance, and outcomes of sepsis. *Crit Care* 2020; **24**: 278 [PMID: 32487252 DOI: 10.1186/s13054-020-02989-1]

33 **Yan H**, Cao S, Li Y, Zhang H, Liu J. Reduced meal frequency alleviates high-fat diet-induced lipid accumulation and inflammation in adipose tissue of pigs under the circumstance of fixed feed allowance. *Eur J Nutr* 2020; **59**: 595-608 [PMID: 30747271 DOI: 10.1007/s00394-019-01928-3]

34 **Muku GE**, Kusnadi A, Kuzu G, Tanos R, Murray IA, Gowda K, Amin S, Perdew GH. Selective Ah receptor modulators attenuate NPC1L1-mediated cholesterol uptake through repression of SREBP-2 transcriptional activity. *Lab Invest* 2020; **100**: 250-264 [PMID: 31417158 DOI: 10.1038/s41374-019-0306-x]

35 **Hu ZB**, Lu J, Chen PP, Lu CC, Zhang JX, Li XQ, Yuan BY, Huang SJ, Ruan XZ, Liu BC, Ma KL. Dysbiosis of intestinal microbiota mediates tubulointerstitial injury in diabetic nephropathy *via* the disruption of cholesterol homeostasis. *Theranostics* 2020; **10**: 2803-2816 [PMID: 32194836 DOI: 10.7150/thno.40571]

36 **Roscam Abbing RLP**, Slijepcevic D, Donkers JM, Havinga R, Duijst S, Paulusma CC, Kuiper J, Kuipers F, Groen AK, Oude Elferink RPJ, van de Graaf SFJ. Blocking Sodium-Taurocholate Cotransporting Polypeptide Stimulates Biliary Cholesterol and Phospholipid Secretion in Mice. *Hepatology* 2020; **71**: 247-258 [PMID: 31136002 DOI: 10.1002/hep.30792]

37 **Hayakawa EH**, Kato H, Nardone GA, Usukura J. A prospective mechanism and source of cholesterol uptake by Plasmodium falciparum-infected erythrocytes co-cultured with HepG2 cells. *Parasitol Int* 2021; **80**: 102179 [PMID: 32853776 DOI: 10.1016/j.parint.2020.102179]

38 **Konishi K**, Du L, Francius G, Linder M, Sugawara T, Kurihara H, Takahashi K. Lipid Composition of Liposomal Membrane Largely Affects Its Transport and Uptake through Small Intestinal Epithelial Cell Models. *Lipids* 2020; **55**: 671-682 [PMID: 32770855 DOI: 10.1002/lipd.12269]

39 **Ceglarek U**, Dittrich J, Leopold J, Helmschrodt C, Becker S, Staab H, Richter O, Rohm S, Aust G. Free cholesterol, cholesterol precursor and plant sterol levels in atherosclerotic plaques are independently associated with symptomatic advanced carotid artery stenosis. *Atherosclerosis* 2020; **295**: 18-24 [PMID: 31981947 DOI: 10.1016/j.atherosclerosis.2019.12.018]

40 **Zhou E**, Hoeke G, Li Z, Eibergen AC, Schonk AW, Koehorst M, Boverhof R, Havinga R, Kuipers F, Coskun T, Boon MR, Groen AK, Rensen PCN, Berbée JFP, Wang Y. Colesevelam enhances the beneficial effects of brown fat activation on hyperlipidaemia and atherosclerosis development. *Cardiovasc Res* 2020; **116**: 1710-1720 [PMID: 31589318 DOI: 10.1093/cvr/cvz253]

41 **Hiebl V**, Schachner D, Ladurner A, Heiss EH, Stangl H, Dirsch VM. Caco-2 Cells for Measuring Intestinal Cholesterol Transport - Possibilities and Limitations. *Biol Proced Online* 2020; **22**: 7 [PMID: 32308567 DOI: 10.1186/s12575-020-00120-w]

42 **Iftikhar M**, Iftikhar A, Zhang H, Gong L, Wang J. Transport, metabolism and remedial potential of functional food extracts (FFEs) in Caco-2 cells monolayer: A review. *Food Res Int* 2020; **136**: 109240 [PMID: 32846508 DOI: 10.1016/j.foodres.2020.109240]

43 **Ulug E**, Nergiz-Unal R. Dietary fatty acids and CD36-mediated cholesterol homeostasis: potential mechanisms. *Nutr Res Rev* 2020; 1-14 [PMID: 32308181 DOI: 10.1017/S0954422420000128]

44 **Nakashima A**, Tomono S, Yamazaki T, Inui M, Morita N, Ichimonji I, Takagi H, Nagaoka F, Matsumoto M, Ito Y, Yanagishita T, Miyake K, Watanabe D, Akashi-Takamura S. Phospholipase A2 from bee venom increases poly(I:C)-induced activation in human keratinocytes. *Int Immunol* 2020; **32**: 371-383 [PMID: 31957789 DOI: 10.1093/intimm/dxaa005]

45 **Qiao S**, Koh SB, Vivekanandan V, Salunke D, Patra KC, Zaganjor E, Ross K, Mizukami Y, Jeanfavre S, Chen A, Mino-Kenudson M, Ramaswamy S, Clish C, Haigis M, Bardeesy N, Ellisen LW. REDD1 loss reprograms lipid metabolism to drive progression of *RAS* mutant tumors. *Genes Dev* 2020; **34**: 751-766 [PMID: 32273287 DOI: 10.1101/gad.335166.119]

46 **Key CC**, Bishop AC, Wang X, Zhao Q, Chen GY, Quinn MA, Zhu X, Zhang Q, Parks JS. Human GDPD3 overexpression promotes liver steatosis by increasing lysophosphatidic acid production and fatty acid uptake. *J Lipid Res* 2020; **61**: 1075-1086 [PMID: 32430316 DOI: 10.1194/jlr.RA120000760]

47 **Wang L**, Huang X, Lim DJ, Laserna AKC, Li SFY. Uptake and toxic effects of triphenyl phosphate

on freshwater microalgae Chlorella vulgaris and Scenedesmus obliquus: Insights from untargeted metabolomics. *Sci Total Environ* 2019; **650**: 1239-1249 [PMID: 30308812 DOI: 10.1016/j.scitotenv.2018.09.024]

48 **Carstens H**, Schumacher F, Keitsch S, Kramer M, Kühn C, Sehl C, Soddemann M, Wilker B, Herrmann D, Swaidan A, Kleuser B, Verhaegh R, Hilken G, Edwards MJ, Dubicanac M, Carpinteiro A, Wissmann A, Becker KA, Kamler M, Gulbins E. Clinical Development of Sphingosine as Anti-Bacterial Drug: Inhalation of Sphingosine in Mini Pigs has no Adverse Side Effects. *Cell Physiol Biochem* 2019; **53**: 1015-1028 [PMID: 31854953 DOI: 10.33594/000000194]

49 **Zhao Y**, Hasse S, Zhao C, Bourgoin SG. Targeting the autotaxin - Lysophosphatidic acid receptor axis in cardiovascular diseases. *Biochem Pharmacol* 2019; **164**: 74-81 [PMID: 30928673 DOI: 10.1016/j.bcp.2019.03.035]

50 **Hosomi R**, Fukunaga K, Nagao T, Shiba S, Miyauchi K, Yoshida M, Takahashi K. Effect of Dietary Oil Rich in Docosahexaenoic Acid-Bound Lysophosphatidylcholine Prepared from Fishery By-Products on Lipid and Fatty Acid Composition in Rat Liver and Brain. *J Oleo Sci* 2019; **68**: 781-792 [PMID: 31366855 DOI: 10.5650/jos.ess19103]

51 **Xu H**, Meng X, Jia L, Wei Y, Sun B, Liang M. Tissue distribution of transcription for 29 lipid metabolism-related genes in Takifugu rubripes, a marine teleost storing lipid predominantly in liver. *Fish Physiol Biochem* 2020; **46**: 1603-1619 [PMID: 32415410 DOI: 10.1007/s10695-020-00815-7]

52 **Yao M**, Li Z, Julian McClements D, Tang Z, Xiao H. Design of nanoemulsion-based delivery systems to enhance intestinal lymphatic transport of lipophilic food bioactives: Influence of oil type. *Food Chem* 2020; **317**: 126229 [PMID: 32078989 DOI: 10.1016/j.foodchem.2020.126229]

53 **Wilson MP**, Plecko B, Mills PB, Clayton PT. Disorders affecting vitamin B_6 metabolism. *J Inherit Metab Dis* 2019; **42**: 629-646 [PMID: 30671974 DOI: 10.1002/jimd.12060]

54 **Dias IH**, Borah K, Amin B, Griffiths HR, Sassi K, Lizard G, Iriondo A, Martinez-Lage P. Localisation of oxysterols at the sub-cellular level and in biological fluids. *J Steroid Biochem Mol Biol* 2019; **193**: 105426 [PMID: 31301352 DOI: 10.1016/j.jsbmb.2019.105426]

55 **Goldberg IJ**, Hussain MM. To absorb fat - supersize my lipid droplets. *J Clin Invest* 2019; **129**: 58-59 [PMID: 30507609 DOI: 10.1172/JCI125318]

56 **Zhao S**, Jang C, Liu J, Uehara K, Gilbert M, Izzo L, Zeng X, Trefely S, Fernandez S, Carrer A, Miller KD, Schug ZT, Snyder NW, Gade TP, Titchenell PM, Rabinowitz JD, Wellen KE. Dietary fructose feeds hepatic lipogenesis *via* microbiota-derived acetate. *Nature* 2020; **579**: 586-591 [PMID: 32214246 DOI: 10.1038/s41586-020-2101-7]

57 **Simon MC**, Reinbeck AL, Wessel C, Heindirk J, Jelenik T, Kaul K, Arreguin-Cano J, Strom A, Blaut M, Bäckhed F, Burkart V, Roden M. Distinct alterations of gut morphology and microbiota characterize accelerated diabetes onset in nonobese diabetic mice. *J Biol Chem* 2020; **295**: 969-980 [PMID: 31822562 DOI: 10.1074/jbc.RA119.010816]

58 **Kemnic TR**, Coleman M. Vitamin E Deficiency. 2020 Jul 10. In: StatPearls [Internet]. Treasure Island (FL): StatPearls Publishing; 2020 Jan– [PMID: 30085593]

59 **Ye Z**, Cao C, Liu Y, Cao P, Li Q. Triglyceride Structure Modulates Gastrointestinal Digestion Fates of Lipids: A Comparative Study between Typical Edible Oils and Triglycerides Using Fully Designed in Vitro Digestion Model. *J Agric Food Chem* 2018; **66**: 6227-6238 [PMID: 29845858 DOI: 10.1021/acs.jafc.8b01577]

60 **Ye Z**, Li R, Cao C, Xu YJ, Cao P, Li Q, Liu Y. Fatty acid profiles of typical dietary lipids after gastrointestinal digestion and absorbtion: A combination study between in-vitro and in-vivo. *Food Chem* 2019; **280**: 34-44 [PMID: 30642504 DOI: 10.1016/j.foodchem.2018.12.032]

61 **Liu T**, Mukosera GT, Blood AB. The role of gasotransmitters in neonatal physiology. *Nitric Oxide* 2020; **95**: 29-44 [PMID: 31870965 DOI: 10.1016/j.niox.2019.12.002]

62 **Binienda A**, Twardowska A, Makaro A, Salaga M. Dietary Carbohydrates and Lipids in the Pathogenesis of Leaky Gut Syndrome: An Overview. *Int J Mol Sci* 2020; **21**: 8368 [PMID: 33171587 DOI: 10.3390/ijms21218368]

63 **Yao Y**, Xu F, Ju X, Li Z, Wang L. Lipid-Lowering Effects and Intestinal Transport of Polyphenol Extract from Digested Buckwheat in Caco-2/HepG2 Coculture Models. *J Agric Food Chem* 2020; **68**: 4205-4214 [PMID: 32141744 DOI: 10.1021/acs.jafc.0c00321]

64 **Song JW**, Lam SM, Fan X, Cao WJ, Wang SY, Tian H, Chua GH, Zhang C, Meng FP, Xu Z, Fu JL, Huang L, Xia P, Yang T, Zhang S, Li B, Jiang TJ, Wang R, Wang Z, Shi M, Zhang JY, Wang FS, Shui G. Omics-Driven Systems Interrogation of Metabolic Dysregulation in COVID-19 Pathogenesis. *Cell Metab* 2020; **32**: 188-202 e5 [PMID: 32610096 DOI: 10.1016/j.cmet.2020.06.016]

65 **Thomas T**, Stefanoni D, Dzieciatkowska M, Issaian A, Nemkov T, Hill RC, Francis RO, Hudson KE, Buehler PW, Zimring JC, Hod EA, Hansen KC, Spitalnik SL, D'Alessandro A. Evidence for structural protein damage and membrane lipid remodeling in red blood cells from COVID-19 patients. *medRxiv* 2020.06.29.20142703 [PMID: 32637980 DOI: 10.1101/2020.06.29.20142703]

66 **Thomas T**, Stefanoni D, Dzieciatkowska M, Issaian A, Nemkov T, Hill RC, Francis RO, Hudson KE, Buehler PW, Zimring JC, Hod EA, Hansen KC, Spitalnik SL, D'Alessandro A. Evidence of Structural Protein Damage and Membrane Lipid Remodeling in Red Blood Cells from COVID-19 Patients. *J Proteome Res* 2020; **19**: 4455-4469 [PMID: 33103907 DOI: 10.1021/acs.jproteome.0c00606]

67 **Mahmud I**, Garrett TJ. Mass Spectrometry Techniques in Emerging Pathogens Studies: COVID-19 Perspectives. *J Am Soc Mass Spectrom* 2020; **31**: 2013-2024 [PMID: 32880453 DOI: 10.1021/jasms.0c00238]

68 **Nicora CD**, Sims AC, Bloodsworth KJ, Kim YM, Moore RJ, Kyle JE, Nakayasu ES, Metz TO.

Metabolite, Protein, and Lipid Extraction (MPLEx): A Method that Simultaneously Inactivates Middle East Respiratory Syndrome Coronavirus and Allows Analysis of Multiple Host Cell Components Following Infection. *Methods Mol Biol* 2020; **2099**: 173-194 [PMID: 31883096 DOI: 10.1007/978-1-0716-0211-9_14]

69 **Schwarz B**, Sharma L, Roberts L, Peng X, Bermejo S, Leighton I, Massana AC, Farhadian S, Ko A, DelaCruz C, Bosio CM. Severe SARS-CoV-2 infection in humans is defined by a shift in the serum lipidome resulting in dysregulation of eicosanoid immune mediators. *medRxiv* 2020; 2020.07.09. 20149849 [PMID: 32676616 DOI: 10.1101/2020.07.09.20149849]

70 **Schwarz B**, Sharma L, Roberts L, Peng X, Bermejo S, Leighton I, Massana AC, Farhadian S, Ko AI; Yale IMPACT Team; Cruz CSD; Bosio CM. Severe SARS-CoV-2 infection in humans is defined by a shift in the serum lipidome resulting in dysregulation of eicosanoid immune mediators. *Res Sq* 2020; rs.3. rs-42999 [PMID: 32743565 DOI: 10.21203/rs.3.rs-42999/v1]

71 **Bruzzone C**, Bizkarguenaga M, Gil-Redondo R, Diercks T, Arana E, García de Vicuña A, Seco M, Bosch A, Palazón A, San Juan I, Laín A, Gil-Martínez J, Bernardo-Seisdedos G, Fernández-Ramos D, Lopitz-Otsoa F, Embade N, Lu S, Mato JM, Millet O. SARS-CoV-2 Infection Dysregulates the Metabolomic and Lipidomic Profiles of Serum. *iScience* 2020; **23**: 101645 [PMID: 33043283 DOI: 10.1016/j.isci.2020.101645]

72 **Balgoma D**, Gil-de-Gómez L, Montero O. Lipidomics Issues on Human Positive ssRNA Virus Infection: An Update. *Metabolites* 2020; **10**: 356 [PMID: 32878290 DOI: 10.3390/metabo10090356]

73 **Yan B**, Zou Z, Chu H, Chan G, Tsang JO, Lai PM, Yuan S, Yip CC, Yin F, Kao RY, Sze KH, Lau SK, Chan JF, Yuen KY. Lipidomic Profiling Reveals Significant Perturbations of Intracellular Lipid Homeostasis in Enterovirus-Infected Cells. *Int J Mol Sci* 2019; **20**: 5952 [PMID: 31779252 DOI: 10.3390/ijms20235952]

74 **Bley H**, Schöbel A, Herker E. Whole Lotta Lipids-from HCV RNA Replication to the Mature Viral Particle. *Int J Mol Sci* 2020; **21**: 2888 [PMID: 32326151 DOI: 10.3390/ijms21082888]

75 **Queiroz A**, Pinto IFD, Lima M, Giovanetti M, de Jesus JG, Xavier J, Barreto FK, Canuto GAB, do Amaral HR, de Filippis AMB, Mascarenhas DL, Falcão MB, Santos NP, Azevedo VAC, Yoshinaga MY, Miyamoto S, Alcantara LCJ. Lipidomic Analysis Reveals Serum Alteration of Plasmalogens in Patients Infected With ZIKA Virus. *Front Microbiol* 2019; **10**: 753 [PMID: 31031729 DOI: 10.3389/fmicb.2019.00753]

76 **Yuan S**, Chu H, Chan JF, Ye ZW, Wen L, Yan B, Lai PM, Tee KM, Huang J, Chen D, Li C, Zhao X, Yang D, Chiu MC, Yip C, Poon VK, Chan CC, Sze KH, Zhou J, Chan IH, Kok KH, To KK, Kao RY, Lau JY, Jin DY, Perlman S, Yuen KY. SREBP-dependent lipidomic reprogramming as a broad-spectrum antiviral target. *Nat Commun* 2019; **10**: 120 [PMID: 30631056 DOI: 10.1038/s41467-018-08015-x]

77 **Yan B**, Chu H, Yang D, Sze KH, Lai PM, Yuan S, Shuai H, Wang Y, Kao RY, Chan JF, Yuen KY. Characterization of the Lipidomic Profile of Human Coronavirus-Infected Cells: Implications for Lipid Metabolism Remodeling upon Coronavirus Replication. *Viruses* 2019; **11**: 73 [PMID: 30654597 DOI: 10.3390/v11010073]

78 **Liebscher S**, Ambrose RL, Aktepe TE, Mikulasova A, Prier JE, Gillespie LK, Lopez-Denman AJ, Rupasinghe TWT, Tull D, McConville MJ, Mackenzie JM. Phospholipase A2 activity during the replication cycle of the flavivirus West Nile virus. *PLoS Pathog* 2018; **14**: e1007029 [PMID: 29709018 DOI: 10.1371/journal.ppat.1007029]

79 **Hofmann S**, Krajewski M, Scherer C, Scholz V, Mordhorst V, Truschow P, Schöbel A, Reimer R, Schwudke D, Herker E. Complex lipid metabolic remodeling is required for efficient hepatitis C virus replication. *Biochim Biophys Acta Mol Cell Biol Lipids* 2018; **1863**: 1041-1056 [PMID: 29885363 DOI: 10.1016/j.bbalip.2018.06.002]

80 **Diwaker D**, Mishra KP, Ganju L, Singh SB. Protein disulfide isomerase mediates dengue virus entry in association with lipid rafts. *Viral Immunol* 2015; **28**: 153-160 [PMID: 25664880 DOI: 10.1089/vim.2014.0095]

81 **Carter CJ**. Interactions between the products of the Herpes simplex genome and Alzheimer's disease susceptibility genes: relevance to pathological-signalling cascades. *Neurochem Int* 2008; **52**: 920-934 [PMID: 18164103 DOI: 10.1016/j.neuint.2007.11.003]

82 **Wang X**, Xu P, Cheng F, Li Y, Wang Z, Hao S, Wang J, Ning K, Ganaie SS, Engelhardt JF, Yan Z, Qiu J. Cellular Cleavage and Polyadenylation Specificity Factor 6 (CPSF6) Mediates Nuclear Import of Human Bocavirus 1 NP1 Protein and Modulates Viral Capsid Protein Expression. *J Virol* 2020; **94**: e01444-19 [PMID: 31666379 DOI: 10.1128/JVI.01444-19]

83 **Wang X**, Hennig T, Whisnant AW, Erhard F, Prusty BK, Friedel CC, Forouzmand E, Hu W, Erber L, Chen Y, Sandri-Goldin RM, Dölken L, Shi Y. Herpes simplex virus blocks host transcription termination *via* the bimodal activities of ICP27. *Nat Commun* 2020; **11**: 293 [PMID: 31941886 DOI: 10.1038/s41467-019-14109-x]

84 **Wendt L**, Brandt J, Bodmer BS, Reiche S, Schmidt ML, Traeger S, Hoenen T. The Ebola Virus Nucleoprotein Recruits the Nuclear RNA Export Factor NXF1 into Inclusion Bodies to Facilitate Viral Protein Expression. *Cells* 2020; **9**: 187 [PMID: 31940815 DOI: 10.3390/cells9010187]

85 **Han S**, Sun S, Li P, Liu Q, Zhang Z, Dong H, Sun M, Wu W, Wang X, Guo H. Ribosomal Protein L13 Promotes IRES-Driven Translation of Foot-and-Mouth Disease Virus in a Helicase DDX3-Dependent Manner. *J Virol* 2020; **94**: e01679-19 [PMID: 31619563 DOI: 10.1128/JVI.01679-19]

86 **Şenbaş Akyazi B**, Pirinçal A, Kawaguchi A, Nagata K, Turan K. Interaction of influenza A virus NS2/NEP protein with the amino-terminal part of Nup214. *Turk J Biol* 2020; **44**: 82-92 [PMID:

32256144 DOI: 10.3906/biy-1909-49]

87 **Thiele S**, Stanelle-Bertram S, Beck S, Kouassi NM, Zickler M, Müller M, Tuku B, Resa-Infante P, van Riel D, Alawi M, Günther T, Rother F, Hügel S, Reimering S, McHardy A, Grundhoff A, Brune W, Osterhaus A, Bader M, Hartmann E, Gabriel G. Cellular Importin-α3 Expression Dynamics in the Lung Regulate Antiviral Response Pathways against Influenza A Virus Infection. *Cell Rep* 2020; **31**: 107549 [PMID: 32320654 DOI: 10.1016/j.celrep.2020.107549]

88 **Ren L**, Ding S, Song Y, Li B, Ramanathan M, Co J, Amieva MR, Khavari PA, Greenberg HB. Profiling of rotavirus 3'UTR-binding proteins reveals the ATP synthase subunit ATP5B as a host factor that supports late-stage virus replication. *J Biol Chem* 2019; **294**: 5993-6006 [PMID: 30770472 DOI: 10.1074/jbc.RA118.006004]

89 **Dave P**, George B, Balakrishnan S, Sharma DK, Raheja H, Dixit NM, Das S. Strand-specific affinity of host factor hnRNP C1/C2 guides positive to negative-strand ratio in Coxsackievirus B3 infection. *RNA Biol* 2019; **16**: 1286-1299 [PMID: 31234696 DOI: 10.1080/15476286.2019.1629208]

90 **Andreev DE**, Hirnet J, Terenin IM, Dmitriev SE, Niepmann M, Shatsky IN. Glycyl-tRNA synthetase specifically binds to the poliovirus IRES to activate translation initiation. *Nucleic Acids Res* 2012; **40**: 5602-5614 [PMID: 22373920 DOI: 10.1093/nar/gks182]

91 **Katsarou K**, Wu Y, Zhang R, Bonar N, Morris J, Hedley PE, Bryan GJ, Kalantidis K, Hornyik C. Insight on Genes Affecting Tuber Development in Potato upon Potato spindle tuber viroid (PSTVd) Infection. *PLoS One* 2016; **11**: e0150711 [PMID: 26937634 DOI: 10.1371/journal.pone.0150711]

92 **Jupatanakul N**, Sim S, Dimopoulos G. Aedes aegypti ML and Niemann-Pick type C family members are agonists of dengue virus infection. *Dev Comp Immunol* 2014; **43**: 1-9 [PMID: 24135719 DOI: 10.1016/j.dci.2013.10.002]

93 **Josset L**, Menachery VD, Gralinski LE, Agnihothram S, Sova P, Carter VS, Yount BL, Graham RL, Baric RS, Katze MG. Cell host response to infection with novel human coronavirus EMC predicts potential antivirals and important differences with SARS coronavirus. *mBio* 2013; **4**: e00165-e00113 [PMID: 23631916 DOI: 10.1128/mBio.00165-13]

94 **Ong EZ**, Chan YFZ, Leong WY, Lee NMY, Kalimuddin S, Haja Mohideen SM, Chan KS, Tan AT, Bertoletti A, Ooi EE, Low JGH. A Dynamic Immune Response Shapes COVID-19 Progression. *Cell Host Microbe* 2020; **27**: 879-882. e2 [PMID: 32359396 DOI: 10.1016/j.chom.2020.03.021]

World Journal of Gastroenterology

Submit a Manuscript: https://www.f6publishing.com

World J Gastroenterol 2021 January 7; 27(1): 55-68

DOI: 10.3748/wjg.v27.i1.55

ISSN 1007-9327 (print) ISSN 2219-2840 (online)

ORIGINAL ARTICLE

Basic Study

Long non-coding ribonucleic acid W5 inhibits progression and predicts favorable prognosis in hepatocellular carcinoma

Guang-Lin Lei, Hong-Xia Fan, Cheng Wang, Yan Niu, Tie-Ling Li, Ling-Xiang Yu, Zhi-Xian Hong, Jin Yan, Xi-Liang Wang, Shao-Geng Zhang, Ming-Ji Ren, Peng-Hui Yang

ORCID number: Guang-Lin Lei 0000-0002-2092-2251; Hong-Xia Fan 0000-0001-9068-8459; Cheng Wang 0000-0001-6213-7027; Yan Niu 0000-0002-1536-8663; Tie-Ling Li 0000-0003-0683-8659; Ling-Xiang Yu 0000-0002-0727-400X; Zhi-Xian Hong 0000-0002-0187-3351; Jin Yan 0000-0002-3743-9477; Xi-Liang Wang 0000-0002-2652-6874; Shao-Geng Zhang 0000-0002-0479-7569; Ming-Ji Ren 0000-0001-6259-1158; Peng-Hui Yang 0000-0001-6519-5927.

Author contributions: Zhang SG and Yang PH contributed to conception and intellectual input; Lei GL, Fan HX, Li TL, Hong ZX and Ren MJ contributed to designing and performing the experiments; Fan HX and Lei GL contributed to sample collection and manuscript drafting; Yan J and Wang XL contributed to statistical analyses and data interpretation; all authors read and approved the final manuscript.

Supported by National High Technology Research and Development Program of China, No. 2015AA020924; Natural Science Foundation of Beijing, China, No. 7202194 and No. 7162185.

Institutional animal care and use committee statement: All animal

Guang-Lin Lei, Hong-Xia Fan, Ling-Xiang Yu, Zhi-Xian Hong, Jin Yan, Shao-Geng Zhang, Peng-Hui Yang, Fifth Medical Center of Chinese PLA General Hospital, Beijing 100039, China

Hong-Xia Fan, Yan Niu, Ming-Ji Ren, College of Basic Medicine, Inner Mongolia Medical University, Hohhot 010110, Inner Mongolia, China

Cheng Wang, Tie-Ling Li, First Medical Center of Chinese PLA General Hospital, Beijing 100853, China

Xi-Liang Wang, Peng-Hui Yang, State Key Laboratory of Pathogens and Biosecurity, Beijing Institute of Microbiology and Epidemiology, Beijing 100071, China

Corresponding author: Peng-Hui Yang, MD, Professor, Fifth Medical Center of Chinese PLA General Hospital, No. 100 Xisihuan Zhong Lu, Fengtai District, Beijing 100039, China. yph3022017@163.com

Abstract

BACKGROUND

Accumulating evidence has revealed that several long non-coding ribonucleic acids (lncRNAs) are crucial in the progress of hepatocellular carcinoma (HCC).

AIM

To classify a long non-coding RNA, *i.e.*, lncRNA W5, and to determine the clinical significance and potential roles of lncRNA W5 in HCC.

METHODS

The results showed that lncRNA W5 expression was significantly downregulated in HCC cell lines and tissues. Analysis of the association between lncRNA W5 expression levels and clinicopathological features suggested that low lncRNA W5 expression was related to large tumor size ($P < 0.01$), poor histological grade ($P < 0.05$) and serious portal vein tumor thrombosis ($P < 0.05$). Furthermore, Kaplan-Meier survival analysis showed that low expression of lncRNA W5 predicts poor overall survival ($P = 0.016$).

RESULTS

Gain-of-loss function experiments, including cell counting kit8 assays, colony formation assays, and transwell assays, were performed *in vitro* to investigate the

biological roles of lncRNA W5. *In vitro* experiments showed that ectopic overexpression of lncRNA W5 suppressed HCC cell proliferation, migration and invasion; conversely, silencing of lncRNA W5 promoted cell proliferation, migration and invasion. In addition, acting as a tumor suppressor gene in HCC, lncRNA W5 inhibited the growth of HCC xenograft tumors *in vivo*.

CONCLUSION

These results showed that lncRNA W5 is down-regulated in HCC, and it may suppress HCC progression and predict poor clinical outcomes in patients with HCC. LncRNA W5 may serve as a potential HCC prognostic biomarker in addition to a therapeutic target.

Key Words: Hepatocellular carcinoma; Long non-coding ribonucleic acid; Long non-coding ribonucleic acid W5

Core Tip: Our results showed that the expression of long non-coding ribonucleic acid (lncRNA) W5 was considerably reduced in hepatocellular carcinoma (HCC) tissues, which suppressed proliferation, migration and invasion of tumor cells *in vitro*. It was also shown that low expression of lncRNA W5 correlated with tumor progression and poor prognosis. Furthermore, manipulation of lncRNA W5 expression affected the biological behavior of HCC. These results suggest that lncRNA W5 may serve as a tumor suppressor in the development and progression of HCC, and has the potential to be a diagnostic and therapeutic target in the clinical management of HCC.

Citation: Lei GL, Fan HX, Wang C, Niu Y, Li TL, Yu LX, Hong ZX, Yan J, Wang XL, Zhang SG, Ren MJ, Yang PH. Long non-coding ribonucleic acid W5 inhibits progression and predicts favorable prognosis in hepatocellular carcinoma. *World J Gastroenterol* 2021; 27(1): 55-68
URL: https://www.wjgnet.com/1007-9327/full/v27/i1/55.htm
DOI: https://dx.doi.org/10.3748/wjg.v27.i1.55

INTRODUCTION

Around 90% of primary liver cancer cases are hepatocellular carcinoma (HCC)[1], approximately 600000 deaths occur globally each year, and half of all deaths occur in China[2,3]. In addition to hepatic resection, liver transplantation, chemotherapy and molecular targeted therapy are often carried out to improve outcomes in patients with HCC; however, the 5-year survival rate of patients with HCC still remains poor[4,5]. The specific signaling mechanisms underlying the development and progression of HCC remain to be defined.

The long non-coding ribonucleic acids (lncRNAs) are a class of noncoding RNAs with more than 200 nucleotides which have no protein-coding potential. Several reports have shown that lncRNAs are critical in numerous biological processes, including tumor development, differentiation, and tumorigenesis[6-10]. The expression of lncRNAs is dysregulated in cancer. Of note, specific lncRNAs are related to cancer recurrence, metastasis and prognosis in various cancers, including HCC[11-14]. To date, several lncRNA have been reported to be associated with the growth and advance of HCC, such as HULC[15], H19[16], MEG3[17], ZFAS1[18], P7[19], ATB[20], GAS8-AS1[21], and so on. In our previous study, we profiled the the expression of lncRNAs in influenza virus infected patients and identified panels of uncharacterized lncRNAs. In the current study, we classified the lncRNA W5 (mitochondrial translation optimization 1homologue; hsa_lncRNA_0007874/hsa_lncRNA_104135) which is notably down-regulated in HCC tissues and strictly associated with the prognosis of HCC patients. Furthermore, we investigated its roles, underlying mechanisms and clinical significance in HCC progression.

experiments were conducted with the approval of the Fifth Medical Center of Chinese PLA General Hospital's Animal Care and Use Committee.

Conflict-of-interest statement: All authors declare no financial or commercial conflicts of interest.

Data sharing statement: All data generated or analyzed during this study are included in this published article.

Manuscript source: Unsolicited manuscript

Specialty type: Gastroenterology and hepatology

Country/Territory of origin: China

Peer-review report's scientific quality classification
Grade A (Excellent): 0
Grade B (Very good): B
Grade C (Good): 0
Grade D (Fair): 0
Grade E (Poor): 0

Received: August 25, 2020
Peer-review started: August 25, 2020
First decision: September 12, 2020
Revised: October 27, 2020
Accepted: November 13, 2020
Article in press: November 13, 2020
Published online: January 7, 2021

P-Reviewer: Zhang L
S-Editor: Zhang L
L-Editor: Webster JR
P-Editor: Ma YJ

MATERIALS AND METHODS

Clinical samples

A total of 86 resected HCC tissues and matched tumor-adjacent tissues were kindly provided by the Department of Hepatobiliary Surgery of the Fifth Medical Center, Chinese PLA General Hospital between October 2013 and June 2018. Tumor tissues and adjacent non-tumor tissue specimens were obtained from the patients after informed consent in accordance with the institutional guidelines of the hospital's Ethics Committee. Table 1 indicates the clinical and pathological characteristics of HCC patients obtained from clinical records.

Cell lines

All human cell lines were provided by the Experimental Center of the Fifth Medical Center, Chinese PLA General Hospital (Beijing, China), and included the normal non-malignant liver cell line LO2 and HCC cell lines Huh7, MHCC-97L, MHCC-97H, PLC, Hep3B and HCCLM3. All cell lines were maintained in DMEM (Gibco, Beijing, China) and were supplemented with 10% fetal bovine serum (Gibco, Beijing, China) in an incubator at 37°C with 5% CO_2.

RNA extraction and reverse transcription-polymerase chain reaction

TRIzol reagent (Invitrogen, United States) was used to isolate total RNA from HCC cells and tissues, and first strand complementary deoxyribonucleic acid (cDNA) was synthesized by the use of reverse transcriptase. Quantitative real-time polymerase chain reaction (PCR) was conducted using the SYBR Green PCR kit (Thermo Fisher Scientific, United States). All reactions were performed on the ABI 7500 system (Applied Biosystems). The lncRNA W5-specific reverse transcription-polymerase chain reaction (qRT-PCR) primers used were as follows: forward: 5'-AAGGAGAACACAAAACAGGCAT-3', reverse: 5'-TGTGAAGCCCTAG ATTTCCCAT-3'; GAPDH forward: 5'-AAG GAGAACACAAAACAG GCAT-3' reverse: 5'-TGTGAAGCCCTAGATTTCCCAT-3'. Human *GAPDH* gene was amplified as an internal control.

Vector construction

The lncRNA W5 vector was constructed and sub-cloned into the pcDNA3.1 (+) vector at the BamHI and EcoRI sites, which produced pcDNA3.1-lncRNA W5. The primers used were as follows: forward: 5'-GCGCGGATCCACTGACTCTTTTCGTTAAGC-3', reverse: 5'-CGCGCGGAATTCATGTTGACTTAAGTTCAGG-3'. Empty vector pcDNA3.1 (+) was used as a negative control. The lncRNA W5 and control were transfected into HCC cells using Polyplus (Invitrogen) according to the manufacturer's instructions and cultured on six-well plates, respectively.

Cell proliferation assay

Cell proliferation experiments were performed using the CCK-8 kit (Dojindo Laboratories) according to the manufacturer's protocol. Briefly, a Huh7 or LM3 cell suspension was adjusted to a final cell concentration of 5×10^3/mL and then added to a 96-well plate. HCC cells were cultured for the indicated time points, and then 10 μL of CCK-8 (5 mg/mL) was added to each well. The cell culture plate was placed in the incubator for 1 h, and the absorbance was measured at 450 nm per well using a Thermomax plate reader (Thermo Fisher, China).

Colony formation assay

Huh7 or LM3 cells were completely dispersed into individual cells in 6-well plates and incubated at 37°C in DMEM with 10% fetal bovine serum, respectively. After 14 d, the cell colonies were washed with PBS, fixed in 4% paraformaldehyde for 20 min, and stained with crystal violet for 20 min. Photographs were subsequently taken and only colonies containing more than 50 cells were recorded.

Cell migration and invasion assays

A chamber assay with Matrigel (invasion) or without Matrigel (migration) was performed at least in triplicate. Twenty-four-well chambers with 8 μm pore size were used in this experiment. Briefly, cells were added to the top chamber without Matrigel (migration) or with Matrigel (invasion) in the 24-well plate (Corning). The medium with 15% forward-based system was added to the lower chambers. After incubator for 48-72 h, the DMEM medium was removed and the cells were washed with PBS, and

Table 1 Association of long non-coding ribonucleic acid W5 expression with clinicopathologic features in hepatocellular carcinoma patients

Parameters	Group	Total	W5 expression		*P* value
			Low	High	
Gender	Male	70	34	36	0.791
	Female	16	10	6	
Age (yr)	≤ 60	30	15	15	0.579
	> 60	56	28	28	
Tumor size (cm)	< 3 cm	21	6	15	0.007[b]
	≥ 3 cm	65	38	27	
AFP	< 20	39	21	18	0.328
	≥ 20	47	22	25	
Histological grade	Well/moderate-poor	52/34	5/28	47/6	0.046[a]
Clinical stage	I/II	50	23	27	0.501
Tumor number	III	36	20	16	
	Solitary	76	36	40	0.312
	Multiple	10	7	3	
Drinking status	Yes	42	24	18	0.276
	No	44	19	25	
Smoking status	Yes	36	18	18	0.584
	No	50	24	26	
PVTT	Yes	32	22	10	0.024[a]
	No	54	21	33	
Microvascular invasion	Yes	70	36	34	0.568
	No	16	6	10	
Liver cirrhosis	Absence	59	30	29	0.489
HBV	Yes	55	25	30	0.365
	No	31	18	13	

[a]$P < 0.05$.
[b]$P < 0.01$. PVTT: Portal vein tumor thrombosis; HBV: Hepatitis B virus.

carefully removed from the top chamber with a cotton swab. The cells were fixed with 4% paraformaldehyde, stained with crystal violet, and then photographed in five randomly selected microscope fields.

In vivo tumor growth

Athymic BALB/C mice (4-6 wk old) were purchased from the Beijing Vital River Laboratory Animal Technology Co., Ltd (Beijing, China) and maintained in a SPF facility. Huh7 cells (5×10^6) over-expressing lncRNA W5 were subcutaneously injected into the flanks of nude mice. Tumor length (L) and width (W) were measured using calipers every 3 d up to 6 wk. Tumor volume was estimated using the formula: π × length × width 2/6. After 6 wk, the mice were sacrificed, and tumor volumes and weights were examined. Proliferation progression was examined and quantified using a noninvasive bioluminescence *in vivo* Imaging System (Xenogen Corporation, Alameda, CA, United States). All animal experiments were conducted with the approval of the Fifth Medical Center of Chinese PLA General Hospital's Animal Care and Use Committee.

Statistical analysis

All statistical analyses were performed using the SPSS 20.0 software package (Chicago, IL, United States). Data were expressed as the mean ± SD. Kaplan-Meier analysis was used to determine whether there was a correlation between the expression of lncRNA W5 and overall survival rate of HCC patients. $P < 0.05$ was considered significant.

RESULTS

HCC cancer tissues and cell lines have low expression of lncRNA W5

Initially, to investigate the potential role of lncRNA W5 in HCC tumorigenesis, we determined the expression of lncRNA W5 in 86 sets of HCC tissues and non-tumor tissues by qRT-PCR. As shown in Figure 1, the expression of lncRNA W5 was significantly reduced in HCC tissues compared with adjacent non-tumor tissues ($P < 0.001$, Figure 1A and B). In addition, we determined the expression of lncRNA W5 in regular liver cells (LO2) and six HCC cancer cell lines (Huh7, MHCC-97L, MHCC-97H, PLC, Hep3B and HCCLM3). The results revealed that lncRNA W5 expression was significantly downregulated in the six HCC cancer cells compared with the regular liver cell line LO2 (Figure 1C). Levels of lncRNA W5 expression were relatively lower in the Huh7 and LM3 HCC cell lines, and were used in subsequent studies. More importantly, a Kaplan-Meier survival analysis indicated that HCC patients with low expression of lncRNA W5 had shorter overall survival than those patients with high expression of lncRNA W5 ($P = 0.016$) (Figure 1D). Cox survival analysis was then used to further confirm the prognostic value of lncRNA W5 in HCC. Univariate analysis showed that the analyzed variables (lncRNA W5 expression, Pathologic-stage and Pathologic-TMN) were markedly associated with the overall survival time of HCC patients. Furthermore, multivariate analysis revealed that lncRNA W5 expression ($P = 0.027$), Pathologic-T ($P = 0.014$) and Pathologic-M ($P = 0.005$) were promising independent prognostic factors of HCC (Table 2). Thus, lncRNA W5 could be used as an independent prognostic factor. Finally, we also measured the expression of lncRNA W5 in nuclear and cytosolic fractions of Huh7 cells by qRT-PCR. The differential enrichments of GAPDH, β-actin and U1 RNA were used as fractionation indicators. Subcellular fractionation location results showed that lncRNA W5 was mainly located in the nucleus (Figure 1E), thus suggesting that lncRNA W5 might play an essential regulatory function at the transcriptional level.

To investigate the relationship between the expression of lncRNA W5 and clinicopathological characteristics, lncRNA W5 expression was detected in 86 HCC patients and distributed into two groups (high–high expression of lncRNA W5 and low–low expression of lncRNA W5) based on the median lncRNA W5 expression. The correlations between lncRNA W5 expression and clinical parameters were analyzed and it was found that low expression of lncRNA W5 was linked to large tumor size ($P < 0.01$), poor histological grade ($P < 0.05$) and serious portal vein tumor thrombosis ($P < 0.05$). Nevertheless, no significant correlation was observed between the expression of lncRNA W5 and other clinicopathological features, such as age, gender, AFP levels, tumor number and with/without HBV infection.

In vitro effects of lncRNA W5 on HCC cell proliferation

To assess the role of lncRNA W5 in regulating the biological behavior of HCC cells, we used the lncRNA W5 expression vector pcDNA3.1-lncRNA W5 and overexpressed lncRNA W5 in the HCC cell lines Huh7 and LM3. LncRNA W5 overexpression in the two cell lines was verified by RT-qPCR (Figure 2A). CCK-8 assays, which were used to show overexpression of lncRNA W5 in the HCC cell lines Huh7 and LM3, demonstrated a significant reduction in cell proliferation from 48 h to 96 h (Figure 2B). Accordingly, colony formation assays, which showed that Huh7 and LM3 cells transfected with lncRNA W5, resulted in significantly decreased clonogenic survival than empty vector control Huh7 and LM3 cell lines (Figure 2C). In addition, we constructed shRNA-1 and shRNA-2 containing the back-splicing region of lncRNA W5 for silencing. The efficiency of lncRNA W5 silencing was confirmed by qPCR following transfection with lncRNA W5 shRNA-1 or-2 in Huh7 and LM3 cells (Figure 2D). As expected, we found that lncRNA W5 silencing significantly promoted cell proliferation of Huh7 and LM3 cells as indicated by MTS (Figure 2E). Furthermore, a clone formation assay verified that following lncRNA W5 knockdown, the HCC population dependence and proliferation ability were considerably increased (Figure 2F). Overall, these data demonstrated that lncRNA W5 may inhibit HCC cell proliferation *in vitro*.

Table 2 Cox proportional hazards model analysis of clinicopathologic features related to overall survival in terms of long non-coding ribonucleic acid W5 expression in hepatocellular carcinoma patients

Variables	Univariate analysis			Multivariate analysis		
	P value	HR	95%CI	*P* value	HR	95%CI
Expression (high/low)	0.041[a]	1.672	1.032-2.159	0.027[a]	1.285	0.867-2.155
Pathologic-Stage (I + II/III + IV)	0.001[a]	2.584	1.934-4.162	0.159	2.436	0.715-7.667
Pathologic-T (T1 + T2/T3 + T4)	0.004[a]	4.068	1.573-8.869	0.014[a]	10.638	2.314-57.649
Pathologic-M (M0/M1)	0.007[a]	5.294	3.195-7.657	0.005[a]	3.082	1.726-5.342
Pathologic-N (N0/N1 + N2 + N3)	0.002[a]	2.413	1.519-3.969	0.246	0.719	0.312-1.911
Age (< 60/ ≥ 60 yrs)	0.342	1.402	0.914-2.357			
Gender (female/male)	0.258	1.324	0.849-1.905			

[a]$P < 0.05$. HR: Hazard ratio; CI: Confidence interval.

In vitro effects of lncRNA W5 on HCC cell migration and invasion

To evaluate the potential role of lncRNA W5 in HCC metastasis, and investigate the effect of lncRNA W5 on cell migration and invasion capacity, we performed transwell assays using Huh7 and LM3 cells. The results revealed that the migration and invasion ability of HCC cells that over-expressed lncRNA W5 was significantly decreased compared with the empty vector group (Figure 3A). On the contrary, lncRNA W5 knockdown with shRNA-1 or-2 significantly promoted cell migration and enhanced cell invasion of Huh7 and LM3 cells, respectively (Figure 3B). These results strongly suggest that lncRNA W5 has a critical effect on the inhibition of HCC cell migration and invasion.

lncRNA W5 inhibits tumor growth in vivo

To elucidate the *in vivo* role of lncRNA W5 in tumorigenesis, we subcutaneously injected the flanks of nude mice with Huh7 cells over-expressing lncRNA W5 and stably expressing luciferase and monitored tumor growth every three days. As shown in Figure 4, mice injected with lncRNA W5 over-expressing cells had a significant decrease in tumor growth at 36 d post-injection as compared with mice injected with control cells. Six weeks after injection, the volumes and weights of tumors examined in mice injected with pcDNA3.1-lncRNA W5 were notably smaller than those in mice injected with the control. At 6 wk after injection, bioluminescent signals were weaker in mice with lncRNA W5 over-expression than in control mice, suggesting that lncRNA W5 may inhibit the growth of HCC xenograft tumors *in vivo*.

DISCUSSION

Increasing evidence has shown that aberrant expression of numerous lncRNAs has been discovered in HCC. Previous studies showed that amplification of lncRNA ZFAS1 promotes metastasis in HCC[18]. Sun SH's group observed in HCC that the lncRNA-activated by TGF-β (lncRNA-ATB) promoted the invasion-metastasis cascade[20]. Hur K's group also reported that lncRNA-ATB could have potential as a biomarker for the prognosis of HCC and as a targeted therapy for HCC patients[22]. Another study showed that the MBNL3 splicing factor promoted HCC by increasing the expression of PXN by the alternative splicing of lncRNA-PXN-AS1[23]. The lncRNA lncHDAC2 may drive the self-renewal of liver cancer stem cells through the activation of Hedgehog signaling[24]. Super-enhancer associated lncRNA HCCL5 is activated by ZEB1 and promotes the malignancy of HCC[25]. Recently, Huang *et al*[26] identified oncofetal lncRNA Ptn-dt which might promote HCC proliferation by regulating the Ptn receptor[26]. These results indicate that lncRNAs may have critical roles in HCC progression and development and can be used in clinical applications.

In this study, we reported an uncharacterized low expression of lncRNA W5 in HCC specimens and cell lines, suggesting that lncRNA W5 expression might be related to HCC carcinogenesis. Decreased expression of lncRNA W5 was associated with aggressive clinicopathological features of HCC tissues, including tumor size,

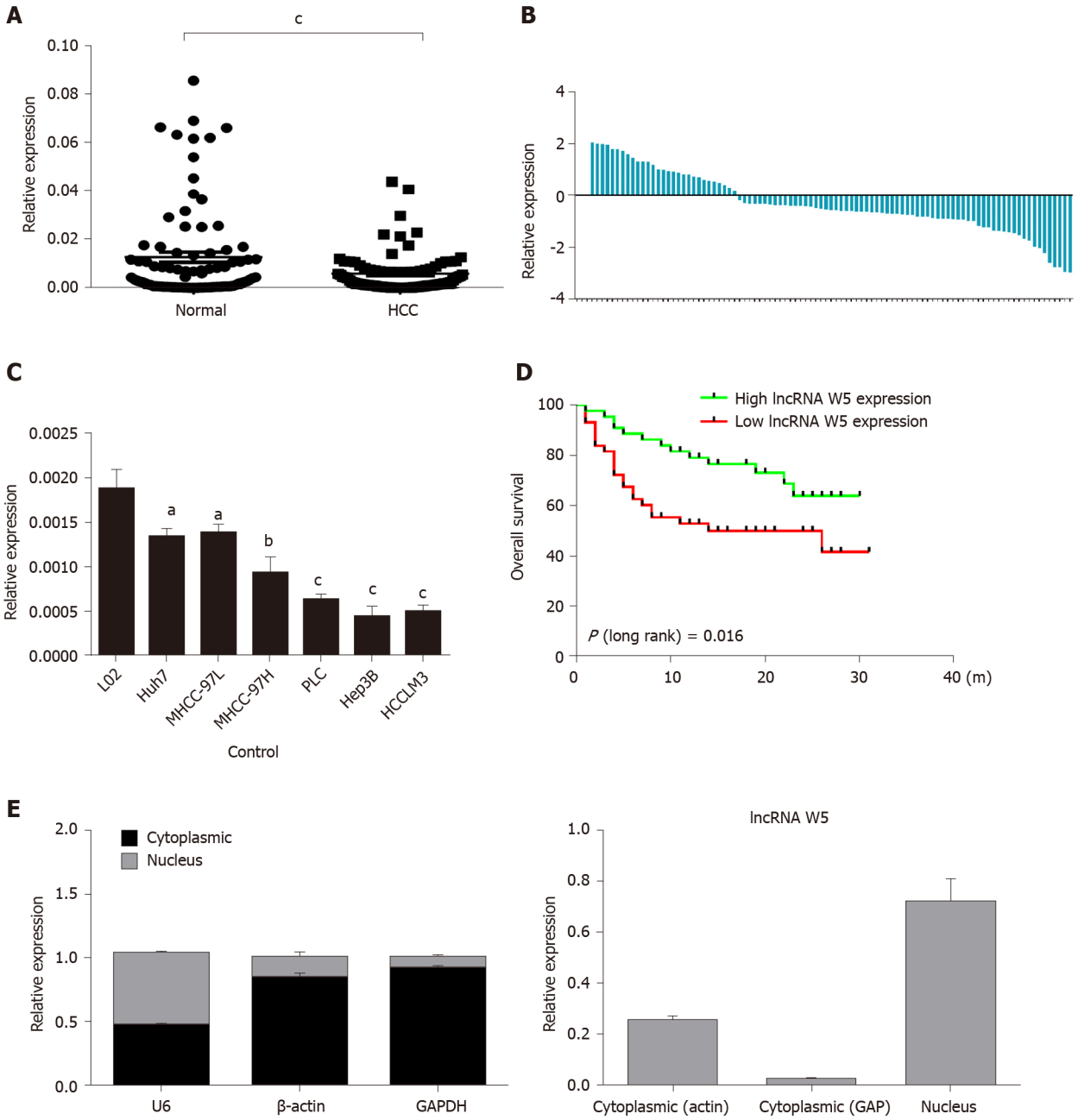

Figure 1 Expression of long non-coding ribonucleic acid W5 is downregulated in hepatocellular carcinoma tissues and cells. A: The expression of long non-coding ribonucleic acid (lncRNA) W5 was detected by reverse transcription-polymerase chain reaction (qRT-PCR) in tumor tissues and non-adjacent normal tissues of hepatocellular carcinoma (HCC) patients (n = 86). LncRNA W5 expression was normalized to GAPDH expression; B: The expression of lncRNA W5 was detected by qRT-PCR in tumor tissues and non-adjacent normal tissues of 86 HCC patients; C: The expression levels of lncRNA W5 in a series of HCC cell lines were reduced compared to that in LO2 cells; D: Analysis of overall survival based on lncRNA W5 expression levels is shown in 86 HCC patients; and E: Subcellular localization of lncRNA W5 in Huh7 cells was examined by qRT-PCR. GAPDH, β-actin and U1 were considered as the control markers, respectively. $^{a}P < 0.05$; $^{b}P < 0.01$; $^{c}P < 0.001$. HCC: Hepatocellular carcinoma; lncRNA: Long non-coding ribonucleic acid; qRT-PCR: Reverse transcription-polymerase chain reaction.

histological grade and the presence of portal vein tumor thrombosis. Gain-and loss function experiments showed that over-expression of lncRNA W5 in Huh7 and LM3 cells decreased cell proliferation, and impaired cell migration and invasion. Moreover, lncRNA W5 over-expression inhibited tumor growth in HCC xenograft-bearing mice. These results demonstrated that lncRNA W5 is involved in the progression of HCC and may be a potential target for therapy. Furthermore, our studies showed that HCC patients with low expression of lncRNA W5 had shorter overall survival than patients with high expression of lncRNA W5, suggesting that lncRNA W5 might be a potential prognostic predictor. Of course, down-regulation of lncRNA W5 should be validated in more HCC cohorts. The interactions of this protein and downstream pathways also warrant further investigation in subsequent studies. In addition, whether lncRNA W5

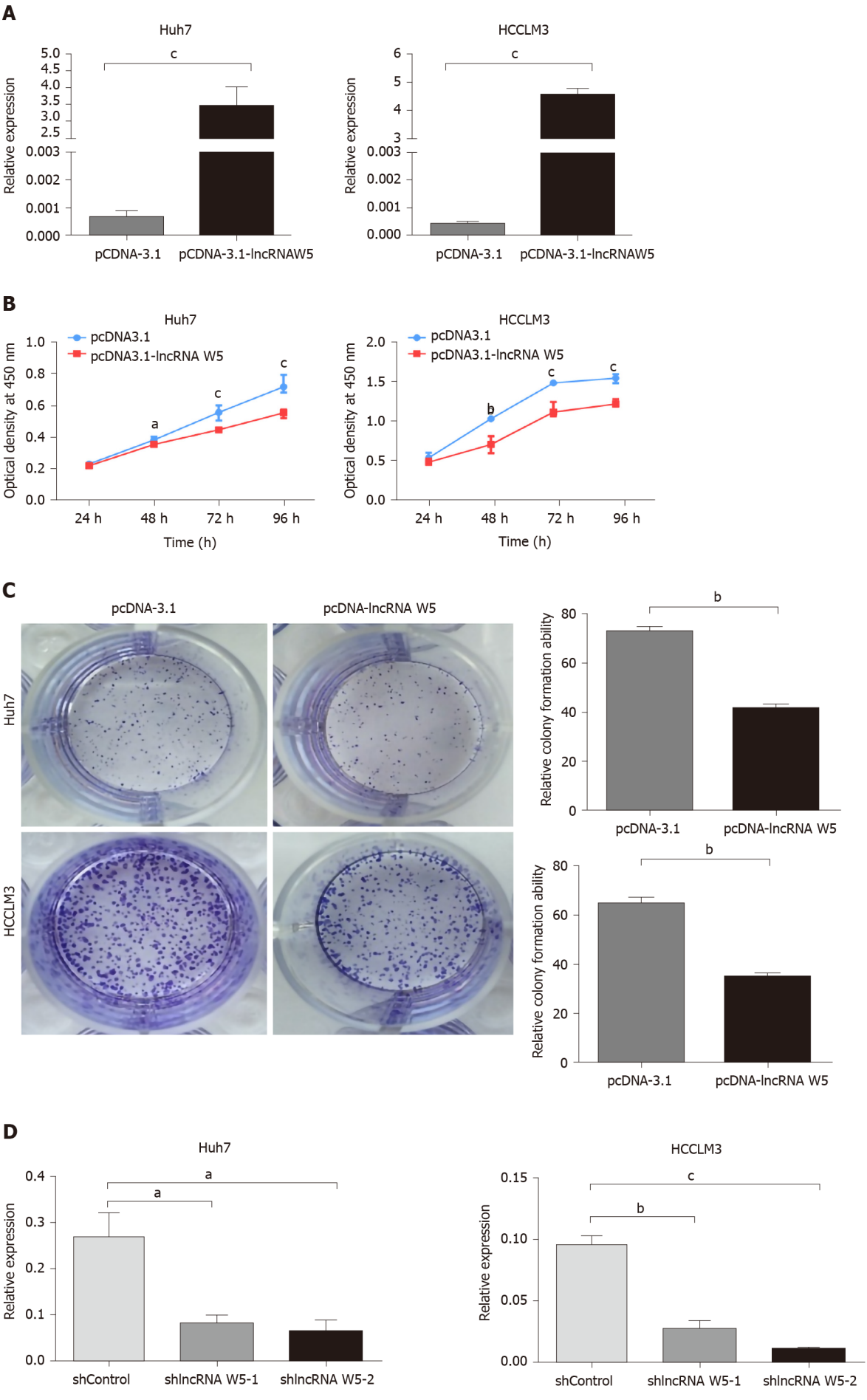
A
Huh7
HCCLM3
Relative expression
pCDNA-3.1
pCDNA-3.1-lncRNAW5
B
Huh7
HCCLM3
pcDNA3.1
pcDNA3.1-lncRNA W5
Optical density at 450 nm
24 h
48 h
72 h
96 h
Time (h)
C
pcDNA-3.1
pcDNA-lncRNA W5
Huh7
HCCLM3
Relative colony formation ability
D
Huh7
HCCLM3
shControl
shlncRNA W5-1
shlncRNA W5-2

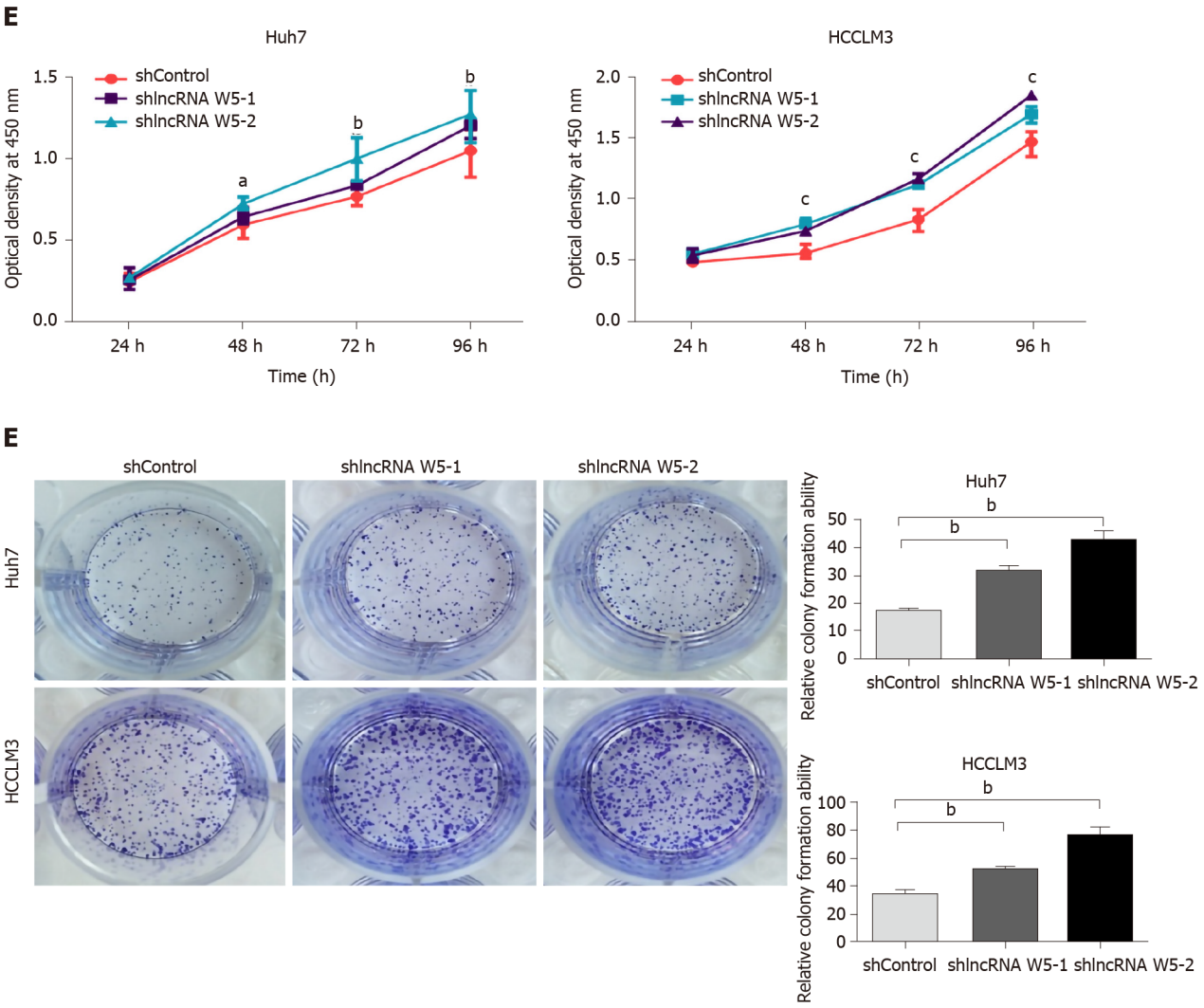

Figure 2 ***In vitro*** **suppression of long non-coding ribonucleic acid W5 in hepatocellular carcinoma proliferation.** A: Increased long non-coding ribonucleic acid (lncRNA) W5 expression in Huh7 and LM3 cells was confirmed after over-expressed lncRNA W5 transfection by reverse transcription-polymerase chain reaction. LncRNA W5 expression was normalized to GAPDH. $^{c}P < 0.001$; B: Cell viability of pCDNA-3.1 LncRNAW5-transfected Huh7 and LM3 cells were detected by CCK-8 assays. Cell number was determined every 24 h up to 96 h. The results are shown as the mean ± SE from three independent experiments. $^{a}P < 0.05$; $^{b}P < 0.01$. $^{c}P < 0.001$, compared with the control by two-sided *t*-test; C: Colony-forming assay was used to determine the effect of lncRNA W5 on the proliferation in Huh7 and LM3 cells; D: Decreased lncRNA W5 expression in Huh7 and LM3 cells was confirmed after sh-1 or sh-2 LncRNAW5 transfection by reverse transcription-polymerase chain reaction. LncRNA W5 expression was normalized to GAPDH. $^{a}P < 0.05$; $^{b}P < 0.01$. $^{c}P < 0.001$; E: Cell viability of sh-1 or sh-2 LncRNAW5-transfected Huh7 and LM3 cells were detected by CCK-8 assays. Cell number was determined every 24 h up to 96 h. The results are shown as the mean ± SE from at least three independent experiments. $^{a}P < 0.05$; $^{b}P < 0.01$. $^{c}P < 0.001$, compared with the control by two-sided *t*-test; and F: Colony-forming assay was used to determine the effect of sh-1 or sh-2 LncRNA W5 on the proliferation of Huh7 and LM3 cells.

exists in other solid tumors remains to be elucidated.

CONCLUSION

In conclusion, our results showed that the expression of lncRNA W5 was considerably reduced in HCC tissues, which suppressed proliferation, migration and invasion of tumor cells *in vitro*. The results also showed that low expression of lncRNA W5 correlated with tumor progression and poor prognosis. Furthermore, manipulation of lncRNA W5 expression impacted the biological behavior of HCC. These results suggest that lncRNA W5 may serve as a tumor suppressor in the development and progression of HCC, and has potential as a diagnostic and therapeutic target in the clinical management of HCC.

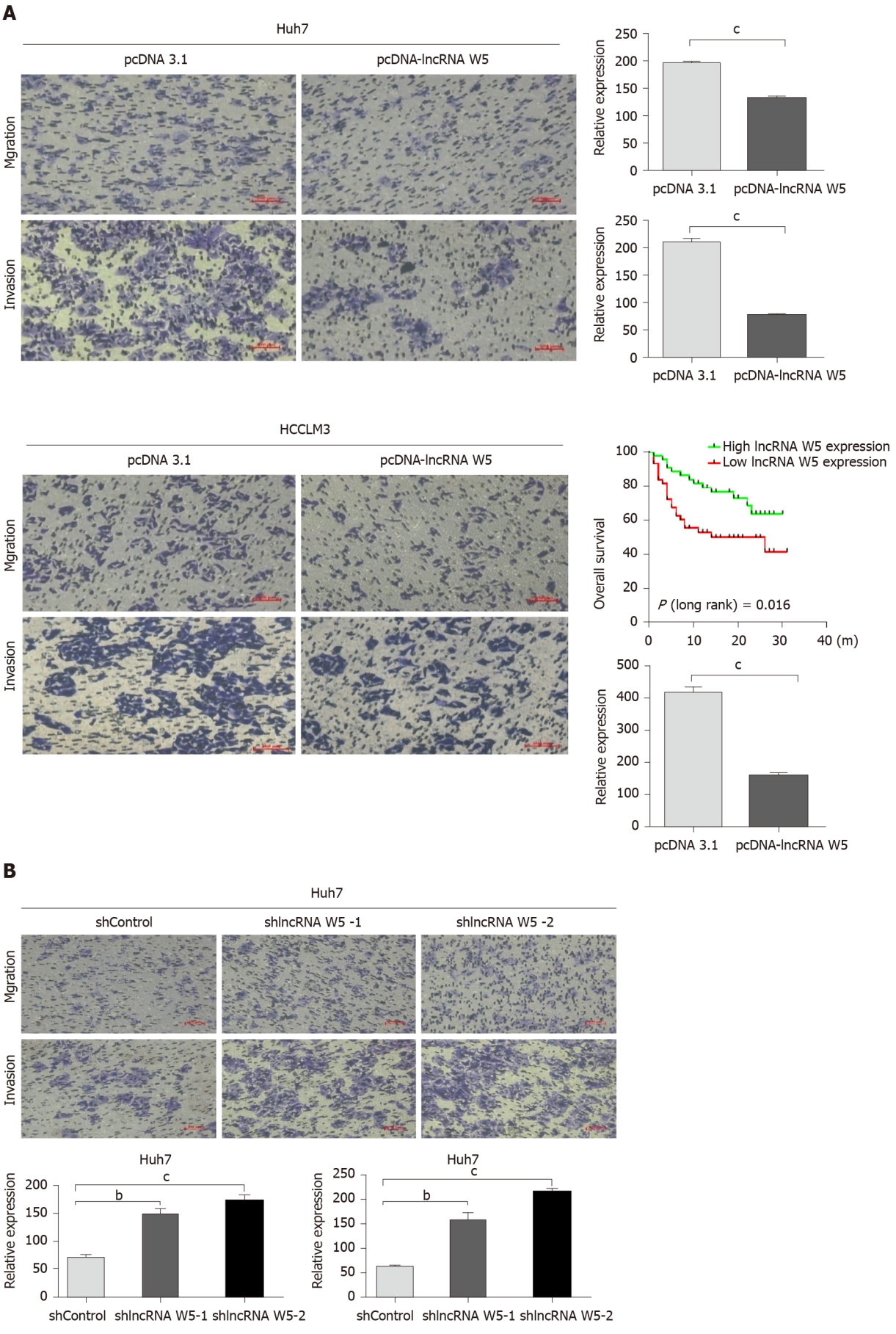
A
Huh7
pcDNA 3.1
pcDNA-lncRNA W5
Mgration
Invasion
Relative expression
c
pcDNA 3.1
pcDNA-lncRNA W5
HCCLM3
High lncRNA W5 expression
Low lncRNA W5 expression
Overall survival
P (long rank) = 0.016
40 (m)
B
shControl
shlncRNA W5 -1
shlncRNA W5 -2
b
shlncRNA W5-1
shlncRNA W5-2

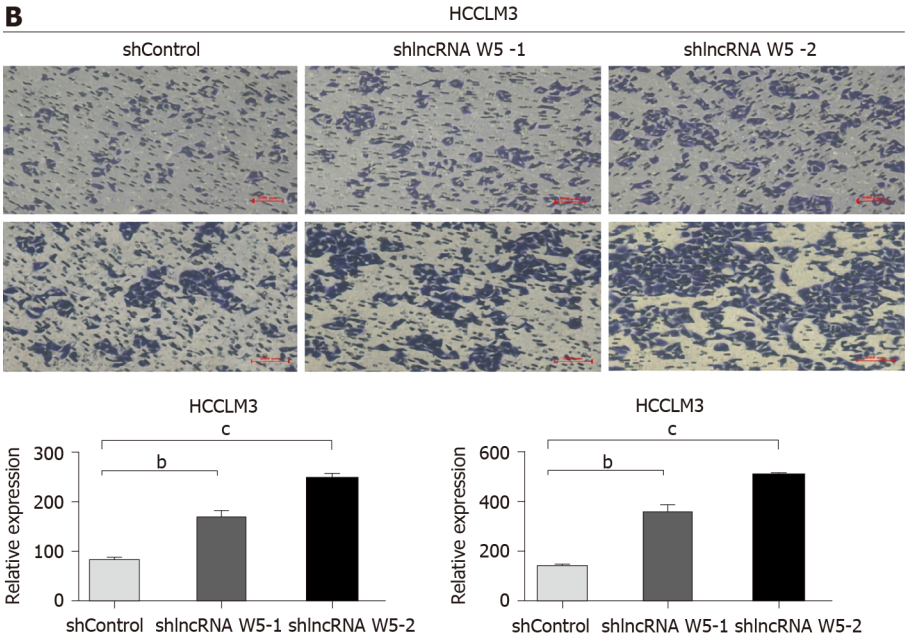

Figure 3 Effects of long non-coding ribonucleic acid W5 on hepatocellular carcinoma migration and invasion. A: Cell migration and invasion abilities were determined after transfection with pcDNA-3.1 and pcDNA-3.1 long non-coding ribonucleic acid W5 in Huh7 and LM3 cell lines, respectively; B: Cell migration and invasion abilities were determined after transfection with sh-1 or sh-2 LncRNA W5 in Huh7 and LM3 cell lines, respectively. All experiments were performed in triplicate. $^{a}P < 0.05$; $^{b}P < 0.01$; $^{c}P < 0.001$.

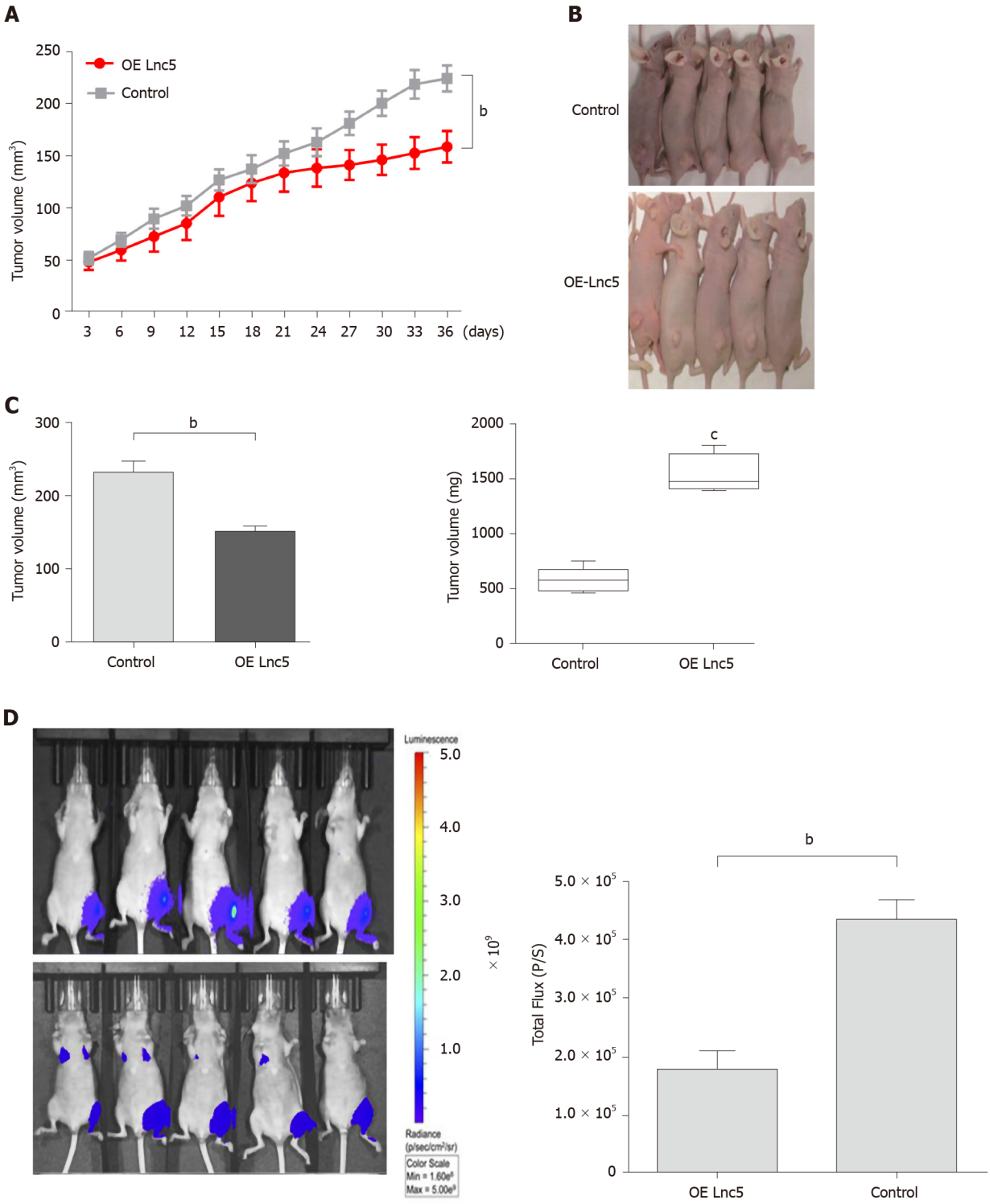

Figure 4 Long non-coding ribonucleic acid W5 inhibits tumor growth *in vivo*. A: Huh7 cells (5×10^6) stably expressed with long non-coding ribonucleic acid W5 (lncRNA W5) were subcutaneously injected into the left flank of nude mice, and the effect of lncRNA W5 on hepatocellular carcinoma tumor growth was examined every 3 d during the course of the experiment ($n = 5$); B: A representative image of the xenograft-bearing mice; C: Tumors were isolated from the nude mice after sacrifice. The effects of lncRNA W5 on hepatocellular carcinoma growth were determined by tumor volume and tumor weight; D: LncRNA W5-overexpressing Huh7 cells which stably expressed luciferase were injected into nude mice ($n = 5$). The bioluminescence photographs of tumor were recorded with the *in vivo* 200 Imaging System. A representative luciferase signal was recorded from each group at 6 wk after injection. $^bP < 0.01$.

ARTICLE HIGHLIGHTS

Research background

Accumulating evidence has revealed that several long non-coding RNAs (lncRNAs) are crucial in the progress of hepatocellular carcinoma (HCC).

Research motivation

To determine the clinical significance and potential roles of lncRNA W5 in HCC.

Research objectives

We classified the long non-coding RNA, lncRNA W5, and examined its clinical significance and potential roles in HCC.

Research methods

Analysis of the association between lncRNA W5 expression levels and clinico-pathological features was performed. In addition, overall survival was determined using Kaplan-Meier survival analysis.

Research results

The results showed that lncRNA W5 was down-regulated in HCC, and it may suppress HCC progression and predict a poor clinical outcome in patients with HCC.

Research conclusions

lncRNA W5 may serve as a potential prognostic biomarker and therapeutic target in HCC.

Research perspectives

lncRNA W5 may serve as a tumor suppressor in the development and progression of HCC, and have potential as a diagnostic and therapeutic target in the clinical management of HCC.

REFERENCES

1 **Hindupur SK**, Colombi M, Fuhs SR, Matter MS, Guri Y, Adam K, Cornu M, Piscuoglio S, Ng CKY, Betz C, Liko D, Quagliata L, Moes S, Jenoe P, Terracciano LM, Heim MH, Hunter T, Hall MN. The protein histidine phosphatase LHPP is a tumour suppressor. *Nature* 2018; **555**: 678-682 [PMID: 29562234 DOI: 10.1038/nature26140]

2 **Zhu J**, Yin T, Xu Y, Lu XJ. Therapeutics for advanced hepatocellular carcinoma: Recent advances, current dilemma, and future directions. *J Cell Physiol* 2019; **234**: 12122-12132 [PMID: 30644100 DOI: 10.1002/jcp.28048]

3 **Okusaka T**, Ikeda M. Immunotherapy for hepatocellular carcinoma: current status and future perspectives. *ESMO Open* 2018; **3**: e000455 [PMID: 30622744 DOI: 10.1136/esmoopen-2018-000455]

4 **Ghouri YA**, Mian I, Rowe JH. Review of hepatocellular carcinoma: Epidemiology, etiology, and carcinogenesis. *J Carcinog* 2017; **16**: 1 [PMID: 28694740 DOI: 10.4103/jcar.JCar_9_16]

5 **Escudier B**, Worden F, Kudo M. Sorafenib: key lessons from over 10 years of experience. *Expert Rev Anticancer Ther* 2019; **19**: 177-189 [PMID: 30575405 DOI: 10.1080/14737140.2019.1559058]

6 **Maracaja-Coutinho V**, Paschoal AR, Caris-Maldonado JC, Borges PV, Ferreira AJ, Durham AM. Noncoding RNAs Databases: Current Status and Trends. *Methods Mol Biol* 2019; **1912**: 251-285 [PMID: 30635897 DOI: 10.1007/978-1-4939-8982-9_10]

7 **Lorenzi L**, Avila Cobos F, Decock A, Everaert C, Helsmoortel H, Lefever S, Verboom K, Volders PJ, Speleman F, Vandesompele J, Mestdagh P. Long noncoding RNA expression profiling in cancer: Challenges and opportunities. *Genes Chromosomes Cancer* 2019; **58**: 191-199 [PMID: 30461116 DOI: 10.1002/gcc.22709]

8 **Zeng Y**, Ren K, Zhu X, Zheng Z, Yi G. Long Noncoding RNAs: Advances in Lipid Metabolism. *Adv Clin Chem* 2018; **87**: 1-36 [PMID: 30342708 DOI: 10.1016/bs.acc.2018.07.001]

9 **Rafiee A**, Riazi-Rad F, Havaskary M, Nuri F. Long noncoding RNAs: regulation, function and cancer. *Biotechnol Genet Eng Rev* 2018; **34**: 153-180 [PMID: 30071765 DOI: 10.1080/02648725.2018.1471566]

10 **Idda ML**, Munk R, Abdelmohsen K, Gorospe M. Noncoding RNAs in Alzheimer's disease. *Wiley Interdiscip Rev RNA* 2018; **9** [PMID: 29327503 DOI: 10.1002/wrna.1463]

11 **Yu WD**, Wang H, He QF, Xu Y, Wang XC. Long noncoding RNAs in cancer-immunity cycle. *J Cell Physiol* 2018; **233**: 6518-6523 [PMID: 29574911 DOI: 10.1002/jcp.26568]

12 **Cheng D**, Deng J, Zhang B, He X, Meng Z, Li G, Ye H, Zheng S, Wei L, Deng X, Chen R, Zhou J.

LncRNA HOTAIR epigenetically suppresses miR-122 expression in hepatocellular carcinoma *via* DNA methylation. *EBioMedicine* 2018; **36**: 159-170 [PMID: 30195653 DOI: 10.1016/j.ebiom.2018.08.055]

13 **Sun QM**, Hu B, Fu PY, Tang WG, Zhang X, Zhan H, Sun C, He YF, Song K, Xiao YS, Sun J, Xu Y, Zhou J, Fan J. Long non-coding RNA 00607 as a tumor suppressor by modulating NF-κB p65/p53 signaling axis in hepatocellular carcinoma. *Carcinogenesis* 2018; **39**: 1438-1446 [PMID: 30169594 DOI: 10.1093/carcin/bgy113]

14 **Noh JH**, Gorospe M. AKTions by Cytoplasmic lncRNA CASC9 Promote Hepatocellular Carcinoma Survival. *Hepatology* 2018; **68**: 1675-1677 [PMID: 30014487 DOI: 10.1002/hep.30165]

15 **Wang Y**, Chen F, Zhao M, Yang Z, Li J, Zhang S, Zhang W, Ye L, Zhang X. The long noncoding RNA HULC promotes liver cancer by increasing the expression of the HMGA2 oncogene *via* sequestration of the microRNA-186. *J Biol Chem* 2017; **292**: 15395-15407 [PMID: 28765279 DOI: 10.1074/jbc.M117.783738]

16 **Zhou Y**, Fan RG, Qin CL, Jia J, Wu XD, Zha WZ. LncRNA-H19 activates CDC42/PAK1 pathway to promote cell proliferation, migration and invasion by targeting miR-15b in hepatocellular carcinoma. *Genomics* 2019; **111**: 1862-1872 [PMID: 30543848 DOI: 10.1016/j.ygeno.2018.12.009]

17 **Zheng Q**, Lin Z, Xu J, Lu Y, Meng Q, Wang C, Yang Y, Xin X, Li X, Pu H, Gui X, Li T, Xiong W, Lu D. Long noncoding RNA MEG3 suppresses liver cancer cells growth through inhibiting β-catenin by activating PKM2 and inactivating PTEN. *Cell Death Dis* 2018; **9**: 253 [PMID: 29449541 DOI: 10.1038/s41419-018-0305-7]

18 **Li T**, Xie J, Shen C, Cheng D, Shi Y, Wu Z, Deng X, Chen H, Shen B, Peng C, Li H, Zhan Q, Zhu Z. Amplification of Long Noncoding RNA ZFAS1 Promotes Metastasis in Hepatocellular Carcinoma. *Cancer Res* 2015; **75**: 3181-3191 [PMID: 26069248 DOI: 10.1158/0008-5472.CAN-14-3721]

19 **Cheng S**, Li T, Wang C, Wang K, Lai C, Yan J, Fan H, Sun F, Wang Z, Zhang P, Yu L, Hong Z, Lei G, Sun B, Gao Y, Xiao Z, Ji X, Wang R, Wu J, Wang X, Zhang S, Yang P. Decreased long intergenic noncoding RNA P7 predicts unfavorable prognosis and promotes tumor proliferation *via* the modulation of the STAT1-MAPK pathway in hepatocellular carcinoma. *Oncotarget* 2018; **9**: 36057-36066 [PMID: 30546827 DOI: 10.18632/oncotarget.23282]

20 **Yuan JH**, Yang F, Wang F, Ma JZ, Guo YJ, Tao QF, Liu F, Pan W, Wang TT, Zhou CC, Wang SB, Wang YZ, Yang Y, Yang N, Zhou WP, Yang GS, Sun SH. A long noncoding RNA activated by TGF-β promotes the invasion-metastasis cascade in hepatocellular carcinoma. *Cancer Cell* 2014; **25**: 666-681 [PMID: 24768205 DOI: 10.1016/j.ccr.2014.03.010]

21 **Pan W**, Zhang N, Liu W, Liu J, Zhou L, Liu Y, Yang M. The long noncoding RNA *GAS8-AS1* suppresses hepatocarcinogenesis by epigenetically activating the tumor suppressor *GAS8*. *J Biol Chem* 2018; **293**: 17154-17165 [PMID: 30228180 DOI: 10.1074/jbc.RA118.003055]

22 **Jang SY**, Kim G, Park SY, Lee YR, Kwon SH, Kim HS, Yoon JS, Lee JS, Kweon YO, Ha HT, Chun JM, Han YS, Lee WK, Chang JY, Park JG, Lee B, Tak WY, Hur K. Clinical significance of lncRNA-ATB expression in human hepatocellular carcinoma. *Oncotarget* 2017; **8**: 78588-78597 [PMID: 29108251 DOI: 10.18632/oncotarget.21094]

23 **Yuan JH**, Liu XN, Wang TT, Pan W, Tao QF, Zhou WP, Wang F, Sun SH. The MBNL3 splicing factor promotes hepatocellular carcinoma by increasing PXN expression through the alternative splicing of lncRNA-PXN-AS1. *Nat Cell Biol* 2017; **19**: 820-832 [PMID: 28553938 DOI: 10.1038/ncb3538]

24 **Wu J**, Zhu P, Lu T, Du Y, Wang Y, He L, Ye B, Liu B, Yang L, Wang J, Gu Y, Lan J, Hao Y, He L, Fan Z. The long non-coding RNA LncHDAC2 drives the self-renewal of liver cancer stem cells *via* activation of Hedgehog signaling. *J Hepatol* 2019; **70**: 918-929 [PMID: 30582981 DOI: 10.1016/j.jhep.2018.12.015]

25 **Peng L**, Jiang B, Yuan X, Qiu Y, Peng J, Huang Y, Zhang C, Zhang Y, Lin Z, Li J, Yao W, Deng W, Zhang Y, Meng M, Pan X, Li C, Yin D, Bi X, Li G, Lin DC. Super-Enhancer-Associated Long Noncoding RNA HCCL5 Is Activated by ZEB1 and Promotes the Malignancy of Hepatocellular Carcinoma. *Cancer Res* 2019; **79**: 572-584 [PMID: 30482773 DOI: 10.1158/0008-5472.CAN-18-0367]

26 **Huang JF**, Jiang HY, Cai H, Liu Y, Zhu YQ, Lin SS, Hu TT, Wang TT, Yang WJ, Xiao B, Sun SH, Ma LY, Yin HR, Wang F. Genome-wide screening identifies oncofetal lncRNA Ptn-dt promoting the proliferation of hepatocellular carcinoma cells by regulating the Ptn receptor. *Oncogene* 2019; **38**: 3428-3445 [PMID: 30643194 DOI: 10.1038/s41388-018-0643-z]

World Journal of Gastroenterology

Submit a Manuscript: https://www.f6publishing.com

World J Gastroenterol 2021 January 7; 27(1): 69-79

DOI: 10.3748/wjg.v27.i1.69

ISSN 1007-9327 (print) ISSN 2219-2840 (online)

ORIGINAL ARTICLE

Retrospective Study

Predictors of pain response after endoscopic ultrasound-guided celiac plexus neurolysis for abdominal pain caused by pancreatic malignancy

Chao-Qun Han, Xue-Lian Tang, Qin Zhang, Chi Nie, Jun Liu, Zhen Ding

ORCID number: Chao-Qun Han 0000-0003-1338-865X; Xue-Lian Tang 0000-0002-1695-7371; Qin Zhang 0000-0001-9156-0772; Chi Nie 0000-0001-6897-2138; Jun Liu 0000-0003-4436-5729; Zhen Ding 0000-0001-8575-5282.

Author contributions: Han CQ performed the literature search and data extraction and drafted of the manuscript; Tang XL and Zhang Q collected the data; Nie C and Liu J contributed important intellectual content; Ding Z designed the study and edited the manuscript as corresponding author.

Supported by National Natural Science Foundation of China, No. 81800467 and No. 81770637.

Institutional review board statement: The study was approved by the Ethics Committee of Tongji Medical College, Huazhong University of Science and Technology (IORG No: IORG0003571).

Informed consent statement: Written informed consent was obtained from the patients.

Conflict-of-interest statement: There is no conflict of interest in this study.

Chao-Qun Han, Xue-Lian Tang, Qin Zhang, Chi Nie, Jun Liu, Zhen Ding, Division of Gastroenterology, Union Hospital, Tongji Medical College, Huazhong University of Science and Technology, Wuhan 430022, Hubei Province, China

Corresponding author: Zhen Ding, MD, PhD, Doctor, Professor, Teacher, Division of Gastroenterology, Union Hospital, Tongji Medical College, Huazhong University of Science and Technology, No. 1277 Jiefang Avenue, Wuhan 430022, Hubei Province, China. 2017xh0122@hust.edu.cn

Abstract

BACKGROUND

Endoscopic ultrasound-guided celiac plexus neurolysis (EUS-CPN) has gained popularity as a minimally invasive approach and is currently widely used to treat pancreatic cancer-associated pain. However, response to treatment is variable.

AIM

To identify the efficacy of EUS-CPN and explore determinants of pain response in EUS-CPN for pancreatic cancer-associated pain.

METHODS

A retrospective study of 58 patients with abdominal pain due to inoperable pancreatic cancer who underwent EUS-CPN were included. The efficacy for palliation of pain was evaluated based on the visual analog scale pain score at 1 wk and 4 wk after EUS-CPN. Univariable and multivariable logistic regression analyses were performed to explore predictors of pain response.

RESULTS

A good pain response was obtained in 74.1% and 67.2% of patients at 1 wk and 4 wk, respectively. Tumors located in the body/tail of the pancreas and patients receiving bilateral treatment were weakly associated with a good outcome. Multivariate analysis revealed patients with invisible ganglia and metastatic disease were significant factors for a negative response to EUS-CPN at 1 wk and 4 wk, respectively, particularly for invasion of the celiac plexus (odds ratio (OR) = 13.20, P = 0.003 for 1 wk and OR = 15.11, P = 0.001 for 4 wk). No severe adverse events were reported.

Data sharing statement: Dataset available from the corresponding author at 271914799@qq.com.

Manuscript source: Unsolicited manuscript

Specialty type: Gastroenterology and Hepatology

Country/Territory of origin: China

Peer-review report's scientific quality classification

Grade A (Excellent): 0
Grade B (Very good): B
Grade C (Good): C
Grade D (Fair): D
Grade E (Poor): 0

Received: July 4, 2020
Peer-review started: July 4, 2020
First decision: August 8, 2020
Revised: August 15, 2020
Accepted: November 12, 2020
Article in press: November 12, 2020
Published online: January 7, 2021

P-Reviewer: Kozarek RA, Thandassery RB
S-Editor: Liu M (Part-Time Editor)
L-Editor: Filipodia
P-Editor: Ma YJ

CONCLUSION

EUS-CPN is a safe and effective form of treatment for intractable pancreatic cancer-associated pain. Invisible ganglia, distant metastasis, and invasion of the celiac plexus were predictors of less effective response in EUS-CPN for pancreatic cancer-related pain. For these patients, efficacy warrants attention.

Key Words: Endoscopic ultrasound; Celiac plexus neurolysis; Pancreatic cancer; Pain; Predictor

Core Tip: Endoscopic ultrasound-guided celiac plexus neurolysis (EUS-CPN) is widely used to treat pancreatic cancer-associated pain. However, response to treatment is variable. The procedure is not always effective, is often variable, and yields transient results. The data on determinants of pain relief response following EUS-CPN are limited and still need to undergo further exploration. Our study found that invisible ganglia, presence of distant metastases, and celiac plexus invasion were considered to be significantly negative variables. The strongest predictor of response was celiac plexus invasion. Moreover, tumors located at the body/tail predicted a better response than those with tumors at the pancreatic head/neck.

Citation: Han CQ, Tang XL, Zhang Q, Nie C, Liu J, Ding Z. Predictors of pain response after endoscopic ultrasound-guided celiac plexus neurolysis for abdominal pain caused by pancreatic malignancy. *World J Gastroenterol* 2021; 27(1): 69-79
URL: https://www.wjgnet.com/1007-9327/full/v27/i1/69.htm
DOI: https://dx.doi.org/10.3748/wjg.v27.i1.69

INTRODUCTION

Up to 90% advanced pancreatic cancer patients experience difficult-to-control pain syndromes[1]. Conventionally, pain is alleviated using a three-step analgesic ladder approach beginning with nonsteroidal anti-inflammatory agents followed by escalating doses of opiates[2]. However, pain is always refractory in some cases, posing a challenge to the physician. A high dose of such drugs still cannot provide adequate analgesia, especially for those patients experiencing intolerable drug-related side effects that can markedly reduce survival. In these patients, interventional pain techniques may be indicated.

In endoscopic ultrasound-guided celiac plexus neurolysis (EUS-CPN), a neurolytic agent disrupts the pain signal transductions from the afferent nerves to the spinal cord, and it has been widely applied as a minimally invasive approach. This procedure is able to decrease significantly the daily usage of morphine medications and relieve pain. The current National Comprehensive Cancer Network guidelines recommends EUS-CPN for treatment of severe cancer-associated pain[3]. Varied studies have reported that over 80% of patients achieved sustainable pain relief after treatment, and many even to the time of death[4,5].

However, the procedure is not always effective, is often variable, and has transient results. Subsequent studies showed the proportion of patients benefiting from pain amelioration is quite variable at 50% to 80%[6-8]. Optimization of treatment outcomes for the technique of neurolysis involves direct injection into the celiac ganglia, broad injection to involve the area around the superior mesenteric artery, and bilateral *vs* unilateral injection; lesion characteristics for optimization have been reported as well, but findings are controversial[7,9-12]. EUS-CPN is not recommended for patients suspected of having unfavorable outcomes. Moreover, the data on determinants of pain relief response following EUS-CPN are limited and still need to undergo further exploration. In this study, we attempt to summarize the predictive factors for response to EUS-CPN in pancreatic cancer with the goal of providing rational selection of the therapeutic strategies to alleviate pancreatic cancer-associated pain.

MATERIALS AND METHODS

Study population

A total of 58 patients who were diagnosed with pancreatic cancer and underwent EUS-CPN over a 4-year period (from January 2015 to December 2018) were included in this study. The inclusion criteria were as follows: (1) Patients over the age of 18 years; (2) Complete information; (3) Presence of unresectable or metastatic pancreatic cancer; (4) No receiving any palliative chemotherapy or radiation therapy; (5) No bleeding tendency (international normalized ratio ≤ 1.5 or platelet count ≥ 50,000 × 10^9/L); (6) No esophageal or gastric varices; and (7) Enduring abdominal or back pain due to confirmed pancreatic malignancy diagnosed by EUS guided fine-needle aspiration/biopsy or percutaneous biopsy. The study was approved by the Ethics Committee of Tongji Medical College, Huazhong University of Science and Technology (IORG No: IORG0003571). All patients signed informed consent for EUS operation, and data were anonymized and de-identified.

Endoscopic procedure in EUS-CPN

Patients were hydrated with 500-1000 mL saline solution during the procedure to minimize the risk of hypotension. They were placed in the left lateral decubitus position, and propofol was administered for deep sedation. Vital signs were continuously monitored with an automated non-invasive blood pressure measurement, electrocardiogram, and pulse oximetry.

EUS-CPN was performed by using the Olympus processor EU-ME2 with a linear array endoscopic ultrasonography (GF-UCT 260; Olympus, Tokyo, Japan). By tracing the aorta under real-time EUS guidance, the base of the celiac artery was identified. Celiac ganglia could be visualized between the celiac artery and the left adrenal gland. Typically for CPN unilateral injection, an Echo Tip 22-gauge needle (Cook Medical, Inc., Winston-Salem, NC, United States) primed with normal saline solution was inserted into the operating channel, affixed to the hub, and placed adjacent to the base of the celiac trunk at its origin from the aorta. In cases with bilateral injection, the same procedure was done, but injections were done at both sides of the celiac trunk with clockwise and counter-clockwise rotation (half of the dehydrated 98% absolute alcohol was injected in each side)[13,14]. After confirming no backflow of blood occurred, the celiac plexus injection by dehydrated 98% absolute alcohol was directly applied. A dense hyperechoic cloud was usually seen in the area of injection, and the injection was continued until spilling to the periganglionic space (Supplemental material). Whether a bilateral injection was carried out depended on the locations of intervening vessels, the tumor status, and invasion of the celiac plexus or not. Tumors extending to the para-aortic region from the level of the celiac axis to the origin of SMA were considered invasive of the celiac plexus. No antibiotics were administered before or post-CPN. All procedures were performed by a single endosonographer.

Pain scores

Pain intensity was evaluated by telephone interview and done objectively using a continuous visual analog scale (VAS), with 0 as no pain and 10 as worst possible pain. Detailed instructions explaining how to assess the VAS were read and the patients then informed the best VAS score that reflected their pain status. Good pain relief was defined as a decrease in the pain score by ≥ 3 or a ≥ 30% reduction in baseline pain without any increase in the narcotic daily dosing[15]. If the patients had no pain improvement or markedly increased pain or required additional doses of narcotic agents 1 wk after the procedure, the procedure was considered to be a failure.

Outcomes measures

Primary outcomes included the efficacy of EUS-CPN and the difference in pain control by VAS was compared. Pain management was evaluated at 1 wk and 4 wk after the CPN procedure. Secondary outcomes included analgesia requirement and adverse events. To minimize subjective variations in the evaluation of outcomes, the same authorized staff who was unaware of the detailed endoscopic procedures collected the outcomes of all patients.

Data collection

To analyze all possible factors that could affect the determinants of pain response in patients undergoing EUS-CPN for abdominal pain caused by pancreatic cancer, the following data were collected for each patient: Information regarding tumor characteristics (*i.e.* size, location, vascular invasion, and distant metastasis), procedure

details (including procedure method, dehydrated alcohol dose, visible or invisible ganglia, and intra-procedural heart rate change), the incidence of adverse events, and the dose of morphine medications administered before and after the assignment intervention. Heart rate change was defined as a decrease of ≥ 5 beats for ≥ 10 s during alcohol injection. Other covariates, including demographics (*i.e.* age, gender, initial VAS score), symptom *(i.e.* abdominal pain concomitant with jaundice and presence of ascites), were also collected.

Statistical analysis

Categorical data are presented as counts and percentages. Continuous variable results were presented as mean ± standard deviation. Associations among various categorical variables were constructed by Pearson's chi-squared test, and non-categorical variables were analyzed by *t* tests. Subsequently, univariable and multivariable logistic regression analyses were carried out to examine potential predictors of pain response to the CPN procedure. All statistical analyses were performed using IBM SPSS software20.0 (SPSS, Armonk, NY, United States). Values were considered to be statistically significant if the *P* value was less than 0.05 (two-sided).

RESULTS

Patient demographic and clinical characteristics

A total of 58 patients with abdominal pain due to inoperable pancreatic cancer who underwent EUS-CPN were included. These cases consisted of 33 men and 25 women with a mean age of 67 years (range: 54-73 years). Predominant distribution of tumor location in pancreas was located in the body/tail (69.0%), and mean tumor diameter was 44.3 mm (range: 24-100 mm). Fifty-one patients were referred for initial evaluation of suspected pancreatic cancer and were first confirmed *via* EUS-fine needle aspiration (FNA) before undergoing EUS-CPN in the same session. The seven remaining patients had been previously diagnosed with pancreatic malignancy and were referred to our center for palliation with EUS-CPN only. The 51 patients had malignant tumors histologically confirmed by EUS-FNA of pancreas (n = 36), enlarged lymph nodes (n = 8), and liver metastases (n = 3) or ascites cytology (n = 4). Of the entire group of patients, visible pre-procedural celiac ganglia were present in 42 patients (72.4%) during the EUS session. Direct invasion of the celiac plexus was detected in 16 (27.6%) patients, whereas 26 (44.8%) patients had distant metastasis. The patient clinical demographics, disease, and treatment characteristics are summarized in Table 1 and Figure 1.

Efficacy for palliation of pain after EUS-CPN

With regard to therapeutic effect, the mean dose of alcohol injection was 10 mL (range: 5-20 mL). The mean initial VAS score was 8, and 51 patients (87.9%) were already taking narcotic analgesics prior to EUS-CPN. The tramadol dose used was 50 mg per time (range: 0–300). The rates of good pain response, defined as a drop of VAS score by ≥ 3 points in pain scale with subjective pain improvements without additional narcotics, were 74.1% and 67.2% of patients at 1 wk and 4 wk after EUS-guided neurolysis, respectively. The other patients were regarded as treatment failures, because either the pain was not better by ≥ 3 points from the baseline VAS score or they were feeling not better and increased their dose of tramadol medication after EUS-CPN. In the successful-treatment group, there was clearly a persistent treatment effect where pain relief lasted for 1–16 wk (until death in eight patients). Overall, there was a significant reduction in pain score from a mean of 8.2 at baseline to 4.4 at 1 wk (P = 0.004) and to 4.9 at 4 wk (P = 0.012) in all patients.

Predictors associated with pain response after EUS-CPN

To assess the predictive factors for pain response at 1 wk and 4 wk in patients who underwent EUS-CPN, variable data between the successful-treatment and the insufficient groups were compared. At 1 wk, tumors located in the body/tail of the pancreas and patients receiving bilateral procedure were weakly associated with a good response, but this was not statistically significant (P = 0.094; P = 0.087, respectively) (Table 2). However, invisible ganglia and presence of distant metastasis were significant negative predictive factors in the univariable analysis [odds ratio (OR) = 3.574, 95% confidence interval (CI): 1.80-14.24, P = 0.003; OR = 5.940, 95%CI: 1.31-11.82, P = 0.015]. Moreover, invasion of the celiac plexus was significantly associated

Table 1 Baseline characteristics of patients who underwent endoscopic ultrasound-guided celiac plexus neurolysis [*n* (%), *n* = 58]

Independent variables	Total number
Age in yr, range (mean)	54–73 (67)
Gender, female/male	25/33
Symptom	
Abdominal pain concomitant with jaundice Tumor largest dimension in mm, range (mean)	6 (10.3)
Ascites, slight or mild	24–100 (44.3)
Tumor location	4 (6.9)
Pancreatic head/neck	
Pancreatic body/tail	18 (31.0)
Initial VAS score, range (mean)	40 (69.0)
Tramadol use before EUS-CPN	6-10 (8)
Dose in mg, range (mean)	51 (87.9)
Ganglia visualized	0-240 (40)
Invasion of celiac plexus	42 (72.4)
Distant metastasis	16 (27.6)
Injected alcohol dose in mL, range (mean)	26 (44.8)
Procedure method	5–20 (10)
Unilateral	
Bilateral	33 (56.9)
Intra-procedural decrease in heart rate	25 (43.1)
decrease of ≥ 5 beats for ≥ 10 s	
	48 (82.8)

EUS-CPN: Endoscopic ultrasound-guided celiac plexus neurolysis; VAS: Visual analog scale.

with a poor pain response (OR = 7.922, P = 0.001). When these factors were subjected to multivariable logistic regression analysis, invisible ganglia, presence of distant metastases, and celiac plexus invasion were identified as significant negative independent pain response factors to EUS-CPN (Table 3). The other factors age, gender, symptom, tumor size, presence of ascites, and initial pain scores did not differ significantly between the two groups (Table 2). Furthermore, neither the pre-intervention tramadol dose use nor injected alcohol dose correlated with the outcome of EUS-CPN. Finally, there was no statistical difference in response to diagnosis between patients who were presenting for initial evaluation by EUS-FNA and those who already had a biopsy-proven pancreatic cancer.

Similarly, at 4 wk, invisible ganglia, presence of distant metastases, and celiac plexus invasion were significant negative predictive factors in univariable analysis (P = 0.003, P = 0.009 and P = 0.001, respectively) (Table 4). At multivariate regression analysis of potential predictors, invisible ganglia, presence of distant metastases, and celiac plexus invasion were associated with a bad pain response (P = 0.037, P = 0.019 and P = 0.001, respectively). The strongest predictor of response was celiac plexus invasion, which yielded a 15-fold higher chance of response for those patients compared with those without celiac plexus invasion (Table 5).

Complication after EUS-CPN

Complications occurred in 10.3% of enrolled patients. No serious adverse events including ischemic, inebriation, and acute paraplegia related to EUS-CPN occurred. Most of the complications were minor and transitory self-limited and included hypotension (1.7%), increase of pain (5.2%), and transient loose stools (3.4%).

Table 2 Univariable analysis of variables associated with pain response after 1 wk in the enrolled cohort of 58 patients

Independent variables	OR	95%CI	*P* value
Age in yr	1.084	0.60-3.88	0.212
Gender, female/male	1.39	0.43-3.79	0.64
Symptom			
Abdominal pain concomitant with jaundice	1.29	0.53–3.26	0.581
Tumor largest dimension	1.32	0.45-4.69	0.665
Ascites	1.772	0.59–6.84	0.437
Tumor location			
Pancreatic head/neck	2.071	0.60-7.09	0.232
Pancreatic body/tail	0.617	0.65-10.40	0.094
Initial VAS score	2.231	0.76-5.41	0.132
Tramadol use before EUS-CPN	1.339	0.54-15.39	0.327
Invisible ganglia	3.574	1.80-14.24	**0.003**
Invasion of celiac plexus	7.922	2.24-25.93	**0.001**
Distant metastasis	5.94	1.31–11.82	**0.015**
Injected alcohol dose	3.825	1.12–13.42	0.437
Procedure method			
Unilateral	1.677	0.84–11.48	0.591
Bilateral	0.489	0.11–1.12	0.087
Intra-procedural decrease in heart rate	1.011	0.91–2.08	0.933

OR: Odds ratio; CI: Confidence interval; EUS-CPN: Endoscopic ultrasound-guided celiac plexus neurolysis; VAS: Visual analogue scale.

Table 3 Multivariate analysis for predictors affecting pain response after 1 wk by endoscopic ultrasound-guided celiac plexus neurolysis

Independent variables	OR	95%CI	*P* value
Ganglia invisible	4.9	2.25-17.91	0.011
Invasion of celiac plexus	13.2	3.02-46.27	0.003
Distant metastasis	6.84	2.34–19.15	0.022

Summarizes the results of the multivariate analyses of the predictive factors associated with pain relief by EUS-CPN. The only independent predictive factors that achieved statistical significance in the univariate analysis were included. CI: Confidence interval; EUS-CPN: Endoscopic ultrasound-guided celiac plexus neurolysis; OR: Odds ratio.

DISCUSSION

Pancreatic cancer is often associated with intense and refractory pain. EUS-CPN was demonstrated to be safe and significantly improved pain control in 88% of patients with pancreatic cancer[16]. However, subsequent studies showed substantial variation in the proportion of patients experiencing pain relief[17]. This wide range is mainly attributable to differences in the characteristics of patients and the lack of standardized operation. For these reasons, it is difficult to compare the efficacy rate of EUS-CPN. Therefore, the current study was designed to analyze potential factors influencing EUS-CPN efficacy in patients with pancreatic cancer. Our data revealed that patients with invisible ganglia, distant metastasis, and invasion of the celiac plexus were predictors of less effective response in EUS-guided neurolysis for pancreatic cancer-related pain.

Our results demonstrated that invisible ganglia, presence of distant metastases, and

Table 4 Univariable analysis of variables associated with pain response after 4 wk in the enrolled cohort of 58 patients

Independent variables	OR	95%CI	*P* value
Age in yr	1.091	0.63-3.94	0.209
Gender, female/male	1.124	0.47-3.99	0.532
Symptom			
Abdominal pain concomitant with	1.384	0.43–4.82	0.618
jaundice	1.496	0.32-5.92	0.701
Tumor largest dimension	1.921	0.79–9.34	0.408
Ascites			
Tumor location	3.59	0.40-10.06	0.184
Pancreatic head/neck	0.42	0.15-12.77	0.082
Pancreatic body/tail	2.93	0.42-8.17	0.101
Initial VAS score	2.91	0.24-19.40	0.149
Tramadol use before EUS-CPN	4.02	1.62-13.27	0.003
Invisible ganglia	8.84	2.11-23.32	0.001
Invasion of celiac plexus	7.83	1.81–15.77	0.009
Distant metastasis	4.90	1.32–17.91	0.394
Injected alcohol dose			
Procedure method	2.87	0.44–17.41	0.502
Unilateral	0.54	0.16–1.99	0.093
Bilateral	0.94	0.42–3.12	0.858
Intra-procedural decrease in heart rate			

CI: Confidence interval; EUS-CPN: Endoscopic ultrasound-guided celiac plexus neurolysis; OR: Odds ratio; VAS: Visual analogue scale.

Table 5 Multivariate analysis for predictors affecting pain response after 4 wk by endoscopic ultrasound-guided celiac plexus neurolysis

Independent variables	OR	95%CI	*P* value
Invisible ganglia	5.85	2.66-22.73	0.037
Invasion of celiac plexus	15.11	4.01-51.22	0.001
Distant metastasis	8.59	2.16–27.02	0.019

Summarizes the results of the multivariate analyses of the predictive factors associated with pain relief by EUS-CPN. The only independent predictive factors that achieved statistical significance in the univariate analysis were included. CI: Confidence interval; EUS-CPN: Endoscopic ultrasound-guided celiac plexus neurolysis; OR: Odds ratio.

celiac plexus invasion were significant negative variables at 1 wk and 4 wk after EUS-CPN by univariable analysis and multivariate regression analysis. The strongest predictor of response was celiac plexus invasion, which may be related to perineural invasion of pancreatic nerves by tumor cells. Direct invasion of the ganglia or plexus may result in patients with pain not mediated by the celiac plexus[1]. In fact, FNA of the celiac ganglia has confirmed invasion by malignant cells in some patients with pancreatic cancer[18]. The reason also may be that cancer invasion restricts the spread of neurolytic solution and limits the subsequent pain relief[19]. Iwata *et al*[20] also suggested that EUS-CPN seems to be less effective in patients with direct invasion of the celiac plexus.

There are mixed findings regarding bilateral or unilateral approach, and a recent meta-analysis showed that the short-term analgesic effect and general risk of bilateral EUS-CPN are comparable with those of unilateral EUS-CPN[9]. There were no

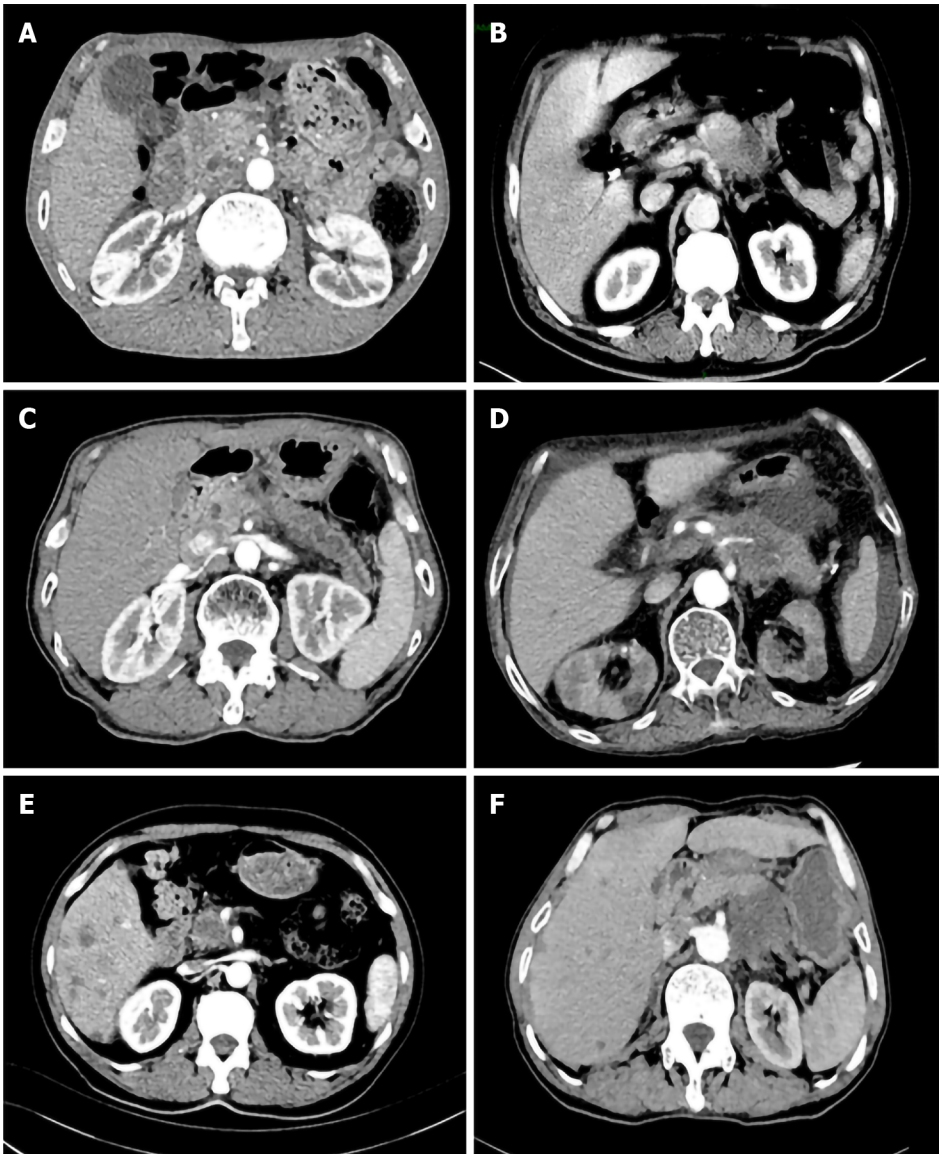

Figure 1 Varied pancreatic lesions are shown by contrast-enhanced computed tomography image. A: The lesion was located in head/neck of pancreas; B: The lesion was located in body/tail of pancreas; C: Pancreatic head lesion was associated with celiac trunk and celiac plexus invasion; D: The image showed a pancreatic body/tail invading the celiac plexus; E: Pancreatic head/neck lesion was accompanied with hepatic metastasis; F: Pancreatic body/tail lesion was accompanied with hepatic metastasis.

differences in onset or duration of pain relief when either one or two injections were used[13,14,21]. In our cohort patients, the bilateral method was associated with a good pain response but no statistical significance (P = 0.087). With regard to the dose of alcohol used in EUS-CPN, the amount of alcohol used in EUS-CPN ranged from 2 mL to 20 mL[22-24]. Our results found that there was no difference in the dose of alcohol used in EUS-CPN, which is consistent with the results described by Leblanc *et al*[25]. Leblanc *et al*[25] indicated that similar clinical outcomes were seen in the 10 mL and 20 mL alcohol groups with respect to overall pain relief, weekly pain scores, onset of pain relief, and proportion of complete responders.

However, according to our data, tumors located at the body/tail predicted a better response than those with tumors at the pancreatic head/neck after 1 wk or 4 wk, although there were no significant differences (P = 0.094 and P = 0.082 L, respectively). This is in contrast to previous literature reports[26]. Ascunce *et al*[1] reported that tumors located outside the head of the pancreas were weakly associated with a good response. Rykowski *et al*[27] also reported that the posterior transcutaneous CPN technique was more effective in tumors involving the pancreatic head than in those affecting the body and tail of the pancreas. On the other hand, our finding was inconsistent with a previous study on heart rate change. Recently, Bang *et al*[28] discussed a direct correlation between the increase in heart rate during alcohol injection and treatment outcomes. They found that during EUS-CPN, the heart rate change cohort had

significantly better adjusted scores for pain, financial difficulties, weight loss, and satisfaction with body image. Especially, a rise in heart rate during alcohol injection appeared to signal successful targeting of the celiac plexus and may be a simple predictor of treatment outcome. However, during alcohol injection in our cohort, the intra-procedural heart rate was decreased in ≥ 80% of patients. The heart rate always decreased when the alcohol was injected into the celiac plexus, and it returned to baseline level after several seconds.

Certainly, the present study has its inherent limitations that should be considered. First, the study is retrospective and the samples of patients are relatively small, suggesting restricted application of the results. A second limitation is the difficulty in measuring pain score, which was variable and a subjective measure. Finally, we failed to supply any results beyond 4 wk, because over time the efficacy of CPN decreased. Also, beyond 4 wk to 16 wk, there were fewer patients for analyzing these data. Therefore, we did not include these patients who received treatment more than 4 wk in the study (data not shown). We also could not compare the survival of patients who did CPN and those who did not. In order to evaluate objectively the significance of these parameters, a large group of multicenter, prospective, randomized trials are required.

CONCLUSION

Our study found that EUS-CPN is a safe and effective form of treatment for intractable pancreatic cancer-associated pain. EUS-CPN seems to be less effective in patients with invisible ganglia, distant metastasis, and direct invasion of the celiac plexus. For these patients, additional attention should be paid to efficacy.

ARTICLE HIGHLIGHTS

Research background

Endoscopic ultrasound-guided celiac plexus neurolysis (EUS-CPN) is widely used to treat pancreatic cancer-associated pain.

Research motivation

Response to the treatment of EUS-CPN is variable.

Research objectives

To explore determinants of pain response in EUS-CPN for pancreatic cancer-associated pain.

Research methods

Univariable and multivariable logistic regression analyses were performed to explore predictors of pain response.

Research results

Invisible ganglia, metastatic disease, and invasion of the celiac plexus were identified as significant factors for a negative response to EUS-CPN. No severe adverse events were reported.

Research conclusions

Invisible ganglia, distant metastasis, and invasion of the celiac plexus were predictors of less effective response in EUS-CPN for pancreatic cancer-related pain. For these patients, attention should be given regarding efficacy.

Research perspectives

These findings could be helpful to endoscopists or oncologists to develop an appropriate treatment scheme for pain management in pancreatic cancer patients.

REFERENCES

1 **Ascunce G**, Ribeiro A, Reis I, Rocha-Lima C, Sleeman D, Merchan J, Levi J. EUS visualization and direct celiac ganglia neurolysis predicts better pain relief in patients with pancreatic malignancy (with video). *Gastrointest Endosc* 2011; **73**: 267-274 [PMID: 21295640 DOI: 10.1016/j.gie.2010.10.029]

2 **Minaga K**, Takenaka M, Kamata K, Yoshikawa T, Nakai A, Omoto S, Miyata T, Yamao K, Imai H, Sakamoto H, Kitano M, Kudo M. Alleviating Pancreatic Cancer-Associated Pain Using Endoscopic Ultrasound-Guided Neurolysis. *Cancers (Basel)* 2018; **10**: 50 [PMID: 29462851 DOI: 10.3390/cancers10020050]

3 **Tempero MA**, Malafa MP, Al-Hawary M, Asbun H, Bain A, Behrman SW, Benson AB, Binder E, Cardin DB, Cha C, Chiorean EG, Chung V, Czito B, Dillhoff M, Dotan E, Ferrone CR, Hardacre J, Hawkins WG, Herman J, Ko AH, Komanduri S, Koong A, LoConte N, Lowy AM, Moravek C, Nakakura EK, O'Reilly EM, Obando J, Reddy S, Scaife C, Thayer S, Weekes CD, Wolff RA, Wolpin BM, Burns J, Darlow S. Pancreatic Adenocarcinoma, Version 2.2017, NCCN Clinical Practice Guidelines in Oncology. *J Natl Compr Canc Netw* 2017; **15**: 1028-1061 [PMID: 28784865 DOI: 10.6004/jnccn.2017.0131]

4 **Eisenberg E**, Carr DB, Chalmers TC. Neurolytic celiac plexus block for treatment of cancer pain: a meta-analysis. *Anesth Analg* 1995; **80**: 290-295 [PMID: 7818115 DOI: 10.1097/00000539-199502000-00015]

5 **Nagels W**, Pease N, Bekkering G, Cools F, Dobbels P. Celiac plexus neurolysis for abdominal cancer pain: a systematic review. *Pain Med* 2013; **14**: 1140-1163 [PMID: 23802777 DOI: 10.1111/pme.12176]

6 **Levy MJ**, Gleeson FC, Topazian MD, Fujii-Lau LL, Enders FT, Larson JJ, Mara K, Abu Dayyeh BK, Alberts SR, Hallemeier CL, Iyer PG, Kendrick ML, Mauck WD, Pearson RK, Petersen BT, Rajan E, Takahashi N, Vege SS, Wang KK, Chari ST. Combined Celiac Ganglia and Plexus Neurolysis Shortens Survival, Without Benefit, *vs* Plexus Neurolysis Alone. *Clin Gastroenterol Hepatol* 2019; **17**: 728-738. e9 [PMID: 30217513 DOI: 10.1016/j.cgh.2018.08.040]

7 **Koulouris AI**, Banim P, Hart AR. Pain in Patients with Pancreatic Cancer: Prevalence, Mechanisms, Management and Future Developments. *Dig Dis Sci* 2017; **62**: 861-870 [PMID: 28229252 DOI: 10.1007/s10620-017-4488-z]

8 **Yasuda I**, Wang HP. Endoscopic ultrasound-guided celiac plexus block and neurolysis. *Dig Endosc* 2017; **29**: 455-462 [PMID: 28160344 DOI: 10.1111/den.12824]

9 **Lu F**, Dong J, Tang Y, Huang H, Liu H, Song L, Zhang K. Bilateral vs. unilateral endoscopic ultrasound-guided celiac plexus neurolysis for abdominal pain management in patients with pancreatic malignancy: a systematic review and meta-analysis. *Support Care Cancer* 2018; **26**: 353-359 [PMID: 28956176 DOI: 10.1007/s00520-017-3888-0]

10 **Wyse JM**, Battat R, Sun S, Saftoiu A, Siddiqui AA, Leong AT, Arturo Arias BL, Fabbri C, Adler DG, Santo E, Kalaitzakis E, Artifon E, Mishra G, Okasha HH, Poley JW, Guo J, Vila JJ, Lee LS, Sharma M, Bhutani MS, Giovannini M, Kitano M, Eloubeidi MA, Khashab MA, Nguyen NQ, Saxena P, Vilmann P, Fusaroli P, Garg PK, Ho S, Mukai S, Carrara S, Sridhar S, Lakhtakia S, Rana SS, Dhir V, Sahai AV. Practice guidelines for endoscopic ultrasound-guided celiac plexus neurolysis. *Endosc Ultrasound* 2017; **6**: 369-375 [PMID: 29251270 DOI: 10.4103/eus.eus_97_17]

11 **Wyse JM**, Carone M, Paquin SC, Usatii M, Sahai AV. Randomized, double-blind, controlled trial of early endoscopic ultrasound-guided celiac plexus neurolysis to prevent pain progression in patients with newly diagnosed, painful, inoperable pancreatic cancer. *J Clin Oncol* 2011; **29**: 3541-3546 [PMID: 21844506 DOI: 10.1200/JCO.2010.32.2750]

12 **Doi S**, Yasuda I, Kawakami H, Hayashi T, Hisai H, Irisawa A, Mukai T, Katanuma A, Kubota K, Ohnishi T, Ryozawa S, Hara K, Itoi T, Hanada K, Yamao K. Endoscopic ultrasound-guided celiac ganglia neurolysis vs. celiac plexus neurolysis: a randomized multicenter trial. *Endoscopy* 2013; **45**: 362-369 [PMID: 23616126 DOI: 10.1055/s-0032-1326225]

13 **Téllez-Ávila FI**, Romano-Munive AF, Herrera-Esquivel Jde J, Ramírez-Luna MA. Central is as effective as bilateral endoscopic ultrasound-guided celiac plexus neurolysis in patients with unresectable pancreatic cancer. *Endosc Ultrasound* 2013; **2**: 153-156 [PMID: 24949384 DOI: 10.7178/eus.06.007]

14 **LeBlanc JK**, Al-Haddad M, McHenry L, Sherman S, Juan M, McGreevy K, Johnson C, Howard TJ, Lillemoe KD, DeWitt J. A prospective, randomized study of EUS-guided celiac plexus neurolysis for pancreatic cancer: one injection or two? *Gastrointest Endosc* 2011; **74**: 1300-1307 [PMID: 22000795 DOI: 10.1016/j.gie.2011.07.073]

15 **Si-Jie H**, Wei-Jia X, Yang D, Lie Y, Feng Y, Yong-Jian J, Ji L, Chen J, Liang Z, De-Liang F. How to improve the efficacy of endoscopic ultrasound-guided celiac plexus neurolysis in pain management in patients with pancreatic cancer: analysis in a single center. *Surg Laparosc Endosc Percutan Tech* 2014; **24**: 31-35 [PMID: 24487155 DOI: 10.1097/SLE.0000000000000032]

16 **Wiersema MJ**, Wiersema LM. Endosonography-guided celiac plexus neurolysis. *Gastrointest Endosc* 1996; **44**: 656-662 [PMID: 8979053 DOI: 10.1016/s0016-5107(96)70047-0]

17 **Puli SR**, Reddy JB, Bechtold ML, Antillon MR, Brugge WR. EUS-guided celiac plexus neurolysis for pain due to chronic pancreatitis or pancreatic cancer pain: a meta-analysis and systematic review. *Dig Dis Sci* 2009; **54**: 2330-2337 [PMID: 19137428 DOI: 10.1007/s10620-008-0651-x]

18 **Levy MJ**, Topazian M, Keeney G, Clain JE, Gleeson F, Rajan E, Wang KK, Wiersema MJ, Farnell M, Chari S. Preoperative diagnosis of extrapancreatic neural invasion in pancreatic cancer. *Clin*

Gastroenterol Hepatol 2006; **4**: 1479-1482 [PMID: 17101297 DOI: 10.1016/j.cgh.2006.08.012]

19 **De Cicco M**, Matovic M, Bortolussi R, Coran F, Fantin D, Fabiani F, Caserta M, Santantonio C, Fracasso A. Celiac plexus block: injectate spread and pain relief in patients with regional anatomic distortions. *Anesthesiology* 2001; **94**: 561-565 [PMID: 11379673 DOI: 10.1097/00000542-200104000-00006]

20 **Iwata K**, Yasuda I, Enya M, Mukai T, Nakashima M, Doi S, Iwashita T, Tomita E, Moriwaki H. Predictive factors for pain relief after endoscopic ultrasound-guided celiac plexus neurolysis. *Dig Endosc* 2011; **23**: 140-145 [PMID: 21429019 DOI: 10.1111/j.1443-1661.2010.01046.x]

21 **Sahai AV**, Lemelin V, Lam E, Paquin SC. Central vs. bilateral endoscopic ultrasound-guided celiac plexus block or neurolysis: a comparative study of short-term effectiveness. *Am J Gastroenterol* 2009; **104**: 326-329 [PMID: 19174816 DOI: 10.1038/ajg.2008.64]

22 **Levy MJ**, Topazian MD, Wiersema MJ, Clain JE, Rajan E, Wang KK, de la Mora JG, Gleeson FC, Pearson RK, Pelaez MC, Petersen BT, Vege SS, Chari ST. Initial evaluation of the efficacy and safety of endoscopic ultrasound-guided direct Ganglia neurolysis and block. *Am J Gastroenterol* 2008; **103**: 98-103 [PMID: 17970834 DOI: 10.1111/j.1572-0241.2007.01607.x]

23 **Sakamoto H**, Kitano M, Kamata K, Komaki T, Imai H, Chikugo T, Takeyama Y, Kudo M. EUS-guided broad plexus neurolysis over the superior mesenteric artery using a 25-gauge needle. *Am J Gastroenterol* 2010; **105**: 2599-2606 [PMID: 20823834 DOI: 10.1038/ajg.2010.339]

24 **Gunaratnam NT**, Sarma AV, Norton ID, Wiersema MJ. A prospective study of EUS-guided celiac plexus neurolysis for pancreatic cancer pain. *Gastrointest Endosc* 2001; **54**: 316-324 [PMID: 11522971 DOI: 10.1067/mge.2001.117515]

25 **Leblanc JK**, Rawl S, Juan M, Johnson C, Kroenke K, McHenry L, Sherman S, McGreevy K, Al-Haddad M, Dewitt J. Endoscopic Ultrasound-Guided Celiac Plexus Neurolysis in Pancreatic Cancer: A Prospective Pilot Study of Safety Using 10 mL *vs* 20 mL Alcohol. *Diagn Ther Endosc* 2013; **2013**: 327036 [PMID: 23365492 DOI: 10.1155/2013/327036]

26 **Minaga K**, Kitano M, Sakamoto H, Miyata T, Imai H, Yamao K, Kamata K, Omoto S, Kadosaka K, Sakurai T, Nishida N, Chiba Y, Kudo M. Predictors of pain response in patients undergoing endoscopic ultrasound-guided neurolysis for abdominal pain caused by pancreatic cancer. *Therap Adv Gastroenterol* 2016; **9**: 483-494 [PMID: 27366217 DOI: 10.1177/1756283X16644248]

27 **Rykowski JJ**, Hilgier M. Efficacy of neurolytic celiac plexus block in varying locations of pancreatic cancer: influence on pain relief. *Anesthesiology* 2000; **92**: 347-354 [PMID: 10691219 DOI: 10.1097/00000542-200002000-00014]

28 **Bang JY**, Hasan MK, Sutton B, Holt BA, Navaneethan U, Hawes R, Varadarajulu S. Intraprocedural increase in heart rate during EUS-guided celiac plexus neurolysis: Clinically relevant or just a physiologic change? *Gastrointest Endosc* 2016; **84**: 773-779.e3 [PMID: 27048974 DOI: 10.1016/j.gie.2016.03.1496]

World Journal of Gastroenterology

Submit a Manuscript: https://www.f6publishing.com

World J Gastroenterol 2021 January 7; 27(1): 80-91

DOI: 10.3748/wjg.v27.i1.80

ISSN 1007-9327 (print) ISSN 2219-2840 (online)

ORIGINAL ARTICLE

Retrospective Study

Evaluation of controlled attenuation parameter in assessing hepatic steatosis in patients with autoimmune liver diseases

Xi-Xi Ni, Min Lian, Hui-Min Wu, Xiao-Yun Li, Li Sheng, Han Bao, Qi Miao, Xiao Xiao, Can-Jie Guo, Hai Li, Xiong Ma, Jing Hua

ORCID number: Xi-Xi Ni 0000-0003-3361-3703; Min Lian 0000-0003-2122-1614; Hui-Min Wu 0000-0002-3991-3857; Xiao-Yun Li 0000-0003-4706-6114; Li Sheng 0000-0002-3641-5211; Han Bao 0000-0003-2934-3990; Qi Miao 0000-0003-3370-9692; Xiao Xiao 0000-0002-7936-336X; Can-Jie Guo 0000-0001-5951-299X; Hai Li 0000-0002-2510-5103; Xiong Ma 0000-0002-2640-2708; Jing Hua 0000-0002-6100-9477.

Author contributions: Ni XX, Lian M, Wu HM, and Li XY contributed equally to this work, and collected and analyzed the data; Sheng L coordinated the research; Bao H and Xiao X performed the transient elastography and coordinated the liver biopsy; Miao Q contributed to histological examination; Ma X, Hua J, Li H, and Guo CJ analyzed the data; Hua J designed the study; Ni XX, Lian M, and Hua J wrote the manuscript; all authors have read and approved the final manuscript.

Supported by National Natural Science Foundation of China, No. 81470842 and No. 81770572.

Institutional review board statement: This study was reviewed and approved by the Ethics Committee of Renji Hospital.

Xi-Xi Ni, Hui-Min Wu, Xiao-Yun Li, Xiao Xiao, Jing Hua, Department of Gastroenterology and Hepatology, Renji Hospital, School of Medicine, Shanghai Jiao Tong University, Shanghai Institute of Digestive Disease, Shanghai 200127, China

Min Lian, Han Bao, Can-Jie Guo, Department of Gastroenterology and Hepatology, Renji Hospital, School of Medicine, Shanghai Jiao Tong University, Shanghai 200127, China

Li Sheng, Xiong Ma, School of Medicine, Shanghai Jiao Tong University, Shanghai Cancer Institute, Shanghai Institute of Digestive Disease, Shanghai 200127, China

Qi Miao, School of Medicine, Shanghai Jiao Tong University, Shanghai Institute of Digestive Disease, Shanghai 200127, China

Hai Li, Department of Gastroenterology, Renji Hospital, Shanghai Jiao Tong University School of Medicine, Shanghai 200127, China

Xiong Ma, Department of Gastroenterology, Renji Hospital, School of Medicine, Shanghai Jiao Tong University, Shanghai Institute of Digestive Disease, Shanghai 200001, China

Corresponding author: Jing Hua, MD, PhD, Professor, Department of Gastroenterology and Hepatology, Renji Hospital, School of Medicine, Shanghai Jiao Tong University, Shanghai Institute of Digestive Disease, No. 160 Pujian Road, Shanghai 200127, China.
hua_jing88@163.com

Abstract

BACKGROUND

Hepatic steatosis commonly occurs in some chronic liver diseases and may affect disease progression.

AIM

To investigate the performance of controlled attenuation parameter (CAP) for the diagnosis of hepatic steatosis in patients with autoimmune liver diseases (AILDs).

METHODS

Patients who were suspected of having AILDs and underwent liver biopsy were consistently enrolled. Liver stiffness measurement (LSM) and CAP were performed by transient elastography. The area under the receiver operating

Informed consent statement: Patients were not required to give informed consent to the study because the analysis used anonymous clinical data that were obtained after each patient agreed to treatment by written consent.

Conflict-of-interest statement: The authors have no financial relationships to disclose.

Data sharing statement: No additional data are available.

Manuscript source: Unsolicited manuscript

Specialty type: Gastroenterology and hepatology

Country/Territory of origin: China

Peer-review report's scientific quality classification

Grade A (Excellent): 0
Grade B (Very good): 0
Grade C (Good): C
Grade D (Fair): 0
Grade E (Poor): 0

Received: September 11, 2020
Peer-review started: September 11, 2020
First decision: November 23, 2020
Revised: December 1, 2020
Accepted: December 11, 2020
Article in press: December 11, 2020
Published online: January 7, 2021

P-Reviewer: Kita K
S-Editor: Huang P
L-Editor: Wang TQ
P-Editor: Li JH

characteristic (AUROC) curve was used to evaluate the performance of CAP for diagnosing hepatic steatosis compared with biopsy.

RESULTS

Among 190 patients with biopsy-proven hepatic steatosis, 69 were diagnosed with autoimmune hepatitis (AIH), 18 with primary biliary cholangitis (PBC), and 27 with AIH-PBC overlap syndrome. The AUROCs of CAP for the diagnosis of steatosis in AILDS were 0.878 (0.791-0.965) for S1, 0.764 (0.676-0.853) for S2, and 0.821 (0.716-0.926) for S3. The CAP value was significantly related to hepatic steatosis grade ($P < 0.001$). Among 69 patients with AIH, the median CAP score was 205.63 ± 47.36 dB/m for S0, 258.41 ± 42.83 dB/m for S1, 293.00 ± 37.18 dB/m for S2, and 313.60 ± 27.89 dB/m for S3. Compared with patients with nonalcoholic fatty liver disease (NAFLD) presenting with autoimmune markers, patients with AIH concomitant with NAFLD were much older and had higher serum IgG levels and LSM values.

CONCLUSION

CAP can be used as a noninvasive diagnostic method to evaluate hepatic steatosis in patients with AILDs. Determination of LSM combined with CAP may help to identify patients with AIH concomitant with NAFLD from those with NAFLD with autoimmune phenomena.

Key Words: Controlled attenuation parameter; Hepatic steatosis; Autoimmune liver diseases; Nonalcoholic fatty liver disease; Liver stiffness measurement; Autoimmune hepatitis

Core Tip: This retrospective study determined that controlled attenuation parameter (CAP) could be used as a noninvasive diagnostic tool to evaluate hepatic steatosis effectively and accurately in patients with autoimmune liver diseases. Patients with autoimmune hepatitis concomitant with nonalcoholic fatty liver disease (NAFLD) had higher IgG levels and liver stiffness measurement values, while patients with NAFLD with autoimmune phenomena had higher gamma-glutamyl transferase levels and CAP values, which benefits the identification of these two kinds of patients.

Citation: Ni XX, Lian M, Wu HM, Li XY, Sheng L, Bao H, Miao Q, Xiao X, Guo CJ, Li H, Ma X, Hua J. Evaluation of controlled attenuation parameter in assessing hepatic steatosis in patients with autoimmune liver diseases. *World J Gastroenterol* 2021; 27(1): 80-91
URL: https://www.wjgnet.com/1007-9327/full/v27/i1/80.htm
DOI: https://dx.doi.org/10.3748/wjg.v27.i1.80

INTRODUCTION

Hepatic steatosis is the accumulation of lipids within hepatocytes and is considered pathologic when it affects more than 5% of hepatocytes[1]. The most common cause of steatosis is insulin resistance associated with nonalcoholic fatty liver disease (NAFLD)[2]. It also occurs in alcoholic liver disease and chronic viral hepatitis, defined as a "cofactor" capable of affecting disease progression and treatment perspectives[3]. Autoimmune liver diseases (AILDs) are a group of autoimmune diseases associated with the liver and are characterized by dysregulation of immune cell homeostasis and inflammation, including autoimmune hepatitis (AIH), primary biliary cholangitis (PBC), primary sclerosing cholangitis, and their overlapping subtypes[4,5]. When hepatic steatosis is present in subjects with AILDs, this coexisting scenario may cause a synergistic combination of steatosis, cellular adaptation, and oxidative damage that aggravates liver injury and affects the treatment effect[6]. Moreover, the standard regimen for AIH involves glucocorticoids[7], the long-term administration of which will further aggravate hepatic steatosis. However, the incidence of AILDs combined with hepatic steatosis has not been reported. Therefore, the evaluation of hepatic steatosis is

a component that cannot be ignored in the management of patients with AILDs.

Liver biopsy is considered the standard method for staging hepatic inflammation, steatosis, and fibrosis. Thus, it plays a vital role in the diagnosis and follow-up of AILDs[7,8]. However, liver biopsy is an invasive procedure, which bears a potential risk of severe complications and is of limited acceptance among patients. Furthermore, the severity of hepatic steatosis may change within weeks after treatment that cannot be sufficiently monitored by repetitive invasive procedures. Accordingly, noninvasive assessments are urgently needed[9].

The controlled attenuation parameter (CAP) measured by transient elastography (TE) is an easy and rapid noninvasive examination method for the detection of hepatic steatosis. It is based on the physical phenomenon that the amplitude of ultrasound waves is attenuated more quickly when they traverse across a steatotic liver[10,11]. TE can also quantify the speed of a mechanically induced shear wave in liver tissue and hence generate a parameter called liver stiffness measurement (LSM) to estimate liver fibrosis[12]. CAP is measured simultaneously with LSM, making it possible to assess hepatic steatosis and fibrosis at the same time. Studies with CAP have been performed in NAFLD, alcoholic liver disease, and viral hepatitis, but very few data are available on AILDs[13-15]. It has been showed that in patients with chronic viral hepatitis and advanced liver fibrosis, CAP performed better than ultrasound for assessing liver steatosis[16]. Besides, a recent meta-analysis showed that CAP diagnosed moderate and severe hepatic steatosis with diagnostic accuracies above 0.85 in patients with liver disease of mixed etiology. However, the analysis did not include patients with AILDs[17].

In this study, we assessed the performance of CAP for evaluating hepatic steatosis in AILDs to determine whether it could be regarded as a reliable tool to monitor disease course.

MATERIALS AND METHODS

Patients

Patients who were suspected of having AILDs and eventually underwent liver biopsy at Shanghai Jiao Tong University Renji Hospital were consistently enrolled from January 2016 to November 2018. A total of 800 patients were analyzed for steatosis in liver histology.

Diagnostic criteria

Diagnosis was made according to the diagnostic criteria described in the clinical practice guidelines for AIH, PBC, AIH-PBC overlap syndrome, and NAFLD. AIH[18] was diagnosed according to a simple score based on four measurements: Liver histology, autoantibody titers, gamma-globulin/IgG levels, and the absence of viral hepatitis. The diagnosis of PBC[19] required fulfilment of two or more of the following criteria: (1) Biochemical evidence of cholestasis based mainly on alkaline phosphatase (AKP) elevation; (2) Detection of anti-mitochondrial autoantibodies (AMA); and (3) Typical histologic evidence of nonsuppurative destructive cholangitis and destruction of interlobular bile ducts. AIH-PBC overlap syndrome[20] was diagnosed based on clinical, biochemical, serological, and histological features overlapping those of PBC and AIH. The diagnosis of NAFLD[21] required imaging or histological evidence of diffuse hepatic steatosis and ruling out other causes of hepatic steatosis, such as excessive alcohol consumption.

Histological examination

Percutaneous liver biopsy guided by ultrasound was performed under local anesthesia using a 16G disposable needle. Liver specimens at least 1 cm in length with eight complete portal tracts were included. The specimens were immediately fixed in 10% neutral formalin and embedded in paraffin. Hematoxylin and eosin staining was used to observe the morphology of the liver, and Masson's trichrome and reticulin staining was performed to detect fibrosis. One single experienced pathologist who was blinded to the patients' clinical data assessed liver histology using a METAVIR-derived scoring system. Hepatic steatosis was scored as S0: < 5%, S1: 5%-33%, S2: > 33%-66%, and S3: > 66%. Fibrosis was staged as follows: F0, no fibrosis; F1, portal fibrosis without septa; F2, portal and periportal fibrosis with few septa; F3, portal and periportal fibrosis with numerous septa without cirrhosis; and F4, cirrhosis. Hepatic inflammatory activity was graded as follows: A0, none; A1, mild; A2, moderate; and A3, severe.

Clinical measurements

Medical records of the patients who were finally included were reviewed, and clinical data and laboratory findings were collected and analyzed. Body mass index (BMI) was calculated. Laboratory evaluations included liver biochemistry [*i.e.*, alanine aminotransferase (ALT), aspartate aminotransferase, AKP, gamma-glutamyl transferase (GGT), total bilirubin, direct bilirubin, globulin, and albumin], serum immunoglobulins (IgG, IgM, and IgA), routine blood tests (white blood cell count and platelet count), and prothrombin time. Serum autoantibodies, including anti-nuclear antibody (ANA), AMA, and anti-smooth muscle actin antibody (ASMA), were detected by indirect immunofluorescence (Euroimmun AG, Hangzhou, China).

CAP and LSM by TE

TE measured with a FibroScan device and an M probe ultrasound transducer (Echosens, Paris, France) was performed in all patients who underwent liver biopsy on the same day. Subjects were placed in the supine position with the right arm in maximal abduction, and measurements were taken over the right hepatic lobe through an intercostal space. We obtained ten valid CAP and LSM measurements from each participant and considered LSM with an interquartile range ≤ 30% and a success rate ≥ 60% as reliable. The median CAP and LSM were taken as the estimates for hepatic steatosis and fibrosis, expressed in dB/m and kilopascals (kPa), respectively.

Statistical analysis

Data were analyzed using SPSS software version 22.0 (SPSS Inc, Chicago, IL, United States). Summary data are reported as the mean ± SD or median (interquartile range) according to distribution. Quantitative variables were compared using independent samples Student's *t*-test or one-way analysis of variance when appropriate. Spearman's rank correlation test was used to explore the correlation between CAP and hepatic steatosis grade. The diagnostic accuracy of CAP for the prediction of hepatic steatosis grade was calculated using a receiver operator characteristic (ROC) curve. Optimal CAP cut-off values for each steatosis stage were determined based on the highest combined sensitivity and specificity (Youden index). The area under the ROC curve (AUROC), sensitivity, specificity, positive predictive value, and negative predictive value for the predefined cut-off values were calculated. A P value < 0.05 was considered statistically significant.

RESULTS

Characteristics of the patients

In 800 patients with liver biopsy, a total of 190 patients were finally included in the study according to the existence of various grades of hepatic steatosis in liver histology, with a mean age of 46.36 ± 12.82 years, including 45 males (23.68%) and 145 females (76.32%). Among these patients, 69 were diagnosed with AIH, 18 with PBC, 27 with AIH-PBC overlap syndrome, 66 with NAFLD, and 10 with other liver diseases. In all patients, the prevalence of autoantibodies, including ANA, AMA, and ASMA, was 70.53%. The average BMI was 23.97 ± 2.69 kg/m^2.

Diagnostic accuracy of CAP to grade hepatic steatosis in patients with mixed etiology liver disease

In all 190 patients, the median CAP score was 270.17 ± 54.52 dB/m, and the median LSM score was 7.66 ± 5.57 kPa (Table 1). The distribution of the CAP value for each steatosis grade in all patients with mixed etiology liver disease is as follows. The median CAP score was 201.6 ± 46.78 dB/m for S0, 260.5 ± 47.92 dB/m for S1, 293.6 ± 40.13 dB/m for S2, and 307.4 ± 45.31 dB/m for S3. The CAP value was significantly related to hepatic steatosis grade (ρ = 0.549, P < 0.001) (Figure 1A).

The AUROCs of CAP for the diagnosis of steatosis were 0.883 (0.807-0.958) for S1, 0.772 (0.705-0.838) for S2, and 0.732 (0.640-0.824) for S3 (Figure 1B-D and Table 2). The optimal cut-off values of CAP for steatosis grades were 229 dB/m for S ≥ 1, 259 dB/m for S ≥ 2, and 283.5 dB/m for S3 with the highest combined sensitivity and specificity (Table 2).

Diagnostic accuracy of CAP for grading hepatic steatosis in AILDs

Next, we further assessed the performance of CAP for evaluating hepatic steatosis in AILDs. The median CAP score for each steatosis grade in AILDs was very similar to

Table 1 Baseline patient characteristics

Variable	All (*n* = 190)	AILDs (*n* = 114)	NAFLD (*n* = 66)
Age, yr	46.36 ± 12.82	48.72 ± 11.57	42.15 ± 13.80
Male sex, *n* (%)	45 (23.68)	23 (20.18)	18 (27.27)
BMI, kg/m^2	23.97 ± 2.69	24.33 ± 1.80	23.63 ± 2.34
Prevalence of autoantibodies, *n* (%)	134 (70.53)	89 (78.07)	37 (56.06)
Laboratory			
AST, U/L	63.96 ± 86.42	72.54 ± 102.23	54.6 ± 59.10
ALT, U/L	83.86 ± 86.42	81.98 ± 92.78	92.81 ± 78.67
LDH, U/L	182.70 ± 35.43	183.02 ± 37.39	182.64 ± 32.86
AKP, U/L	80.00 (63.00, 108.50)	85.00 (62.25, 129.5)	75.00 (64.00, 94.00)
GGT, U/L	103.67 ± 126.83	126.00 ± 151.92	76.82 ± 73.15
Total bilirubin, mg/dL	10.90 (8.10, 15.30)	11.20 (8.30, 16.70)	9.80 (6.95, 14.15)
Direct bilirubin, mg/dL	3.60 (2.80, 4.90)	3.70 (2.90, 5.70)	3.45 (2.52, 4.50)
Histological steatosis stage, *n* (%)			
S0 (< 5%)	22 (11.6)	20 (11.1)	0 (0.0)
S1 (5%-33%)	85 (44.7)	61 (33.9)	16 (24.2)
S2 (> 33%-66%)	55 (28.9)	28 (15.6)	27 (40.9)
S3 (> 66%)	28 (14.7)	5 (2.8)	23 (34.8)
Histological fibrosis stage, *n* (%)			
F0 (no fibrosis)	12 (6.3)	1 (0.9)	10 (15.2)
F1 (portal fibrosis without septa)	70 (36.8)	38 (33.3)	30 (45.5)
F2 (portal and periportal fibrosis with few septa)	64 (33.7)	40 (35.1)	18 (27.3)
F3 (portal and periportal fibrosis with numerous septa without cirrhosis)	35 (18.4)	26 (22.8)	8 (12.1)
F4 (cirrhosis)	9 (4.7)	9 (7.9)	0 (0.0)
CAP, dB/m	270.17 ± 54.52	261.73 ± 53.80	290.97 ± 50.68
LSM, kPa	7.66 ± 5.57	8.48 ± 6.50	6.61 ± 3.66

Distributions are expressed as the mean ± SD or median (interquartile range) or number (percentage). AIH: Autoimmune hepatitis; NAFLD: Nonalcoholic fatty liver disease; BMI: Body mass index; AKP: Alkaline phosphatase; ALT: Alanine aminotransferase; AST: Aspartate aminotransferase; CAP: Controlled attenuation parameter; GGT: Gamma-glutamyl transferase; LDH: Lactate dehydrogenase; LSM: Liver stiffness measurement.

that in all patients. The CAP value was also significantly related to hepatic steatosis grade (ρ = 0.553, P < 0.001) (Figure 2A). The AUROCs of CAP for the diagnosis of steatosis in AILDs were 0.878 (0.791-0.965) for S1, 0.764 (0.676-0.853) for S2, and 0.821 (0.716-0.926) for S3 (Figure 2D-F and Table 2). The optimal cut-off values of CAP for steatosis grades were 220.5 dB/m for S ≥ 1, 271.5 dB/m for S ≥ 2, and 283.5 dB/m for S3 (Table 2).

Considering the relatively high incidence and clinical significance of AIH, we focused on calculating the median CAP value for patients with AIH. Among 69 patients with AIH, the median CAP score was 205.63 ± 47.36 dB/m for S0, 258.41 ± 42.83 dB/m for S1, 293.00 ± 37.18 dB/m for S2, and 313.60 ± 27.89 dB/m for S3 (Figure 2B). Furthermore, there was no significant difference in the median CAP value between patients with AIH and NAFLD in each hepatic steatosis grade (Figure 2C).

Factors affecting the performance of CAP

Univariate and multivariate analyses showed that the CAP value was significantly correlated with BMI and hepatic steatosis (P < 0.001, P < 0.001). When patients were divided into three subgroups according to BMI < 24 kg/m^2, 24-27 kg/m^2, and BMI ≥ 27 kg/m^2, patients with BMI ≥ 27 kg/m^2 had a significantly higher CAP value than the

Table 2 Diagnostic performance of controlled attenuation parameter for assessment of hepatic steatosis in patients with mixed etiology liver disease and in patients with autoimmune liver diseases

Etiology	Grade	AUROC (95%CI)	Cut-off, dB/m (kPa)	Sensitivity	Specificity	PPV	NPV
Mixed etiology	S ≥ 1	0.883 (0.807-0.958)	229	0.852	0.714	0.960	0.375
	S ≥ 2	0.772 (0.705-0.838)	259	0.875	0.636	0.636	0.875
	S = 3	0.732 (0.640-0.824)	283.5	0.750	0.654	0.273	0.938
AILDs	S ≥ 1	0.878 (0.791-0.965)	220.5	0.874	0.737	0.937	0.538
	S ≥ 2	0.764 (0.676-0.853)	271.5	0.818	0.704	0.510	0.937
	S = 3	0.821 (0.716-0.926)	283.5	1.000	0.688	0.128	1.000

AUROC: Area under receiver operating characteristic; CAP: Controlled attenuation parameter; NPV: Negative predictive value; PPV: Positive predictive value.

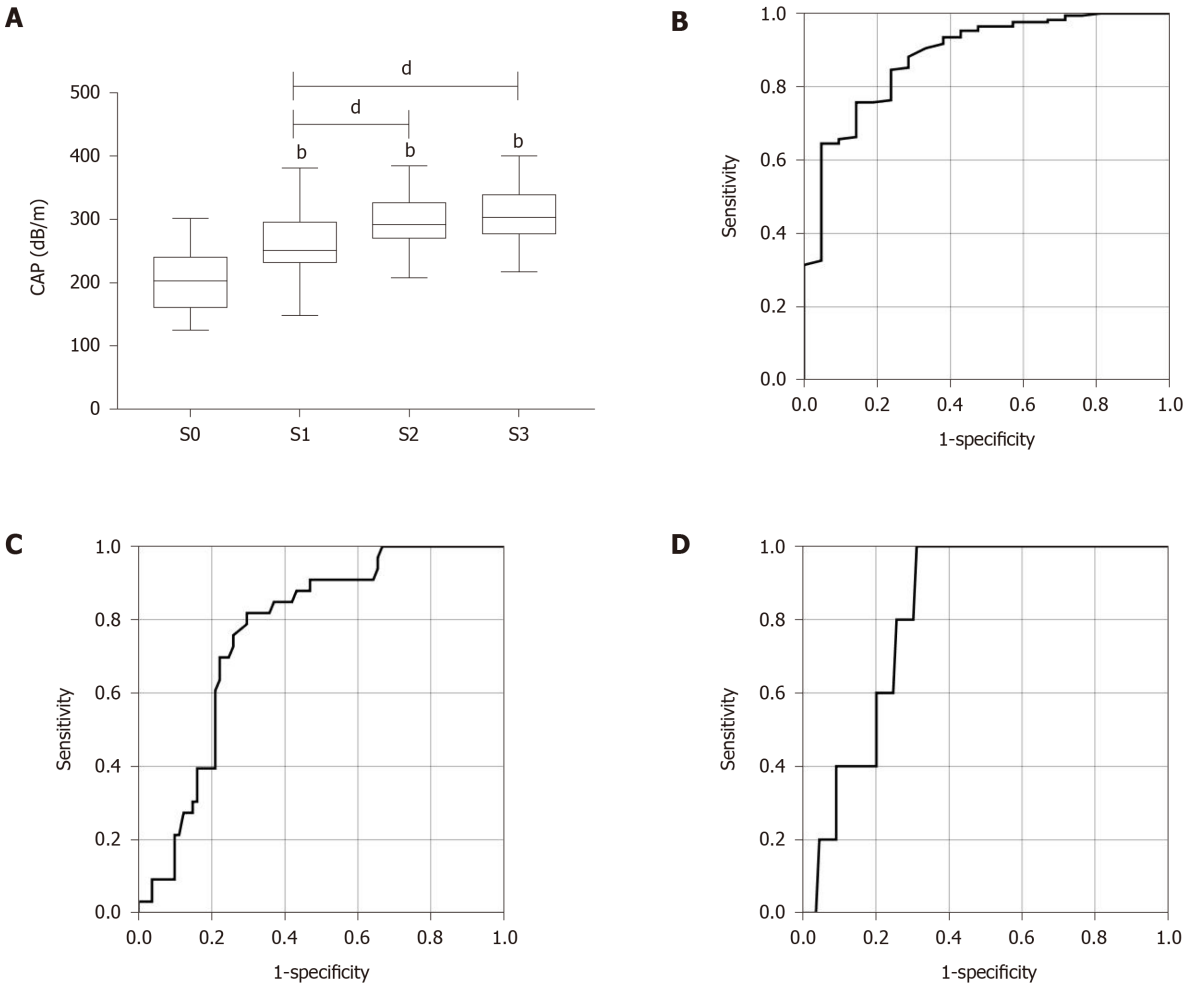

Figure 1 The receiver operator characteristic curve of controlled attenuation parameter for diagnosis of hepatic steatosis grade in patients with mixed etiology liver disease. A: Correlation between the controlled attenuation parameter (CAP) and the grade of hepatic steatosis (ρ = 0.549, P < 0.001); B-D: The receiver operator characteristic curve of CAP for diagnosis of (B) steatosis grade ≥ S1, (C) steatosis grade ≥ S2, and (D) steatosis grade ≥ S3 in patients with mixed etiology liver disease. ^{b}P < 0.01 *vs* S0; ^{d}P < 0.01. CAP: Controlled attenuation parameter.

other two groups (Figure 3). The performance of CAP was stable across fibrosis stages. In addition, traditional factors affecting the performance of LSM, such as bilirubin and serum ALT level, did not affect the performance of CAP (data not shown).

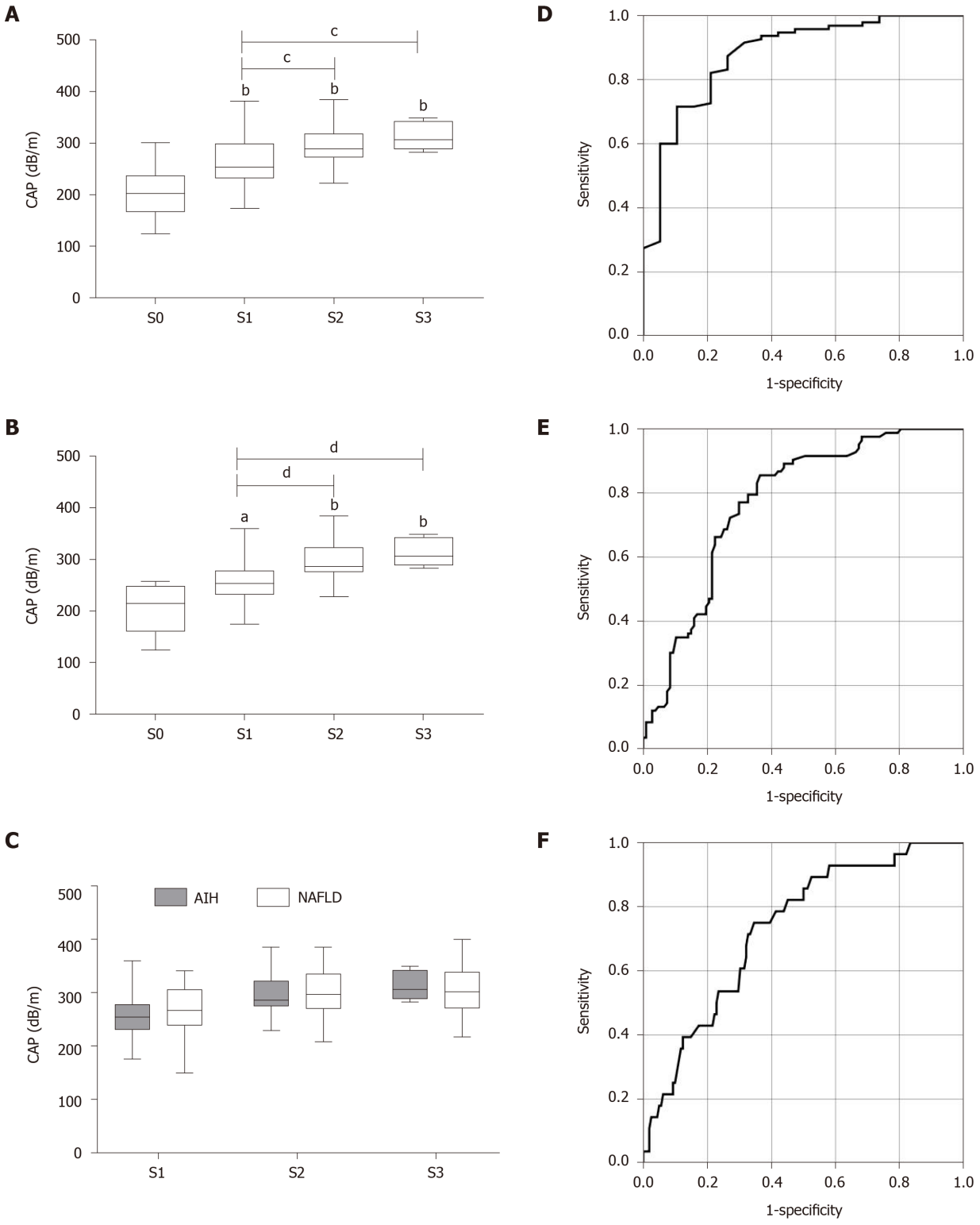

Figure 2 Controlled attenuation parameter value in different hepatic steatosis grades and etiologies and the receiver operator characteristic curve of controlled attenuation parameter for diagnosis of hepatic steatosis grade in patients with autoimmune liver diseases. A and B: Correlation between the controlled attenuation parameter (CAP) and the grade of hepatic steatosis in patients with (A) autoimmune liver diseases (AILDs) or (B) autoimmune hepatitis (AIH); C: Comparison of the CAP value in patients with AIH and nonalcoholic fatty liver disease in different hepatic steatosis grades; D-F: The receiver operator characteristic curve of CAP for diagnosis of (D) steatosis grade ≥ S1, (E) steatosis grade ≥ S2, and (F) steatosis grade ≥ S3 in patients with AILDs. $^{a}P < 0.05$; $^{b}P < 0.01$ *vs* S0; $^{c}P < 0.05$; $^{d}P < 0.01$. CAP: Controlled attenuation parameter; AIH: Autoimmune hepatitis; NAFLD: Nonalcoholic fatty liver disease.

Comparative analysis of patients with AIH concomitant with NAFLD and patients with NAFLD with autoimmune phenomena

In this study, we defined patients with histologic evidence of both AIH and NAFLD as patients with AIH concomitant with NAFLD and patients with histologic evidence of NAFLD and positive autoantibodies or elevated IgG or IgM as patients with NAFLD with autoimmune phenomena.

The results showed that patients with AIH concomitant with NAFLD were older and had higher IgG levels and LSM values than patients with NAFLD with autoimmune phenomena. In contrast, the GGT level and CAP value were higher in patients with NAFLD with autoimmune phenomena (Table 3). Interestingly, when we compared the LSM value in each steatosis grade of the two groups, patients with AIH concomitant with NAFLD were higher in both S1 and S3 grades, suggesting a potential diagnostic marker for patients with AIH concomitant with NAFLD.

DISCUSSION

The prevalence of hepatic steatosis is rising in association with the global increase in obesity. The overall prevalence of NAFLD over the past two decades is 29.6%, up to 46.4% in heavy drinkers and 50%-80% in the obese population[22]. Close attention was paid to the potential interactions between chronic liver disease and hepatic steatosis with the growing NAFLD prevalence. However, the particular role of hepatic steatosis has been less of a focus of attention in AILDs than in other chronic liver diseases, partly due to the lack of proper evaluation tools. Herein, we demonstrated that CAP measured by TE could be used as a noninvasive diagnostic tool to evaluate hepatic steatosis effectively and accurately in patients with AILDs.

In this study, we confirmed that CAP correlated well with hepatic steatosis on histology, and we were able to establish cut-off values with high diagnostic accuracies. The cut-off values for each steatosis grade in patients with mixed etiology liver disease were similar to the previously proposed cut-off values in an individual patient data meta-analysis (229 dB/m for S ≥ 1, 258 dB/m for S ≥ 2)[17]. However, the accuracy of CAP in separating steatosis grades 2 and 3 was suboptimal, which was similar to prior reports[13]. Nevertheless, in clinical practice, the identification of moderate steatosis is of greater utility than distinctions between S2 and S3, and thus, the Youden cut-off for S2 of 258 dB/m is sufficient.

Given the high risk of glycolipid metabolism disorder and increased possibility of hepatic steatosis in patients with AIH due to the long-term administration of immunosuppressive drugs such as glucocorticoids, the noninvasive method may be particularly suited for monitoring current hepatic histological changes and therapeutic effects[7,23]. Here, we found that CAP was closely related to hepatic steatosis in patients with AILDs, as well as patients with AIH. Surprisingly, the performance of CAP for the diagnosis of hepatic steatosis grade in patients with AIH remained stable, which supported that CAP can be used as a noninvasive and reliable diagnostic method to monitor steatosis and disease course.

Notably, we found a strong correlation between CAP and BMI, in agreement with previous studies[24,25]. The skin capsular distance (SCD) has also been shown to be associated with increased CAP values[26]. Since BMI and SCD are both surrogate markers of adiposity, it is difficult to determine the mechanism underlying the association. However, we did not find a correlation between CAP and LSM as reported for patients with NAFLD[27].

It is found in the clinic that elevated immunoglobulin and/or positive autoantibodies may occur during the progression of NAFLD, which we defined as "patients with NAFLD with autoimmune phenomena" here. On the other hand, patients with AIH can also have NAFLD, thereby affecting the diagnosis and treatment. In this study, we found that patients with AIH concomitant with NAFLD were older and had higher IgG levels and LSM values than patients with NAFLD with autoimmune phenomena, which could be related to the repeated and long-term course of AILDs. In contrast, the GGT level was higher in patients with NAFLD with autoimmune phenomena. Therefore, serum IgG and GGT levels and the LSM value can benefit the identification of these two kinds of patients.

There are a few limitations in this study. First, our study is retrospective in nature due to the data collection despite the "blinded" analysis of histology. Second, the sample size is limited due to the low prevalence of AILDs, especially PBC and AIH-PBC overlap syndrome. Third, for historical reasons, CAP was measured only using the M probe. However, a recent multicenter prospective study has shown that there

Table 3 Comparative analysis of patients with autoimmune hepatitis concomitant with nonalcoholic fatty liver disease and patients with nonalcoholic fatty liver disease with autoimmune phenomena

Variable	Patients with AIH concomitant with NAFLD (*n* = 61)	Patients with NAFLD with autoimmune phenomena (*n* = 34)	*P* value
Age, yr	52.05 ± 11.11	43.68 ± 13.71	< 0.001
Male sex, *n* (%)	13 (21.3)	6 (17.6)	
BMI, kg/m^2	24.21 ± 3.10	24.65 ± 2.02	
Laboratory			
AST, U/L	55.03 ± 47.31	50.03 ± 29.26	
ALT, U/L	66.62 ± 74.94	86.01 ± 62.59	
AKP, U/L	63.00 (45.00, 84.00)	75.00 (54.00, 87.00)	
GGT, U/L	49.27 ± 32.24	69.26 ± 44.07	< 0.05
Total bilirubin, mg/dL	10.20 (8.60, 14.10)	10.25 (7.40, 13.67)	
Direct bilirubin, mg/dL	4.20 (3.20, 5.00)	3.70 (2.92, 4.65)	
IgG	15.60 ± 4.57	13.81 ± 2.67	< 0.05
IgM	1.18 ± 0.45	1.28 ± 0.57	
Histological steatosis stage, *n* (%)			
S1	39 (63.9)	8 (23.5)	
S2	17 (27.9)	10 (29.4)	
S3	5 (8.2)	16 (47.1)	
Histological fibrosis stage, *n* (%)			
F1	17 (27.9)	6 (17.6)	
F2	22 (36.1)	14 (41.2)	
F3	16 (26.2)	11 (32.4)	
F4	6 (9.8)	3 (8.8)	
CAP, dB/m	272.57 ± 44.39	293.41 ± 51.04	< 0.05
LSM in total, kPa	9.34 ± 7.14	6.49 ± 2.44	< 0.05
In steatosis S1	9.19 ± 8.11	5.28 ± 1.88	< 0.05
In steatosis S2	7.80 ± 3.47	6.31 ± 2.18	
In steatosis S3	15.76 ± 6.25	7.20 ± 2.69	< 0.01

Distributions are expressed as the mean ± SD or median [interquartile range] or number (percentage). AKP: Alkaline phosphatase; ALT: Alanine aminotransferase; AST: Aspartate aminotransferase; BMI: Body mass index; CAP: Controlled attenuation parameter; GGT: Gamma-glutamyl transferase; LSM: Liver stiffness measurement; AIH: Autoimmune hepatitis; NAFLD: Nonalcoholic fatty liver.

was no significant difference in diagnostic accuracy between the two probes to diagnose liver fibrosis and steatosis in patients with NAFLD[28].

CONCLUSION

In summary, this study revealed that CAP could be used as a noninvasive diagnostic method to evaluate hepatic steatosis in patients with AILDs. Determination of LSM combined with CAP may help to identify patients with AIH concomitant with NAFLD from those with NAFLD with autoimmune phenomena.

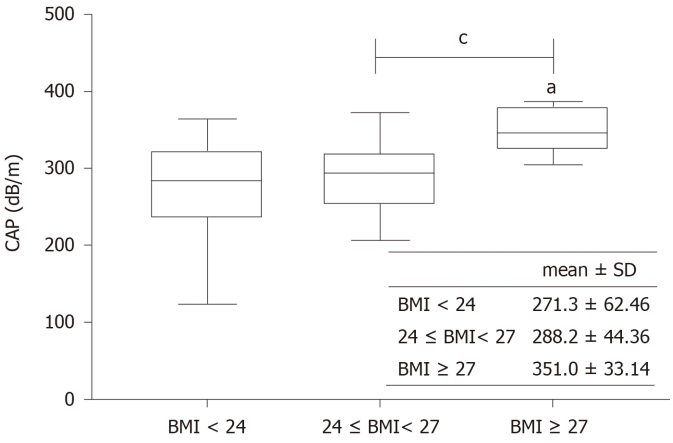

Figure 3 Controlled attenuation parameter in patients with different body mass indexes. [a]*P* < 0.05 *vs* S0; [c]*P* < 0.05. CAP: Controlled attenuation parameter; BMI: Body mass index.

ARTICLE HIGHLIGHTS

Research background

The controlled attenuation parameter (CAP) assesses hepatic steatosis with high diagnostic accuracies among several chronic liver diseases. However, it has not been studied in patients with autoimmune liver diseases (AILDs).

Research motivation

This study aimed to investigate the performance of CAP for the diagnosis of hepatic steatosis in patients with AILDs.

Research objectives

We evaluated the performance and usefulness of CAP for detection of hepatic steatosis in patients with AILDs.

Research methods

The area under the receiver operating characteristic curve was used to evaluate the performance of CAP for diagnosing hepatic steatosis compared with biopsy. Optimal CAP cut-off values were determined based on the highest combined sensitivity and specificity.

Research results

CAP can accurately detect hepatic steatosis as a noninvasive method in patients with AILDs. Compared with patients with nonalcoholic fatty liver disease (NAFLD) presenting with autoimmune markers, patients with autoimmune hepatitis (AIH) concomitant with NAFLD were much older and had higher serum IgG levels and liver stiffness measurement (LSM) values.

Research conclusions

CAP can be used as a noninvasive diagnostic method to evaluate hepatic steatosis in patients with AILDs. Determination of LSM combined with CAP may help to identify patients with AIH concomitant with NAFLD from patients with NAFLD with autoimmune phenomena.

Research perspectives

Larger multicenter studies using both M and XL probes are needed to confirm our results.

REFERENCES

1 **Yeh MM**, Brunt EM. Pathological features of fatty liver disease. *Gastroenterology* 2014; **147**: 754-764 [PMID: 25109884 DOI: 10.1053/j.gastro.2014.07.056]

2 **Sasso M**, Miette V, Sandrin L, Beaugrand M. The controlled attenuation parameter (CAP): a novel tool for the non-invasive evaluation of steatosis using Fibroscan. *Clin Res Hepatol Gastroenterol* 2012; **36**: 13-20 [PMID: 21920839 DOI: 10.1016/j.clinre.2011.08.001]

3 **Persico M**, Iolascon A. Steatosis as a co-factor in chronic liver diseases. *World J Gastroenterol* 2010; **16**: 1171-1176 [PMID: 20222159 DOI: 10.3748/wjg.v16.i10.1171]

4 **Tanaka A**, Mori M, Matsumoto K, Ohira H, Tazuma S, Takikawa H. Increase trend in the prevalence and male-to-female ratio of primary biliary cholangitis, autoimmune hepatitis, and primary sclerosing cholangitis in Japan. *Hepatol Res* 2019; **49**: 881-889 [PMID: 30932290 DOI: 10.1111/hepr.13342]

5 **Beringer A**, Miossec P. IL-17 and IL-17-producing cells and liver diseases, with focus on autoimmune liver diseases. *Autoimmun Rev* 2018; **17**: 1176-1185 [PMID: 30321671 DOI: 10.1016/j.autrev.2018.06.008]

6 **Powell EE**, Jonsson JR, Clouston AD. Steatosis: co-factor in other liver diseases. *Hepatology* 2005; **42**: 5-13 [PMID: 15962320 DOI: 10.1002/hep.20750]

7 **European Association for the Study of the Liver**. EASL Clinical Practice Guidelines: Autoimmune hepatitis. *J Hepatol* 2015; **63**: 971-1004 [PMID: 26341719 DOI: 10.1016/j.jhep.2015.06.030]

8 **European Association for the Study of the Liver**. European Association for the Study of the Liver. EASL Clinical Practice Guidelines: The diagnosis and management of patients with primary biliary cholangitis. *J Hepatol* 2017; **67**: 145-172 [PMID: 28427765 DOI: 10.1016/j.jhep.2017.03.022]

9 **Castera L**, Vilgrain V, Angulo P. Noninvasive evaluation of NAFLD. *Nat Rev Gastroenterol Hepatol* 2013; **10**: 666-675 [PMID: 24061203 DOI: 10.1038/nrgastro.2013.175]

10 **Sasso M**, Beaugrand M, de Ledinghen V, Douvin C, Marcellin P, Poupon R, Sandrin L, Miette V. Controlled attenuation parameter (CAP): a novel VCTE™ guided ultrasonic attenuation measurement for the evaluation of hepatic steatosis: preliminary study and validation in a cohort of patients with chronic liver disease from various causes. *Ultrasound Med Biol* 2010; **36**: 1825-1835 [PMID: 20870345 DOI: 10.1016/j.ultrasmedbio.2010.07.005]

11 **Sasso M**, Audière S, Kemgang A, Gaouar F, Corpechot C, Chazouillères O, Fournier C, Golsztejn O, Prince S, Menu Y, Sandrin L, Miette V. Liver Steatosis Assessed by Controlled Attenuation Parameter (CAP) Measured with the XL Probe of the FibroScan: A Pilot Study Assessing Diagnostic Accuracy. *Ultrasound Med Biol* 2016; **42**: 92-103 [PMID: 26386476 DOI: 10.1016/j.ultrasmedbio.2015.08.008]

12 **Sandrin L**, Fourquet B, Hasquenoph JM, Yon S, Fournier C, Mal F, Christidis C, Ziol M, Poulet B, Kazemi F, Beaugrand M, Palau R. Transient elastography: a new noninvasive method for assessment of hepatic fibrosis. *Ultrasound Med Biol* 2003; **29**: 1705-1713 [PMID: 14698338 DOI: 10.1016/j.ultrasmedbio.2003.07.001]

13 **Eddowes PJ**, Sasso M, Allison M, Tsochatzis E, Anstee QM, Sheridan D, Guha IN, Cobbold JF, Deeks JJ, Paradis V, Bedossa P, Newsome PN. Accuracy of FibroScan Controlled Attenuation Parameter and Liver Stiffness Measurement in Assessing Steatosis and Fibrosis in Patients With Nonalcoholic Fatty Liver Disease. *Gastroenterology* 2019; **156**: 1717-1730 [PMID: 30689971 DOI: 10.1053/j.gastro.2019.01.042]

14 **Seto WK**, Hui RWH, Mak LY, Fung J, Cheung KS, Liu KSH, Wong DK, Lai CL, Yuen MF. Association Between Hepatic Steatosis, Measured by Controlled Attenuation Parameter, and Fibrosis Burden in Chronic Hepatitis B. *Clin Gastroenterol Hepatol* 2018; **16**: 575-583. e2 [PMID: 28970146 DOI: 10.1016/j.cgh.2017.09.044]

15 **Thiele M**, Rausch V, Fluhr G, Kjærgaard M, Piecha F, Mueller J, Straub BK, Lupşor-Platon M, De-Ledinghen V, Seitz HK, Detlefsen S, Madsen B, Krag A, Mueller S. Controlled attenuation parameter and alcoholic hepatic steatosis: Diagnostic accuracy and role of alcohol detoxification. *J Hepatol* 2018; **68**: 1025-1032 [PMID: 29343427 DOI: 10.1016/j.jhep.2017.12.029]

16 **Ferraioli G**, Tinelli C, De Silvestri A, Lissandrin R, Above E, Dellafiore C, Poma G, Di Gregorio M, Maiocchi L, Maserati R, Filice C. The clinical value of controlled attenuation parameter for the noninvasive assessment of liver steatosis. *Liver Int* 2016; **36**: 1860-1866 [PMID: 27439331 DOI: 10.1111/liv.13207]

17 **Karlas T**, Petroff D, Sasso M, Fan JG, Mi YQ, de Lédinghen V, Kumar M, Lupsor-Platon M, Han KH, Cardoso AC, Ferraioli G, Chan WK, Wong VW, Myers RP, Chayama K, Friedrich-Rust M, Beaugrand M, Shen F, Hiriart JB, Sarin SK, Badea R, Jung KS, Marcellin P, Filice C, Mahadeva S, Wong GL, Crotty P, Masaki K, Bojunga J, Bedossa P, Keim V, Wiegand J. Individual patient data meta-analysis of controlled attenuation parameter (CAP) technology for assessing steatosis. *J Hepatol* 2017; **66**: 1022-1030 [PMID: 28039099 DOI: 10.1016/j.jhep.2016.12.022]

18 **Hennes EM**, Zeniya M, Czaja AJ, Parés A, Dalekos GN, Krawitt EL, Bittencourt PL, Porta G, Boberg KM, Hofer H, Bianchi FB, Shibata M, Schramm C, Eisenmann de Torres B, Galle PR, McFarlane I, Dienes HP, Lohse AW; International Autoimmune Hepatitis Group. Simplified criteria for the diagnosis of autoimmune hepatitis. *Hepatology* 2008; **48**: 169-176 [PMID: 18537184 DOI: 10.1002/hep.22322]

19 **Lindor KD**, Gershwin ME, Poupon R, Kaplan M, Bergasa NV, Heathcote EJ; American Association for Study of Liver Diseases. Primary biliary cirrhosis. *Hepatology* 2009; **50**: 291-308 [PMID: 19554543 DOI: 10.1002/hep.22906]

20 **Chazouillères O**, Wendum D, Serfaty L, Montembault S, Rosmorduc O, Poupon R. Primary biliary cirrhosis-autoimmune hepatitis overlap syndrome: clinical features and response to therapy. *Hepatology* 1998; **28**: 296-301 [PMID: 9695990 DOI: 10.1002/hep.510280203]

21 **National Workshop on Fatty Liver and Alcoholic Liver Disease CSoH**; Chinese Medical

Association. Guidelines of prevention and treatment for nonalcoholic fatty liver disease: a 2018 update. *Linchuang Gandan Bing Zazhi* 2018; **34**: 947-957

22 **Zhou J**, Zhou F, Wang W, Zhang XJ, Ji YX, Zhang P, She ZG, Zhu L, Cai J, Li H. Epidemiological Features of NAFLD From 1999 to 2018 in China. *Hepatology* 2020; **71**: 1851-1864 [PMID: 32012320 DOI: 10.1002/hep.31150]

23 **Mieli-Vergani G**, Vergani D, Czaja AJ, Manns MP, Krawitt EL, Vierling JM, Lohse AW, Montano-Loza AJ. Autoimmune hepatitis. *Nat Rev Dis Primers* 2018; **4**: 18017 [PMID: 29644994 DOI: 10.1038/nrdp.2018.17]

24 **Wong VW**, Petta S, Hiriart JB, Cammà C, Wong GL, Marra F, Vergniol J, Chan AW, Tuttolomondo A, Merrouche W, Chan HL, Le Bail B, Arena U, Craxì A, de Lédinghen V. Validity criteria for the diagnosis of fatty liver by M probe-based controlled attenuation parameter. *J Hepatol* 2017; **67**: 577-584 [PMID: 28506907 DOI: 10.1016/j.jhep.2017.05.005]

25 **de Lédinghen V**, Vergniol J, Capdepont M, Chermak F, Hiriart JB, Cassinotto C, Merrouche W, Foucher J, Brigitte le B. Controlled attenuation parameter (CAP) for the diagnosis of steatosis: a prospective study of 5323 examinations. *J Hepatol* 2014; **60**: 1026-1031 [PMID: 24378529 DOI: 10.1016/j.jhep.2013.12.018]

26 **Shen F**, Zheng RD, Shi JP, Mi YQ, Chen GF, Hu X, Liu YG, Wang XY, Pan Q, Chen GY, Chen JN, Xu L, Zhang RN, Xu LM, Fan JG. Impact of skin capsular distance on the performance of controlled attenuation parameter in patients with chronic liver disease. *Liver Int* 2015; **35**: 2392-2400 [PMID: 25689614 DOI: 10.1111/liv.12809]

27 **Petta S**, Wong VW, Cammà C, Hiriart JB, Wong GL, Marra F, Vergniol J, Chan AW, Di Marco V, Merrouche W, Chan HL, Barbara M, Le-Bail B, Arena U, Craxì A, de Ledinghen V. Improved noninvasive prediction of liver fibrosis by liver stiffness measurement in patients with nonalcoholic fatty liver disease accounting for controlled attenuation parameter values. *Hepatology* 2017; **65**: 1145-1155 [PMID: 27639088 DOI: 10.1002/hep.28843]

28 **Oeda S**, Takahashi H, Imajo K, Seko Y, Ogawa Y, Moriguchi M, Yoneda M, Anzai K, Aishima S, Kage M, Itoh Y, Nakajima A, Eguchi Y. Accuracy of liver stiffness measurement and controlled attenuation parameter using FibroScan® M/XL probes to diagnose liver fibrosis and steatosis in patients with nonalcoholic fatty liver disease: a multicenter prospective study. *J Gastroenterol* 2020; **55**: 428-440 [PMID: 31654131 DOI: 10.1007/s00535-019-01635-0]

World Journal of Gastroenterology

Submit a Manuscript: https://www.f6publishing.com

World J Gastroenterol 2021 January 7; 27(1): 92-106

DOI: 10.3748/wjg.v27.i1.92

ISSN 1007-9327 (print) ISSN 2219-2840 (online)

ORIGINAL ARTICLE

Retrospective Study

Valuable clinical indicators for identifying infantile-onset inflammatory bowel disease patients with monogenic diseases

Wen Su, Yi Yu, Xu Xu, Xin-Qiong Wang, Jie-Bin Huang, Chun-Di Xu, Yuan Xiao

ORCID number: Wen Su 0000-0002-7853-4606; Yi Yu 0000-0002-5680-1195; Xu Xu 0000-0002-5720-945X; Xin-Qiong Wang 0000-0003-0057-3653; Jie-Bin Huang 0000-0001-9362-3511; Chun-Di Xu 0000-0002-2314-9188; Yuan Xiao 0000-0002-4927-8199.

Author contributions: Su W and Yu Y contributed equally to this work; Su W and Yu Y were in charge of the data analysis and writing; Xu X and Wang XQ contributed to data collection; Huang JB contributed to literature search and figure preparation; Xu CD and Xiao Y contributed to study design and data interpretation, and they contributed equally to this work; all authors have read and approved the final manuscript.

Supported by Scientific Research Fund of Shanghai Municipal Health Commission, No. 201640368; National Natural Science Foundation of China, No. 81741103; and The Shanghai Plan for Women and Children's Health Service Capacity Construction (Enhancing the Service Capacity of Shanghai Women and Children Health Care Institutions).

Institutional review board statement: This study was approved by the ethics committee of Ruijin Hospital, Shanghai

Wen Su, Yi Yu, Xu Xu, Xin-Qiong Wang, Jie-Bin Huang, Chun-Di Xu, Yuan Xiao, Department of Pediatrics, Ruijin Hospital, Shanghai Jiao Tong University, School of Medicine, Shanghai 200025, China

Corresponding author: Yuan Xiao, MD, PhD, Associate Chief Physician, Doctor, Department of Pediatrics, Ruijin Hospital, Shanghai Jiao Tong University, School of Medicine, No. 197 Ruijin 2 Road, Shanghai 200025, China. yxiao.penicilinum@gmail.com

Abstract

BACKGROUND

Infantile-onset inflammatory bowel disease (IO-IBD) occurs in very young children and causes severe clinical manifestations, which has poor responses to traditional inflammatory bowel disease (IBD) treatments. At present, there are no simple and reliable laboratory indicators for early screening IO-IBD patients, especially those in whom the disease is caused by monogenic diseases.

AIM

To search for valuable indicators for early identifying IO-IBD patients, especially those in whom the disease is caused by monogenic diseases.

METHODS

A retrospective analysis was performed in 73 patients with IO-IBD admitted to our hospital in the past 5 years. Based on the next-generation sequencing results, they were divided into a monogenic IBD group (M-IBD) and a non-monogenic IBD group (NM-IBD). Forty age-matched patients with allergic proctocolitis (AP) were included in a control group. The clinical manifestations and the inflammatory factors in peripheral blood were evaluated. Logistic regression analysis and receiver operating characteristic (ROC) curve analysis were used to identify the screening factors and cut-off values of IO-IBD as well as monogenic IO-IBD, respectively.

RESULTS

Among the 44 M-IBD patients, 35 carried *IL-10RA* mutations, and the most common mutations were c.301C>T (p.R101W, 30/70) and the c.537G>A (p.T179T, 17/70). Patients with higher serum tumor necrosis factor (TNF)-α value were more likely to have IBD [odds ratio (OR) = 1.25, 95% confidence interval (CI): 1.05-1.50, P = 0.013], while higher serum albumin level was associated with lower risk of IBD (OR = 0.86, 95%CI: 0.74-1.00, P = 0.048). The cut-off values of TNF-α and

Jiaotong University School of Medicine.

Informed consent statement: All guardians of the enrolled pediatric patients who experienced the gene test signed an informed consent form.

Conflict-of-interest statement: The authors have no conflicts of interest to declare.

Data sharing statement: No additional data are available.

Manuscript source: Unsolicited manuscript

Specialty type: Gastroenterology and hepatology

Country/Territory of origin: China

Peer-review report's scientific quality classification
Grade A (Excellent): 0
Grade B (Very good): B
Grade C (Good): 0
Grade D (Fair): 0
Grade E (Poor): 0

Received: October 16, 2020
Peer-review started: October 16, 2020
First decision: November 23, 2020
Revised: December 2, 2020
Accepted: December 11, 2020
Article in press: December 11, 2020
Published online: January 7, 2021

P-Reviewer: Tanabe S
S-Editor: Gao CC
L-Editor: Wang TQ

albumin were 17.40 pg/mL (sensitivity: 0.78; specificity: 0.88) and 36.50 g/L (sensitivity: 0.80; specificity: 0.90), respectively. The increased ferritin level was indicative of a genetic mutation in IO-IBD patients. Its cut-off value was 28.20 ng/mL (sensitivity: 0.93; specificity: 0.92). When interleukin (IL)-10 level was higher than 33.05 pg/mL (sensitivity: 1.00; specificity: 0.84), or the onset age was earlier than 0.21 mo (sensitivity: 0.82; specificity: 0.94), the presence of disease-causing mutations in *IL-10RA* in IO-IBD patients was strongly suggested.

CONCLUSION
Serum TNF-α and albumin level could differentiate IO-IBD patients from allergic proctocolitis patients, and serum ferritin and IL-10 levels are useful indicators for early diagnosing monogenic IO-IBD.

Key Words: Infantile-onset inflammatory bowel disease; Immunodeficiency; Clinical indicators; Interleukin 10; Ferritin; *IL10RA*

Core Tip: It is very important to identify infantile-onset inflammatory bowel disease (IO-IBD) patients, especially those in whom the disease is caused by monogenic diseases, as early as possible because these patients have poor responses to traditional inflammatory bowel disease treatments. However, there are no simple and reliable laboratory indicators for early differential diagnosis. This is the first study focusing on the laboratory indicators that could be used to distinguish O-IBD patients from allergic enteritis patients and screening IO-IBD patients with monogenic diseases. We believe that these results may be valuable in the initial investigations and diagnosis of IO-IBD.

Citation: Su W, Yu Y, Xu X, Wang XQ, Huang JB, Xu CD, Xiao Y. Valuable clinical indicators for identifying infantile-onset inflammatory bowel disease patients with monogenic diseases. *World J Gastroenterol* 2021; 27(1): 92-106
URL: https://www.wjgnet.com/1007-9327/full/v27/i1/92.htm
DOI: https://dx.doi.org/10.3748/wjg.v27.i1.92

INTRODUCTION

Inflammatory bowel disease (IBD) is a chronic recurrent gastrointestinal inflammatory disease, which could be classified into Crohn's disease (CD), ulcerative colitis (UC), and IBD-unclassified (IBD-U)[1]. Common clinical manifestations include diarrhea, hematochezia, abdominal pain, growth retardation, and weight loss. Many studies have reported that the phenotypic characteristics are different in very early onset-IBD (VEO-IBD, the onset age was younger than 6 years old) children from those in adolescent-onset or adult-onset IBD patients[2]. An increasing number of studies[3] have indicated the presence of monogenic defects in VEO-IBD children, especially in infantile patients (< 2 years old). Gene sequencing, especially next generation-sequencing (NGS), could help to find the mutations to explain the cause of the disease; however, this method has high costs, and is time-consuming and not suitable for regular application at the early stage of the disease, particularly in economically underdeveloped areas. Besides, many variants of uncertain significance (VUS) after NGS was applied need laboratory indicators to verify their pathogenicity. However, there have been no reliable clinical indicators reported to identify pediatric IBD patients early, especially those who have potential gene mutations. In this retrospective study, we intended to search for early diagnostic indicators for IO-IBD children with or without the gene mutation, in order to shorten the diagnosis time, reduce medical costs, simplify the analysis of NGS, and administer targeted intervention as early as possible.

P-Editor: Wang LL

MATERIALS AND METHODS

Study participants and groups

This study was approved by the ethics committee of Ruijin Hospital, Shanghai Jiaotong University School of Medicine. All guardians of the enrolled pediatric patients who experienced the gene test signed an informed consent form. This study retrospectively analyzed 73 IO-IBD patients with a disease onset before 2 years of age who were admitted to the Department of Pediatrics, Ruijin Hospital, Shanghai Jiaotong University School of Medicine from January 2014 to February 2019. The diagnostic criteria were based on the Consensus on the Diagnosis and Management of Pediatric Inflammatory Bowel Disease[4] formulated by the Chinese Society of Pediatric Gastroenterology, the Chinese Medical Association. According to the NGS results, the patients were divided into either a monogenic IBD (M-IBD) group, which comprised IO-IBD patients caused by Mendelian diseases, or a non-monogenic IBD (NM-IBD) group, which comprised IO-IBD patients without disease-causing gene mutations. Forty age-matched children who were hospitalized due to diarrhea and hematochezia during the same period and ultimately diagnosed with allergic proctocolitis (AP) were enrolled in the study as a control group.

Clinical data analysis

The clinical data of all patients were collected, including sex, age of onset, body weight and height on admission, average daily frequency of diarrhea, hematochezia, perianal lesions, recurrent fever, and treatment outcomes (remission, non-remission, and death). The results of complete blood count, C-reactive protein (CRP), erythrocyte sedimentation rate (ESR), serum albumin, and serum iron levels were collected and analyzed. Tumor necrosis factor (TNF)-α, interleukin (IL)-6, and IL-10 levels were determined using chemiluminescence immunoassays with a commercial kit (Siemens). The serum ferritin concentration was detected using a double-site enzyme immunoassay with a commercial ferritin kit (ACCES).

Next-generation sequencing and validation

Peripheral blood was collected from all IO-IBD patients for the genetic test. A FlexiGene DNA Kit (Qiagen GmbH, D-40724 Hilden) was used to extract DNA according to the manufacturer's instructions. NGS of targeted genes including primary immunodeficiency diseases and congenital diarrheal diseases (20 cases) was performed by Beijing Mygeno Gene Technology Co., Ltd and whole-exome sequencing (53 cases) was performed by Beijing Berry Genomics Co., Ltd. For the mutations found *via* NGS, Sanger sequencing was used to retest the corresponding gene sequences of the patients and their parents to verify and confirm the genetic origin. The genetic variations were identified using online databases, such as the Single Nucleotide Polymorphism Database (dbSNP), Clinvar, the Human Gene Mutation Database (HGMD), the 1000 Genomes Project, and Online Mendelian Inheritance in Man (OMIM), to verify whether they were the known pathogenic mutations. For novel mutations not included in the databases, pathogenicity was further evaluated according to the American College of Medical Genetics and Genomics (ACMG) guidelines[5].

Statistical analysis

Z scores for height and weight were calculated using WHO Anthro V3.2.2 software. All data were statistically analyzed using IBM SPSS Statistics 25.0. Measurement data with a normal distribution are expressed as the mean ± standard deviation (SD), and nonnormally distributed data are expressed as the median and interquartile range (IQR). Data with a normal distribution and homogeneity of variance were analyzed using ANOVA analysis, and abnormally distributed data were analyzed by nonparametric Kruskal-Wallis analysis. Categorical data were analyzed using the chi-square test, or Fisher's exact Chi-square test. Multivariate binary logistic regression analysis was performed to identify risk factors for IO-IBD and monogenic IO-IBD. Receiver operating characteristic (ROC) curve analysis was performed to assess the diagnostic value of the identified indicators. *P* values were adjusted using the Bonferroni method for pairwise comparison. $P < 0.05$ was considered statistically significant. The statistical methods of this study were reviewed by Li J from the Clinical Research Center, Ruijin Hospital, Shanghai Jiao Tong University School of Medicine.

RESULTS

Genotypes of IO-IBD patients

Among the 73 IO-IBD patients, 24 did not carry any disease-causing mutations in IBD-associated genes, and 49 had the gene mutations related to the disease. Among 49 patients with mutations, 39 carried *IL-10RA* mutations, 2 carried *CYBB* mutations, and *WAS*, *IKBKG*, *SLC37A4*, *CD40LG*, *LIG4*, *CARD11*, *PIK3CD*, and *CXCR4* mutations were observed in one patient each (Table 1). Four of them carried the *IL-10RA* heterozygous mutation which did not meet the criteria of Mendelian disease, and one of them had a heterozygous *CXCR4* mutation which was inherited from his father with ankylosing spondylitis and recognized as a VUS according to the ACMG guidelines because of absence of typical manifestations of autosome dominant WHIM syndrome. Therefore, these five patients were included in the NM-IBD group. There were 14 different missense mutations found in *IL-10RA* among M-IBD patients. Two variations, the c.301C>T (p.R101W) and the c.537G>A (p.T179T), were considered hotspot mutations in the M-IBD patient cohort, the mutation frequencies were 42.86% (30/70) and 24.29% (17/70) respectively. We also found nine novel mutations: c.109G>T, c.302G>A, c.569T>G, and c.787C>T in *IL-10RA* gene; c.674+2T>C in *CYBB* gene; c.267delC in *CD40LG* gene; c.1144_1145delCT in *LIG4* gene; c.155T>C in *CARD11* gene; and c.1001G>A in *CXCR4* gene. The amino acid substitutions and pathogenicity of these variations that were assessed according to the ACMG guidelines are summarized in Table 1.

Clinical characteristics

As shown in Table 2, the proportions of male patients in the AP group, the M-IBD group, and the NM-IBD group was higher than those of female patients; however, no significant difference was observed among the three groups. The median onset age of patients in the M-IBD group was 0.51 (0.04-1.79) mo, which was much younger than that in the AP group [4.44 (1.25-11.76) mo; $P = 0.003$] and the NM-IBD group [3.99 (3-9) mo; $P = 0.001$]. The proportions of all IO-IBD patients who had severe diarrhea (more than 8 times/d, 86.4% in the M-IBD group and 58.6% in the NM-IBD group) and recurrent fever (63.6% in the M-IBD group and 41.4% in the NM-IBD group) were significantly higher than those in AP patients (25% of patients had severe diarrhea [$P < 0.001$] and 5% of patients had a recurrent fever [$P = 0.01$]). The percentages of the patients who had severe diarrhea and perianal lesions in the M-IBD group (86.4% and 79.5%, respectively) were much higher than those in the NM-IBD group (58.6% [$P = 0.007$] and 24.1% [$P = 0.005$]). The anthropometric results showed that the *Z* scores for body weight (-1.95 ± 0.26 for the M-IBD group and -1.15 ± 0.29 for the NM-IBD group) and body height (-1.95 ± 0.25 for the M-IBD group and -1.32 ± 0.31 for the NM-IBD group) of the IBD patients were all lower than those of the children in the AP group (-0.05 ± 0.21 for weight [$P < 0.001$] and 0.17 ± 0.19 for height [$P < 0.001$]), while there was no significant difference between the M-IBD group and the NM-IBD group. Regarding the outcomes of treatment, mortality in the M-IBD group was significantly higher than that in the NM-IBD group (20.5% *vs* 3.4%, $P = 0.001$), whereas no death occurred in the AP group.

As shown in Table 3, the blood test results showed that peripheral white blood cell count (WBC), platelet count (PLT), CRP, ESR, TNF-α, and IL-6 levels in the IO-IBD group were significantly higher than those in the AP group ($P < 0.01$ for all), while serum albumin level was lower than that in the AP group ($P < 0.001$). Differences in serum iron levels were not significant among the three groups. Notably, serum IL-10 [85.50 (42.75-127.25) pg/mL] and ferritin [55.90 (36.10-231.20) ng/mL] levels in the M-IBD group were significantly higher than those in the AP group [IL-10: 5.00 (5.00-5.00) pg/mL, $P < 0.001$; ferritin: 22.90 (14.90-37.05) ng/mL, $P = 0.002$] and in the NM-IBD group [IL-10: 6.37 (5.00-14.80) pg/mL, $P < 0.001$; ferritin: 15.30 (9.40-27.60) ng/mL, $P < 0.001$].

Binary logistic regression analysis and ROC curve analysis

Clinical indicators for risk of IO-IBD: Binary logistic regression analysis was performed for the parameters with significant differences between the AP group and the IO-IBD group [including diarrhea (> 8 times/d), recurrent fever, *Z*-scores for weight, *Z*-scores for height, WBC, hemoglobin (Hb), PLT, CRP, ESR, TNF-α, IL-6, and albumin levels]. The results showed that increased peripheral WBC (odds ratio [OR] = 1.19, 95% confidence interval [CI]: 1.01-1.40, $P = 0.040$), ESR (OR = 1.10, 95%CI: 1.01-1.20, $P = 0.037$) and levels of TNF-α (OR =1.25, 95%CI: 1.05-1.50, $P = 0.013$), as well as reduced albumin levels were risk factors (OR = 0.86, 95%CI: 0.74-1.00, $P = 0.048$) for

Table 1 Genotypes of 49 infantile-onset inflammatory bowel disease patients

Patient	Gene	Variant (allele 1)	Amino acid	ACMG (P/LP)	Variant (allele 2)	Amino acid	ACMG (P/LP)
1	*IL10RA*	c.301C>T	R101W	P (PS1+PS3+PM1+PM2+PP3+PP4)	c.301C>T	R101W	P (PS1+PS3+PM1+PM2+PP3+PP4)
2	*IL10RA*	c.299T>G	V100G	P (PS1+PS3+PM2+PP3+PP4)	c.301C>T	R101W	P (PS1+PS3+PM1+PM2+PP3+PP4)
3	*IL10RA*	c.191A>G	Y64C	LP (PM1+PM2+PM3+PP3+PP4)	c.537G>A	T179T	P (PS1+PS3+PM2+PP3+PP4)
4	*IL10RA*	c.301C>T	R101W	P (PS1+PS3+PM1+PM2+PP3+PP4)	c.537G>A	T179T	P (PS1+PS3+PM2+PP3+PP4)
5	*IL10RA*	c.301C>T	R101W	P (PS1+PS3+PM1+PM2+PP3+PP4)	c.301C>T	R101W	P (PS1+PS3+PM1+PM2+PP3+PP4)
6	*IL10RA*	c.493C>T	R165X	P (PVS1+PS1+PM2+PP4)	c.301C>T	R101W	P (PS1+PS3+PM1+PM2+PP3+PP4)
7	*IL10RA*	c.301C>T	R101W	P (PS1+PS3+PM1+PM2+PP3+PP4)	c.537G>A	T179T	P (PS1+PS3+PM2+PP3+PP4)
8	*IL10RA*	c.350G>A	R117H	P (PS1+PM1+PM2+PP3+PP4)	c.493C>T	R165X	P (PVS1+PS1+PM2+PP4)
9	*IL10RA*	c.301C>T	R101W	P (PS1+PS3+PM1+PM2+PP3+PP4)	c.436delC	P146fs	P (PVS1+PS1+PM2+PP4)
10	*IL10RA*	c.301C>T	R101W	P (PS1+PS3+PM1+PM2+PP3+PP4)	c.537G>A	T179T	P (PS1+PS3+PM2+PP3+PP4)
11	*IL10RA*	c.421G>A	G141R	P (PS1+PM2+PM3+PP3+PP4)	c.537G>A	T179T	P (PS1+PS3+PM2+PP3+PP4)
12	*IL10RA*	c.301C>T	R101W	P (PS1+PS3+PM1+PM2+PP3+PP4)	c.301C>T	R101W	P (PS1+PS3+PM1+PM2+PP3+PP4)
13	*IL10RA*	c.301C>T	R101W	P (PS1+PS3+PM1+PM2+PP3+PP4)	c.350G>A	R117H	P (PS1+PM1+PM2+PP3+PP4)
14	*IL10RA*	c.537G>A	T179T	P (PS1+PS3+PM2+PP3+PP4)	c.537G>A	T179T	P (PS1+PS3+PM2+PP3+PP4)
15	*IL10RA*	c.301C>T	R101W	P (PS1+PS3+PM1+PM2+PP3+PP4)	c.537G>A	T179T	P (PS1+PS3+PM2+PP3+PP4)
16	*IL10RA*	c.99G>A	W33X	P (PVS1+PS1+PM2+PP4)	c.301C>T	R101W	P (PS1+PS3+PM1+PM2+PP3+PP4)
17	*IL10RA*	c.493C>T	R165X	P (PVS1+PS1+PM2+PP4)	c.493C>T	R165X	P (PVS1+PS1+PM2+PP4)
18	*IL10RA*	c.109G>T	E37X	LP (PVS1+PM2+PM3+PP4)	c.301C>T	R101W	P (PS1+PS3+PM1+PM2+PP3+PP4)
19	*IL10RA*	c.301C>T	R101W	P (PS1+PS3+PM1+PM2+PP3+PP4)	c.537G>A	T179T	P (PS1+PS3+PM2+PP3+PP4)
20	*IL10RA*	c.301C>T	R101W	P (PS1+PS3+PM1+PM2+PP3+PP4)	c.537G>A	T179T	P (PS1+PS3+PM2+PP3+PP4)
21	*IL10RA*	c.301C>T	R101W	P (PS1+PS3+PM1+PM2+PP3+PP4)	c.537G>A	T179T	P (PS1+PS3+PM2+PP3+PP4)
22	*IL10RA*	c.301C>T	R101W	P (PS1+PS3+PM1+PM2+PP3+PP4)	c.350G>A	R117H	P (PS1+PM1+PM2+PP3+PP4)
23	*IL10RA*	c.99G>A	W33X	P (PVS1+PS1+PM2+PP4)	c.299T>G	V100G	P (PS1+PS3+PM2+PP3+PP4)
24	*IL10RA*	c.301C>T	R101W	P (PS1+PS3+PM1+PM2+PP3+PP4)	c.537G>A	T179T	P (PS1+PS3+PM2+PP3+PP4)
25	*IL10RA*	c.301C>T	R101W	P (PS1+PS3+PM1+PM2+PP3+PP4)	c.537G>A	T179T	P (PS1+PS3+PM2+PP3+PP4)
26	*IL10RA*	c.301C>T	R101W	P(PS1+PS3+PM1+PM2+PP3+PP4)	c.493C>T	R165X	P (PVS1+PS1+PM2+PP4)
27	*IL10RA*	c.301C>T	R101W	P (PS1+PS3+PM1+PM2+PP3+PP4)	c.537G>A	T179T	P (PS1+PS3+PM2+PP3+PP4)
28	*IL10RA*	c.493C>T	R165X	P (PVS1+PS1+PM2+PP4)	c.537G>A	T179T	P (PS1+PS3+PM2+PP3+PP4)
29	*IL10RA*	c.301C>T	R101W	P (PS1+PS3+PM1+PM2+PP3+PP4)	c.301C>T	R101W	P (PS1+PS3+PM1+PM2+PP3+PP4)
30	*IL10RA*	c.302G>A	R101Q	LP (PM1+PM2+PM3+PM5+PP3+PP4)	c.349C>T	R117C	P (PS1+PM1+PM2+PP3+PP4)
31	*IL10RA*	c.301C>T	R101W	P (PS1+PS3+PM1+PM2+PP3+PP4)	c.301C>T	R101W	P (PS1+PS3+PM1+PM2+PP3+PP4)
32	*IL10RA*	c.301C>T	R101W	P (PS1+PS3+PM1+PM2+PP3+PP4)	c.301C>T	R101W	P (PS1+PS3+PM1+PM2+PP3+PP4)
33	*IL10RA*	c.299T>G	V100G	P (PS1+PS3+PM2+PP3+PP4)	c.569T>G	F190C	LP (PS1+PM2+PM3_VeryStrong+PP3+PP4)
34	*IL10RA*	c.537G>A	T179T	P (PS1+PS3+PM2+PP3+PP4)	c.537G>A	T179T	P (PS1+PS3+PM2+PP3+PP4)
35	*IL10RA*	c.299T>G	V100G	P (PS1+PS3+PM2+PP3+PP4)	c.299T>G	V100G	P (PS1+PS3+PM2+PP3+PP4)
36	*WAS*	IVS8: +3- +6 GAGT del		LP (PS1+PM2+PP3+PP4)			
37	*IKBKG*	c.1217A>T	D406V	P (PS1+PM1+PM2+PP3+PP4)			
38	*SLC37A4*	c.310 ins T		P (PVS1+PM2+PP4)	c.1014-1120 del107		P (PVS1+PM2+PP4)

39	*CYBB*	c.674+2T>C		P (PVS1+PM2+PP4)			
40	*CYBB*	c.1272G>A	W424X	P (PVS1+PS1+PM2+PP4)			
41	*CD40LG*	c.267delC	Q90Sfs*6	LP (PVS1+PM2+PP4)			
42	*LIG4*	c.833G>T	R278L	LP (PM1+PM2+PM3+PM5+PP3+PP4)	c.1144_1145delCT	L382Efs*5	LP (PVS1+PS1+PM2+PP4)
43	*CARD11*	c.155T>C	I52T	LP (PS2+PM2+PP4)			
44	*PIK3CD*	c.3061G>A	E1021K	P (PS1+PS3+PM2+PP3+PP4)			
45	*IL10RA*	c.350G>A	R117H	P (PS1+PM1+PM2+PP3+PP4)			
46	*IL10RA*	c.537G>A	T179T	P (PS1+PS3+PM2+PP3+PP4)			
47	*IL10RA*	c.787C>T	R263X	LP (PVS1+PM2+PP4)			
48	*IL10RA*	c.301C>T	R101W	P (PS1+PS3+PM1+PM2+PP3+PP4)			
49	*CXCR4*	c.1001G>A	R334Q	VUS (PM2+PP3+PP4:BS4)			

ACMG: American College of Medical Genetics and Genomics; P/LP: Pathogenic/likely pathogenic; VUS: Variants of uncertain significance.

Table 2 Clinical features and growth parameters among three groups of patients

	AP	M-IBD	NM-IBD	*P* value
Total number	40	44	29	
Male (%)	25 (62.50)	27 (61.36)	21 (72.41)	0.591
Median onset age (mo, IQR)	4.44 (1.25,11.76)	0.51 (0.04,1.79)[1]	3.99 (3.00,9.00)	< 0.001
Diarrhea (≥ 8 times/d, %)	10 (25.00)[1]	38 (86.40)[1]	17 (58.60)	< 0.001
Diarrhea with blood (%)	30 (75.00)	29 (65.90)	24 (82.80)	0.320
Perianal disease (%)	0 (0)	35 (79.54)[1]	7 (24.14)	0.005
Fever (%)	2 (5.00)[1]	28 (63.63)	12 (41.38)	< 0.001
Death (%)	0 (0.00)	9 (20.45)	1 (3.45)[2]	0.001
Z scores for weight (mean ± SD)	-0.05 ± 0.21[1]	-1.95 ± 0.26	-1.15 ± 0.29	< 0.001
Z scores for height (mean ± SD)	0.19 ± 0.19[1]	-1.95 ± 0.25	-1.32 ± 0.31	< 0.001
Z scores for BMI (mean ± SD)	-0.21 ± 0.24[2]	-1.30 ± 0.28	-0.52 ± 0.27	0.026

[1]Compared with the other two groups, adjusted *P* value < 0.05.
[2]Compared with the monogenic inflammatory bowel disease (M-IBD) group, adjusted *P* value < 0.05. AP: Allergic proctocolitis; M-IBD: Monogenic inflammatory bowel disease; NM-IBD: Non-monogenic inflammatory bowel disease; IQR: Interquartile range; SD: Standard deviation; BMI: Body mass index.

the diagnosis of IO-IBD (Table 4). We further investigated these four indicators using ROC curve analysis to explore their diagnostic value. The areas under the curves (AUCs) and the cut-off values are shown in Figure 1A and B. For WBC, the AUC was 0.78 (95%CI: 0.69-0.86, $P < 0.001$) and the cut-off value was 11.96 × 10^9/L (sensitivity: 0.66; specificity: 0.88). For ESR, the AUC was 0.81 (95%CI: 0.73-0.89, $P < 0.001$), and the cut-off value was 12.50 mm/h (sensitivity: 0.70; specificity: 0.90). For TNF-α, the AUC was 0.80 (95%CI: 0.72-0.89, $P < 0.001$) and the cut-off value was 17.40 pg/mL (sensitivity: 0.78; specificity: 0.88). For albumin, the AUC was 0.88 (95%CI: 0.81-0.94, $P < 0.001$), and the cut-off value was 36.50 g/L (sensitivity: 0.80; specificity: 0.90). Based on the results, WBC and ESR had a low sensitivity for recognizing IO-IBD. While TNF-α and albumin level had a higher sensitivity and specificity, and we speculated they may be used for early identifying IO-IBD patients.

Clinical indicators for risk of M-IBD: Binary logistic regression analysis was performed using the parameters with significant differences between the M-IBD group and the NM-IBD group [including median onset age, diarrhea (> 8 times/d), perianal disease, CRP, IL-10, and ferritin levels]. The results showed that very early onset age

Table 3 Results of blood test and inflammatory factors among three groups of patients (median, interquartile range)

	AP	M-IBD	NM-IBD	*P* value
WBC (× 10^9)	8.77 (6.78, 10.75)[1]	14.88 (9.84, 19.37)	13.77 (8.87,18.51)	< 0.001
Hemoglobin (mg/L)	119 (115, 126)[1]	98 (90, 113)	100 (80.50,116)	< 0.001
PLT (× 10^9)	304 (254, 383)[1]	447 (306.75, 591.50)	477 (323.50, 601.50)	0.002
CRP (mg/L)	1 (0.20, 1.00)[1]	48 (7.98, 75.23)[1]	21 (1.00, 44.35)	< 0.001
ESR (mm/h)	6 (4, 8)[1]	18.50 (8, 39)	21 (6, 42)	< 0.001
TNF-α (pg/mL)	14.60 (10.68, 17.03)[1]	21.50 (17.58, 27.88)	22.90 (14.48, 61.28)	< 0.001
IL-6 (pg/mL)	2.85 (2.00, 3.35)[1]	21.00 (10.20, 50.30)	14.55 (6.81, 30.00)	< 0.001
IL-10 (pg/mL)	500 (5, 5)	85.50 (42.75, 127.25)[1]	6.37 (5.00, 14.80)	< 0.001
Ferritin (ng/mL)	22.90 (14.90, 37.05)	55.90 (36.10, 231.20)[1]	15.50 (10.60, 27.72)	< 0.001
Albumin (g/L)	41 (38, 43)[1]	31 (27, 35)	33 (27.00, 36.50)	< 0.001
Serum iron (μmol/L)	8.00 (5.90, 10.20)	3.90 (2.60, 6.88)	5.70 (4.35, 11.38)	0.069

[1]Compared with the other two groups, adjusted *P* value < 0.05. AP: Allergic proctocolitis; M-IBD: Monogenic inflammatory bowel disease; NM-IBD: Non-monogenic inflammatory bowel disease; WBC: White blood cells; PLT: Platelets; CRP: C-reactive protein; ESR: Erythrocyte sedimentation rate; TNF: Tumor necrosis factor; IL: Interleukin.

Table 4 Binary logistic analysis for identifying risk factors for infantile-onset inflammatory bowel disease

	AP (median, IQR)	IO-IBD (median, IQR)	Adjusted OR (95%CI)	*P* value
WBC (× 10^9)	8.77 (6.78, 10.75)	14.12 (8.85, 18.27)	1.19 (1.01, 1.40)	0.040
ESR (mm/h)	6 (4, 8)	19.00 (8.00, 39.00)	1.10 (1.01, 1.20)	0.037
TNF-α (pg/mL)	14.60 (10.68, 17.03)	21.65 (17.33, 29.45)	1.25 (1.05, 1.50)	0.013
Albumin (g/L)	41 (38, 43)	32 (27, 36)	0.86 (0.74, 1.00)	0.048

Binary logistic analysis showed that white blood cell (WBC) count, erythrocyte sedimentation rate (ESR), tumor necrosis factor (TNF)-α, and albumin in peripheral blood could be used to identify the infantile-onset inflammatory bowel disease from AP if a child had diarrhea and hematochezia in early childhood. Higher WBC, ESR, and TNF-α, as well as lower level of albumin suggested a higher probability of inflammatory bowel disease. AP: Allergic proctocolitis; IO-IBD: Infantile-onset inflammatory bowel disease; IQR: Interquartile range; OR: Odds ratio; CI: Confidence interval; WBC: White blood cells; ESR: Erythrocyte sedimentation rate; TNF: Tumor necrosis factor.

(OR = 3.47, 95%CI: 1.29-9.29, *P* = 0.013], presence of perianal diseases (OR = 11.42, 95%CI: 1.71-76.23, *P* = 0.012), and high levels of serum ferritin (OR = 1.14, 95%CI: 1.06-1.24, *P* = 0.001) and IL-10 (OR = 1.04, 95%CI: 1.01-1.08, *P* = 0.005) were the main risk factors for M-IBD diagnosis (Table 5). Because the *IL-10RA* mutations in this study accounted for a dominant proportion (79.6%) in the M-IBD group, to avoid bias caused by sample selection, we further compared the above high-risk factors among patients with *IL-10RA* mutations or non-*IL-10RA* mutations in the M-IBD group, and those without any disease-causing mutations in the NM-IBD group. The results showed that only serum ferritin could discriminate M-IBD and NM-IBD regardless of genotypes. The level of serum ferritin was significantly lower in the NM-IBD group than in the other two groups (Table 6) and could be used as an indicator for recognizing IO-IBD children with genetic mutations. The ROC curve analysis was also performed to explore the indicators for the diagnosis of M-IBD. Using gene sequencing results as the gold standard, all IO-IBD patients were included in the analysis. The AUC of ferritin for diagnosing M-IBD was 0.94 (95%CI: 0.87-1.00, *P* < 0.001), with a cut-off value of 28.20 ng/mL (sensitivity: 0.93; specificity: 0.92; Figure 1C), which showed high diagnostic value. Besides, we further analyzed the value of serum IL-10 level and onset age for early noticing *IL-10RA* mutation in M-IBD patients. The AUC for IL-10 was 0.91 (95%CI: 0.86-0.99, *P* < 0.001), and the cut-off value was 33.05 pg/mL (sensitivity: 1.00; specificity: 0.84); the AUC for onset age was 0.87 (95%CI: 0.78-0.96, *P* < 0.001), and the cut-off value was 0.21 mo (sensitivity: 0.82; specificity: 0.94; Figure 1D and E). These results indicated that the two indicators had high diagnostic value and may be

Table 5 Binary logistic analysis for identifying risk factors for monogenic inflammatory bowel disease

	M-IBD (median, IQR)	NM-IBD (median, IQR)	Ajusted OR (95%CI)	*P* value
Ferritin (ng/mL)	55.90 (36.10, 231.20)	15.30 (9.40, 27.60)	1.14 (1.06, 1.24)	0.001
IL-10 (pg/mL)	85.20 (43.30, 126.50)	5.00 (5.00, 9.11)	1.04 (1.01, 1.08)	0.005
Median onset age (mo)	0.51 (0.04, 1.79)	3.99 (3.00, 9.00)	3.47 (1.29, 9.29)	0.013
Perianal disease (%)	35 (79.50)	7 (24.10)	11.42 (1.71, 76.23)	0.012

Binary logistic analysis showed that higher levels of ferritin and interleukin (IL)-10 in peripheral blood, earlier onset age, and presence of perianal disease suggested that inflammatory bowel disease children may have the gene mutation. However, most of the mutations (79.6%) in this study occurred in *IL-10RA*, and in order to avoid the bias, we did further analyses as showed in Table 6. M-IBD: Monogenic inflammatory bowel disease; NM-IBD: Non-monogenic inflammatory bowel disease; IL: Interleukin; IQR: Interquartile range; OR: Odds ratio; CI: Confidence interval.

Table 6 Comparison of risk factors among infantile-onset inflammatory bowel disease patients with or without *IL-10RA* mutation and non-monogenic inflammatory bowel disease (median, interquartile range)

	IL-10RA M-IBD	Non-*IL-10RA* M-IBD	NM-IBD	*P* value
Ferritin (ng/mL)	55.90 (53.12, 74.73)	45.25 (16.58, 68.70)	15.30 (14.55, 17.95)[1]	< 0.001
IL-10 (pg/mL)	85.20 (66.20, 125.00)[1]	8.90 (5.00, 85.20)	5.00 (5.00, 9.11)	< 0.001
Median onset age (mo)	0.04 (0.00, 0.08)[1]	2 (0.41, 4.08)	3.99 (3, 9)	< 0.001
Perianal disease (%)	32 (91.43)[1]	3 (33.33)	7 (24.14)	0.002

[1]Compared with the other two groups, adjusted *P* value < 0.01. M-IBD: Monogenic inflammatory bowel disease; NM-IBD: Non-monogenic inflammatory bowel disease; IL: Interleukin.

used in clinical practice. All above results suggested that, when serum ferritin levels were higher than 28.20 ng/mL, it might indicate the existence of pathogenic gene mutations in IO-IBD patients. If the infant got IO-IBD within 1 wk after the birth or their serum IL-10 levels were higher than 33.05 pg/mL, it might strongly suggest the presence of *IL-10RA* gene mutations.

DISCUSSION

Approximately 15% of pediatric patients were categorized as having VEO-IBD[2], and approximately 1% of pediatric patients developed symptoms during infancy (IO-IBD). Over the past decade, the prevalence of VEO-IBD had increased by more than 50%[6,7]. Increasing studies believed that genetic factors, such as monogenic diseases, play important roles in the development of VEO-IBD, especially IO-IBD. Currently, there is no epidemiological data for IO-IBD patients in China. However, in the past 5 years, more than 200 cases of VEO-IBD have been reported by our hospital and other hospitals in China[8-13], and more than half of the patients presented genetic defects. Among the 73 pediatric patients in this study, 49 (67.12%) carried disease-related gene mutations, which was much higher than the reported proportions in European and American countries[14,15] but similar to the proportion reported by Huang *et al*[10], suggesting that the presence of monogenic diseases is more common in Chinese VEO-IBD patients.

A total of ten mutated genes were identified in this study, among which the *IL-10RA* mutation was the most common (39/49). This finding was similar to those reported by other researchers in China[8], while *IL-10RB* and *IL-10* mutations were not observed. Among the 14 *IL-10RA* variants, ten have been reported previously, among which c.537G>A, c.493C>T, c.436delC, c.299T>G, and c.191A>G mutations were observed in children only in China or other Asian countries[11,16,17] but have not been reported in Western countries, suggesting a genetic founder effect in *IL-10RA*. The four identified novel variants were c.109G>T, c.302G>A, c.569T>G, and c.787C>T, which were likely pathogenic mutations according to the ACMG guidelines. In this study, the most common *IL-10RA* mutation locus was c.301C>T, followed by c.537G>A, which was

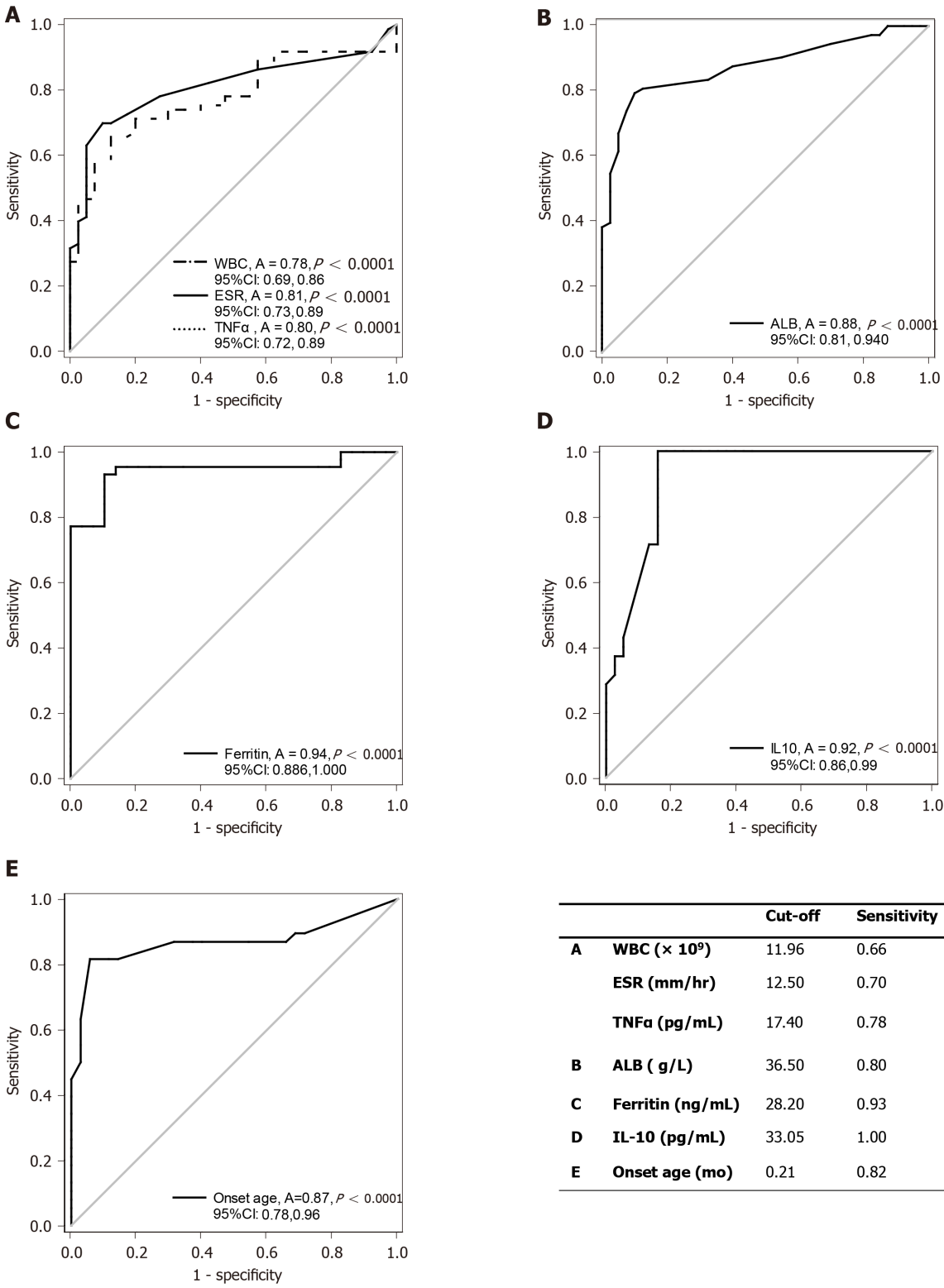

		Cut-off	Sensitivity	Specipicity
A	**WBC (× 10⁹)**	11.96	0.66	0.88
	ESR (mm/hr)	12.50	0.70	0.90
	TNFα (pg/mL)	17.40	0.78	0.88
B	**ALB (g/L)**	36.50	0.80	0.90
C	**Ferritin (ng/mL)**	28.20	0.93	0.92
D	**IL-10 (pg/mL)**	33.05	1.00	0.84
E	**Onset age (mo)**	0.21	0.82	0.94

Figure 1 Receiver operating characteristic curve analysis for diagnostic indicators. A and B: Parameters that may be used to distinguish allergic proctocolitis from infantile-onset inflammatory bowel disease (IO-IBD). The increased peripheral white blood cell count, erythrocyte sedimentation, rate and tumor necrosis factor (TNF)-α, as well as the reduced albumin levels were risk factors for the diagnosis of IO-IBD, and TNF-α and albumin levels had higher sensitivity and specificity; C: Serum ferritin level has high diagnostic value in discriminating IO-IBD patients with gene mutation (M-IBD) or without (NM-IBD) when serum ferritin levels are above 28.20 ng/mL. It might indicate the existence of pathogenic gene mutations in IO-IBD patients; D and E: Serum interleukin (IL)-10 level and onset age can be used to screen *IL-10RA* mutation in M-IBD patients. If an infant got IO-IBD within a week in life or a patient's serum IL-10 levels were higher than 33.05 pg/mL, the presence of *IL-10RA* gene mutations was strongly suggested. WBC: White blood cell; ESR: Erythrocyte sedimentation rate; TNF: Tumor necrosis factor; ALB: Albumin; IL: Interleukin; CI: Confidence interval.

consistent with the previous reports in Asian children[8]. Notably, c.537G>A mutation was located in exon 4, which was always missed in the reports as it was mistaken for a synonymous mutation; however, it had been confirmed as a splicing mutation that has a deleterious effect on IL-10 receptor[11]. For IBD children who are highly suspected of having abnormal IL-10 signaling pathways, especially those who have a heterozygous *IL-10RA* mutation after gene sequencing, clinicians should be aware of the sequencing report and not to miss the c.537G>A mutation.

In addition to *IL-10RA*, the other eight genetic mutations that could cause immunodeficiency diseases were also observed in this study. These included *CYBB* mutation, which caused X-linked chronic granulomatous disease[18], *IKBKG* mutation, which caused ectodermal dysplasia and immunodeficiency[19,20], *PIK3CD* mutation, which caused activated phosphoinositide 3-kinase δ syndrome[21], *CD40LG* mutation, which caused X-linked hyper-IgM syndrome[22], *SLC37A4* mutation, which caused glycogen storage disease type 1B[23], *LIG4* mutation, which caused LIG4 syndrome[24], *WAS* mutation, which caused Wiskott-Aldrich syndrome[25], and *CARD11* mutation, which caused immunodeficiency type 11B with atopic dermatitis[26]. These diseases have been confirmed to cause IBD-like colitis in infants, such as recurrent diarrhea, hematochezia, infections, perianal abscess, and growth retardation.

Because of an insufficient understanding of IO-IBD, especially that caused by monogenic diseases, most patients could not be diagnosed as early as possible. It has been reported that the median time from the occurrence of symptoms to disease diagnosis was approximately 6 mo[15]. The most common misdiagnosis was allergic diseases, therefore, this study included a group of age-matched patients who were admitted to the hospital due to diarrhea and hematochezia and were eventually diagnosed as allergic proctocolitis. Although the AP children had diarrhea, hematochezia, or other similar symptoms with the IBD children, there was less onset of failure to thrive, perianal lesions, and death in AP patients; meanwhile, the daily frequency of diarrhea was significantly higher in IO-IBD children than in AP children. Inflammatory markers in peripheral blood such as WBC, CRP, ESR, PLT, TNF-α, and IL-6 in IO-IBD children were significantly higher than those in AP children, while the nutritional indicators such as albumin and hemoglobin were lower in IBD patients than in AP patients. Logistic regression analysis further confirmed that increased levels of WBC, ESR, and TNF-α, as well as lower serum albumin level were associated with a higher likelihood of IBD. Although it has been reported that hematological examinations had little value in the differential diagnosis of food allergy and IBD[15],the ROC curve analysis in this study showed that TNF-α and serum albumin level had moderate value for differentiating IBD from allergic disease. Moreover, the high sensitivities and specificities of cut-off values for TNF-α and serum albumin may help clinicians, especially those in areas with limited medical resources, to identify IO-IBD patients earlier.

Genetic diagnosis is currently the gold standard for the diagnosis of IO-IBD caused by gene defects. However, the economic and time costs of this detection are relatively high in China. Most parents are not willing to choose this method at initial visits, and this would delay the diagnosis and treatment. The binary logistic regression analysis showed the serum ferritin (OR = 1.14) and IL-10 (OR = 1.04) may indicate the presence of gene defects in IO-IBD children; however, in view of the high proportion of IL-10RA mutations in our cohort, we further compared these factors among patients with *IL-10RA* mutations, those with non-*IL-10RA* mutations, and those without any disease-causing mutations. The final results showed that serum ferritin was abnormally elevated in IO-IBD patients with gene mutations and was not affected by the genotypes. Further ROC curve analysis showed that serum ferritin might be a valuable diagnostic indicator for monogenic IBD. Serum ferritin was acknowledged as an inflammatory marker, which would reflect the acute and chronic inflammatory state in infectious diseases, immunological diseases, hematological diseases, and malignant diseases[27]. A variety of cells could synthesize and secrete ferritin, of which macrophages were the main source and could induce diseases[27]. The role of ferritin in inflammatory responses is still unclear. It was hypothesized that in the inflammatory state, the Toll-like receptor (TLR) 9 signaling pathway is activated, IL-1β and IL-18 levels increased, then macrophages were activated, and synthesized more ferritin, which could further amplify the inflammatory response through the TLR9 signaling pathway, thereby forming a positive feedback loop and resulting in continuous aggravation of inflammation[28-32]. Some researchers believed that serum ferritin could bind to T and B lymphocytes directly[32,33], then inhibit T cell proliferation, B cell maturation, and immunoglobulin synthesis[33-35]. In addition, serum ferritin could also promote regulatory T cell differentiation through the IL-10 signaling pathway and play an immunoregulatory role[36]. In our study, the serum ferritin level was

significantly elevated in M-IBD children, but whether it plays a pro-inflammatory or immunomodulatory role needs further study.

Both in our study and other studies in China, *IL-10RA* is the most common mutated gene in Chinese VEO-IBD patients. We also found that compared to the patients with other gene mutations, patients with the *IL-10RA* deficiency had unique features. First, the age of onset was particularly early. The median onset age was 0.04-mo-old, while it was 2-mo-old in patients with other gene mutations, indicating that diarrhea and hematochezia existed from birth in *IL-10RA* mutated children. Second, serum IL-10 level in these patients was particularly high. IL-10 is an important anti-inflammatory factor secreted by a variety of immune cells. After binding to IL-10R, IL-10 can activate a series of cascade reactions to maintain immune homeostasis by inhibiting inflammatory factors such as TNF-α[37]. IL-10R is composed of two subunits, IL-10RA and IL-10RB, and IL-10RA only binds to IL-10[38]. It was previously believed that the increased expression of IL-10 in IBD patients indicated a good steroid response and prognosis[39]. However, when IL-10R is deficient, the anti-inflammatory function of IL-10 could not be achieved. Glocker *et al*[40] confirmed that human peripheral blood mononuclear cells (PBMCs) could secrete large amounts of TNF-α after stimulation with lipopolysaccharide (LPS) *in vitro*, but its level decreased significantly when exogenous IL-10 was added into the culture medium, while this phenomenon could not be observed in the PBMC culture supernatant from *IL-10RA* deficient children, indicating the important role of the IL-10 signaling pathway in anti-inflammatory processes. In our study, both high IL-10 and TNF-α levels were observed in patients with *IL-10RA* mutation, which indicated that even such a high level of IL-10 could not inhibit TNF-α release and alleviate the inflammation in these children. These findings were similar to the *in vitro* research mentioned above. Therefore, we speculated that IL-10 level could be used as an *in vivo* detective indicator to verify the function of novel mutations of the *IL-10RA* gene. In this study, ROC curve analysis also confirmed that serum IL-10 level had a high sensitivity and specificity for identifying the presence of *IL-10RA* mutations, which suggested that if IO-IBD patients have a remarkably elevated IL-10 level, the gene sequencing is strongly recommended to identify the existence of *IL-10RA* deficiency. In fact, we did further investigation by whole-genome sequencing (WGS) in two patients of this cohort, whose clinical manifestations were similar to those of *IL-10RA* mutated patients, especially the increased significantly IL-10 level but whole-exsome sequencing only found heterozygous mutations in *IL-10RA*. However, the results of WGS showed that there was another heterozygous deletion of 333bp in *IL-10RA* which led to exon 1 absence. This result further supported that serum IL-10 level may help distinguish *IL-10RA* mutated patients.

IO-IBD patients, especially those caused by gene mutations, are rare. Although the cohort included in this study was larger than many published studies, the absolute number was not large, which may lead to statistical bias. Besides, we needed further prospective studies to evaluate the diagnostic value of the indicators identified in this study.

CONCLUSION

Children with IO-IBD have a higher proportion of Mendelian diseases. For Chinese Han pediatric patients, *IL-10RA* mutation is the most common pathogenic gene. A complete medical history and clinical evaluation are necessary to differentiate IBD and allergic proctocolitis earlier. Diarrhea frequency, body weight, height, serum albumin, and TNF-α level could help distinguish IO-IBD and allergy. Elevated serum ferritin level could be used for identifying IO-IBD caused by gene mutations, and the remarkably increased serum IL-10 level strongly suggests the presence of *IL-10RA* gene mutation. These clinical characteristics and hematological parameters would help to shorten the time of diagnosis so that the patients are able to receive timely and correct treatment and then reduce social and financial burdens.

ARTICLE HIGHLIGHTS

Research background

Infantile-onset inflammatory bowel disease (IO-IBD) causes severe clinical manifestations and responds poorly to traditional inflammatory bowel disease (IBD)

treatments. At present, there are no simple and reliable laboratory indicators for early screening IO-IBD patients, especially those in whom the disease is caused by monogenic diseases.

Research motivation

Because of an insufficient understanding of IO-IBD, especially that caused by monogenic diseases, most patients could not be diagnosed as early as possible. It is hard to persuade the parents to accept endoscopic examination or genetic diagnosis at initial visits, especially those in areas with limited medical resources.

Research objectives

We intended to search for early diagnostic indicators for IO-IBD children with or without gene mutations, in order to shorten the diagnosis time, reduce medical costs, simplify the analysis of next generation-sequencing, and administer targeted intervention as early as possible.

Research methods

A retrospective analysis was performed in 73 patients with IO-IBD admitted to our hospital in the past 5 years. Based on the next-generation sequencing results, they were divided into either a monogenic IBD group (M-IBD) or non-monogenic IBD group (NM-IBD). Forty age-matched patients with allergic proctocolitis (AP) were included as a control group. The clinical manifestations and the inflammatory factors in peripheral blood were evaluated. Logistic regression analysis and receiver operating characteristic (ROC) curve analysis were performed to find the screening factors and cut-off values of IO-IBD as well as monogenic IO-IBD.

Research results

Among the 44 M-IBD patients, 35 carried *IL-10RA* mutations, and the most common mutations were c.301C>T (p.R101W, 30/70) and c.537G>A (p.T179T, 17/70). Patients with higher serum tumor necrosis factor (TNF)-α value were more likely have IBD [odds ratio (OR) = 1.25, 95% confidence interval (CI): 1.05-1.50, P = 0.013), while higher serum albumin level was associated with lower risk of IBD (OR = 0.86, 95%CI: 0.74-1.00, P = 0.048). The cut-off values of TNF-α and albumin were 17.40 pg/mL (sensitivity: 0.78; specificity: 0.88) and 36.50 g/L (sensitivity: 0.80; specificity: 0.90), respectively. The increased ferritin level was indicative of a genetic mutation in IO-IBD patients. Its cut-off value was 28.20 ng/mL (sensitivity: 0.93; specificity: 0.92). When interleukin (IL)-10 level was higher than 33.05 pg/mL (sensitivity: 1.00; specificity: 0.84), or the onset age was earlier than 0.21 mo (sensitivity: 0.82; specificity: 0.94), the presence of disease-causing mutations in *IL-10RA* in IO-IBD patients was strongly suggested.

Research conclusions

Serum TNF-α and albumin level could differentiate IO-IBD patients from allergic proctocolitis patients, and serum ferritin and IL-10 level are useful indicators for early diagnosing monogenic IO-IBD.

Research perspectives

Using serum TNF-α and albumin level may contribute to distinguishing IO-IBD which needs further investigations, such as gastrointestinal endoscopy. High levels of serum ferritin and IL-10 can infer a monogenic disease in IO-IBD patients, especially the mutations in the *IL-10RA* gene. The diagnostic value of the indicators identified in this study should be evaluated by prospective studies.

ACKNOWLEDGEMENTS

We thank Li J at the Ruijin Hospital for statistics assistance and Chen XY at the Ruijin Hospital for pathological diagnosis.

REFERENCES

1 **Levine A**, Koletzko S, Turner D, Escher JC, Cucchiara S, de Ridder L, Kolho KL, Veres G, Russell RK, Paerregaard A, Buderus S, Greer ML, Dias JA, Veereman-Wauters G, Lionetti P, Sladek M,

Martin de Carpi J, Staiano A, Ruemmele FM, Wilson DC; European Society of Pediatric Gastroenterology; Hepatology; and Nutrition. ESPGHAN revised porto criteria for the diagnosis of inflammatory bowel disease in children and adolescents. *J Pediatr Gastroenterol Nutr* 2014; **58**: 795-806 [PMID: 24231644 DOI: 10.1097/MPG.0000000000000239]

2 **Heyman MB**, Kirschner BS, Gold BD, Ferry G, Baldassano R, Cohen SA, Winter HS, Fain P, King C, Smith T, El-Serag HB. Children with early-onset inflammatory bowel disease (IBD): analysis of a pediatric IBD consortium registry. *J Pediatr* 2005; **146**: 35-40 [PMID: 15644819 DOI: 10.1016/j.jpeds.2004.08.043]

3 **Chandrakasan S**, Venkateswaran S, Kugathasan S. Nonclassic Inflammatory Bowel Disease in Young Infants: Immune Dysregulation, Polyendocrinopathy, Enteropathy, X-Linked Syndrome, and Other Disorders. *Pediatr Clin North Am* 2017; **64**: 139-160 [PMID: 27894441 DOI: 10.1016/j.pcl.2016.08.010]

4 **Pediatircs' Inflammation bowl diesease collaborating group attached to the Chinese society of pediatric gastroenterology of Chinese Medical Association**, Chen J, Xu CD, Huang ZH, Gong ST, Dong YS, Dong M, Sun M, Ye LY, Huang YK, Wang BX, Wang LL, Xu XW, Jiang MZ, Yang WL, Zhu CM, You JY, Wu QB, Jiang LR, Li ZL, Shao CH, Huang Y, Zhang YL, Xu XH, Liu FL, Mang M. Consensus on the Diagnosis and Management of Pediatric Inflammatory Bowel Disease. *Zhongguo Shiyong Erke Zazhi* 2010; **25**: 263-265

5 **Richards S**, Aziz N, Bale S, Bick D, Das S, Gastier-Foster J, Grody WW, Hegde M, Lyon E, Spector E, Voelkerding K, Rehm HL; ACMG Laboratory Quality Assurance Committee. Standards and guidelines for the interpretation of sequence variants: a joint consensus recommendation of the American College of Medical Genetics and Genomics and the Association for Molecular Pathology. *Genet Med* 2015; **17**: 405-424 [PMID: 25741868 DOI: 10.1038/gim.2015.30]

6 **Benchimol EI**, Guttmann A, Griffiths AM, Rabeneck L, Mack DR, Brill H, Howard J, Guan J, To T. Increasing incidence of paediatric inflammatory bowel disease in Ontario, Canada: evidence from health administrative data. *Gut* 2009; **58**: 1490-1497 [PMID: 19651626 DOI: 10.1136/gut.2009.188383]

7 **Benchimol EI**, Mack DR, Nguyen GC, Snapper SB, Li W, Mojaverian N, Quach P, Muise AM. Incidence, outcomes, and health services burden of very early onset inflammatory bowel disease. *Gastroenterology* 2014; **147**: 803-813. quiz e14-5 [PMID: 24951840 DOI: 10.1053/j.gastro.2014.06.023]

8 **Zheng C**, Huang Y, Hu W, Shi J, Ye Z, Qian X, Huang Z, Xue A, Wang Y, Lu J, Tang Z, Wu J, Wang L, Peng K, Zhou Y, Miao S, Sun H. Phenotypic Characterization of Very Early-Onset Inflammatory Bowel Disease with Interleukin-10 Signaling Deficiency: Based on a Large Cohort Study. *Inflamm Bowel Dis* 2019; **25**: 756-766 [PMID: 30212871 DOI: 10.1093/ibd/izy289]

9 **Su W**, Xu CD, Wang XQ, Yu Y, Guo Y, Xu X, Xiao Y. Analysis of clinical phenotype and genotype of 30 Chinese pediatric patients suffering very early onset inflammatory bowel disease. *Zhonghua Yanxingchangbing Zazhi* 2018; **2**: 83-88 [DOI: 10.3760/cma.j.issn.2096-367X.2018.02.003]

10 **Huang Z**, Peng K, Li X, Zhao R, You J, Cheng X, Wang Z, Wang Y, Wu B, Wang H, Zeng H, Yu Z, Zheng C, Wang Y, Huang Y. Mutations in Interleukin-10 Receptor and Clinical Phenotypes in Patients with Very Early Onset Inflammatory Bowel Disease: A Chinese VEO-IBD Collaboration Group Survey. *Inflamm Bowel Dis* 2017; **23**: 578-590 [PMID: 28267044 DOI: 10.1097/MIB.0000000000001058]

11 **Xu YB**, Chen YB, Zeng P, Chen HS, Zeng HS. Interleukin-10 receptor mutations in children with neonatal onset inflammatory bowel disease: genetic diagnosis and pathogenesis. *Zhonghua Erke Zazhi* 2015; **53**: 348-354 [DOI: 10.3760/cma.j.issn.0578-1310.2015.05.007]

12 **Liu LL**, Jiang Y, HOU XL, Tang ZZ, Zhou CL, Sun GW. Clinical characteristics and genetic diagnosis of infantile inflammatory bowel disease within four months after birth: seven case report. *Zhongguo Xunzheng Erke Zazhi* 2016; **11**: 285-289 [DOI: 10.3969/j.issn.1673-5501.2016.04.009]

13 **Xiao Y**, Wang XQ, Yu Y, Guo Y, Xu X, Gong L, Zhou T, Li XQ, Xu CD. Comprehensive mutation screening for 10 genes in Chinese patients suffering very early onset inflammatory bowel disease. *World J Gastroenterol* 2016; **22**: 5578-5588 [PMID: 27350736 DOI: 10.3748/wjg.v22.i24.5578]

14 **Kotlarz D**, Beier R, Murugan D, Diestelhorst J, Jensen O, Boztug K, Pfeifer D, Kreipe H, Pfister ED, Baumann U, Puchalka J, Bohne J, Egritas O, Dalgic B, Kolho KL, Sauerbrey A, Buderus S, Güngör T, Enninger A, Koda YK, Guariso G, Weiss B, Corbacioglu S, Socha P, Uslu N, Metin A, Wahbeh GT, Husain K, Ramadan D, Al-Herz W, Grimbacher B, Sauer M, Sykora KW, Koletzko S, Klein C. Loss of interleukin-10 signaling and infantile inflammatory bowel disease: implications for diagnosis and therapy. *Gastroenterology* 2012; **143**: 347-355 [PMID: 22549091 DOI: 10.1053/j.gastro.2012.04.045]

15 **Kammermeier J**, Dziubak R, Pescarin M, Drury S, Godwin H, Reeve K, Chadokufa S, Huggett B, Sider S, James C, Acton N, Cernat E, Gasparetto M, Noble-Jamieson G, Kiparissi F, Elawad M, Beales PL, Sebire NJ, Gilmour K, Uhlig HH, Bacchelli C, Shah N. Phenotypic and Genotypic Characterisation of Inflammatory Bowel Disease Presenting Before the Age of 2 years. *J Crohns Colitis* 2017; **11**: 60-69 [PMID: 27302973 DOI: 10.1093/ecco-jcc/jjw118]

16 **Yanagi T**, Mizuochi T, Takaki Y, Eda K, Mitsuyama K, Ishimura M, Takada H, Shouval DS, Griffith AE, Snapper SB, Yamashita Y, Yamamoto K. Novel exonic mutation inducing aberrant splicing in the IL10RA gene and resulting in infantile-onset inflammatory bowel disease: a case report. *BMC Gastroenterol* 2016; **16**: 10 [PMID: 26822028 DOI: 10.1186/s12876-016-0424-5]

17 **Oh SH**, Baek J, Liany H, Foo JN, Kim KM, Yang SC, Liu J, Song K. A Synonymous Variant in

IL10RA Affects RNA Splicing in Paediatric Patients with Refractory Inflammatory Bowel Disease. *J Crohns Colitis* 2016; **10**: 1366-1371 [PMID: 27177777 DOI: 10.1093/ecco-jcc/jjw102]

18 **Schäppi MG**, Smith VV, Goldblatt D, Lindley KJ, Milla PJ. Colitis in chronic granulomatous disease. *Arch Dis Child* 2001; **84**: 147-151 [PMID: 11159292 DOI: 10.1136/adc.84.2.147]

19 **Mizukami T**, Obara M, Nishikomori R, Kawai T, Tahara Y, Sameshima N, Marutsuka K, Nakase H, Kimura N, Heike T, Nunoi H. Successful treatment with infliximab for inflammatory colitis in a patient with X-linked anhidrotic ectodermal dysplasia with immunodeficiency. *J Clin Immunol* 2012; **32**: 39-49 [PMID: 21993693 DOI: 10.1007/s10875-011-9600-0]

20 **Orange JS**, Jain A, Ballas ZK, Schneider LC, Geha RS, Bonilla FA. The presentation and natural history of immunodeficiency caused by nuclear factor kappaB essential modulator mutation. *J Allergy Clin Immunol* 2004; **113**: 725-733 [PMID: 15100680 DOI: 10.1016/j.jaci.2004.01.762]

21 **Nunes-Santos CJ**, Uzel G, Rosenzweig SD. PI3K pathway defects leading to immunodeficiency and immune dysregulation. *J Allergy Clin Immunol* 2019; **143**: 1676-1687 [PMID: 31060715 DOI: 10.1016/j.jaci.2019.03.017]

22 **Levy J**, Espanol-Boren T, Thomas C, Fischer A, Tovo P, Bordigoni P, Resnick I, Fasth A, Baer M, Gomez L, Sanders EA, Tabone MD, Plantaz D, Etzioni A, Monafo V, Abinun M, Hammarstrom L, Abrahamsen T, Jones A, Finn A, Klemola T, DeVries E, Sanal O, Peitsch MC, Notarangelo LD. Clinical spectrum of X-linked hyper-IgM syndrome. *J Pediatr* 1997; **131**: 47-54 [PMID: 9255191 DOI: 10.1016/s0022-3476(97)70123-9]

23 **Gerin I**, Veiga-da-Cunha M, Achouri Y, Collet J-F, Van Schaftingen E. Sequence of a putative glucose 6-phosphate translocase, mutated in glycogen storage disease type Ib1. *FEBS Lett* 1997; **419**: 235-238 [DOI: 10.1016/s0014-5793(97)01463-4]

24 **Felgentreff K**, Perez-Becker R, Speckmann C, Schwarz K, Kalwak K, Markelj G, Avcin T, Qasim W, Davies EG, Niehues T, Ehl S. Clinical and immunological manifestations of patients with atypical severe combined immunodeficiency. *Clin Immunol* 2011; **141**: 73-82 [PMID: 21664875 DOI: 10.1016/j.clim.2011.05.007]

25 **Catucci M**, Castiello MC, Pala F, Bosticardo M, Villa A. Autoimmunity in wiskott-Aldrich syndrome: an unsolved enigma. *Front Immunol* 2012; **3**: 209 [PMID: 22826711 DOI: 10.3389/fimmu.2012.00209]

26 **Dorjbal B**, Stinson JR, Ma CA, Weinreich MA, Miraghazadeh B, Hartberger JM, Frey-Jakobs S, Weidinger S, Moebus L, Franke A, Schäffer AA, Bulashevska A, Fuchs S, Ehl S, Limaye S, Arkwright PD, Briggs TA, Langley C, Bethune C, Whyte AF, Alachkar H, Nejentsev S, DiMaggio T, Nelson CG, Stone KD, Nason M, Brittain EH, Oler AJ, Veltri DP, Leahy TR, Conlon N, Poli MC, Borzutzky A, Cohen JI, Davis J, Lambert MP, Romberg N, Sullivan KE, Paris K, Freeman AF, Lucas L, Chandrakasan S, Savic S, Hambleton S, Patel SY, Jordan MB, Theos A, Lebensburger J, Atkinson TP, Torgerson TR, Chinn IK, Milner JD, Grimbacher B, Cook MC, Snow AL. Hypomorphic caspase activation and recruitment domain 11 (CARD11) mutations associated with diverse immunologic phenotypes with or without atopic disease. *J Allergy Clin Immunol* 2019; **143**: 1482-1495 [PMID: 30170123 DOI: 10.1016/j.jaci.2018.08.013]

27 **Kernan KF**, Carcillo JA. Hyperferritinemia and inflammation. *Int Immunol* 2017; **29**: 401-409 [PMID: 28541437 DOI: 10.1093/intimm/dxx031]

28 **Gray CP**, Arosio P, Hersey P. Heavy chain ferritin activates regulatory T cells by induction of changes in dendritic cells. *Blood* 2002; **99**: 3326-3334 [PMID: 11964300 DOI: 10.1182/blood.v99.9.3326]

29 **Carcillo JA**, Sward K, Halstead ES, Telford R, Jimenez-Bacardi A, Shakoory B, Simon D, Hall M; Eunice Kennedy Shriver National Institute of Child Health and Human Development Collaborative Pediatric Critical Care Research Network Investigators. A Systemic Inflammation Mortality Risk Assessment Contingency Table for Severe Sepsis. *Pediatr Crit Care Med* 2017; **18**: 143-150 [PMID: 27941423 DOI: 10.1097/PCC.0000000000001029]

30 **Fautrel B**, Le Moël G, Saint-Marcoux B, Taupin P, Vignes S, Rozenberg S, Koeger AC, Meyer O, Guillevin L, Piette JC, Bourgeois P. Diagnostic value of ferritin and glycosylated ferritin in adult onset Still's disease. *J Rheumatol* 2001; **28**: 322-329 [PMID: 11246670]

31 **Garcia PC**, Longhi F, Branco RG, Piva JP, Lacks D, Tasker RC. Ferritin levels in children with severe sepsis and septic shock. *Acta Paediatr* 2007; **96**: 1829-1831 [PMID: 18001337 DOI: 10.1111/j.1651-2227.2007.00564.x]

32 **Recalcati S**, Invernizzi P, Arosio P, Cairo G. New functions for an iron storage protein: the role of ferritin in immunity and autoimmunity. *J Autoimmun* 2008; **30**: 84-89 [PMID: 18191543 DOI: 10.1016/j.jaut.2007.11.003]

33 **Fargion S**, Fracanzani AL, Brando B, Arosio P, Levi S, Fiorelli G. Specific binding sites for H-ferritin on human lymphocytes: modulation during cellular proliferation and potential implication in cell growth control. *Blood* 1991; **78**: 1056-1061 [PMID: 1831058 DOI: 10.1182/blood.V78.4.1056.bloodjournal7841056]

34 **Broxmeyer HE**, Williams DE, Geissler K, Hangoc G, Cooper S, Bicknell DC, Levi S, Arosio P. Suppressive effects *in vivo* of purified recombinant human H-subunit (acidic) ferritin on murine myelopoiesis. *Blood* 1989; **73**: 74-79 [PMID: 2910370 DOI: 10.1182/blood.V73.1.74.bloodjournal73174]

35 **Yamashita M**, Harada G, Matsumoto SE, Aiba Y, Ichikawa A, Fujiki T, Udono M, Kabayama S, Yoshida T, Zhang P, Fujii H, Shirahata S, Katakura Y. Suppression of immunoglobulin production in human peripheral blood mononuclear cells by monocytes *via* secretion of heavy-chain ferritin.

Immunobiology 2014; **219**: 149-157 [PMID: 24157279 DOI: 10.1016/j.imbio.2013.08.011]

36 **Li R**, Luo C, Mines M, Zhang J, Fan GH. Chemokine CXCL12 induces binding of ferritin heavy chain to the chemokine receptor CXCR4, alters CXCR4 signaling, and induces phosphorylation and nuclear translocation of ferritin heavy chain. *J Biol Chem* 2006; **281**: 37616-37627 [PMID: 17056593 DOI: 10.1074/jbc.M607266200]

37 **Hutchins AP**, Diez D, Miranda-Saavedra D. The IL-10/STAT3-mediated anti-inflammatory response: recent developments and future challenges. *Brief Funct Genomics* 2013; **12**: 489-498 [PMID: 23943603 DOI: 10.1093/bfgp/elt028]

38 **Commins S**, Steinke JW, Borish L. The extended IL-10 superfamily: IL-10, IL-19, IL-20, IL-22, IL-24, IL-26, IL-28, and IL-29. *J Allergy Clin Immunol* 2008; **121**: 1108-1111 [PMID: 18405958 DOI: 10.1016/j.jaci.2008.02.026]

39 **Santaolalla R**, Mañé J, Pedrosa E, Lorén V, Fernández-Bañares F, Mallolas J, Carrasco A, Salas A, Rosinach M, Forné M, Espinós JC, Loras C, Donovan M, Puig P, Mañosa M, Gassull MA, Viver JM, Esteve M. Apoptosis resistance of mucosal lymphocytes and IL-10 deficiency in patients with steroid-refractory Crohn's disease. *Inflamm Bowel Dis* 2011; **17**: 1490-1500 [PMID: 21674705 DOI: 10.1002/ibd.21507]

40 **Glocker EO**, Kotlarz D, Boztug K, Gertz EM, Schäffer AA, Noyan F, Perro M, Diestelhorst J, Allroth A, Murugan D, Hätscher N, Pfeifer D, Sykora KW, Sauer M, Kreipe H, Lacher M, Nustede R, Woellner C, Baumann U, Salzer U, Koletzko S, Shah N, Segal AW, Sauerbrey A, Buderus S, Snapper SB, Grimbacher B, Klein C. Inflammatory bowel disease and mutations affecting the interleukin-10 receptor. *N Engl J Med* 2009; **361**: 2033-2045 [PMID: 19890111 DOI: 10.1056/NEJMoa0907206]

World Journal of Gastroenterology

Submit a Manuscript: https://www.f6publishing.com

World J Gastroenterol 2021 January 7; 27(1): 107-128

DOI: 10.3748/wjg.v27.i1.107

ISSN 1007-9327 (print) ISSN 2219-2840 (online)

ORIGINAL ARTICLE

Randomized Controlled Trial

Effect of probiotic *Lactobacillus plantarum* Dad-13 powder consumption on the gut microbiota and intestinal health of overweight adults

Endang Sutriswati Rahayu, Mariyatun Mariyatun, Nancy Eka Putri Manurung, Pratama Nur Hasan, Phatthanaphong Therdtatha, Riko Mishima, Husnita Komalasari, Nurul Ain Mahfuzah, Fathyah Hanum Pamungkaningtyas, Wahyu Krisna Yoga, Dina Aulia Nurfiana, Stefanie Yolanda Liwan, Mohammad Juffrie, Agung Endro Nugroho, Tyas Utami

ORCID number: Endang Sutriswati Rahayu 0000-0002-6101-3433; Mariyatun Mariyatun 0000-0002-7998-2531; Nancy Eka Putri Manurung 0000-0002-5182-7433; Pratama Nur Hasan 0000-0001-7780-2421; Phatthanaphong Therdtatha 0000-0002-1443-5270; Riko Mishima 0000-0003-0961-1628; Husnita Komalasari 0000-0001-8399-6015; Nurul Ain Mahfuzah 0000-0002-2156-8645; Fathyah Hanum Pamungkaningtyas 0000-0002-2106-0040; Wahyu Krisna Yoga 0000-0002-7350-0589; Dina Aulia Nurfiana 0000-0003-0192-8217; Stefanie Yolanda Liwan 0000-0001-5753-233X; Mohammad Juffrie 0000-0002-2862-3897; Agung Endro Nugroho 0000-0001-7840-8493; Tyas Utami 0000-0003-3600-6060.

Author contributions: Rahayu ES leaded the research project and together with Utami T designed the study; Juffrie M supervised the ethical approval and acted as the consultant for the clinical trial; Nugroho AE supervised the production of probiotic powder; Mariyatun M and Hasan PN supervised the on-site study; Putri Manurung NE, Komalasari H, Yoga WK, Therdtatha P, Mishima

Endang Sutriswati Rahayu, Mariyatun Mariyatun, Nancy Eka Putri Manurung, Pratama Nur Hasan, Husnita Komalasari, Nurul Ain Mahfuzah, Fathyah Hanum Pamungkaningtyas, Wahyu Krisna Yoga, Dina Aulia Nurfiana, Stefanie Yolanda Liwan, Tyas Utami, Department of Food and Agricultural Technology, Faculty of Agricultural Technology, Universitas Gadjah Mada, Yogyakarta 55281, Indonesia

Endang Sutriswati Rahayu, Mariyatun Mariyatun, Nancy Eka Putri Manurung, Pratama Nur Hasan, Fathyah Hanum Pamungkaningtyas, Dina Aulia Nurfiana, Tyas Utami, Center for Food and Nutrition Studies, Universitas Gadjah Mada, Yogyakarta 55281, Indonesia

Phatthanaphong Therdtatha, Riko Mishima, Department of Bioscience and Biotechnology, Faculty of Agriculture, Kyushu University, 774 Motooka, Nishi-ku, Fukuoka, Japan

Mohammad Juffrie, Department of Public Health, Faculty of Medicine, Public Health and Nursery, Universitas Gadjah Mada, Yogyakarta 55281, Indonesia

Agung Endro Nugroho, Department of Pharmacology and Clinical Pharmacy, Faculty of Pharmacy, Universitas Gadjah Mada, Yogyakarta 55281, Indonesia

Corresponding author: Endang Sutriswati Rahayu, Dr, Professor, Department of Food and Agricultural Technology, Faculty of Agricultural Technology, Universitas Gadjah Mada, Jalan Flora No. 1, Bulaksumur, Sleman, Yogyakarta 55281, Yogyakarta, Indonesia.
endangsrahayu@ugm.ac.id

Abstract

BACKGROUND

Shifting on lifestyle, diet, and physical activity contributed on increasing number of obese people around the world. Multiple factors influence the development of obesity. Some research suggested that gut microbiota (GM) plays an important role in nutrient absorption and energy regulation of individuals, thus affecting their nutritional status. Report of Indonesia Basic Health Research showed that the prevalence of obesity in every province tended to increase. Although the root

R performed the work on-site and maintained the coordination with subject as well as conducted sampling; Nurfiana DA, Mahfuzah NA, Liwan SY performed analysis at the laboratory; Mariyatun M and Pamungkaningtyas FH analysed the laboratory data and took part in preparing the manuscript.

Supported by Ristekdikti Kalbe - Science Awards, No. 048/KF-Legal/RKSA/I/2019.

Institutional review board statement: The study was reviewed and approved by the Ethic Comittee Faculty of Medicine Universitas Gadjah Mada, Institutional Review Board, Approval No. KE/1267/11/2018.

Clinical trial registration statement: This study is registered on the Health Research and Development Agency, Ministry of Health of the Republic of Indonesia, registration No. INA-2A8RG4R.

Informed consent statement: All subjects agreed to participate in this study after informed consent and ethical permission was obtained.

Conflict-of-interest statement: The authors declare that they have no conflicts of interest related to this manuscript.

Data sharing statement: No additional data are available.

CONSORT 2010 statement: The authors have read the CONSORT 2010 Statement, and the manuscript was prepared and revised according to the CONSORT 2010 Statement.

cause of obesity is excessive calorie intake compared with expenditure, the differences in gut microbial ecology between healthy and obese humans may affect energy homeostasis. GM affect body weight, especially obesity. Probiotics that are consumed while alive and able to colonize in the intestine are expected to increase the population of good bacteria, especially *Bifidobacteria* and Lactobacilli, and suppress pathogens such as *Enterobacteriaceae* and *Staphylococcus*. The strain of *L. plantarum* Dad-13 has been demonstrated to survive and colonize in the gastrointestinal tract of healthy Indonesian adults who consume fermented milk containing *L. plantarum* Dad-13. The consumption of probiotic *L. plantarum* Dad-13 powder decreased *E. coli* and non-*E. coli* coliform bacteria in school-aged children in Indonesia. *L. plantarum* is a dominant bacterium in the average Indonesian's GM. For this reason, this bacterium is probably a more suitable probiotic for Indonesians.

AIM

To determine the effect of the consumption of indigenous probiotic *Lactobacillus plantarum* Dad-13 powder in overweight adults in Yogyakarta (Indonesia).

METHODS

Sixty overweight volunteers with a body mass index (BMI) equal to or greater than 25 consume indigenous probiotic powder *L. plantarum* Dad-13 (2×10^9 CFU/gram/sachet) for 90 d. The study was a randomized, double-blind, placebo-controlled study. The volunteers filled in a diary on a daily basis, which consisted of questions on study product intake (only during ingestion period), other food intake, number of bowel movements, fecal quality (consistency and color), any medications received, and any symptom of discomfort, such as diarrhea, constipation, vomiting, gassing, sensation of illness, *etc.* Fecal samples and the subjects' diaries were collected on the morning of day 10 + 1, which was marked as the end of the baseline period and the start of the ingestion period. During the ingestion period (from day 11 to day 101), several parameters to measure and analyze the results included body weight and height (once a month), the lipid profile, GM analysis using MiSeq, short-chain fatty acid (SCFA) analysis using gas chromatography, and the measurement of fecal pH using a pH meter.

RESULTS

The consumption of indigenous probiotic powder *L. plantarum* Dad-13 caused the average body weight and BMI of the probiotic group to decrease from 84.54 ± 17.64 kg to 83.14 ± 14.71 kg and 33.10 ± 6.15 kg/m^2 to 32.57 ± 5.01 kg/m^2, respectively. No significant reduction of body weight and BMI in the placebo group was observed. An analysis of the microbiota showed that the number of *Bacteroidetes*, specifically *Prevotella*, increased significantly, while that of *Firmicutes* significantly decreased. No significant change in lipid profile in both groups was found. Also, no significant change in SCFAs (*e.g.*, butyrate, propionate, acetic acid) and pH level was found after the consumption of the probiotic.

CONCLUSION

No significant differences in pH before and after ingestion were observed in both the probiotic and placebo groups as well as in the lipid profile of both cholesterol and triglyceride, high-density lipoprotein (HDL), low-density lipoprotein (LDL), and the LDL/HDL ratio. In addition, no significant changes in the concentration of SCFAs (*e.g.*, acetic acid, propionate, and butyrate) were found after consumption. Interestingly, a significant decrease in body weight and BMI ($P < 0.05$) was determined in the treatment group. An analysis of GM shows that *L. plantarum* Dad-13 caused the *Firmicutes* population to decrease and the *Bacteroidetes* population (especially *Prevotella*) to increase.

Key Words: Obesity; Body mass index; Lipid profile; Gut microbiota; Short chain fatty acid; Probiotic *Lactobacillus plantarum* Dad-13

Manuscript source: Unsolicited manuscript

Specialty type: Gastroenterology and hepatology

Country/Territory of origin: Indonesia

Peer-review report's scientific quality classification

Grade A (Excellent): 0
Grade B (Very good): 0
Grade C (Good): C
Grade D (Fair): 0
Grade E (Poor): 0

Received: November 9, 2020
Peer-review started: November 9, 2020
First decision: November 23, 2020
Revised: December 7, 2020
Accepted: December 16, 2020
Article in press: December 16, 2020
Published online: January 7, 2021

P-Reviewer: Jin X
S-Editor: Huang P
L-Editor: A
P-Editor: Ma YJ

Core Tip: Obesity and overweight are corelated with unhealthy lifestyle that affect the health of intestine and affect the ecosystem of gut microbiota (GM). Consumption of probiotics help to maintain the ecosystem of GM to stay balance and healthy. *L. plantarum* Dad-13 is potential probiotics for Indonesians to maintain health of the gastrointestinal ecosystem. This research was conducted to investigate and determine the effect of consumption of indigenous probiotic *L. plantarum* Dad-13 powder in overweight adults in Yogyakarta (Indonesia). The results show decreasing body mass index and weight on overweight subject and increasing of *Bacteroidetes* specifically *Prevotella*.

Citation: Rahayu ES, Mariyatun M, Putri Manurung NE, Hasan PN, Therdtatha P, Mishima R, Komalasari H, Mahfuzah NA, Pamungkaningtyas FH, Yoga WK, Nurfiana DA, Liwan SY, Juffrie M, Nugroho AE, Utami T. Effect of probiotic *Lactobacillus plantarum* Dad-13 powder consumption on the gut microbiota and intestinal health of overweight adults. *World J Gastroenterol* 2021; 27(1): 107-128
URL: https://www.wjgnet.com/1007-9327/full/v27/i1/107.htm
DOI: https://dx.doi.org/10.3748/wjg.v27.i1.107

INTRODUCTION

Changes in lifestyle, diet, and physical activity have resulted in an exponential increase in the number of obese people around the world. Multiple factors influence the development of this disease, and gut microbiota (GM) have been suggested to play an important role in the nutrient absorption and energy regulation of individuals, thus affecting their nutritional status. Different levels of GM have been observed between individuals with normal nutritional status and those who are obese.

The World Health Organization defines obesity as an accumulation of abnormal or excessive fat that can interfere with health[1]. Body mass index (BMI) is the easiest way to identify whether someone is obese or not, namely, by calculating body weight (kg) divided by height squared (m^2). A person is categorized as overweight if his/her BMI is greater than or equal to 25.0, while an obese person is someone with a BMI greater than or equal to 30.0[2]. A report from Indonesia Basic Health Research showed that the prevalence of obesity in every province tended to increase from 2007 to 2013 to 2018. In addition, it reported that adult women had higher obesity prevalence compared with adult men[3].

Although the root cause of obesity is excessive calorie intake compared with expenditure, the differences in gut microbial ecology between healthy and obese humans may affect energy homeostasis. In other words, individuals predisposed to obesity may have gut microbial communities that promote the more efficient extraction and/or storage of energy from a given diet compared with the communities in lean individuals[4].

GM affect body weight, especially obesity. A study showed that after the GM of fat mice were moved to thin mice, the latter gradually increased in weight and became fat[5]. A link is presumed to exist between GM and body weight. The biomarker of the GM of obesity is high-phylum *Firmicutes* bacteria[6]. Delzenne *et al*[7] found that the number of *Bifidobacteria* in obese individuals is lower than that in normal individuals. Other bacteria that were reported to consistently increase in obese individuals include *Enterobacteriaceae*, *Escherichia coli*, and *Staphylococcus* aureus[7].

Bifidobacteria are known as good bacteria as they produce short-chain fatty acids (SCFAs), such as acetate, propionate, butyrate, and lactate. This metabolite result has important effects on host metabolism. SCFAs can regulate (suppress or activate) the expression of specific genes associated with adiposity and inflammation that somewhat benefits the host. Given this description, we know that the population of *Bifidobacteria* is decreasing and that some pathogen bacteria, such as *Enterobacteriaceae* and *Staphylococcus*, are inclined to increase in obese individuals. Probiotics that are consumed while alive and able to colonize in the intestine are expected to increase the population of good bacteria, especially *Bifidobacteria* and Lactobacilli, and suppress pathogens such as *Enterobacteriaceae* and *Staphylococcus*. Kobyliak *et al*[8] proved that the consumption of probiotics, especially Lactobacilli, for nine weeks could suppress body weight gain and reduce adipose tissue in obese mice.

The probiotic research team of Universitas Gadjah Mada (UGM) came up with an indigenous probiotic from Indonesia that was obtained from various sources, but it has not been thoroughly studied. A study by Rahayu *et al*[9] revealed that the Indonesian indigenous probiotic strains have been molecularly confirmed and could inhibit the growth of pathogenic bacteria. In addition, the indigenous probiotic strains were shown to be resistant to pH 2 and bile salt of 3% concentration. Some probiotic cultures owned by the UGM research team are *Lactobacillus plantarum* Dad-13 (obtained from dadih, fermented buffalo milk), *L. plantarum* Mut-7 and Mut-13 (taken from gatot, fermented cassava), *L. plantarum* T3 (obtained from growol, fermented raw cassava), and *Lactobacillus paracasei* SNP-2 (taken from healthy baby feces).

The strain of *L. plantarum* Dad-13 has been demonstrated to survive and colonize in the gastrointestinal tract of healthy Indonesian adults who consume fermented milk containing *L. plantarum* Dad-13[10]. A safety assessment of *L. plantarum* Dad-13 on Sprague Dawley rats reported no adverse effects in general health, organ weight, leukocyte profiles, GOT activity, MDA concentration, and intestinal morphology after the consumption of the probiotic[11]. The indigenous probiotic *L. plantarum* Dad-13 also did not cause translocation in the organs and blood of the rats[11].

Apart from significantly increasing the population of *L. plantarum* and *Lactobacillus*, the consumption of probiotic *L. plantarum* Dad-13 powder decreased *E. coli* and non–*E. coli* coliform bacteria in school-aged children in Indonesia[12]. *L. plantarum* is a dominant bacterium in the average Indonesian's GM[13]. For this reason, this bacterium is probably a more suitable probiotic for Indonesians. Thus, this study aimed to determine the effect of the consumption of indigenous probiotic *L. plantarum* Dad-13 powder in overweight adults in Yogyakarta (Indonesia).

MATERIALS AND METHODS

Study subjects

This study involved 60 overweight volunteers, consisting of 24 males and 36 females. The age of the subjects ranged between 35 and 56 years old. The inclusion criteria of the subjects covered having a BMI equal to or greater than 25, no history of gastrointestinal disorder (such as constipation, diarrhea, abdominal pain, and irritable bowel syndrome), and no allergies to certain foods. The subjects had not taken antibiotics/antimycotics or any specific drugs and did not consume antidiarrheal or laxative medicine for 100 d during the study.

Ethical approval

This study was conducted in accordance with Good Clinical Practice (GCP) as defined by the International Conference of Harmonization (ICH) and in accordance with the Indonesian National Agency for Drug and Food Control Guidance. Approval by the Ethics Committee of the Faculty of Medicine, Public Health, and Nursing of UGM, Yogyakarta, was received on January 2, 2018, as stated in the committee's letter, with reference number KE/FK/0002/2018.

Study products

The product of this study was 1 g of skimmed milk powder containing the probiotic *L. plantarum* Dad-13 of 2×10^9 CFU in sachet packing. The product was prepared using a halal medium by the Center for Food and Nutrition Studies, UGM. One gram of skimmed milk obtained from a local supermarket was used in the placebo group. The study products were stored in a refrigerator (< 4 °C) before being consumed. *L. plantarum* Dad-13, the indigenous probiotic strain, was deposited in ampoules at the Food and Nutrition Culture Collection (FNCC), Center for Food and Nutrition Studies, UGM. Labelling and product blinding were prepared by the Unit Production of Probiotics and Starter Cultures, Center for Food and Nutrition Studies, UGM.

Materials

DNA fecal extraction was performed using phenol–chloroform extraction. The SsoFast™ Evagreen®Supermix Kit from PT Sciencewerke (Indonesia) was used as a mixture of DNA extracts in super-mix real-time PCR. The primers for qPCR analysis consisted of *Bifidobacteria*[14], the *L. plantarum* subgroup[15], *Clostridium coccoides*[15], and *Enterobacteriaceae*[14]. The main instrument used for GM analysis was real-time PCR. Stool sampling equipment included stool tubes, sterile tissue paper, gloves, masks, ice gel, and cool boxes. DNA extraction equipment included a centrifuge, a vortex,

analytical scales, and other kinds of glassware. The equipment for the probiotic powder included freeze dryers and vacuum sealing.

Study design

The study was a randomized, placebo-controlled study; 60 volunteers were divided into an intervention group (probiotic) and a control group (placebo). All the subjects and the researcher were blinded to the treatment administrated (double-blind study). This study used simple randomization, performed in such a way that leaves no significant difference between the study groups (BMI, age, or sex). The placebo product used was skimmed milk without probiotics. The study consisted of 10 d without the consumption of the study product (baseline period) followed by 90 d of ingestion, as shown in Figure 1. During the baseline period, the volunteers consumed their normal dietaries with the exception of probiotic products. The baseline period was a "washout" period to eliminate the effect of previously used probiotics. The volunteers filled in a diary on a daily basis, which consisted of questions on study product intake (only during the ingestion period), other food intake, number of bowel movements, fecal quality (consistency and color), any medications received, and any symptom of discomfort, such as diarrhea, constipation, vomiting, gassing, sensation of illness, *etc*. Fecal samples and the subjects' diaries were collected on the morning of day 10 ± 1, which was marked as the end of the baseline period and the start of the ingestion period. During the ingestion period (from day 11 to day 101), the volunteers consumed one sachet of the study product per day after having lunch for 90 consecutive days. The volunteers were not allowed to consume any other probiotic products. They were requested to fill in a new diary on a daily basis. Upon the completion of the ingestion period, on the morning of day 100 ± 1, fecal samples and the subjects' diaries were collected.

Fecal collection

A fecal sample was collected into a sterile tube with a kind of scoop built into the inside of the lid by the subjects at home, and the sample was immediately transported to the laboratory in a cold storage container (< 10 °C). Two tubes were used to collect the samples, containing buffer/stabilizer RNA later and glass beads, one tube for GM analysis and the other for SCFA analysis. The materials and instructions for fecal sample collection were provided to the subjects prior to the fecal collection schedule. The subjects were instructed to defecate on the trail paper (smooth side up) and were prevented from wetting the fecal paper with urine or water. Then they were required to immediately take a sample by scraping the feces with the scooper and capping the tube tightly.

Analysis

Several parameters to measure and analyze the results included: (1) The measurement of body weight and height once a month; (2) The lipid profile; (3) GM analysis; (4) SCFA analysis using gas chromatography; and (5) The measurement of fecal pH using a pH meter.

GM analysis using next-genome sequencing - MiSeq

A high-throughput analysis of 16 rRNA gene sequences was carried out according to the previous method. Areas V3-V4 of the sequences from the bacteria were amplified with the fecal DNA genome (approximately 1 ng) using TaKaRa Ex TaqTM HS (Takara Bio, Japan) and universal primer Bakt_341F (5'-CGCTCTTCCGATCTCTG CCTACGGGGGGGCWGCAG-355)GGCTATICCCACCATTCCCCATTCCACCA CCACCACCACCACCACCACCACCA UTAA. The amplification results were used as a template for the second PCR using barcode-tag primers. The second PCR results were purified using the FastGene Gel/PCR Extraction Kit (NIPPON Genetics, Japan) according to company protocol. The purified products were quantified using the PicoGreen® dsDNA Assay Kit (Life Technologies, United States) based on company protocol. All the PCR samples were of the same total amount (approximately 200 ng total), and they were purified using electrophoresis in 2% (w/v) agarose gel (classic-type Agarose-LE: Nacalai Tesque, Japan), followed by extraction from the gel by the FastGene Gel/PCR Extraction Kit. The purified mixture was applied to the final-pair sequence of Illumina MiSeq v3 (Illumina, United States).

Statistical analysis

The data was displayed as mean ± standard deviation unless stated otherwise. IBM Statistic SPSS 20.0 with a 95% confidence interval (a = 5%) was used to perform

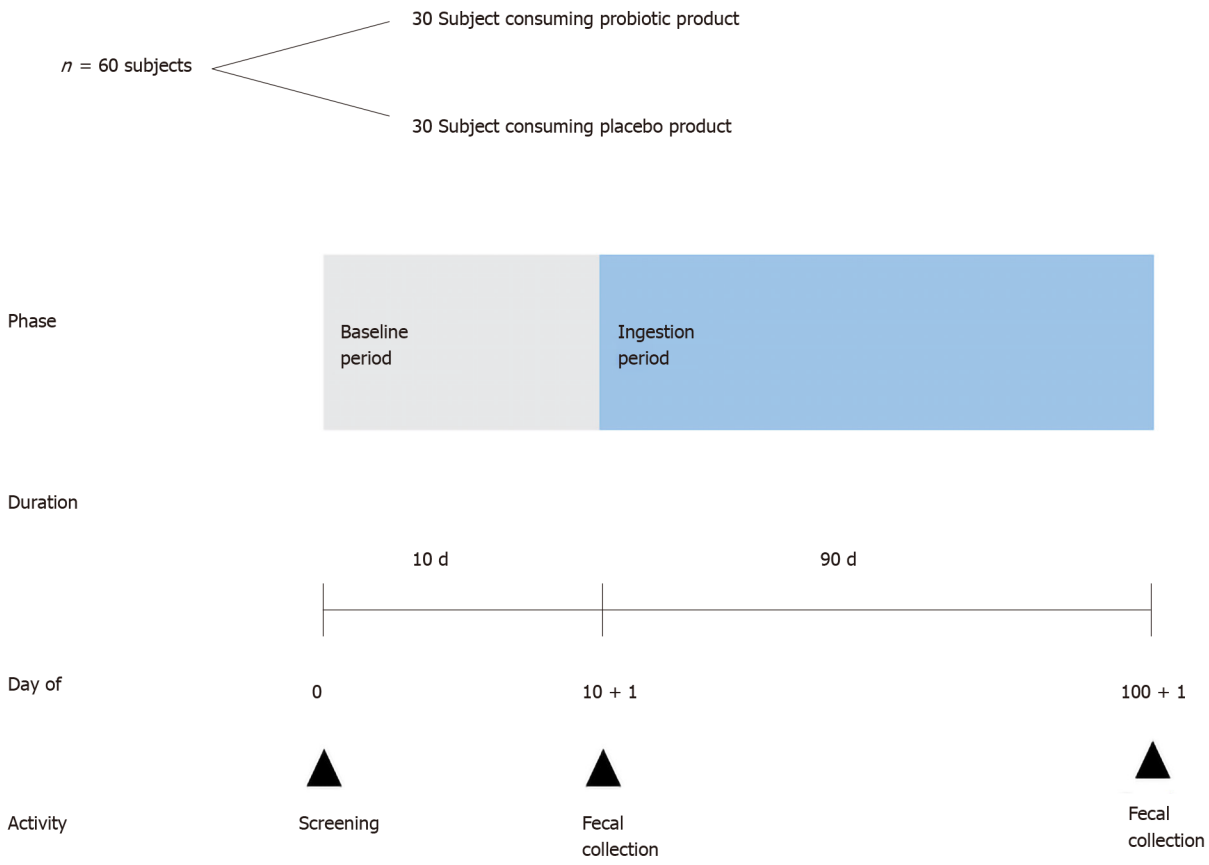

Figure 1 Study design.

statistical analysis. A chi-square test or independent *t*-test or Wilcoxon test was carried out to evaluate the significant differences of the observed parameters between the probiotic-treated group and the placebo group depending on the normality and equality of variance of the data. In addition, a paired *t*-test was used to analyze the observed parameters before and after the consumption of the indigenous probiotic powder or placebo powder.

RESULTS

Demographic data of study subjects

Sixty overweight subjects who participated in the research signed informed consent forms. The subjects were divided into two groups, namely, the probiotic-treated group and the placebo group. Neither the researcher nor the participants knew which subject entered the probiotic group or the placebo group. The research began on January 5, 2019. Fifteen days were allotted for the prescreening period, and the baseline period started on January 21-30, 2019, the intervention period started on January 31 and ended on April 30, 2019. The research ended when all the subjects finished giving their fecal samples to the researcher. The demographic data of the subjects showed no significant differences in age, height, weight, and BMI, and the number of female participants was higher than that of male participants (Table 1).

Body weight, height, and BMI

The body weight, height, and BMI of the subjects were measured every 10 d. Table 2 presents a significant decrease ($P < 0.05$) in the body weight and BMI of the subjects after 90 d of probiotic ingestion. Table 3 further shows the different effects of consuming probiotics between the female and male subjects.

Some studies also reported that probiotics could reduce body weight. Kadooka *et al*[16] found that the probiotic *Lactobacillus gasseri* SBT2055 (LG2055) caused abdominal adiposity, body weight, and other measures to decrease, suggesting its

Table 1 Demographic data of study subjects

	Probiotic-treated group (*n* = 30)	Placebo group (*n* = 30)	*P* value
Age (yr)	44.07 ± 6.23	44.67 ± 5.66	0.42[1]
Height (cm)	159.66 ± 8.27	157.92 ± 9.58	0.40[1]
Weight (kg)	83.45 ± 14.61	79.58 ± 11.79	0.21[1]
BMI (kg/m^2)	32.69 ± 5.07	31.88 ± 3.77	0.18[1]
Women, *n* (%)	18 (60)	18 (60)	0.00[2]
Men, *n* (%)	12 (40)	12 (40)	0.00[2]

[1]Independent sample *t*-test.
[2]Chi-square. BMI: Body mass index.

Table 2 Changes of body weight, height, and body mass index

	Group	Baseline period	Ingestion period	*P* value
Weight	Probiotic-treated	84.54 ± 17.62	83.14 ± 14.71	0.04[2a]
	Placebo	79.37 ± 11.76	78.80 ± 11.77	0.12[1]
Height	Probiotic-treated	159.66 ± 8.27	159.66 ± 8.27	1.00[2]
	Placebo	157.92 ± 9.58	157.92 ± 9.58	1.00[2]
BMI	Probiotic-treated	33.10 ± 6.15	32.57 ± 5.01	0.04[2a]
	Placebo	31.80 ± 3.71	31.56 ± 3.67	0.18[1]

[1]Independent sample *t*-test.
[2]Wilcoxon signed-rank test. A significantly different ([a]$P < 0.05$). BMI: Body mass index.

beneficial influence on metabolic disorders. According to Higashikawa *et al*[17], the heat-killed *Pediococcus pentosaceus* LP28 displayed an anti-obesity effect that reduced BMI, body fat, and waist circumference. Another study revealed that the mean of weight loss in female subjects consuming *Lactobacillus rhamnosus* CGMCC1.3724 (LPR) supplementation was significantly higher than that in women who belonged to the placebo group after the first 12 wk. The body weight and fat mass of the male subjects were not affected by the treatment[18].

Lipid profile

The lipid profile showed that in both groups, there was no significant difference in each parameter measured after consuming the study product. The results of the lipid profile are shown in Table 4.

Fecal characteristics and defecation frequency

Fecal characteristics indicate intestinal conditions in humans. These characteristics include volume, type, color, odor, and pH. The fecal volume of 1 is equal to the volume of a chicken egg. The color is indicated in four scales (1: yellow; 2: brownish yellow; 3: brown; 4: green). The Bristol stool chart was used to identify the type of feces. The aroma of the feces was expressed using a three-point scale (1: normal; 2: strong; 3: very strong). Table 5 shows the fecal characteristics and defecation frequency.

Table 5 indicates that in both the probiotic-treated group and the placebo group, the volume, type, color, odor, and pH of the feces during the baseline and ingestion periods were not significantly changed. The defecation frequency was expressed as the total number or frequency of defecation in 10 d. Overall, the fecal samples from both groups had the following characteristics: Banana-like shape, brownish yellow color, normal odor, and pH of 5.58-5.76.

SCFA

An analysis of SCFAs was performed using gas chromatography. The SCFAs analyzed

Table 3 Different changes of body weight, height, and body mass index in female and male subjects

Gender		Group	Baseline period	Ingestion period	*P* value
Women	Weight	Probiotic-treated	77.91 ± 14.16	77.08 ± 13.68	0.01[1a]
		Placebo	73.20 ± 9.93	72.69 ± 9.93	0.33[1]
	Height	Probiotic-treated	153.82 ± 4.05	153.82 ± 4.05	1.00[2]
		Placebo	151.42 ± 5.92	151.42 ± 5.92	1.00[2]
	BMI	Probiotic-treated	32.90 ± 5.73	32.58 ± 5.58	0.02[1a]
		Placebo	31.96 ± 4.25	31.72 ± 4.14	0.31[1]
Men	Weight	Probiotic-treated	94.48 ± 18.11	92.22 ± 11.45	0.38[1]
		Placebo	88.63 ± 7.51	87.97 ± 7.77	0.16[1]
	Height	Probiotic-treated	168.42 ± 3.92	168.42 ± 3.92	1.00[2]
		Placebo	167.67 ± 3.87	167.67 ± 3.87	1.00[2]
	BMI	Probiotic-treated	33.39 ± 6.98	32.54 ± 4.25	0.37[1]
		Placebo	31.56 ± 2.87	31.32 ± 2.96	0.15[1]

[1]Independent sample *t*-test.
[2]Wilcoxon signed-rank test. A significantly different ([a]$P < 0.05$). BMI: Body mass index.

Table 4 Lipid profile

Lipid profile	Group	Baseline period	Ingestion period	*P* value
Cholesterol (mg/dL)	Probiotic-treated	194.93 ± 37.64	192.20 ± 36.55	0.46[2]
	Placebo	193.70 ± 29.47	192.37 ± 29.75	0.41[2]
Triglyceride (mg/dL)	Probiotic-treated	151.50 ± 63.92	166.83 ± 75.02	0.16[2]
	Placebo	191.40 ± 133.60	187.73 ± 111.58	0.54[2]
HDL (mg/dL)	Probiotic-treated	40.33 ± 9.77	40.00 ± 9.28	0.69[1]
	Placebo	39.93 ± 7.29	40.60 ± 8.18	0.39[1]
LDL (mg/dL)	Probiotic-treated	141.43 ± 32.17	136.97 ± 33.12	0.18[2]
	Placebo	134.50 ± 24.84	133.50 ± 27.06	0.71[1]
Ratio of LDL/HDL	Probiotic-treated	3.63 ± 0.95	3.55 ± 0.87	0.38[1]
	Placebo	3.44 ± 0.70	3.39 ± 0.84	0.61[1]

[1]Paired *t*-test.
[2]Wilcoxon signed-rank test. A significantly different ($P < 0.05$). LDL: Low-density lipoprotein; HDL: High-density lipoprotein.

in this study included acetic acid, propionate, and butyrate. Table 6 shows the SCFA concentration of the probiotic-treated and placebo groups. It also shows that the SCFAs did not significantly change ($P > 0.05$) in both groups after the ingestion period. The SCFAs function *via* diverse host molecular mechanisms to regulate host energy intake, energy expenditure, and storage[19]. The production of SCFAs by bacteria that ferment carbohydrates contribute 10% of the total energy to be absorbed in the colon, and the rest would be lost through the feces[20]. One study proved that the administration of *L. salivarius* Ls-33 to obese adolescent subjects did not have a significant effect[21]. Likewise, the administration of *L. plantarum* Dad-13 in this study did not affect the SCFA concentration of the overweight subjects. The pH value in the treatment group was 5.72 ± 0.31 before ingestion and 5.76 ± 0.28 after ingestion. The pH value in the placebo group was 5.58 ± 0.40 before ingestion and 5.75 ± 0.34 after ingestion. This insignificant change of fecal pH was attributed to insignificant SCFA concentration, so the intestines' condition did not change.

Table 5 Fecal characteristic (volume, type, color, odor, pH) and defecation frequency

	Group	Baseline period	Ingestion period	*P* value
Volume	Probiotic-treated	2.20 ± 0.79	2.23 ± 0.96	0.86[1]
	Placebo	2.37 ± 0.95	2.29 ± 0.90	0.23[2]
Type	Probiotic-treated	3.59 ± 0.93	3.22 ± 1.17	0.08[1]
	Placebo	4.02 ± 1.14	3.89 ± 0.93	0.34[2]
Color	Probiotic-treated	1.86 ± 0.57	1.73 ± 0.55	0.20[1]
	Placebo	2.00 ± 0.59	1.95 ± 0.54	0.70[1]
Odor	Probiotic-treated	1.11 ± 0.37	1.10 ± 0.28	0.93[2]
	Placebo	1.26 ± 0.35	1.32 ± 0.41	0.57[2]
pH	Probiotic-treated	5.72 ± 0.31	5.76 ± 0.28	0.51[3]
	Placebo	5.58 ± 0.40	5.75 ± 0.34	0.07[3]
Defecation frequency[4]	Probiotic-treated	12.93 ± 3.61	13.40 ± 4.52	0.58[2]
	Placebo	14.67 ± 4.93	15.70 ± 7.57	0.51[2]

[1]Independent sample *t*-test.
[2]Wilcoxon signed-rank test.
[3]Paired *t*-test.
[4]Every 10 d.

Table 6 Short-chain fatty acid (acetic acid, propionic acid, and butyrate acid) of feces

	Group	Baseline period	Ingestion period	*P* value[a]
Acetic acid (mmol/kg)	Probiotic-treated	63.19 ± 34.97	64.76 ± 17.61	0.89
	Placebo	67.09 ± 19.56	63.76 ± 13.05	0.65
Propionic acid (mmol/kg)	Probiotic-treated	22.02 ± 14.17	20.65 ± 9.76	0.67
	Placebo	21.98 ± 10.44	17.16 ± 2.04	0.17
Butyrate acid (mmol/kg)	Probiotic-treated	14.78 ± 6.68	14.97 ± 7.24	0.95
	Placebo	19.45 ± 8.60	15.59 ± 9.40[a]	0.33

[a]Paired *t*-test with significance level of 5%.

Diet profile

Diet or food intake is associated with obesity. This study also recorded the daily diet of the subjects. The dietary records were analyzed using the NutriSurvey 2007 software. The household size based on the standard issued by the Republic of Indonesia Ministry of Health in 2014 was used to measure the amount of food intake. Table 7 below summarizes the diet profile of the subjects.

Based on the analysis of the dietary patterns of the subjects, the standard deviation was high, which indicates that the nutrient intake of the subjects was very diverse. Compared to the intake during the baseline period, both the probiotic-treated group and the placebo group consumed less energy, protein, lipid, carbohydrate, and PUFA sources in the last month of the ingestion period. In addition, the average daily energy intake of the subjects was around 1518.17-1642.88 kcal/d, less than that of a normal adult (around 2000 kcal/d)[22]. The consumption of dietary fiber sources experienced a gradual drop from day 41 to the end of the study period. Meanwhile, no significant differences were observed in the intake of cholesterol between the baseline period and the end of the ingestion period in both the probiotic-treated group and the placebo group.

Table 7 Diet profile of subjects

	Group	Baseline period	Ingestion day 11-20	Ingestion day 21-30	Ingestion day 31-40	Ingestion day 41-60	Ingestion day 61-80	Ingestion day 81-100
Energy (kcal)	Probiotic-treated	1518.17 ± 484.46	1322.04 ± 431.90	1338.23 ± 376.17	1274.13 ± 390.37	1124.89 ± 378.82[a]	1060.65 ± 286.86[a]	1103.54 ± 311.74[a]
	Placebo	1642.88 ± 599.33	1660.02 ± 611.62	1562.79 ± 1144.53	1396.65 ± 476.01[a]	1085.16 ± 346.08[a]	1047.90 ± 313.37[a]	1105.73 ± 313.58[a]
Water (g)	Probiotic-treated	744.06 ± 526.92	633.17 ± 397.27	593.60 ± 377.72	691.70 ± 470.44	720.66 ± 551.62	656.24 ± 419.94	712.81 ± 438.11
	Placebo	1122.19 ± 615.82	1016.66 ± 665.44	1041.80 ± 568.23	1100.16 ± 601.35	688.97 ± 533.39[a]	813.86 ± 565.46	841.27 ± 595.64
Protein (g)	Probiotic-treated	52.72 ± 19.49	44.69 ± 16.73	46.23 ± 14.61	46.81 ± 12.61	38.49 ± 14.10[a]	38.30 ± 10.23[a]	39.62 ± 11.30[a]
	Placebo	53.92 ± 24.02	55.03 ± 25.52	47.12 ± 33.52	47.02 ± 18.70	38.38 ± 12.95[a]	35.67 ± 10.98[a]	39.09 ± 9.72[a]
Lipid (g)	Probiotic-treated	61.41 ± 30.24	47.15 ± 26.32	47.60 ± 21.41	49.86 ± 19.25	40.78±15.24[a]	39.63 ± 12.02[a]	40.78 ± 12.99[a]
	Placebo	64.15 ± 34.36	63.17 ± 38.78	54.22 ± 36.98	52.15 ± 25.09[a]	36.99 ± 13.85[a]	36.88 ± 12.74[a]	37.68 ± 9.70[a]
Carbo-hydrate (g)	Probiotic-treated	190.85 ± 68.00	179.93 ± 57.44	180.95 ± 65.23	160.50 ± 59.23	150.80 ± 56.88	137.97 ± 43.53[a]	144.63 ± 46.33[a]
	Placebo	216.39 ± 88.21	221.71 ± 83.07	224.10 ± 190.74	186.27 ± 71.98	149.82 ± 48.91[a]	144.70 ± 49.45[a]	153.74 ± 60.37[a]
Fiber (g)	Probiotic-treated	10.96 ± 5.88	8.66 ± 3.04	8.71 ± 2.91	8.49 ± 2.63	7.08 ± 2.16[a]	6.24 ± 2.01[a]	6.61 ± 2.48[a]
	Placebo	12.17 ± 7.15	13.34 ± 9.00	11.90 ± 8.61	10.20 ± 4.67	6.96 ± 2.99[a]	7.17 ± 2.30[a]	7.45 ± 2.30[a]
PUFA (g)	Probiotic-treated	16.87 ± 13.02	12.80 ± 7.73	12.17 ± 5.87	13.03 ± 7.64	12.17 ± 7.36	10.91 ± 4.50	10.86 ± 4.31
	Placebo	18.20 ± 13.73	18.49 ± 15.71	15.70 ± 13.47	16.29 ± 13.52	10.50 ± 5.94[a]	10.03 ± 4.70[a]	9.73 ± 3.1[a]
Choles-terol (mg)	Probiotic-treated	191.39 ± 163.58	163.28 ± 83.55	168.44 ± 92.31	182.29 ± 68.95	160.32 ± 84.56	172.70 ± 77.78	179.23 ± 57.13
	Placebo	170.42 ± 154.32	168.91 ± 169.50	142.45 ± 159.96	164.19 ± 124.86	173.22 ± 86.80	165.31 ± 85.03	182.64 ± 81.91

[a]$P < 0.05$ based on Independent sample *t*-test compared to the nutrient intake in baseline. PUFA: Polyunsaturated fatty acid.

Population of GM in overweight subjects

Based on the results of the 16 RNA sequences using MiSeq performed in both the probiotic-treated and placebo groups, the bacterial group was dominated by the phyla *Firmicutes*, *Bacteroidetes*, *Actinobacteria*, *Proteobacteria*, *Fusobacteria*, and *Verrucomicrobia* (Figure 2). A small portion of the phyla *Cyanobacteria*, *Lentisphaerae*, *Elusimicrobia*, and *Synergistetes* appeared in both the treatment and control groups (Table 8).

The phylum distribution composition of each subject from both the treatment and control groups can be seen in Figure 3. Three genera - *Firmicutes*, *Bacteroidetes*, and *Actinobacteria* - are the most dominant genera appearing on almost all the subjects, while some phyla, such as *Proteobacteria* and *Fusobacteria*, appear dominantly in only a few subjects.

Concerning the two dominant phyla, the number of *Bacteroidetes* significantly increased ($P < 0.05$) in both the treatment and placebo groups after the ingestion period (Table 9), and the number of *Firmicutes* significantly decreased ($P < 0.05$) in the treatment group (Figure 4). Meanwhile, the *Fusobacteria* population was only found in a few subjects. The *Verrucomicrobia* population significantly decreased in both the treatment and placebo groups after the ingestion period. *Verrucomicrobia* was often associated with gastrointestinal health and glucose homeostasis. No significant changes ($P > 0.05$) were found in the phyla of *Cyanobacteria*, *Elusimicrobia*, *Lentisphaerae*, and *Synergistetes* in the treatment and placebo groups before and after the ingestion period. The changes in phylum of bacterial composition in both the probiotic-treated and placebo groups before and after the ingestion period are presented in Figure 4.

At the genus level (as shown in Table 8), some microbiota showed some changes in

Table 8 Gut microbiota composition based on genus

Phylum	Genus	Probiotic-treated			Placebo		
		Baseline, mean (%) ± SD	Ingestion, mean (%) ± SD	*P* value	Baseline, mean (%) ± SD	Ingestion, mean (%) ± SD	*P* value
Firmicutes	*Faecalibacterium*	11.43 ± 5.03	10.94 ± 4.21	0.614	15.30 ± 7.07	11.82 ± 5.50	0.01[a]
	Coprococcus	7.53 ± 3.55	6.23 ± 1.85	0.037[a]	7.34 ± 3.71	5.82 ± 2.67	0.116
	Other	7.63 ± 5.05	8.22 ± 4.15	0.491	6.03 ± 4.13	8.40 ± 4.56	0.012[a]
	Ruminococcus	4.49 ± 4.06	3.69 ± 2.90	0.271	3.80 ± 3.84	3.70 ± 4.79	0.572
	Roseburia	1.36 ± 1.31	1.54 ± 1.10	0.072[b]	1.49 ± 1.55	2.04 ± 1.28	0.037[a]
	Clostridium	0.16 ± 0.22	0.16 ± 0.27	0.829	0.25 ± 0.53	0.35 ± 0.49	0.202
	Paenibacillus	0.01 ± 0.01	0.00 ± 0.01	0.1	0.03 ± 0.06	0.00 ± 0.01	0.002[a]
Bacteroidetes	*Prevotella*	14.56 ± 11.57	19.25 ± 13.03	0.066[b]	14.15 ± 13.69	14.28 ± 14.13	0.75
	Bacteroides	3.78 ± 5.43	5.57 ± 8.21	0.019[a]	5.59 ± 9.97	10.30 ± 13.83	0.04[a]
Actino-bacteria	*Bifidobacterium*	3.38 ± 4.96	2.74 ± 4.01	0.6	3.07 ± 3.95	2.71 ± 2.91	0.957
	Collinsella	2.02 ± 1.40	1.52 ± 0.94	0.069[b]	2.00 ± 1.80	1.51 ± 0.98	0.271
	Brevibacterium	0.01 ± 0.01	0.00 ± 0.01	0.307	0.03 ± 0.07	0.01 ± 0.02	0.082[b]
Proteo-bacteria	*Succinivibrio*	2.19 ± 4.51	1.44 ± 3.37	0.548	2.06 ± 5.29	2.51 ± 6.89	0.534
	Phyllobacterium	0.02 ± 0.04	0.02 ± 0.02	0.037[a]	0.01 ± 0.03	0.01 ± 0.03	0.167
	Sphingomonas	0.02 ± 0.03	0.02 ± 0.02	0.75	0.01 ± 0.03	0.01 ± 0.03	0.833
Verrucomicrobia	*Akkermansia*	0.13 ± 0.56	0.04 ± 0.18	0.028[a]	0.35 ± 1.64	0.02 ± 0.07	0.024[a]

[a]Paired *t*-test with significance level of 5% ($P < 0.05$).
[b]Significance level 10% ($P < 0.1$).

composition. However, not all genera of the whole phylum experienced some changes. In the phylum *Firmicutes*, *Faecalibacterium* was quite significant in the placebo group compared with the treatment group ($P < 0.05$). One species of *Faecalibacterium* that is quite abundant in the human digestive tract is *Faecalibacterium prausnitzii*. *Faecalibacterium* is a fairly dominant digestive microbiota, as indicated by the fact that 5%-15% of total bacteria are *F. prausnitzii* species[23]. *F. prausnitzii* is also considered one of the health indicators of gastrointestinal health. Healthy subjects normally showed an abundance of *F. prausnitzii* compared with subjects with Crohn's disease[24]. The genus *Coprococcus* showed a significant decrease in the treatment group ($P < 0.05$). *Coprococcus* is characterized as comprising anaerobic microbes able to produce butyrate acid. Countless studies have associated *Coprococcus* with the health conditions of the human digestive tract. One study showed that its healthy subjects had a high abundance of *Coprococcus* compared with subjects with colorectal cancer[25]. Other studies showed that the number of *Bacteroides* and *Coprococcus* in subjects with colorectal pre-cancerous conditions was much lower than that in healthy subjects[26]. Body conditions in humans, such as obesity or being overweight, can also affect the conditions of microbiota. The populations of *Blautia*, *Coprococcus*, and *Enterobacteriaceae* were quite high in overweight children in Mexico compared with those with normal conditions[27].

Table 8 shows that *Roseburia* significantly increased in both the treatment ($P < -0.01$) and placebo groups ($P < 0.05$). *Roseburia* is a microbiota of the genus *Firmicutes* that has the characteristics of gram-positive, obligate anaerobes and can produce the SCFA butyrate. In the human digestive tract, one of the species of *Roseburia* - namely, *Roseburia hominis* - can regulate immunity[28]. An increase in the population of *Roseburia* can also be attributed to the type of food consumed. The consumption of resistant starch is said to increase *Eubacterium rectale* and *Roseburia*[29]. The *Roseburia* population in humans is quite varied. A study of groups of obese and overweight children showed a fairly high *Roseburia* population compared with the normal group[27].

The *Paenibacillus* genus, as shown in Table 8, decreased in both groups, but only the placebo control group experienced a significant decrease. The genus *Clostridium* did not significantly change in both groups, but the placebo group experienced a slight

Table 9 Composition of gut microbiota (based on the most abundant in phylum population) in the probiotic-treated and placebo groups before and after ingestion period

No.	Phylum	Group	Baseline period	Ingestion period	*P* value[a]
1	*Firmicutes*	Probiotic-treated	69.90 ± 15.95	64.13 ± 15.22	0.037[a]
		Placebo	70.66 ± 14.41	65.30 ± 14.52	0.153
2	*Bacteroidetes*	Probiotic-treated	20.63 ± 11.49	28.27 ± 14.26	0.008[a]
		Placebo	21.30 ± 12.72	26.71 ± 13.93	0.045[a]
3	*Actinobacteria*	Probiotic-treated	6.11 ± 5.37	5.07 ± 5.48	0.237
		Placebo	5.55 ± 4.90	4.63 ± 3.61	0.453
4	*Proteobacteria*	Probiotic-treated	2.87 ± 6.39	2.04 ± 6.05	0.491
		Placebo	1.84 ± 4.32	1.69 ± 3.77	0.572
5	*Fusobacteria*	Probiotic-treated	0.23 ± 0.57	0.34 ± 0.86	0.701
		Placebo	0.20 ± 0.94	1.58 ± 6.57	0.044[a]
6	*Verrucomicrobia*	Probiotic-treated	0.13 ± 0.57	0.04 ± 1.66	0.028[a]
		Placebo	0.35 ± 0.19	0.02 ± 0.07	0.024[a]
7	*Cyanobacteria*	Probiotic-treated	0.09 ± 0.29	0.07 ± 0.21	0.537
		Placebo	0.06 ± 0.24	0.04 ± 0.10	0.427
8	*Lentisphaerae*	Probiotic-treated	0.02 ± 0.05	0.01 ± 0.08	0.681
		Placebo	0.03 ± 0.02	0.03 ± 0.11	0.334
9	*Elusimicrobia*	Probiotic-treated	0.00 ± 0.01	0.00 ± 0.03	0.655
		Placebo	0.01 ± 0.02	0.00 ± 0.00	0.317
10	*Synergistetes*	Probiotic-treated	0.00 ± 0.00	0.00 ± 0.00	0.655
		Placebo	0.00 ± 0.00	0.00 ± 0.01	0.273

[a]Paired *t*-test with significance level of 5%.

increase in abundance. The genus *Ruminococcus* decreased significantly in the probiotic-treated group.

The *Coprococcus* genus experienced a significant decrease in the treatment group after consumption, inversely proportional to the genus *Roseburia*, which experienced a significant increase in the treatment group after consumption. *Roseburia* also experienced a significant increase in the control group after the ingestion period. The genera *Faecalibacterium* and *Paenibacillus* experienced a decrease in the placebo group after the ingestion period. No significant differences were observed in the genera *Clostridium* and *Ruminococcus* in both the treatment and placebo groups after the ingestion period.

The second dominant phylum (Table 9) is *Bacteroidetes*, which increased in the treatment group. The genus *Bacteroides* significantly increased in both the probiotic-treated and placebo groups ($P < 0.05$). However, the genus *Prevotella* significantly increased ($P < 0.1$) in the probiotic-treated group. Previous papers mentioned that *Prevotella* is the dominant genus in the phylum *Bacteroidetes* for healthy school-aged children (Murugesan *et al*[27] 2015) and adult Indonesians (Rahayu *et al*[13] 2019). In this study, the population of *Prevotella* is much higher than that of *Bacteroides*. This finding supports previous reports stating that Indonesians have the *Prevotella* enterotype.

The relative abundance of the phylum *Actinobacteria* - namely, the genera Brevibacterium, *Bifidobacteria*, and *Collinsella* - is shown in Table 8. *Brevibacterium* in the treatment group significantly decreased after the ingestion period and showed a significant decrease in the genus *Collinsella* in the treatment group ($P < 0.1$) compared with the placebo group. *Collinsella* is a microbiota of the phylum *Actinobacteria*. These microbiota were often said to be pathobionts, which have the potential to influence the nature of the pathogen to its host[30]. Subjects with obesity and having type 2 diabetes are said to have a high abundance of *Collinsella* compared with healthy people[31].

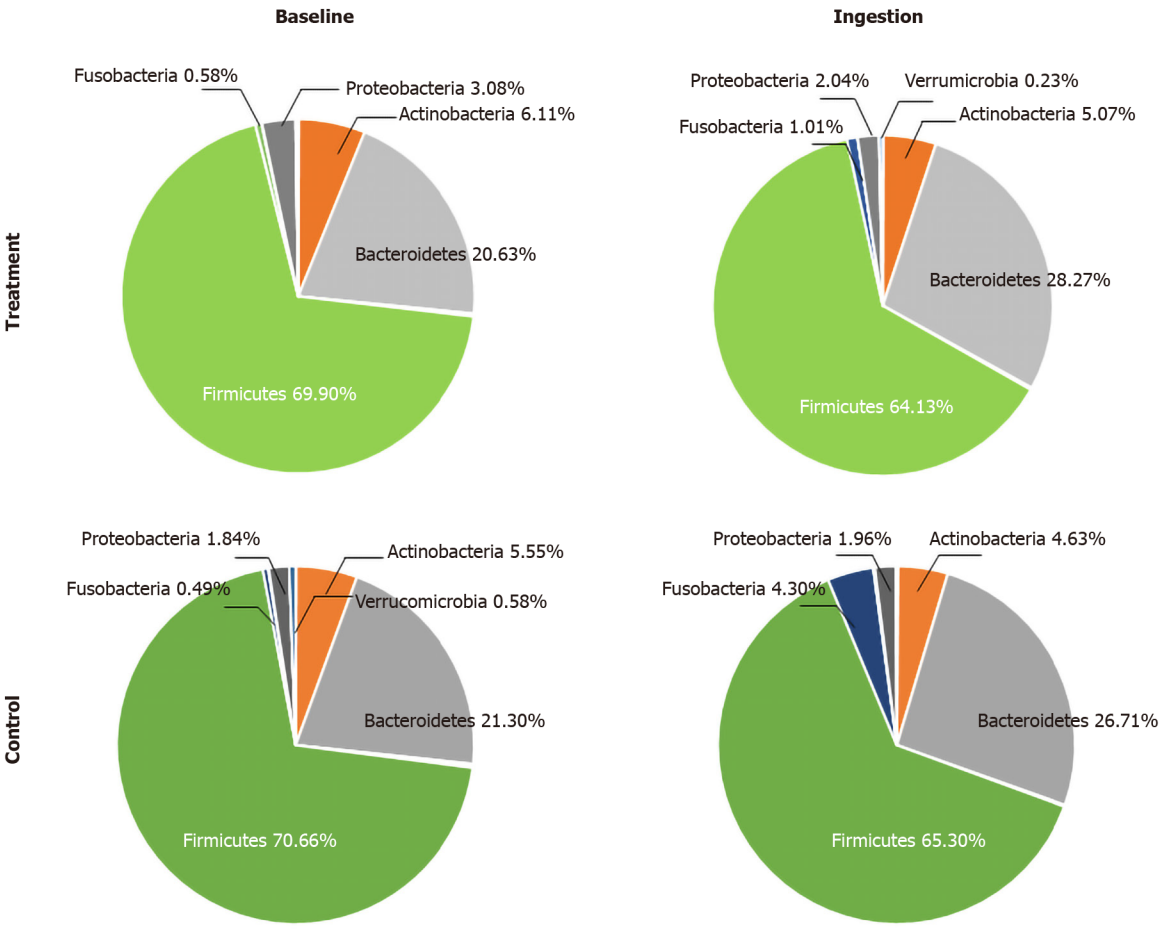

Figure 2 The composition of gut microbiota [relative abundance (%) in the probiotic-treated and placebo groups before and after ingestion period].

Table 8 shows that the genus Phyllobacterium of the phylum *Proteobacteria* increased significantly in the treatment group, while no significant change in the genera *Succinivibrio* and *Sphingomonas* was found in both the treatment and placebo groups. Meanwhile, the abundance of the genus *Akkermansia* in the phylum *Verrucomicrobia* decreased significantly.

From the analyses using LeSfe with a *P* value of < 0.05 (LDA > 2.0), one against all showed a significant difference in bacterial abundance in the probiotic-treated and placebo groups before and after the ingestion period. Alpha diversity analysis (Figure 5) showed that the abundance of bacteria in the probiotic-treated group significantly increased after they consumed the probiotic powder. This indicates that the consumption of probiotics could increase the abundance of bacteria in obese people, who have a diversity and wealth of microbiota gut components compared with eutrophic subjects[32]. At the genus level, a significant increase was observed in the abundance of the genus Phyllobacterium in the probiotic-treated group after consumption, whereas in the control group, *Roseburia* abundance increased significantly after consumption. The Brevibacterium, *Paenibacillus*, *Bacillales*, and *Faecalibacterium* groups were abundant in the placebo group before the consumption of the placebo product.

DISCUSSION

Ley *et al*[33] authored one of the first studies linking GM to obesity in humans[4]. The results from the 16 rRNA gene sequences in mouse models indicated that the two most abundant bacterial phyla were *Firmicutes* (60%-80%) and *Bacteroidetes* (20%-40%). In particular, the *ob*/*ob* mice had a 50% decrease in the population of *Bacteroidetes* and a proportional increase in *Firmicutes*. These changes indicate that obesity affects the diversity of GM and suggest that the intentional manipulation of the community

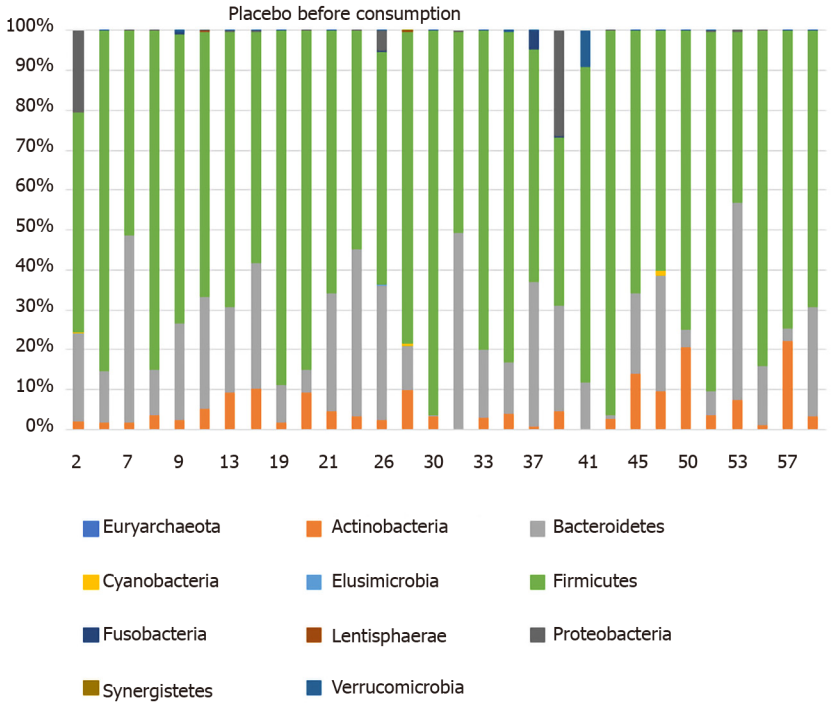
Placebo before consumption
100%
90%
80%
70%
60%
50%
40%
30%
20%
10%
0%
2 7 9 13 19 21 26 30 33 37 41 45 50 53 57
Euryarchaeota
Actinobacteria
Bacteroidetes
Cyanobacteria
Elusimicrobia
Firmicutes
Fusobacteria
Lentisphaerae
Proteobacteria
Synergistetes
Verrucomicrobia

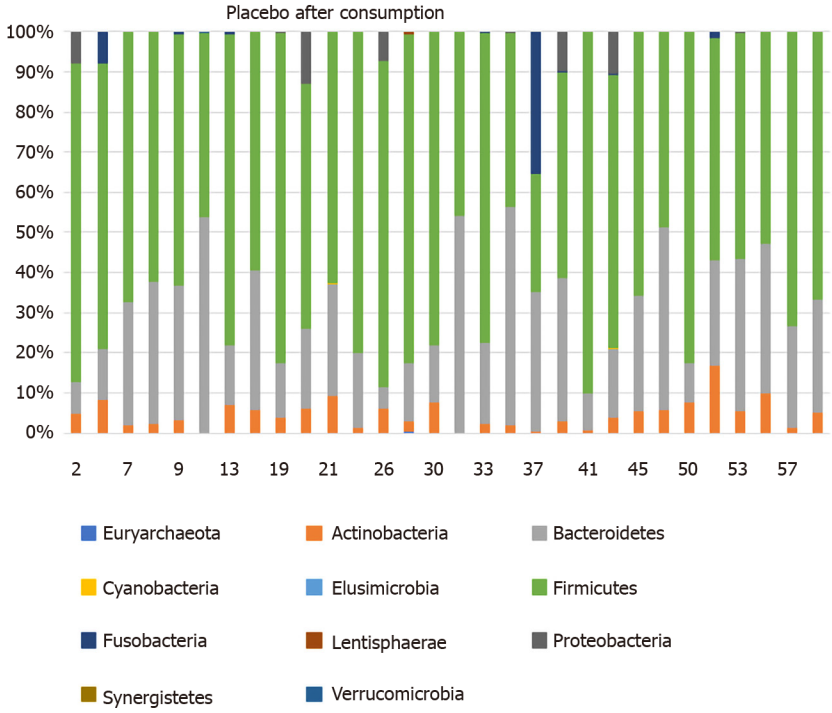
Placebo after consumption
100%
90%
80%
70%
60%
50%
40%
30%
20%
10%
0%
2 7 9 13 19 21 26 30 33 37 41 45 50 53 57
Euryarchaeota
Actinobacteria
Bacteroidetes
Cyanobacteria
Elusimicrobia
Firmicutes
Fusobacteria
Lentisphaerae
Proteobacteria
Synergistetes
Verrucomicrobia

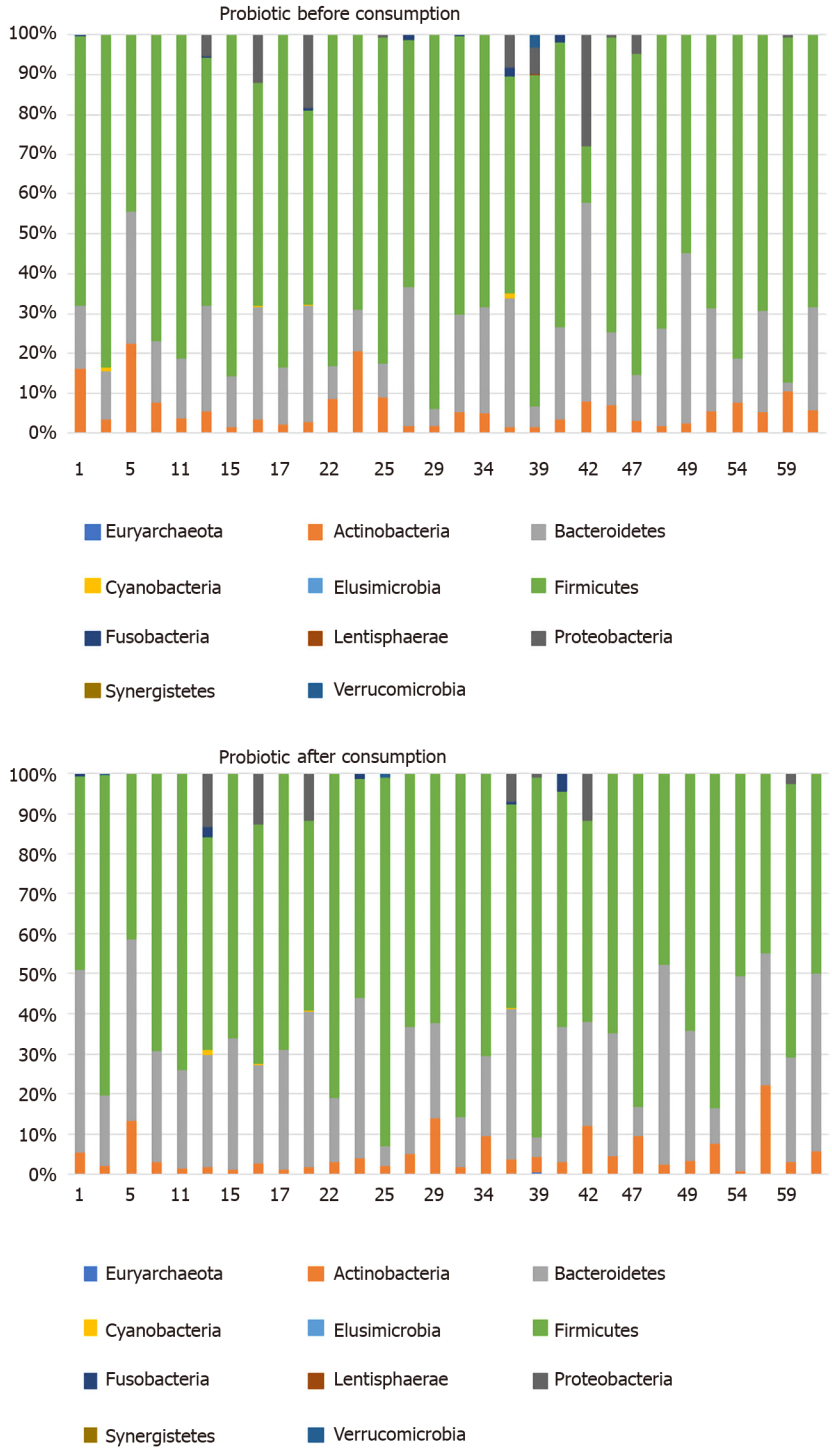

Figure 3 The phylum distribution composition of each subject from both probiotic-treated and placebo groups. The number on the X-axis represents the code of subject.

structure may be useful to regulate the energy balance in the obese individual[4,33]. Meanwhile, Turnbaugh *et al*[34] and Furet *et al*[35] found a lower representation of *Bacteroidetes* (*Bacteroides*/*Prevotella*) in obese individuals, with no differences in the *Firmicutes phylum*.

In addition, an ongoing review of GM and obesity found evidence of the association between gut bacteria and obesity[36,37]. Normally, the subclass distributions of GM are composed of the following: *Bacteroidetes* (23%), comprising the genus *Bacteroides*; *Firmicutes* (64%), including *Bacilli*, *Clostridia*, and *Mollicutes*; *Proteobacteria* (8%), gram-negative bacteria, such as *E. coli* and *Helicobacter pylori*; *Fusobacteria*, *Verrucomicrobia*, and *Actinobacteria* (3%), which include species such as *Bifidobacteria*; and only about 2% of other phyla. Our findings also indicate that an obese person has a different microbial proportion of the dominant phyla, which consists of the higher *Firmicutes* of

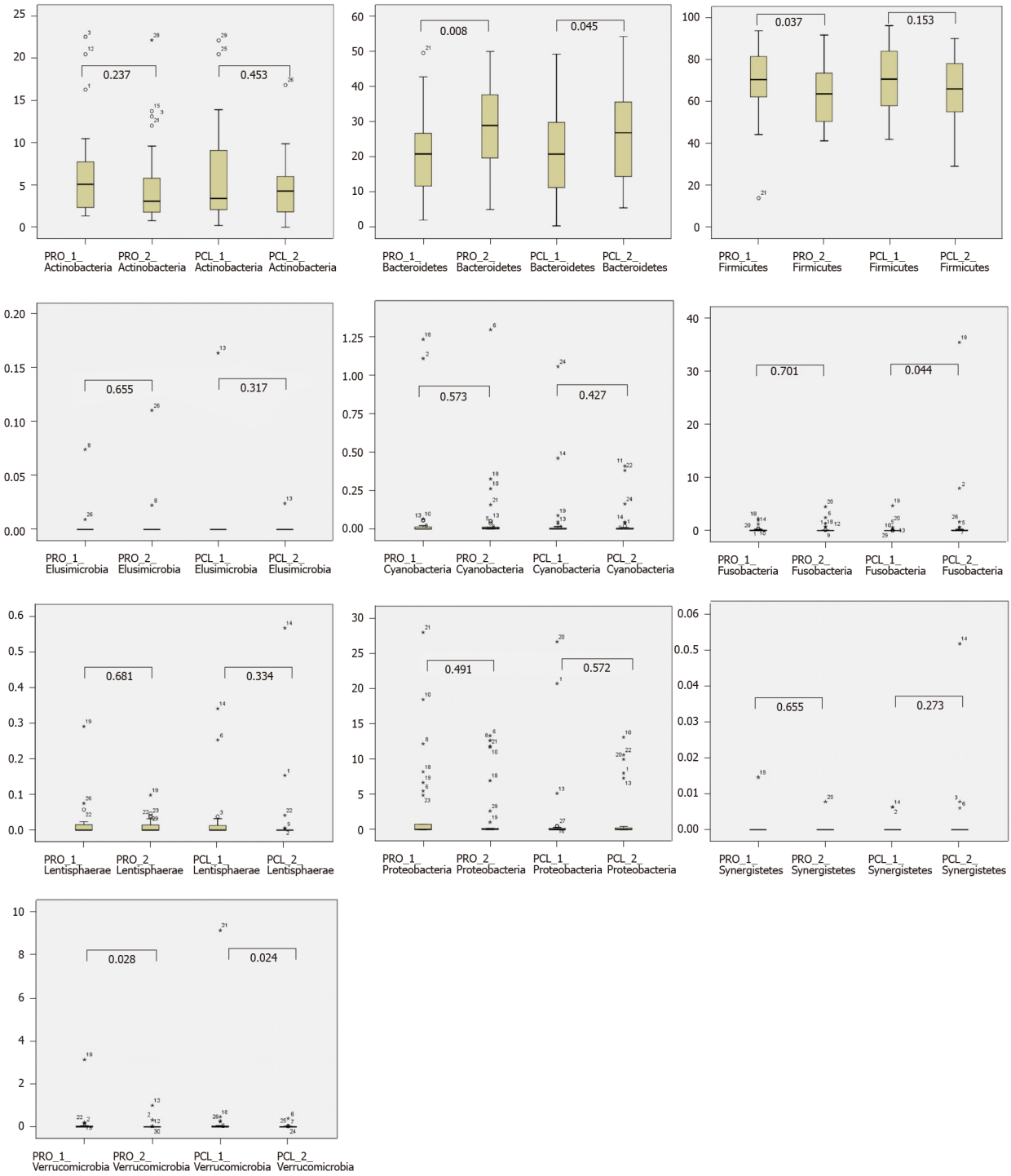

Figure 4 The changes in phylum of bacterial composition in both probiotic-treated and placebo groups before and after ingestion period.
PRO1: Probiotic before ingestion; PRO2: Probiotic after ingestion; PLC1: Placebo before ingestion; PLC2: Placebo after ingestion.

about 70% and the lower *Bacteroidetes* of about 21%, compared with a normal person, as mentioned in another study by Abenavoli *et al*[37]. The other phyla comprise *Actinobacteria* at about 6%, *Proteobacteria* at 3%, and less than 1% of other bacteria, such as *Fusobacteria*, *Verrucomicrobia*, *Cyanobacteria*, and *Lentisphaerae*.

Jumpertz *et al*[38] investigated the dynamic changes of GM during diets that varied in caloric content in the feces of lean and obese individuals by measuring ingested and stool calories using bomb calorimetry. The alteration of the nutrient load induced rapid changes in the GM. These changes were directly correlated with stool energy loss in lean individuals, such as a 20% increase in *Firmicutes* and a corresponding decrease in *Bacteroidetes*, which were associated with an increased energy harvest. A high degree of overfeeding in lean individuals was accompanied by a greater fractional decrease in stool energy loss. These results show that the nutrient load is a

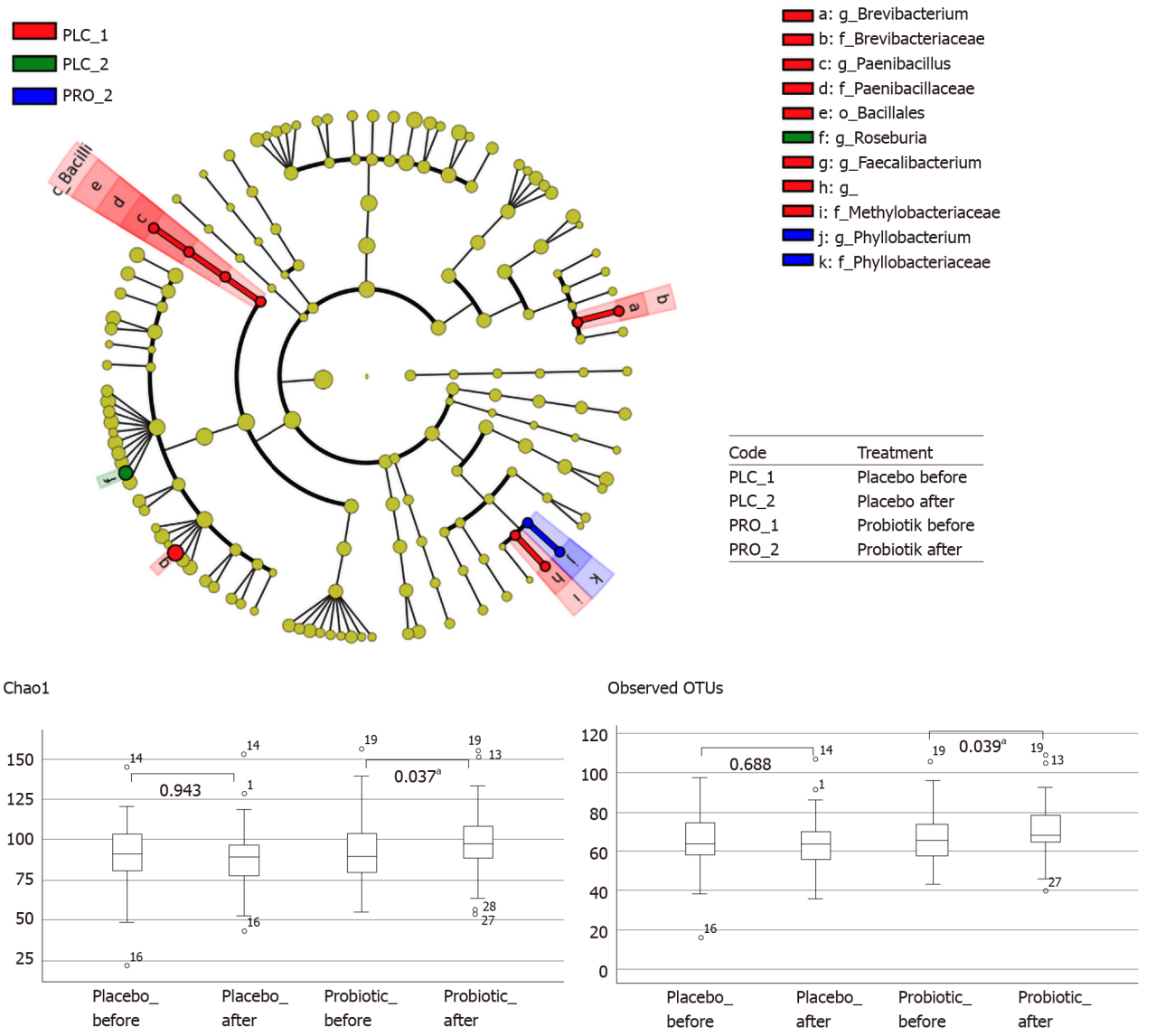

Figure 5 Cladogram and Alpha diversity on the treatment group and placebo group before and after the ingestion period. PRO1: Probiotic before ingestion; PRO2: Probiotic after ingestion; PLC1: Placebo before ingestion; PLC2: Placebo after ingestion.

key variable that can influence the gut (fecal) bacterial community structure over short periods. Furthermore, the observed associations between gut microbes and nutrient absorption indicate a possible role of the human GM in the regulation of the nutrient harvest. Recent studies have shown that the increase of bile acids in the intestine when comparing sterile rats with normal rats would show that the GM are related to not only obesity but also a diverse range of metabolic diseases[39].

Several mechanisms have been proposed for GM causative action in obesity physiopathology. In fact, gut commensal bacteria interact with our metabolism at several points. They help convert ingested complex nutrients to SCFAs, transform mucins and dietary fibers into simple sugars ready for absorption, stimulate intestinal epithelial proliferation, and favor nutrient absorption and metabolism. They are the main actor in shaping the gut crucial defense barrier constituted by the systemic and mucosal immune system and activate bio-inactive compounds[40]. Nevertheless, GM play an important role in human adipose tissue formation and deposition. Indeed, our intestinal bacteria can maintain the human body's energy balance mainly because of their ability to share the otherwise indigestible components of a mammalian's diet[41]. In this study, the average daily energy intake of the subjects was around 1518.17-1642.88 kcal/d, less than that of a normal adult (around 2000 kcal/d). No significant differences were observed in the diet profile of the subjects in both the probiotic-treated and placebo groups.

Abenavoli *et al*[37] mentioned in their review that evidence of the association between gut bacteria and obesity exists in both infants and adults. Several genetic, metabolic,

and inflammatory pathophysiological mechanisms are involved in the interplay between gut microbes and obesity. Microbial changes in the human gut can be considered a factor in obesity development in humans. The modulation of the bacterial strains in the digestive tract can help reshape the metabolic profile in the human obese host, as suggested by data from several animal and human studies. Several reports have also been conducted on the probiotic treatment of obese individuals. In adults, different strains of *Lactobacillus* and *Bifidobacterium*, alone or in combination, as well as *P. pentosaceus* led to a significant reduction of body weight, BMI, waist circumference, and fat mass[17,42-46].

As the administered dosage of probiotics affects the efficacy of the treatment, reduced visceral adiposity and waist circumference were observed after exposure to a high dose of *L. gasseri* BNR17[44]. These results were not so unambiguous given the different doses of Ecologic® (a mixture of multi-strains of *Lactobacillus* and *Bifidobacterium*), although this study was only conducted on obese women[47]. Interestingly, a report by Sanchez *et al*[48] showed the gender-specific effects of probiotics in human obese subjects. Indeed, the administration of *L. rhamnosus* CGMCC1.3724 and a restricted caloric diet resulted in significantly higher weight loss in obese women than in men. This finding can be explained by a greater impact on satiety, eating habits, and mood in women *vs* men[48]. Finally, scant evidence exists on the potential preventive effect on obesity of some probiotics in non-obese subjects. Specifically, VSL#3 can reduce body weight and fat accumulation *via L. gasseri* SBT2055 administration[16,49].

CONCLUSION

No significant differences in pH were found before and after ingestion in both the probiotic and placebo groups as well as in the lipid profile of both cholesterol and triglyceride, high-density lipoprotein (HDL), low-density lipoprotein (LDL), and the LDL/HDL ratio. In addition, no significant changes in the concentration of SCFAs (acetic acid, propionate, and butyrate) were observed after the consumption of the probiotic powder *L. plantarum* Dad-13.

An interesting finding is a significant decrease in body weight and BMI ($P < 0.05$) in the treatment group. This weight loss was particularly observed in the female subjects. GM analysis shows that *L. plantarum* Dad-13 was able to decrease *Firmicutes* and increase *Bacteroidetes* (especially *Prevotella*).

ARTICLE HIGHLIGHTS

Research background

Gut microbiota (GM) play an important role in the nutrient absorption and energy regulation of individuals, thus affecting their nutritional status. GM also affect body weight, especially obesity, a condition wherein the accumulation of abnormal or excessive fat can interfere with health. Obesity in Indonesia showed an increasing prevalence in every province from 2007 to 2018. One study found a link between GM and body weight. Probiotics, as healthy bacteria, can improve an individual's health status by affecting GM composition. The consumption of probiotics may maintain this status and reduce the weight gain of adults with obesity in Indonesia.

Research motivation

This research aimed to investigate the effect of the consumption of an indigenous probiotic on overweight people. The results obtained may be used to determine the condition of GM in overweight people and the effect of indigenous probiotics on the GM of overweight adults. These results may also be used to determine the treatment of probiotic consumption that is most suitable and effective for overweight individuals in Indonesia to improve their health status.

Research objectives

The objective of this study was to determine the effect of the consumption of the indigenous probiotic powder *L. plantarum* Dad-13 on overweight adults in Indonesia.

Research methods

Sixty overweight volunteers with body mass index (BMI) equal to or greater than 25 consumed indigenous probiotic powder *L. plantarum* Dad-13 (2×10^9 CFU/gram/sachet) for 90 d. The study was a randomized, double-blind, placebo-controlled study. The volunteers filled in a diary on a daily basis, which consisted of questions on study product intake (only during the ingestion period), other food intake, number of bowel movements, fecal quality (consistency and color), any medications received, and any symptom of discomfort, such as diarrhea, constipation, vomiting, gassing, sensation of illness, *etc*. Fecal samples and the subjects' diaries were collected on the morning of day 10 + 1, marked as the end of the baseline period and the start of the ingestion period. During the ingestion period (from day 11 to day 101), several parameters to measure and analyze the results included body weight and height (once a month), the lipid profile, GM analysis using MiSeq, short-chain fatty acid (SCFA) analysis using gas chromatography, and the measurement of fecal pH using a pH meter.

Research results

The consumption of indigenous probiotic powder *L. plantarum* Dad-13 by overweight people caused the average body weight and BMI of the probiotic group to decrease from 84.54 ± 17.64 kg to 83.14 ± 14.71 kg and from 33.10 ± 6.15 kg/m^2 to 32.57 ± 5.01 kg/m^2, respectively. No significant reduction in the body weight and BMI of the placebo group was found. An analysis of the microbiota showed that the number of *Bacteroidetes*, specifically *Prevotella*, increased significantly, while *Firmicutes* significantly decreased. No significant change in lipid profile was observed in both groups. Also, no significant change in SCFAs (butyrate, propionate, acetic acid) and pH level were found after the consumption of the probiotic.

Research conclusions

No significant differences in pH were found before and after ingestion in both the probiotic and placebo groups as well as in the lipid profile of both cholesterol and triglyceride, high-density lipoprotein (HDL), low-density lipoprotein (LDL), and the LDL/HDL ratio. In addition, no significant changes were observed in the concentration of SCFAs (acetic acid, propionate, and butyrate) after consumption. Interestingly, a significant decrease in body weight and BMI ($P < 0.05$) was found in the treatment group. An analysis of the GM shows that *L. plantarum* Dad-13 was able to decrease *Firmicutes* and increase *Bacteroidetes* (especially *Prevotella*).

Research perspectives

These results proved that the consumption of probiotics among overweight adults helps significantly reduce body weight, especially in women, and affects the composition of GM.

ACKNOWLEDGEMENTS

The researchers would like to sincerely thank the Indonesian Ministry of Research and Higher Education and Kalbe PT for providing support, as well as the study subjects for their participation.

REFERENCES

1 **World Health Organization**. What is malnutrition? [Internet]. 2020. Available from: https://www.who.int/features/qa/malnutrition/en/
2 **World Health Organization**. Obesity and overweight [Internet]. 2020. Available from: https://www.who.int/news-room/fact-sheets/detail/obesity-and-overweight
3 **Ministry of Health of the Republic of Indonesia**. Report of Indonesia Basic Health Research in 2018. 2018. Available from: https://www.litbang.kemkes.go.id/Laporan-riset-kesehatan-dasar-riskesdas/
4 **Ley RE**, Bäckhed F, Turnbaugh P, Lozupone CA, Knight RD, Gordon JI. Obesity alters gut microbial ecology. *Proc Natl Acad Sci USA* 2005; **102**: 11070-11075 [PMID: 16033867 DOI: 10.1073/pnas.0504978102]
5 **Turnbaugh PJ**, Bäckhed F, Fulton L, Gordon JI. Diet-induced obesity is linked to marked but reversible alterations in the mouse distal gut microbiome. *Cell Host Microbe* 2008; **3**: 213-223

[PMID: 18407065 DOI: 10.1016/j.chom.2008.02.015]
6 **De Filippo C**, Cavalieri D, Di Paola M, Ramazzotti M, Poullet JB, Massart S, Collini S, Pieraccini G, Lionetti P. Impact of diet in shaping gut microbiota revealed by a comparative study in children from Europe and rural Africa. *Proc Natl Acad Sci USA* 2010; **107**: 14691-14696 [PMID: 20679230 DOI: 10.1073/pnas.1005963107]
7 **Delzenne NM**, Cani PD. Interaction between obesity and the gut microbiota: relevance in nutrition. *Annu Rev Nutr* 2011; **31**: 15-31 [PMID: 21568707 DOI: 10.1146/annurev-nutr-072610-145146]
8 **Kobyliak N**, Conte C, Cammarota G, Haley AP, Styriak I, Gaspar L, Fusek J, Rodrigo L, Kruzliak P. Probiotics in prevention and treatment of obesity: a critical view. *Nutr Metab (Lond)* 2016; **13**: 14 [PMID: 26900391 DOI: 10.1186/s12986-016-0067-0]
9 **Rahayu ES**, Yogeswara A, Mariyatun, Windiarti L, Utami T, Watanabe K. Molecular characteristics of indigenous probiotic strains from Indonesia. *Int J Probiotics Prebiotics* 2016; **11**: 109-116
10 **Rahayu ES**, Cahyanto M, Windiarti L, Sutriyanto J, Kandarina T, Utami T. Effects of Consumption of Fermented Milk Containing Indigenous Probiotic Lactobacillus Plantarum Dad-13 on the Fecal Microbiota of Healthy Indonesian Volunteers. *Int J Probiotics Prebiotics* 2016; **11**: 91-98
11 **Rahayu ES**, Rusdan IH, Athennia A, Kamil RZ, Pramesi PC, Marsono Y, Utami T, Widada J. Safety Assessment of Indigenous Probiotic Strain Lactobacillus plantarum Dad-13 Isolated from Dadih Using Sprague Dawley Rats as a Model. *Am J Pharmacol Toxicol* 2019; **1**: 38-47 [DOI: 10.3844/ajptsp.2019.38.47]
12 **Maghfirotin Marta B**, Tyas U, Muhammad Nur C, Jaka W, Endang Sutriswati R. Effects of Consumption of Probiotic Powder Containing Lactobacillus Plantarum Dad-13 on Fecal Bacterial Population in School-Age Children in Indonesia. *Int J Probiotics Prebiotics* 2019; **14**: 1-8 [DOI: 10.37290/ijpp2641-7197.14:1-8]
13 **Rahayu ES**, Utami T, Mariyatun M, Hasan PN, Kamil RZ, Setyawan RH, Pamungkaningtyas FH, Harahap IA, Wiryohanjoyo DV, Pramesi PC, Cahyanto MN, Sujaya IN, Juffrie M. Gut microbiota profile in healthy Indonesians. *World J Gastroenterol* 2019; **25**: 1478-1491 [PMID: 30948911 DOI: 10.3748/wjg.v25.i12.1478]
14 **Matsuki T**, Watanabe K, Fujimoto J, Kado Y, Takada T, Matsumoto K, Tanaka R. Quantitative PCR with 16S rRNA-gene-targeted species-specific primers for analysis of human intestinal bifidobacteria. *Appl Environ Microbiol* 2004; **70**: 167-173 [PMID: 14711639 DOI: 10.1128/AEM.70.1.167-173.2004]
15 **Matsuda K**, Tsuji H, Asahara T, Matsumoto K, Takada T, Nomoto K. Establishment of an analytical system for the human fecal microbiota, based on reverse transcription-quantitative PCR targeting of multicopy rRNA molecules. *Appl Environ Microbiol* 2009; **75**: 1961-1969 [PMID: 19201979 DOI: 10.1128/AEM.01843-08]
16 **Kadooka Y**, Sato M, Imaizumi K, Ogawa A, Ikuyama K, Akai Y, Okano M, Kagoshima M, Tsuchida T. Regulation of abdominal adiposity by probiotics (Lactobacillus gasseri SBT2055) in adults with obese tendencies in a randomized controlled trial. *Eur J Clin Nutr* 2010; **64**: 636-643 [PMID: 20216555 DOI: 10.1038/ejcn.2010.19]
17 **Higashikawa F**, Noda M, Awaya T, Danshiitsoodol N, Matoba Y, Kumagai T, Sugiyama M. Antiobesity effect of Pediococcus pentosaceus LP28 on overweight subjects: a randomized, double-blind, placebo-controlled clinical trial. *Eur J Clin Nutr* 2016; **70**: 582-587 [PMID: 26956126 DOI: 10.1038/ejcn.2016.17]
18 **Sanchez M**, Darimont C, Drapeau V, Emady-Azar S, Lepage M, Rezzonico E, Ngom-Bru C, Berger B, Philippe L, Ammon-Zuffrey C, Leone P, Chevrier G, St-Amand E, Marette A, Doré J, Tremblay A. Effect of Lactobacillus rhamnosus CGMCC1.3724 supplementation on weight loss and maintenance in obese men and women. *Br J Nutr* 2014; **111**: 1507-1519 [PMID: 24299712 DOI: 10.1017/S0007114513003875]
19 **Shen J**, Obin MS, Zhao L. The gut microbiota, obesity and insulin resistance. *Mol Aspects Med* 2013; **34**: 39-58 [PMID: 23159341 DOI: 10.1016/j.mam.2012.11.001]
20 **Flint HJ**, Scott KP, Duncan SH, Louis P, Forano E. Microbial degradation of complex carbohydrates in the gut. *Gut Microbes* 2012; **3**: 289-306 [PMID: 22572875 DOI: 10.4161/gmic.19897]
21 **Larsen N**, Vogensen FK, Gøbel RJ, Michaelsen KF, Forssten SD, Lahtinen SJ, Jakobsen M. Effect of Lactobacillus salivarius Ls-33 on fecal microbiota in obese adolescents. *Clin Nutr* 2013; **32**: 935-940 [PMID: 23510724 DOI: 10.1016/j.clnu.2013.02.007]
22 **Institute of Medicine**, Food and Nutrition Board. A Report of the Panel on Macronutrients, Subcommittees on Upper Reference Levels of Nutrients and Interpretation and Uses of Dietary Reference Intakes, Standing Committee on the Scientific Evaluation of Dietary Reference Intakes. Dietary Reference intakes for energy, carbohydrates, fiber, fat, fatty acids, cholesterol, protein and amino acids. The National Academies Press. 2005 [DOI: 10.17226/10490]
23 **Duncan SH**, Hold GL, Harmsen HJM, Stewart CS, Flint HJ. Growth requirements and fermentation products of Fusobacterium prausnitzii, and a proposal to reclassify it as Faecalibacterium prausnitzii gen. nov., comb. nov. *Int J Syst Evol Microbiol* 2002; **52**: 2141-2146 [PMID: 12508881 DOI: 10.1099/00207713-52-6-2141]
24 **Miquel S**, Martín R, Rossi O, Bermúdez-Humarán LG, Chatel JM, Sokol H, Thomas M, Wells JM, Langella P. Faecalibacterium prausnitzii and human intestinal health. *Curr Opin Microbiol* 2013; **16**: 255-261 [PMID: 23831042 DOI: 10.1016/j.mib.2013.06.003]
25 **Ai D**, Pan H, Li X, Gao Y, Liu G, Xia LC. Identifying Gut Microbiota Associated With Colorectal Cancer Using a Zero-Inflated Lognormal Model. *Front Microbiol* 2019; **10**: 826 [PMID: 31068913

DOI: 10.3389/fmicb.2019.00826]

26 **Brugère JF**, Borrel G, Gaci N, Tottey W, O'Toole PW, Malpuech-Brugère C. Archaebiotics: proposed therapeutic use of archaea to prevent trimethylaminuria and cardiovascular disease. *Gut Microbes* 2014; **5**: 5-10 [PMID: 24247281 DOI: 10.4161/gmic.26749]

27 **Murugesan S**, Ulloa-Martínez M, Martínez-Rojano H, Galván-Rodríguez FM, Miranda-Brito C, Romano MC, Piña-Escobedo A, Pizano-Zárate ML, Hoyo-Vadillo C, García-Mena J. Study of the diversity and short-chain fatty acids production by the bacterial community in overweight and obese Mexican children. *Eur J Clin Microbiol Infect Dis* 2015; **34**: 1337-1346 [PMID: 25761741 DOI: 10.1007/s10096-015-2355-4]

28 **Patterson AM**, Mulder IE, Travis AJ, Lan A, Cerf-Bensussan N, Gaboriau-Routhiau V, Garden K, Logan E, Delday MI, Coutts AGP, Monnais E, Ferraria VC, Inoue R, Grant G, Aminov RI. Human Gut Symbiont *Roseburia hominis* Promotes and Regulates Innate Immunity. *Front Immunol* 2017; **8**: 1166 [PMID: 29018440 DOI: 10.3389/fimmu.2017.01166]

29 **Walker AW**, Ince J, Duncan SH, Webster LM, Holtrop G, Ze X, Brown D, Stares MD, Scott P, Bergerat A, Louis P, McIntosh F, Johnstone AM, Lobley GE, Parkhill J, Flint HJ. Dominant and diet-responsive groups of bacteria within the human colonic microbiota. *ISME J* 2011; **5**: 220-230 [PMID: 20686513 DOI: 10.1038/ismej.2010.118]

30 **Chow J**, Tang H, Mazmanian SK. Pathobionts of the gastrointestinal microbiota and inflammatory disease. *Curr Opin Immunol* 2011; **23**: 473-480 [PMID: 21856139 DOI: 10.1016/j.coi.2011.07.010]

31 **Bunney PE**, Zink AN, Holm AA, Billington CJ, Kotz CM. Orexin activation counteracts decreases in nonexercise activity thermogenesis (NEAT) caused by high-fat diet. *Physiol Behav* 2017; **176**: 139-148 [PMID: 28363838 DOI: 10.1016/j.physbeh.2017.03.040]

32 **Al-Assal K**, Martinez AC, Torrinhas RS, Cardinelli C, Waitzberg D. Gut microbiota and obesity. *Clin Nutr Exp* 2018; **20**: 60-64 [DOI: 10.1016/j.yclnex.2018.03.001]

33 **Ley RE**, Turnbaugh PJ, Klein S, Gordon JI. Microbial ecology: human gut microbes associated with obesity. *Nature* 2006; **444**: 1022-1023 [PMID: 17183309 DOI: 10.1038/4441022a]

34 **Turnbaugh PJ**, Gordon JI. The core gut microbiome, energy balance and obesity. *J Physiol* 2009; **587**: 4153-4158 [PMID: 19491241 DOI: 10.1113/jphysiol.2009.174136]

35 **Furet JP**, Kong LC, Tap J, Poitou C, Basdevant A, Bouillot JL, Mariat D, Corthier G, Doré J, Henegar C, Rizkalla S, Clément K. Differential adaptation of human gut microbiota to bariatric surgery-induced weight loss: links with metabolic and low-grade inflammation markers. *Diabetes* 2010; **59**: 3049-3057 [PMID: 20876719 DOI: 10.2337/db10-0253]

36 **Yu M**, Stott S, Toner M, Maheswaran S, Haber DA. Circulating tumor cells: approaches to isolation and characterization. *J Cell Biol* 2011; **192**: 373-382 [PMID: 21300848 DOI: 10.1083/jcb.201010021]

37 **Abenavoli L**, Scarpellini E, Colica C, Boccuto L, Salehi B, Sharifi-Rad J, Aiello V, Romano B, De Lorenzo A, Izzo AA, Capasso R. Gut Microbiota and Obesity: A Role for Probiotics. *Nutrients* 2019; **11**: 2690 [PMID: 31703257 DOI: 10.3390/nu11112690]

38 **Jumpertz R**, Le DS, Turnbaugh PJ, Trinidad C, Bogardus C, Gordon JI, Krakoff J. Energy-balance studies reveal associations between gut microbes, caloric load, and nutrient absorption in humans. *Am J Clin Nutr* 2011; **94**: 58-65 [PMID: 21543530 DOI: 10.3945/ajcn.110.010132]

39 **Devaraj S**, Hemarajata P, Versalovic J. The human gut microbiome and body metabolism: implications for obesity and diabetes. *Clin Chem* 2013; **59**: 617–628 [PMID: 23401286 DOI: 10.1373/clinchem.2012.187617]

40 **Sanmiguel C**, Gupta A, Mayer EA. Gut Microbiome and Obesity: A Plausible Explanation for Obesity. *Curr Obes Rep* 2015; **4**: 250-261 [PMID: 26029487 DOI: 10.1007/s13679-015-0152-0]

41 **Stephens RW**, Arhire L, Covasa M. Gut Microbiota: From Microorganisms to Metabolic Organ Influencing Obesity. *Obesity (Silver Spring)* 2018; **26**: 801-809 [PMID: 29687647 DOI: 10.1002/oby.22179]

42 **Jung S**, Lee YJ, Kim M, Kim M, Kwak JH, Lee JW, Ahn YT, Sim JH, Lee JH. Supplementation with two probiotic strains, Lactobacillus curvatus HY7601 and Lactobacillus plantarum KY1032, reduced body adiposity and Lp-PLA2 activity in overweight subjects. *J Funct Foods* 2015; **19**: 744-752 [DOI: 10.1016/j.jff.2015.10.006]

43 **Gomes AC**, de Sousa RG, Botelho PB, Gomes TL, Prada PO, Mota JF. The additional effects of a probiotic mix on abdominal adiposity and antioxidant Status: A double-blind, randomized trial. *Obesity (Silver Spring)* 2017; **25**: 30-38 [PMID: 28008750 DOI: 10.1002/oby.21671]

44 **Kim J**, Yun JM, Kim MK, Kwon O, Cho B. Lactobacillus gasseri BNR17 Supplementation Reduces the Visceral Fat Accumulation and Waist Circumference in Obese Adults: A Randomized, Double-Blind, Placebo-Controlled Trial. *J Med Food* 2018; **21**: 454-461 [PMID: 29688793 DOI: 10.1089/jmf.2017.3937]

45 **Minami J**, Iwabuchi N, Tanaka M, Yamauchi K, Xiao JZ, Abe F, Sakane N. Effects of *Bifidobacterium breve* B-3 on body fat reductions in pre-obese adults: a randomized, double-blind, placebo-controlled trial. *Biosci Microbiota Food Health* 2018; **37**: 67-75 [PMID: 30094122 DOI: 10.12938/bmfh.18-001]

46 **Pedret A**, Valls RM, Calderón-Pérez L, Llauradó E, Companys J, Pla-Pagà L, Moragas A, Martín-Luján F, Ortega Y, Giralt M, Caimari A, Chenoll E, Genovés S, Martorell P, Codoñer FM, Ramón D, Arola L, Solà R. Effects of daily consumption of the probiotic Bifidobacterium animalis subsp. lactis CECT 8145 on anthropometric adiposity biomarkers in abdominally obese subjects: a randomized controlled trial. *Int J Obes (Lond)* 2019; **43**: 1863-1868 [PMID: 30262813 DOI: 10.1038/s41366-018-0220-0]

47 **Szulińska M**, Łoniewski I, van Hemert S, Sobieska M, Bogdański P. Dose-Dependent Effects of Multispecies Probiotic Supplementation on the Lipopolysaccharide (LPS) Level and Cardiometabolic Profile in Obese Postmenopausal Women: A 12-Week Randomized Clinical Trial. *Nutrients* 2018; **10**: 773 [PMID: 29914095 DOI: 10.3390/nu10060773]

48 **Sanchez M**, Darimont C, Panahi S, Drapeau V, Marette A, Taylor VH, Doré J, Tremblay A. Effects of a Diet-Based Weight-Reducing Program with Probiotic Supplementation on Satiety Efficiency, Eating Behaviour Traits, and Psychosocial Behaviours in Obese Individuals. *Nutrients* 2017; **9**: 284 [PMID: 28294985 DOI: 10.3390/nu9030284]

49 **Osterberg KL**, Boutagy NE, McMillan RP, Stevens JR, Frisard MI, Kavanaugh JW, Davy BM, Davy KP, Hulver MW. Probiotic supplementation attenuates increases in body mass and fat mass during high-fat diet in healthy young adults. *Obesity (Silver Spring)* 2015; **23**: 2364-2370 [PMID: 26466123 DOI: 10.1002/oby.21230]

World Journal of Gastroenterology

Submit a Manuscript: https://www.f6publishing.com

World J Gastroenterol 2021 January 7; 27(1): 129-142

DOI: 10.3748/wjg.v27.i1.129

ISSN 1007-9327 (print) ISSN 2219-2840 (online)

CASE REPORT

Spontaneous regression of gastric gastrinoma after resection of metastases to the lesser omentum: A case report and review of literature

Takeshi Okamoto, Takaaki Yoshimoto, Nobuyuki Ohike, Aoi Fujikawa, Takayoshi Kanie, Katsuyuki Fukuda

ORCID number: Takeshi Okamoto 0000-0001-9719-0282; Takaaki Yoshimoto 0000-0003-3014-1392; Nobuyuki Ohike 0000-0001-8631-821X; Aoi Fujikawa 0000-0003-2299-3931; Takayoshi Kanie 0000-0002-6955-0671; Katsuyuki Fukuda 0000-0001-6273-4227.

Author contributions: Okamoto T cared for the patient, performed endoscopic procedures, wrote the manuscript, and reviewed the literature; Yoshimoto T cared for the patient and contributed to manuscript drafting; Ohike N interpreted the pathological findings and contributed to manuscript drafting; Fujikawa A performed the surgical procedure and contributed to manuscript drafting; Kanie T cared for the patient, performed cardiology procedures and contributed to manuscript drafting; Fukuda K provided oversight for the manuscript and revised the manuscript for important intellectual content; and all authors issued final approval for the version to be submitted.

Informed consent statement: The patient has provided written informed consent for the publication of this article and associated images.

Takeshi Okamoto, Takaaki Yoshimoto, Katsuyuki Fukuda, Department of Gastroenterology, St. Luke's International Hospital, Tokyo 104-8560, Japan

Nobuyuki Ohike, Department of Pathology, Shizuoka Cancer Center, Shizuoka 411-8777, Japan

Aoi Fujikawa, Department of Surgery, St. Luke's International Hospital, Tokyo 104-8560, Japan

Takayoshi Kanie, Department of Cardiology, St. Luke's International Hospital, Tokyo 104-8560, Japan

Corresponding author: Takeshi Okamoto, MD, Staff Physician, Department of Gastroenterology, St. Luke's International Hospital, 9-1 Akashicho, Chuo-ku, Tokyo 104-8560, Japan. tak@afia.jp

Abstract

BACKGROUND

Gastric gastrinoma and spontaneous tumor regression are both very rarely encountered. We report the first case of spontaneous regression of gastric gastrinoma.

CASE SUMMARY

A 37-year-old man with a 9-year history of chronic abdominal pain was referred for evaluation of an 8 cm mass in the lesser omentum discovered incidentally on abdominal computed tomography. The tumor was diagnosed as grade 2 neuroendocrine neoplasm (NEN) on endoscopic ultrasound-guided fine-needle aspiration. Screening esophagogastroduodenoscopy revealed a 7 mm red polypoid lesion with central depression in the gastric antrum, also confirmed to be a grade 2 NEN. Laparoscopic removal of the abdominal mass confirmed it to be a metastatic gastrinoma lesion. The gastric lesion was subsequently diagnosed as primary gastric gastrinoma. Three months later, the gastric lesion had disappeared without treatment. The patient remains symptom-free with normal fasting serum gastrin and no recurrence of gastrinoma during 36 mo of follow-up.

CONCLUSION

Gastric gastrinoma may arise as a polypoid lesion in the gastric antrum. Spontaneous regression can rarely occur after biopsy.

Conflict-of-interest statement: The authors have no financial disclosures or conflicts of interest to declare.

CARE Checklist (2016) statement: The authors have read the CARE Checklist (2016), and the manuscript was prepared and revised according to the CARE Checklist (2016).

Manuscript source: Unsolicited manuscript

Specialty type: Gastroenterology and hepatology

Country/Territory of origin: Japan

Peer-review report's scientific quality classification

Grade A (Excellent): 0
Grade B (Very good): B
Grade C (Good): 0
Grade D (Fair): 0
Grade E (Poor): 0

Received: October 11, 2020
Peer-review started: October 11, 2020
First decision: November 23, 2020
Revised: November 28, 2020
Accepted: December 16, 2020
Article in press: December 16, 2020
Published online: January 7, 2021

P-Reviewer: Sun Q
S-Editor: Huang P
L-Editor: A
P-Editor: Liu JH

Key Words: Neuroendocrine neoplasm; Functional tumor; Biopsy; Gastrin; Stomach; Case report

Core Tip: Gastrinoma is a functional neuroendocrine tumor which can cause refractory gastrointestinal symptoms. We present a rare case of gastrinoma originating in the stomach, with metastasis to the lesser omentum. Tumors including neuroendocrine tumors are rarely known to regress spontaneously following biopsy or surgical insult. This is the first report of spontaneous regression of a gastric gastrinoma. We also review the literature on gastric gastrinoma, gastrinoma arising in the lesser omentum, and spontaneous regression of gastrinomas and other neuroendocrine tumors.

Citation: Okamoto T, Yoshimoto T, Ohike N, Fujikawa A, Kanie T, Fukuda K. Spontaneous regression of gastric gastrinoma after resection of metastases to the lesser omentum: A case report and review of literature. *World J Gastroenterol* 2021; 27(1): 129-142
URL: https://www.wjgnet.com/1007-9327/full/v27/i1/129.htm
DOI: https://dx.doi.org/10.3748/wjg.v27.i1.129

INTRODUCTION

Gastrinoma is a type of neuroendocrine neoplasm (NEN) with high malignant potential. It is known to cause Zollinger-Ellison syndrome (ZES), a state of gastrin hypersecretion causing peptic ulcers in over 90% of affected cases[1]. The annual incidence has been reported at 0.5-2 per million. About 25% are associated with multiple endocrine neoplasia (MEN) type 1, while the remainder are sporadic[2]. Most arise in the gastrinoma triangle, an area with borders formed by the porta hepatis, duodenum, and pancreatic head[1]. Duodenal and pancreatic gastrinomas make up over 80% of all gastrinomas; other potential sites for primary lesions include the liver, biliary tree, ovary, kidney, jejunum, greater and lesser omentum, heart, and stomach[2-4].

Gastric NENs have an annual incidence of 2-5 per 100000 persons and account for 0.3%-1.8% of all gastric tumors, 5.6%-7.4% of NENs, and 6.9%-8.7% of all digestive NENs[5-8]. A large majority arise from enterochromaffin-like (ECL) cells which are stimulated by gastrin and secrete histamines[9-11]. As ECL cells are distributed in the gastric fundus and corpus, antral NENs are rare and originate from G-cells (which produce gastrin), D-cells (somatostatin) and enterochromaffin cells (serotonin).

NENs arising from ECL cells (ECLomas) are classified into 3 types based on etiology[5,6]. Type 1 is the most common and often presents with small, multiple polypoid lesions in the setting of autoimmune atrophic gastritis. Type 2 is the rarest type, accounting for 5%-6% of gastric NENs. It also commonly presents with small, multiple polypoid lesions in the fundus or body, but arises in the setting of gastrinoma or MEN type 1. Both type 1 and type 2 have high fasting serum gastrin (FSG) but type 2 has lower gastric pH and higher rates of metastasis (10%-30%). Type 3 commonly presents with large neuroendocrine carcinoma, has normal FSG, and metastatic disease is observed in a majority of cases. More recently, a fourth type involving multiple lesions associated with hypergastrinemia, endocrine cell hyperplasia, and parietal cell hypertrophy has been reported[12]. Gastric NENs originate in the deep mucosa and invade the submucosa, creating dome-like protrusions with or without central depressions when observed endoscopically[13].

Gastric gastrinomas do not fit into this framework, as they are not ECLomas. To the extent of our search, there are only 12 reports of gastric gastrinoma in the English literature[4,5,14-23]. While gastrinomas can occur sporadically or in connection with MEN type 1, all reported gastric cases in the English language are sporadic gastrinomas. There is one French report of a gastric gastrinoma associated with the latter[24].

Spontaneous regression is defined as the complete or partial disappearance of a tumor with no or inadequate treatment[25]. It is not equivalent to cure; the tumor may reappear in the same location or elsewhere in the body. While initially estimated to occur once in every 60000-100000 cases, recent studies suggest that at least partial

regression may be much more common[26-28]. The frequency of spontaneous regression varies widely depending on the tumor, with a large number of reports in renal cell carcinoma, melanoma, and neuroblastoma[25,26,28]. Reports in gastric NENs are scarce[29-31]. Immunological response by tumor infiltrating leukocytes such as cytotoxic T lymphocytes has been implicated as a possible explanation, while the impact of hormones, infection, diet and nutrition, toxins, genetics, and invasive procedures such as biopsies and surgery have also been suggested[26,28,32,33].

Here, we present a case of gastric gastrinoma with large metastases to the lesser omentum. The primary gastric lesion regressed spontaneously following biopsy of the gastric lesion and surgical resection of the metastatic lesion. We also review the existing literature on gastric gastrinomas, gastrinomas of the lesser omentum, and spontaneous regression of NENs.

CASE PRESENTATION

Chief complaints

A 37-year-old man presented to the emergency department after sudden cardiopulmonary arrest while outdoors.

History of present illness

Return of spontaneous circulation was achieved due to bystander cardiopulmonary resuscitation and 2 electric shocks from an automated external defibrillator.

History of past illness

His medical history was only significant for gastric mucosal erosions diagnosed 9 years prior to admission. The patient had chronic abdominal pain and occasional reflux symptoms despite continued treatment with proton pump inhibitors (PPIs).

Personal and family history

He had never consumed alcohol or smoked cigarettes. He had no known food or drug allergies. He had also never experienced syncope or palpitations in the past.

Physical examination

Body temperature of 36.2 degrees Celsius, blood pressure of 139/111 mmHg, sinus tachycardia with a heart rate of 130 beats/min, and respiratory rate of 32 times/min were noted upon arrival. The patient's eyes were open but he could not speak (Glasgow Coma Scale: E4V1M4). Physical examination was otherwise unremarkable.

Laboratory examinations

Laboratory values were significant for leukocytosis, mild increase in liver enzymes and creatinine, lactic acidosis (pH of 7.118 and lactate of 8.1 mmol/L on arterial blood gas analysis), and a severely elevated D-dimer of over 100 mcg/mL. Electrolytes were within their normal ranges. Rapid improvement was observed on serial follow-up examinations.

Imaging examinations

Computed tomography (CT) with contrast at admission revealed an incidental 8 cm mass in the lesser omentum (Figure 1). The mass appeared to result from the fusion of 3 similar solid tumors, of which 1 contained a non-enhancing, low-density area suggestive of necrosis or hematoma.

Further diagnostic work-up

Esophagogastroduodenoscopy (EGD) incidentally revealed a red, 7 mm submucosal tumor with central depression, which was biopsied (Figure 2A). Prominent gastric folds and shallow duodenal ulcers were also noted despite prolonged intravenous PPI treatment during admission (Figure 2B and C). No signs of gastroesophageal reflux disease or duodenal submucosal tumors were observed. Endoscopic ultrasound revealed 3 clearly delineated, hyperechoic masses with uniform texture, of which 1 had a hypoechoic center (Figure 2D). No pancreatic tumors were noted. Endoscopic ultrasound-guided fine-needle aspiration was performed. Pathology of both the gastric and lesser omentum specimens stained positive for chromogranin A and synaptophysin and were diagnosed as grade 2 NENs.

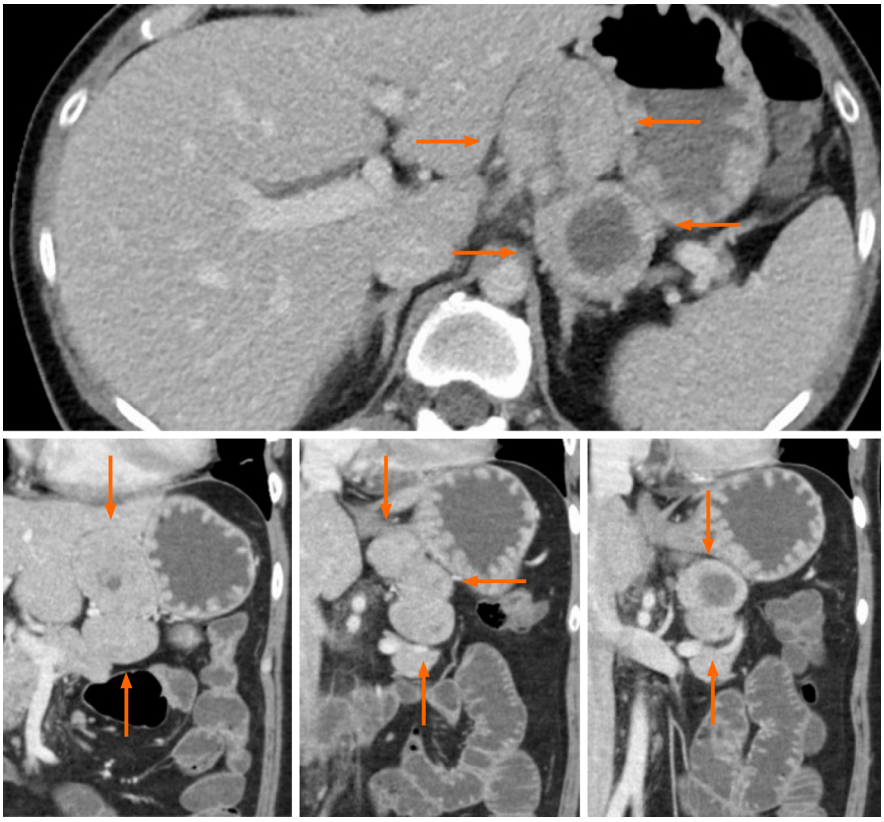

Figure 1 Axial (top) and coronal (bottom) views of computed tomography with contrast at admission revealed an incidental 8 cm mass in the lesser omentum (orange arrows). The mass appeared to result from the fusion of 3 similar tumors, of which 1 contained a non-enhancing, low-density area suggestive of necrosis or hematoma.

MULTIDISCIPLINARY EXPERT CONSULTATION

Takayoshi Kanie, MD, Department of Cardiology, St. Luke's International Hospital

After admission, targeted temperature management was performed under total anesthesia. The patient recovered completely after 2 d, with no neurological sequelae. While coronary angiogram including various stress tests was unremarkable, electrocardiogram findings were suggestive of Brugada's syndrome. An implantable cardiac defibrillator (EMBLEM MRI S-ICD System, Boston Scientific, Marlborough, MA, United States) was implanted during admission.

Aoi Fujikawa, MD, Department of Surgery, St. Luke's International Hospital

As the gastric and omental lesions were initially assumed to be independent lesions, laparoscopic omental tumor resection with possible gastrectomy was planned. The intention was to perform endoscopic submucosal dissection (ESD) to treat the gastric lesion once post-operative recovery was confirmed. The patient provided informed consent for the surgery and the overall treatment plan based on an adequate understanding of the risks involved in each procedure, particularly given his post-resuscitation status.

Laparoscopic surgery revealed an 83 mm × 80 mm × 37 mm mass in the lesser omentum which appeared to be formed from the fusion of 3 spherical tumors (Figure 3). No adhesion to the stomach was observed, enabling *en bloc* resection without partial gastrectomy. A macroscopic examination of the resected specimen revealed a brown, well-defined, encapsulated 75 mm × 40 mm solid tumor inside adipose tissue of the lesser omentum with a central hematoma. Pathology revealed nests of tumor cells characterized by small ovoid nuclei and mildly eosinophilic cytoplasms with intervening dilated capillary networks (Figure 4A). The tumor was positive for chromogranin A, synaptophysin, and gastrin (Figure 4B-D). Mitotic count was less than 2 per 2 mm^2 and the Ki67 index was 6%. No lymphatic or vascular invasion was noted. While initially suspected to be lymph nodes, the fused tumor was completely composed on uniform tumor cells with almost no lymphocytes except outside the encapsulated tumor. The differential at the time included primary

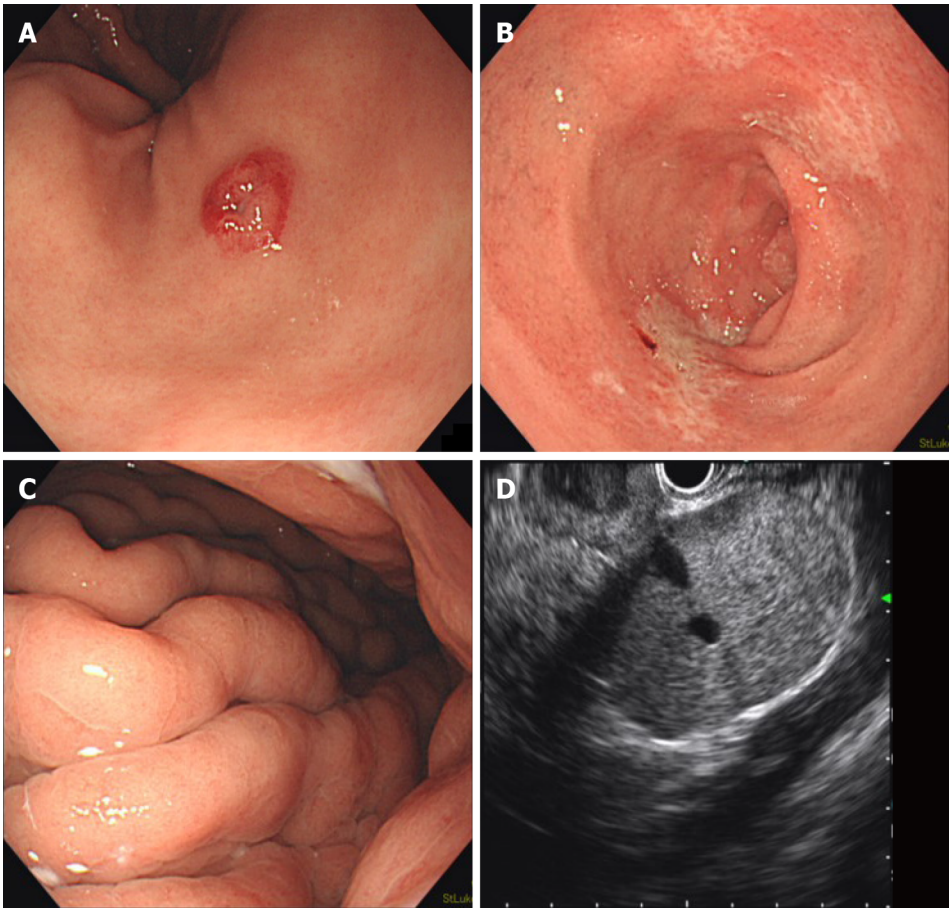

Figure 2 Esophagogastroduodenoscopy incidentally revealed a red, 7 mm submucosal tumor with a central depression (A); prominent gastric folds (B) and shallow duodenal ulcers (C) were also noted; endoscopic ultrasound revealed 3 clearly delineated, hyperechoic masses with uniform texture, of which 1 had a hypoechoic center with clear borders (D).

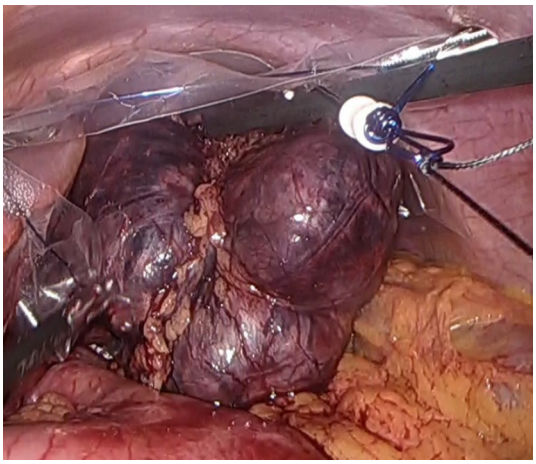

Figure 3 Laparoscopic surgery revealed an 83 mm × 80 mm × 37 mm mass in the lesser omentum which appeared to be formed from the fusion of 3 spherical tumors.

gastrinoma of lesser omentum lymph node, lymph node metastasis from primary gastric or undetected duodenal gastrinoma, and tumor-forming hematogenous spread of gastrinoma. While the gastric lesion had not been resected, the Tumor-Node-Metastasis staging was clinically considered to be T1N1M0, stage III (Union for International Cancer Control, 8th edition) assuming the lesion was a locoregional lymph node metastasis from a gastric NEN primary.

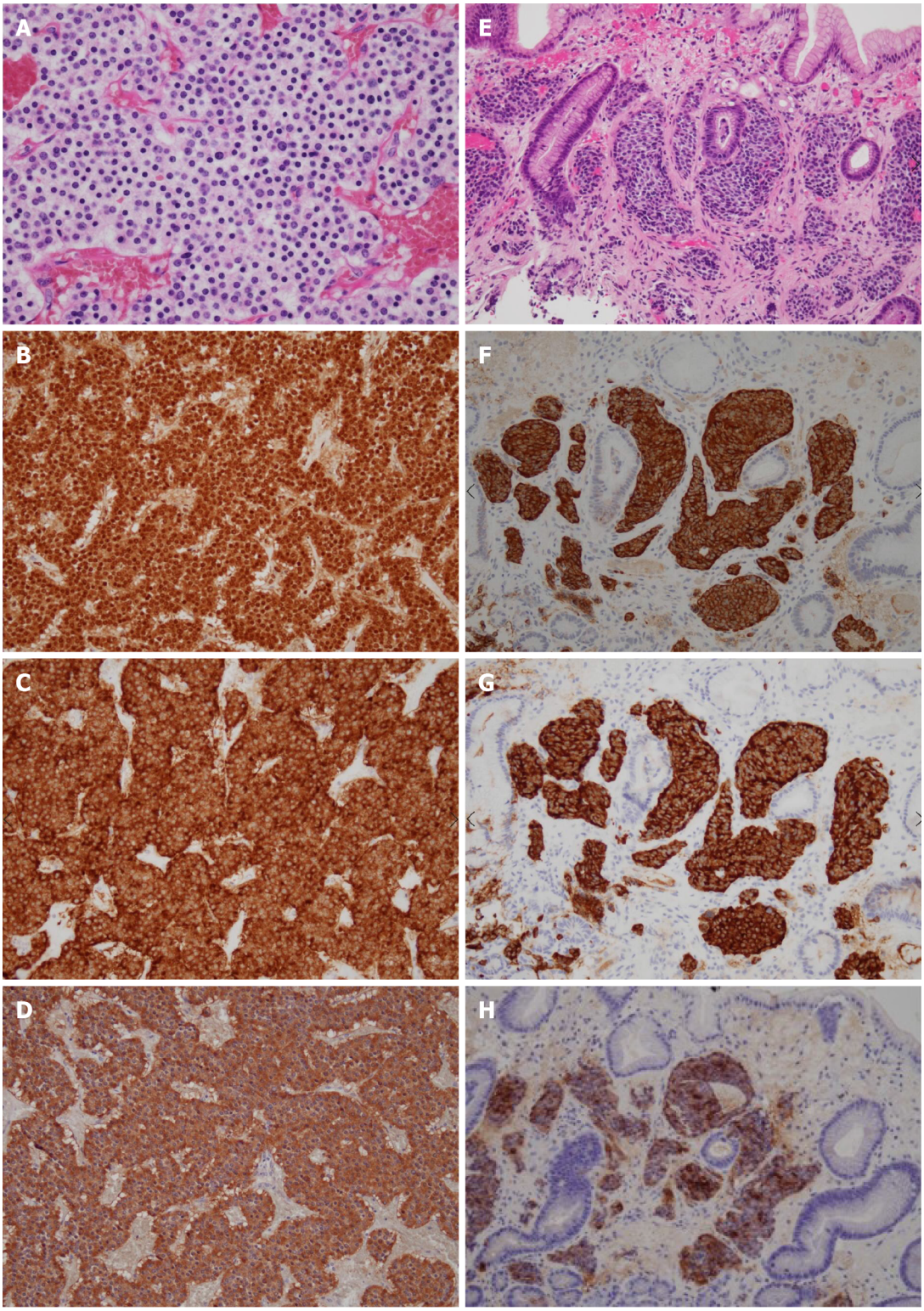

Figure 4 Pathology of the surgical specimen (A-D) and gastric biopsy (E-H). Nests of tumor cells characterized by small ovoid nuclei and mildly eosinophilic cytoplasms with intervening dilated capillary networks were observed in the omental lesion (A). The tumor was positive for chromogranin A (B), synaptophysin (C), and gastrin (D) stains. Biopsy of the gastric lesion showed similar cells in the mucosal layer (E) which were also positive for chromogranin A (F), synaptophysin (G), and gastrin (H) stains.

Nobuyuki Ohike, MD, PhD, Department of Pathology, Shizuoka Cancer Center

After the surgery, results of the pre-operative FSG test returned and showed marked elevation (41100 pg/mL without discontinuation of PPIs; reference range: 37-172 pg/mL). Pathology of the stomach biopsy was re-evaluated by an expert pathologist specializing in gastrointestinal tumors and was found to have a striking resemblance to the resected lesser omentum mass (Figure 4E-G). Strong immunoreactivity with gastrin was also confirmed for the first time (Figure 4H).

FINAL DIAGNOSIS

The patient denied a family history of MEN type 1, of pituitary, parathyroid, or pancreatic tumors, or of peptic ulcers. Gastric pH was not evaluated as the primary cardiology team believed PPIs should not be withheld for testing. Calcium, parathyroid hormone, vitamin B12, and thyroid function tests were within their normal ranges. Parietal cell and intrinsic factor antibodies and *Helicobacter pylori* antibodies were negative. Brain, neck, and abdominal imaging showed no pituitary, parathyroid, or pancreatic tumors.

As a result, the patient was diagnosed with sporadic gastric gastrinoma with metastases to the lesser omentum.

TREATMENT

In part due to stress from a long hospital stay, the patient left the hospital against medical advice after surgery.

OUTCOME AND FOLLOW-UP

He voluntarily returned for follow-up EGD 3 mo later to be re-evaluated before a possible distal gastrectomy. However, the gastric gastrinoma had reduced to a red dot with no visible elevation and was barely identifiable (Figure 5A). Biopsy of the lesion was negative for tumor, with only regenerative and fibrous changes (Figure 5B). Chromogranin A and synaptophysin stains were also negative (Figure 5C). In addition, duodenal ulcers had healed completely, allowing the patient to discontinue PPIs for the first time in 9 years. The prominent gastric folds observed in the gastric corpus had also normalized. FSG decreased dramatically to the normal range (167 pg/mL) and somatostatin-receptor scintigraphy (Octreoscan) showed no focal uptake throughout the body, including the stomach and lesser omentum. Based on a careful discussion of the risks involved, the patient decided to forgo surgery and opted for close observation.

Subsequent endoscopic findings have remained unchanged, FSG has remained within the normal range, and CT and scintigraphy have shown no recurrence of gastrinoma during 36 mo of follow-up. The patient remains asymptomatic without PPIs. No shocks from his implantable cardiac defibrillator have been triggered to date.

DISCUSSION

Gastric gastrinoma

G-cells are neuroendocrine cells which secrete gastrin. G-cells are stimulated by vagal stimulation *via* gastrin-releasing peptide, producing gastrin which in turn stimulate ECL cells to produce histamines. While G-cell NENs are strongly positive for the gastrin stain, they are not considered gastrinomas unless they present with symptoms consistent with ZES; gastrinoma is a clinical diagnosis[4-6]. Primary gastric gastrinoma is a rare clinical entity, even though most G-cells in the human body residing in the gastric antrum. La Rosa *et al*[11] found only 1 case of gastric gastrinoma among 8 antral G-cell NENs and among 209 gastric NENs.

Huang *et al*[14] reported an exceptionally high rate of gastrinomas among NENs at their institution: 20 cases of gastrinoma, of which 9 were gastric gastrinomas, out of 109 upper gastrointestinal NENs studied. However, they state in their discussion that type 1 and type 2 gastric NENs were considered gastrinomas. Their report appears to be focused on NENs (ECLomas) induced by hypergastrinemia instead of gastrin-producing primary NENs, which is our topic of discussion.

We conducted a PubMed search using the search terms "gastrinoma AND (stomach OR gastric)" and investigated all sources cited in each relevant report. We found 12 reports in the English language (excluding abstracts), mostly from the twentieth century (Table 1)[4,5,15-23]. Among the 13 reports including our case, there was a male preponderance (83%). Ages varied broadly, from 11 to 91 years of age. Most had a long history of abdominal symptoms and all lesions with specified locations were found in the distal half of the stomach, mainly in the antrum. Surgery was generally the treatment of choice, after which FSG normalized in a majority of cases. Lymph nodes

Table 1 Case reports of gastric gastrinoma

Case	Ref.	Year	Age	Gender	Symptoms	Symptom duration (yr)	History of peptic ulcer	Location	Size (mm)	Metastases	Gastrin before surgery (pg/mL)	Gastrin after surgery (pg/mL)	Treatment	Follow-up (mo)	Recurrence
1	Royston *et al*[16]	1972	65	M	Abdominal pain	14	+	Whole stomach	Large	-	> 1000	Undetectable	Total gastrectomy	15	-
2	Larsson *et al*[17]	1973	65	M	Abdominal pain, hematemesis	10	+	Antro-pylorus	10	-	NA	NA	Gastrectomy	12	-
3	Bhagavan *et al*[18]	1974	11	M	Acute peritonitis	0	-	Antrum (multiple)	Micro-scopic	-	> 1000	11000	Total gastrectomy	12	NA
4	Russo *et al*[19]	1980	51	F	Dyspepsia	7	-	Antrum-body junction	10	-	265	< 100	Polypectomy, antrectomy + splenectomy	36	-
5	Thompson *et al*[20]	1985	19	M	NA	3	+	Antrum	20	Liver	3000-4000	Normal	Total gastrectomy + segmental hepatectomy	NA	-
6	Liu *et al*[21]	1989	50	M	Pain, diarrhea, vomiting, weight loss	1.5	+	Antrum	< 10	Lymph node	1100-3000	153	Total gastrectomy	36	+
7	Liu *et al*[21]	1989	36	F	Pain, diarrhea, vomiting, weight loss	3.5	+	Lower body/antrum-body junction (multiple)	60	Lymph node, liver	518	4900	Subtotal gastrectomy	29 (dead)	NA
8	Werbel *et al*[22]	1989	72	M	Nausea, vomiting, anorexia, weight loss	8	+	Antrum	15	-	340	40	Antrectomy + vagotomy	12	-
9	Rindi *et al*[5]	1993	NA	NA	NA	NA	+	Pylorus	20	-	Elevated	Normal	Distal gastrectomy	NA	-
10	Wu *et al*[4]	1997	40	M	NA	NA	NA	Pylorus	NA	-	373	250	Enucleation	140	+
11	de Leval *et al*[23]	2002	91	M	Nausea, vomiting, anorexia, weight loss	4	+	Antrum	55	Lymph node, liver	3500	NA	None	0 (dead)	NA
12	Tartaglia *et al*[15]	2005	37	M	Abdominal pain, nausea	8	+	Angulus	7	Hepatogastric ligament	420	95	Endoscopic resection, subtotal gastrectomy + left hepatic lobectomy, lanreotide	72	+
13	Our case	2020	37	M	Abdominal pain	9	+	Antrum	7	Lesser omentum	41100	167	Tumor resection	30	-

and the liver were the most common sites for metastases.

Treatment for gastric gastrinoma has not been elucidated due to its rarity.

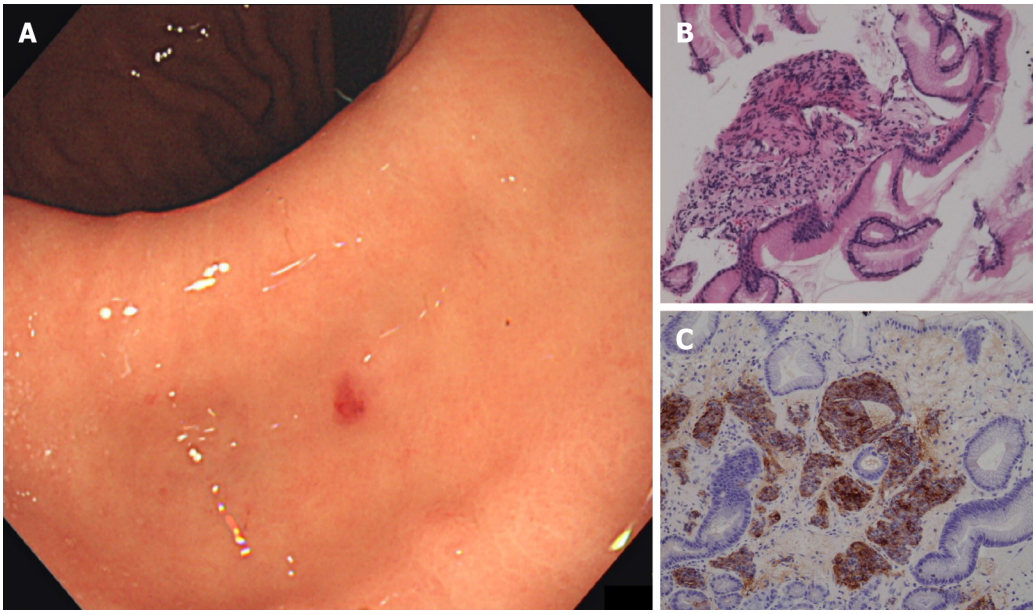

Figure 5 The gastric neuroendocrine neoplasm was barely identifiable on follow-up esophagogastroduodenoscopy, reducing to a red dot with no visible elevation (A); biopsy of the lesion was negative for tumor, with only regenerative and fibrous changes (B); synaptophysin (C) stain was also negative.

Guidelines from the National Comprehensive Cancer Network (NCCN) and the European Neuroendocrine Tumor Society (ENETS) both recommend radical resection with lymph node sampling for duodenal and pancreatic gastrinomas[7,34]. While both NCCN and ENETS guidelines permit endoscopic resection for certain types of small gastric NENs, radical resection with lymph node sampling should be performed for gastric gastrinomas due to the potential for metastases. Although some authors suggest a role for endoscopic resection of gastric gastrinomas[35], our preferred approach is open surgery with intraoperative digital and ultrasound exploration to investigate undetected duodenal primaries. In the present case, laparoscopy was performed instead of open surgery as the diagnosis of gastrinoma was not reached before surgery.

A gastrinoma work-up is generally considered when encountering NENs in the gastric fundus or corpus. We propose that gastric gastrinoma should be included in the differential diagnosis for a NEN in the gastric antrum, particularly when accompanied by peptic ulcers and prominent gastric folds.

Relationship between the gastric and omental lesions

Before reaching the final diagnosis of primary gastric gastrinoma with metastasis to the lesser omentum, we considered several other possibilities for the relationship between the gastric and lesser omentum lesions.

Primary omental gastrinoma with gastric NEN from ectopic ECL cells: While ECL cells generally do not exist in the gastric antrum, type 2 antral NENs arising from ectopic ECL cells were observed in at least 2 of 4 antral NEN cases in one report[36]. However, the positive gastrin stain in our case supports a G-cell origin.

Primary gastrinoma of the lesser omentum with gastric metastasis: We initially entertained the possibility that the large lesser omentum lesion was the primary site. Primary tumors of the lesser omentum are rare. Most are benign tumors such as lymphangiomas and hemangiomas, with isolated reports of gastrointestinal stroma tumors and malignancies such as soft tissue sarcoma, lymphoma, and small cell carcinoma[37-40]. There are 5 reports of primary gastrinoma of the lesser omentum (Table 2)[41-44]. Four cases were relatively young males (average age: 26.3 years) including 2 teenagers, while the fifth was an elderly woman. All had solitary tumors and none had any evidence of MEN type 1. Tumors in most cases exceeded 4 cm but had no metastases. Normalization of serum gastrin and recurrence-free status was achieved in all cases. Tumor resection without gastrectomy was possible in 3 cases, while total gastrectomy was performed in 2 cases. These is also one report of primary gastrinoma of the greater omentum in which serum gastrin similarly normalized after

Table 2 Case reports of primary gastrinoma of the lesser omentum

Case	Ref.	Year	Age	Gender	Symptoms	Size (mm)	Gastrin before surgery (pg/mL)	Gastrin after surgery (pg/mL)	Treatment	Follow-up (mo)	Recurrence
1	Wolfe *et al*[41]	1982	51	M	Recurrent duodenal ulcer	NA	753	112	Total gastrectomy	60	-
2	Wolfe *et al*[41]	1982	15	M	Hematemesis, abdominal pain, diarrhea	25	455	41	Tumor resection	12	-
3	Kohyama *et al*[42]	2007	74	F	Abdominal pain	40	1850	118	Resection of remnant stomach with tumor	24	-
4	Chang *et al*[43]	2010	13	M	Abdominal pain, diarrhea	45 × 37	1263	Normal	Tumor resection	36	-
5	Labidi *et al*[44]	2018	26	M	Melena, abdominal pain	50 × 40	306	Normal	Tumor resection	6	-

surgery and no recurrence was observed[45].

There is no known method of determining whether the gastric lesion or the omental lesion was the primary gastrinoma. However, both sub-centimeter duodenal gastrinomas and sub-centimeter gastric NENs have been reported to metastasize[11,15]. To the extent of our search, there are no reports of gastrinomas metastasizing to the stomach. It therefore appears natural to consider the gastric lesion as the primary site.

Primary lymph node gastrinoma with gastric metastasis: The existence of primary lymph node gastrinoma remains in dispute among experts. Sub-centimeter duodenal primaries commonly exhibit distant metastases and may be undetected despite careful evaluation, including autopsy. In a study of 176 ZES patients, lymph nodes were the only lesions discovered initially in 45 cases[46]. While small duodenal gastrinomas had been missed in several cases, 26 appeared to be completely cured after surgical resection of the involved lymph node. None of these cases arose in the omentum.

Furthermore, primary lymph node gastrinoma is currently diagnosed when diagnostic criteria for gastrinoma are met without any confirmed lesions other than lymph nodes and their resection leads to normalization of FSG and other laboratory or radiological findings suggestive of gastrinoma. This definition fails to account for spontaneous regression of an undetected primary after surgery, discussed below.

Gastric and omental metastases from undiscovered primary duodenal tumor: Most gastrinomas arise in the duodenum and small duodenal gastrinomas undetected by endoscopic or imaging studies are known to metastasize. As surgery was not performed in our patient, this possibility is the most difficult to rule out. There is no way to confirm whether or not spontaneous regression, which occurred in the stomach, also occurred in the duodenum. However, as stated previously, we found no reports of gastrinoma metastasizing to the stomach.

Gastric NEN triggered by chronic PPI use: Chronic PPI use is widely known to cause ECL cell hyperplasia as well as hypergastrinemia, albeit at mild levels of approximately 1-3 times the upper limit of normal which generally plateaus after 1-2 years. A systematic review of 1920 patients on PPIs found no found gastric NENs[47]. On the other hand, a single center study reported that 3 of 31 gastric NENs arose in patients with long-term PPI use in the absence of autoimmune atrophic gastritis, *Helicobacter pylori* infection, or ZES. ECL hyperplasia was not observed in 1 of the 3 cases, while another was a 6 mm, grade 2 NEN with normal FSG[48]. A study of 66 gastric NENs in long-term PPI users reported that 9% of NENs arose in the antrum or pylorus, but did not specify whether these were ECL-cell NENs[49]. In any event, the strongly positive gastrin stain and strong resemblance to the omental lesion makes this an unlikely explanation in our case.

Multicentric or incidental simultaneous occurrence of gastric and omental NENs: Simultaneous multicentric occurrence of NENs is another possibility. The negative tests for MEN type 1 and the strong pathological resemblance between the gastric primary and omental metastasis does not allow us to rule this out completely.

Additional molecular genetic testing, not available at our institution, may shed light on this possibility[50].

It is also possible for sporadic NENs in 2 separate organs to be discovered incidentally at the same time. This premature assumption led to a delay in the diagnosis in our patient. There are no reports on this phenomenon and other possibilities should be considered first, particularly in young patients with no apparent risk factors for NEN development. Had gastrinoma been suspected in advance, open laparotomy with digital and ultrasound exploration would have been selected over laparoscopy. The pathological resemblance between the 2 lesions was too strong for them to be considered unrelated lesions.

Spontaneous regression

Complete and partial spontaneous regressions of NENs have been observed in various organs. Most reports involve Merkel cell carcinomas and neuroblastomas, which are neuroendocrine carcinomas of the skin and sympathetic nervous system, respectively[51,52]. Isolated cases of spontaneous regression of NENs in the pancreas, lung, bile duct, thymus, and pelvis have been reported, as well as in metastatic disease[53-58]. Biopsy, surgery for another condition, and pregnancy have been suggested as possible triggers[54-56].

Focusing on this placebo arms of randomized controlled trials conducted from 1980 to 2014, Ghatalia *et al*[27] investigated spontaneous regression in various solid tumors including 2 trials relating to pancreatic NENs. Partial spontaneous regression was observed in 4 of 252 patients receiving placebo, for an overall response ratio (ORR) of 1.6%. Amoroso expanded this idea to include 5 trials on NENs and found an ORR of 1.52% among 531 patients receiving placebo[53]. The authors also found minor response, defined as a 10%-30% reduction in tumor size from baseline, in almost 6% of NEN patients receiving placebo. While no complete spontaneous regressions were observed in these studies, partial spontaneous regressions may not be as rare as once believed.

Spontaneous regression of metastatic gastrinomas after biopsy and/or surgery was reported as far back as the 1960s. Disappearance of biopsy-proven liver and/or lung metastases on imaging or during second-look operations were observed in 2 out of 44 gastrinoma patients in one study and 4 out of 267 metastatic reports in another, all following total gastrectomy[59,60]. There are also sparse reports of spontaneous regression of gastric NENs. An Indian report detailed the complete spontaneous regression of an 11 cm gastric NEN after exploratory laparotomy[29]. Another report from Hong Kong found no residual tumor in the gastrectomy specimen after biopsy revealed a 4 cm high-grade large-cell neuroendocrine carcinoma in the gastric cardia[30]. Complete spontaneous regression was observed in both cases after either biopsy or surgical insult. Three cases of autoimmune atrophic gastritis in which multiple small gastric carcinoids regressed spontaneously during follow-up have also been reported[31].

In our case, we believe that complete spontaneous regression was achieved based on normalized FSG, cure of peptic ulcers, no signs of recurrence on imaging, and the negative biopsy of the gastric lesion. However, the biopsy was limited to the mucosal layer and remnants of tumor in the submucosal layer cannot be completely ruled out without surgery or ESD. While the patient did not consent to such additional treatment, at least a partial spontaneous regression was clearly achieved. We speculate biopsy of the primary lesion and subsequent surgery triggered the spontaneous regression.

To the extent of our search, we could not find any relationship between ZES and Brugada's syndrome, which was the cause of our patient's cardiopulmonary arrest. While cardiopulmonary arrest due to carcinoid syndrome has been reported, there were no clinical manifestations to raise any suspicion of this rare event[61]. We suspect that the gastrinoma was unrelated to the cardiopulmonary arrest.

CONCLUSION

In conclusion, we report a case of gastric gastrinoma which regressed spontaneously after biopsy and resection of a metastatic lesion in the lesser omentum. ZES can be left undetected for years and should be suspected in longstanding reflux disease or abdominal pain refractory to PPIs. NENs in the antrum should alert the physician for possible gastrinoma as well as NENs of other non-ECL cell origins. Further research is

required to further clarify the mechanisms behind spontaneous regression and to determine the characteristics of lesions or patients who may experience this extraordinary phenomenon. Such research may contribute to the discovery of new immunotherapies and to the reduction of unnecessary surgeries.

REFERENCES

1 **Jensen RT**, Cadiot G, Brandi ML, de Herder WW, Kaltsas G, Komminoth P, Scoazec JY, Salazar R, Sauvanet A, Kianmanesh R; Barcelona Consensus Conference participants. ENETS Consensus Guidelines for the management of patients with digestive neuroendocrine neoplasms: functional pancreatic endocrine tumor syndromes. *Neuroendocrinology* 2012; **95**: 98-119 [PMID: 22261919 DOI: 10.1159/000335591]

2 **Gibril F**, Schumann M, Pace A, Jensen RT. Multiple endocrine neoplasia type 1 and Zollinger-Ellison syndrome: a prospective study of 107 cases and comparison with 1009 cases from the literature. *Medicine (Baltimore)* 2004; **83**: 43-83 [PMID: 14747767 DOI: 10.1097/01.md.0000112297.72510.32]

3 **Jensen RT**, Niederle B, Mitry E, Ramage JK, Steinmuller T, Lewington V, Scarpa A, Sundin A, Perren A, Gross D, O'Connor JM, Pauwels S, Kloppel G; Frascati Consensus Conference; European Neuroendocrine Tumor Society. Gastrinoma (duodenal and pancreatic). *Neuroendocrinology* 2006; **84**: 173-182 [PMID: 17312377 DOI: 10.1159/000098009]

4 **Wu PC**, Alexander HR, Bartlett DL, Doppman JL, Fraker DL, Norton JA, Gibril F, Fogt F, Jensen RT. A prospective analysis of the frequency, location, and curability of ectopic (nonpancreaticoduodenal, nonnodal) gastrinoma. *Surgery* 1997; **122**: 1176-1182 [PMID: 9426435 DOI: 10.1016/s0039-6060(97)90224-5]

5 **Rindi G**, Luinetti O, Cornaggia M, Capella C, Solcia E. Three subtypes of gastric argyrophil carcinoid and the gastric neuroendocrine carcinoma: a clinicopathologic study. *Gastroenterology* 1993; **104**: 994-1006 [PMID: 7681798 DOI: 10.1016/0016-5085(93)90266-f]

6 **Rindi G**, Klimstra DS, Abedi-Ardekani B, Asa SL, Bosman FT, Brambilla E, Busam KJ, de Krijger RR, Dietel M, El-Naggar AK, Fernandez-Cuesta L, Klöppel G, McCluggage WG, Moch H, Ohgaki H, Rakha EA, Reed NS, Rous BA, Sasano H, Scarpa A, Scoazec JY, Travis WD, Tallini G, Trouillas J, van Krieken JH, Cree IA. A common classification framework for neuroendocrine neoplasms: an International Agency for Research on Cancer (IARC) and World Health Organization (WHO) expert consensus proposal. *Mod Pathol* 2018; **31**: 1770-1786 [PMID: 30140036 DOI: 10.1038/s41379-018-0110-y]

7 **Delle Fave G**, O'Toole D, Sundin A, Taal B, Ferolla P, Ramage JK, Ferone D, Ito T, Weber W, Zheng-Pei Z, De Herder WW, Pascher A, Ruszniewski P; Vienna Consensus Conference participants. ENETS Consensus Guidelines Update for Gastroduodenal Neuroendocrine Neoplasms. *Neuroendocrinology* 2016; **103**: 119-124 [PMID: 26784901 DOI: 10.1159/000443168]

8 **Grozinsky-Glasberg S**, Alexandraki KI, Angelousi A, Chatzellis E, Sougioultzis S, Kaltsas G. Gastric Carcinoids. *Endocrinol Metab Clin North Am* 2018; **47**: 645-660 [PMID: 30098721 DOI: 10.1016/j.ecl.2018.04.013]

9 **WHO of Tumours Editorial Board**. Digestive system tumors. Lyon: International Agency for Research on Cancer. 5th ed. 2019; 1: 104-109. Available from: https://publications.iarc.fr/Book-And-Report-Series/Who-Classification-Of-Tumours/Digestive-System-Tumours-2019

10 **La Rosa S**, Vanoli A. Gastric neuroendocrine neoplasms and related precursor lesions. *J Clin Pathol* 2014; **67**: 938-948 [PMID: 25053544 DOI: 10.1136/jclinpath-2014-202515]

11 **La Rosa S**, Inzani F, Vanoli A, Klersy C, Dainese L, Rindi G, Capella C, Bordi C, Solcia E. Histologic characterization and improved prognostic evaluation of 209 gastric neuroendocrine neoplasms. *Hum Pathol* 2011; **42**: 1373-1384 [PMID: 21531442 DOI: 10.1016/j.humpath.2011.01.018]

12 **Ooi A**, Ota M, Katsuda S, Nakanishi I, Sugawara H, Takahashi I. An Unusual Case of Multiple Gastric Carcinoids Associated with Diffuse Endocrine Cell Hyperplasia and Parietal Cell Hypertrophy. *Endocr Pathol* 1995; **6**: 229-237 [PMID: 12114744 DOI: 10.1007/BF02739887]

13 **Sato Y**, Hashimoto S, Mizuno K, Takeuchi M, Terai S. Management of gastric and duodenal neuroendocrine tumors. *World J Gastroenterol* 2016; **22**: 6817-6828 [PMID: 27570419 DOI: 10.3748/wjg.v22.i30.6817]

14 **Huang SF**, Kuo IM, Lee CW, Pan KT, Chen TC, Lin CJ, Hwang TL, Yu MC. Comparison study of gastrinomas between gastric and non-gastric origins. *World J Surg Oncol* 2015; **13**: 202 [PMID: 26077245 DOI: 10.1186/s12957-015-0614-6]

15 **Tartaglia A**, Vezzadini C, Bianchini S, Vezzadini P. Gastrinoma of the stomach: a case report. *Int J Gastrointest Cancer* 2005; **35**: 211-216 [PMID: 16110123 DOI: 10.1385/IJGC:35:3:211]

16 **Royston CM**, Brew DS, Garnham JR, Stagg BH, Polak J. The Zollinger-Ellison syndrome due to an infiltrating tumour of the stomach. *Gut* 1972; **13**: 638-642 [PMID: 4562021 DOI: 10.1136/gut.13.8.638]

17 **Larsson LI**, Ljungberg O, Sundler F, Håkanson R, Svensson SO, Rehfeld J, Stadil R, Holst J. Antor-pyloric gastrinoma associated with pancreatic nesidioblastosis and proliferation of islets. *Virchows Arch A Pathol Pathol Anat* 1973; **360**: 305-314 [PMID: 4201098 DOI: 10.1007/BF00548351]

18 **Bhagavan BS**, Hofkin GA, Woel GM, Koss LG. Zollinger-Ellison syndrome. Ultrastructural and histochemical observations in a child with endocrine tumorlets of gastric antrum. *Arch Pathol* 1974; **98**: 217-222 [PMID: 4416924]

19 **Russo A**, Buffa R, Grasso G, Giannone G, Sanfilippo G, Sessa F, Solcia E. Gastric gastrinoma and diffuse G cell hyperplasia associated with chronic atrophic gastritis. Endoscopic detection and removal. *Digestion* 1980; **20**: 416-419 [PMID: 6250933 DOI: 10.1159/000198484]

20 **Thompson NW**, Vinik AI, Eckhauser FE, Strodel WE. Extrapancreatic gastrinomas. *Surgery* 1985; **98**: 1113-1120 [PMID: 4071387]

21 **Liu TH**, Zhong SX, Chen YF, Lin Y, Chen J, Li DC, Wang DT, Gu CF, Yie SF. Gastric gastrinoma. *Chin Med J (Engl)* 1989; **102**: 774-782 [PMID: 2517058]

22 **Werbel GB**, Nelson SP, Robinson PG, Anastasi J, Joehl RJ, Rege RV. A foregut carcinoid tumor causing Zollinger-Ellison syndrome. *Arch Surg* 1989; **124**: 381-384 [PMID: 2919971 DOI: 10.1001/archsurg.1989.01410030131022]

23 **de Leval L**, Hardy N, Deprez M, Delwaide J, Belaïche J, Boniver J. Gastric collision between a papillotubular adenocarcinoma and a gastrinoma in a patient with Zollinger-Ellison syndrome. *Virchows Arch* 2002; **441**: 462-465 [PMID: 12447676 DOI: 10.1007/s00428-002-0707-9]

24 **Buyse S**, Charachon A, Petit T, Marmuse JP, Mignon M, Soule JC. [The gastric antrum: a rare primitive location of a gastrinoma within a type I multiple endocrine neoplasia]. *Gastroenterol Clin Biol* 2006; **30**: 625-628 [PMID: 16733391 DOI: 10.1016/s0399-8320(06)73240-7]

25 **COLE WH**, EVERSON TC. Spontaneous regression of cancer: preliminary report. *Ann Surg* 1956; **144**: 366-383 [PMID: 13363274 DOI: 10.1097/00000658-195609000-00007]

26 **Cole WH**. Efforts to explain spontaneous regression of cancer. *J Surg Oncol* 1981; **17**: 201-209 [PMID: 6166811 DOI: 10.1002/jso.2930170302]

27 **Ghatalia P**, Morgan CJ, Sonpavde G. Meta-analysis of regression of advanced solid tumors in patients receiving placebo or no anti-cancer therapy in prospective trials. *Crit Rev Oncol Hematol* 2016; **98**: 122-136 [PMID: 26597016 DOI: 10.1016/j.critrevonc.2015.10.018]

28 **Challis GB**, Stam HJ. The spontaneous regression of cancer. A review of cases from 1900 to 1987. *Acta Oncol* 1990; **29**: 545-550 [PMID: 2206563 DOI: 10.3109/02841869009090048]

29 **Sawant PD**, Nanivadekar SA, Shroff CP, Srinivas A, Dewoolkar VV. Spontaneous regression of large gastric carcinoid. *Indian J Gastroenterol* 1989; **8**: 289-290 [PMID: 2689331]

30 **Ip YT**, Pong WM, Kao SS, Chan JK. Spontaneous complete regression of gastric large-cell neuroendocrine carcinoma: mediated by cytomegalovirus-induced cross-autoimmunity? *Int J Surg Pathol* 2011; **19**: 355-358 [PMID: 21665860 DOI: 10.1177/1066896911404412]

31 **Harvey RF**. Spontaneous resolution of multifocal gastric enterochromaffin-like cell carcinoid tumours. *Lancet* 1988; **1**: 821 [PMID: 2895334 DOI: 10.1016/s0140-6736(88)91677-7]

32 **Bodey B**. Spontaneous regression of neoplasms: new possibilities for immunotherapy. *Expert Opin Biol Ther* 2002; **2**: 459-476 [PMID: 12079483 DOI: 10.1517/14712598.2.5.459]

33 **Abdelrazeq AS**. Spontaneous regression of colorectal cancer: a review of cases from 1900 to 2005. *Int J Colorectal Dis* 2007; **22**: 727-736 [PMID: 17146588 DOI: 10.1007/s00384-006-0245-z]

34 **National Comprehensive Cancer Network: NCCN Clinical Practice Guidelines in Oncology (NCCN Guidelines®)**. Neuroendocrine and Adrenal Tumors Version 2.2020 – July 24, 2020. Available from: https://www.nccn.org/

35 **Shao QQ**, Zhao BB, Dong LB, Cao HT, Wang WB. Surgical management of Zollinger-Ellison syndrome: Classical considerations and current controversies. *World J Gastroenterol* 2019; **25**: 4673-4681 [PMID: 31528093 DOI: 10.3748/wjg.v25.i32.4673]

36 **Bordi C**, Corleto VD, Azzoni C, Pizzi S, Ferraro G, Gibril F, Delle Fave G, Jensen RT. The antral mucosa as a new site for endocrine tumors in multiple endocrine neoplasia type 1 and Zollinger-Ellison syndromes. *J Clin Endocrinol Metab* 2001; **86**: 2236-2242 [PMID: 11344233 DOI: 10.1210/jcem.86.5.7479]

37 **Ninomiya S**, Hiroishi K, Shiromizu A, Ueda Y, Shiraishi N, Inomata M, Arita T. Gastrointestinal stromal tumor of the lesser omentum: a case report and review of the literature. *J Surg Case Rep* 2019; **2019**: rjz035 [PMID: 30792845 DOI: 10.1093/jscr/rjz035]

38 **Feng JF**, Guo YH, Chen WY, Chen DF, Liu J. Primary small cell carcinoma of the lesser omentum. *Kaohsiung J Med Sci* 2012; **28**: 115-119 [PMID: 22313540 DOI: 10.1016/j.kjms.2011.10.028]

39 **Wang B**, Ren KW, Yang YC, Wan DL, Li XJ, Zhai ZL, Zhang LL, Zheng SS. Carcinosarcoma of the Lesser Omentum: A Unique Case Report and Literature Review. *Medicine (Baltimore)* 2016; **95**: e3246 [PMID: 27057865 DOI: 10.1097/MD.0000000000003246]

40 **Onodera H**, Maetani S, Imamura M, Hayashi K, Nakayama T, Aoki T. [A case of a huge malignant lymphoma in the lesser omentum showing a long-term survival after combined treatment of surgery and VEP-THP chemotherapy]. *Gan To Kagaku Ryoho* 1994; **21**: 689-692 [PMID: 8154894]

41 **Wolfe MM**, Alexander RW, McGuigan JE. Extrapancreatic, extraintestinal gastrinoma: effective treatment by surgery. *N Engl J Med* 1982; **306**: 1533-1536 [PMID: 6281644 DOI: 10.1056/NEJM198206243062506]

42 **Kohyama A**, Shibata C, Funayama Y, Fukushima K, Takahashi K, Ueno T, Kobayashi T, Kinouchi M, Sasaki I, Moriya T. Primary Gastrinoma in the Lesser Omentum: A Case Report. *Jpn J Gastroenterol Surg* 2007; **40**: 1582-1586 [DOI: 10.5833/jjgs.40.1582]

43 **Chang FY**, Liao KY, Wu L, Lin SP, Lai YT, Liu CS, Tsay SH, Wu TC. An uncommon cause of abdominal pain and diarrhea-gastrinoma in an adolescent. *Eur J Pediatr* 2010; **169**: 355-357 [PMID:

19565263 DOI: 10.1007/s00431-009-1013-1]
44 **Labidi A**, Hamdi S, Ben Othman A, Chelly B, Daghfous A, Fekih M. A rare cause of upper gastrointestinal bleeding: Primary gastrinoma of the lesser omentum. *Presse Med* 2018; **47**: 913-915 [PMID: 30361100 DOI: 10.1016/j.lpm.2018.08.013]
45 **Pisegna JR**, Norton JA, Slimak GG, Metz DC, Maton PN, Gardner JD, Jensen RT. Effects of curative gastrinoma resection on gastric secretory function and antisecretory drug requirement in the Zollinger-Ellison syndrome. *Gastroenterology* 1992; **102**: 767-778 [PMID: 1537514 DOI: 10.1016/0016-5085(92)90157-t]
46 **Norton JA**, Alexander HR, Fraker DL, Venzon DJ, Gibril F, Jensen RT. Possible primary lymph node gastrinoma: occurrence, natural history, and predictive factors: a prospective study. *Ann Surg* 2003; **237**: 650-7; discussion 657 [PMID: 12724631 DOI: 10.1097/01.SLA.0000064375.51939.48]
47 **Lundell L**, Vieth M, Gibson F, Nagy P, Kahrilas PJ. Systematic review: the effects of long-term proton pump inhibitor use on serum gastrin levels and gastric histology. *Aliment Pharmacol Ther* 2015; **42**: 649-663 [PMID: 26177572 DOI: 10.1111/apt.13324]
48 **Cavalcoli F**, Zilli A, Conte D, Ciafardini C, Massironi S. Gastric neuroendocrine neoplasms and proton pump inhibitors: fact or coincidence? *Scand J Gastroenterol* 2015; **50**: 1397-1403 [PMID: 26059834 DOI: 10.3109/00365521.2015.1054426]
49 **Trinh VQ**, Shi C, Ma C. Gastric neuroendocrine tumours from long-term proton pump inhibitor users are indolent tumours with good prognosis. *Histopathology* 2020; **77**: 865-876 [PMID: 32702178 DOI: 10.1111/his.14220]
50 **Ahmadi Moghaddam P**, Cornejo KM, Hutchinson L, Tomaszewicz K, Dresser K, Deng A, O'Donnell P. Complete Spontaneous Regression of Merkel Cell Carcinoma After Biopsy: A Case Report and Review of the Literature. *Am J Dermatopathol* 2016; **38**: e154-e158 [PMID: 27759689 DOI: 10.1097/DAD.0000000000000614]
51 **Wang B**, Xia CY, Lau WY, Lu XY, Dong H, Yu WL, Jin GZ, Cong WM, Wu MC. Determination of clonal origin of recurrent hepatocellular carcinoma for personalized therapy and outcomes evaluation: a new strategy for hepatic surgery. *J Am Coll Surg* 2013; **217**: 1054-1062 [PMID: 24246620 DOI: 10.1016/j.jamcollsurg.2013.07.402]
52 **De Bernardi B**, Gerrard M, Boni L, Rubie H, Cañete A, Di Cataldo A, Castel V, Forjaz de Lacerda A, Ladenstein R, Ruud E, Brichard B, Couturier J, Ellershaw C, Munzer C, Bruzzi P, Michon J, Pearson AD. Excellent outcome with reduced treatment for infants with disseminated neuroblastoma without MYCN gene amplification. *J Clin Oncol* 2009; **27**: 1034-1040 [PMID: 19171711 DOI: 10.1200/JCO.2008.17.5877]
53 **Amoroso V**, Agazzi GM, Roca E, Fazio N, Mosca A, Ravanelli M, Spada F, Maroldi R, Berruti A. Regression of advanced neuroendocrine tumors among patients receiving placebo. *Endocr Relat Cancer* 2017; **24**: L13-L16 [PMID: 27965278 DOI: 10.1530/ERC-16-0475]
54 **Venkatram S**, Sinha N, Hashmi H, Niazi M, Diaz-Fuentes G. Spontaneous Regression of Endobronchial Carcinoid Tumor. *J Bronchology Interv Pulmonol* 2017; **24**: 70-74 [PMID: 27367850 DOI: 10.1097/LBR.0000000000000232]
55 **Sewpaul A**, Bargiela D, James A, Johnson SJ, French JJ. Spontaneous Regression of a Carcinoid Tumor following Pregnancy. *Case Rep Endocrinol* 2014; **2014**: 481823 [PMID: 25587468 DOI: 10.1155/2014/481823]
56 **Rayson D**, Pitot HC, Kvols LK. Regression of metastatic carcinoid tumor after valvular surgery for carcinoid heart disease. *Cancer* 1997; **79**: 605-611 [PMID: 9028374]
57 **Sano I**, Kuwatani M, Sugiura R, Kato S, Kawakubo K, Ueno T, Nakanishi Y, Mitsuhashi T, Hirata H, Haba S, Hirano S, Sakamoto N. Hepatobiliary and Pancreatic: A rare case of a well-differentiated neuroendocrine tumor in the bile duct with spontaneous regression diagnosed by EUS-FNA. *J Gastroenterol Hepatol* 2017; **32**: 11 [PMID: 28052461 DOI: 10.1111/jgh.13585]
58 **Kawaguchi K**, Usami N, Okasaka T, Yokoi K. Multiple thymic carcinoids. *Ann Thorac Surg* 2011; **91**: 1973-1975 [PMID: 21619996 DOI: 10.1016/j.athoracsur.2010.11.067]
59 **Delcore R**, Friesen SR. Zollinger-Ellison syndrome. A new look at regression of gastrinomas. *Arch Surg* 1991; **126**: 556-558 [PMID: 2021333 DOI: 10.1001/archsurg.1991.01410290028004]
60 **Fox PS**, Hofmann JW, Decosse JJ, Wilson SD. The influence of total gastrectomy on survival in malignant Zollinger-Ellison tumors. *Ann Surg* 1974; **180**: 558-566 [PMID: 4416322 DOI: 10.1097/00000658-197410000-00020]
61 **Magabe PC**, Bloom AL. Sudden death from carcinoid crisis during image-guided biopsy of a lung mass. *J Vasc Interv Radiol* 2014; **25**: 484-487 [PMID: 24581473 DOI: 10.1016/j.jvir.2013.10.054]

Published by **Baishideng Publishing Group Inc**
7041 Koll Center Parkway, Suite 160, Pleasanton, CA 94566, USA
Telephone: +1-925-3991568
E-mail: bpgoffice@wjgnet.com
Help Desk: https://www.f6publishing.com/helpdesk
https://www.wjgnet.com